



UNIVERSIDAD DE BURGOS

Departamento de Biotecnología y Ciencia de los Alimentos

**Integral valorization of brewer's spent grain  
by emerging technologies**

**PhD Thesis**

Patricia Alonso Riaño

Burgos, 2022



# **Integral valorization of brewer's spent grain by emerging technologies**

Memoria que para optar al grado de  
Doctor por la Universidad de Burgos  
en el programa Avances en Ciencia y  
Biotecnología Alimentarias presenta:

**Patricia Alonso Riaño**

Burgos, 2022





## UNIVERSIDAD DE BURGOS

### Departamento de Biotecnología y Ciencia de los Alimentos

**Dña. MARÍA TERESA SANZ DIEZ y Dña. SAGRARIO BELTRÁN CALVO**, Profesoras del Departamento de Biotecnología y Ciencia de los Alimentos de la Universidad de Burgos,

CERTIFICAN:

Que la Licenciada en Química **Dña. Patricia Alonso Riaño** ha realizado bajo su dirección el trabajo titulado **“Integral valorization of brewer’s spent grain by emerging technologies”**, cuyo título en castellano es: “Valorización integral del bagazo de cerveza mediante tecnologías emergentes”.

Considerando que dicho trabajo reúne los requisitos exigidos para ser presentado como Tesis Doctoral, expresan su conformidad con dicha presentación.

Para que conste, firman el presente certificado.

En Burgos, a 30 de Marzo de 2022

Fdo. María Teresa Sanz Diez

Fdo. Sagrario Beltrán Calvo





## UNIVERSIDAD DE BURGOS

### Departamento de Biotecnología y Ciencia de los Alimentos

D. JOSÉ MANUEL BENITO MORENO, coordinador del programa de doctorado “Avances en Ciencia y Biotecnología Alimentarias” de la Universidad de Burgos,

CERTIFICA:

Que la memoria titulada “Integral valorization of brewer’s spent grain by emerging technologies” presentada por Dña Patricia Alonso Riaño, Licenciada en Química, ha sido realizada en el Departamento de Biotecnología y Ciencia de los Alimentos bajo la dirección de las Dras. María Teresa Sanz Diez y Sagrario Beltrán Calvo, y en representación de la Comisión Académica del Programa de Doctorado, autoriza su presentación para ser defendida como Tesis Doctoral.

Para que conste, y surta los efectos oportunos, firmo el presente certificado.

En Burgos, a 30 de Marzo de 2022

Fdo. José Manuel Benito Moreno

Coordinador del Programa de Doctorado





## AGRADECIMIENTOS

---

Este trabajo ha sido desarrollado en el seno del Grupo de Investigación Biotecnología Industrial y Medioambiental, reconocido por la Universidad de Burgos (GIR-UBU BIOIND) y por la Junta de Castilla y León como Unidad de Investigación Consolidada UIC-128, en el marco de los siguientes proyectos de investigación:

- VALORIZACIÓN DE LA FRACCIÓN PROTEICA DE SUBPRODUCTOS DE LA INDUSTRIA AGROALIMENTARIA DE CASTILLA Y LEÓN MEDIANTE TECNOLOGÍAS DE FLUIDOS PRESURIZADOS (PROVALOR), financiado por la Junta de Castilla y León y el Fondo Europeo de Desarrollo Regional (BU050P20).

- VALORIZACIÓN DE SUBPRODUCTOS MARINOS MEDIANTE TECNOLOGÍAS DE FLUIDOS SUB- Y SUPERCRÍTICOS PARA LA OBTENCIÓN DE BIOCOMPUESTOS VALIOSOS, financiado por la Agencia Estatal de Investigación (10.13039/501100011033).

- VALORIZACIÓN INTEGRAL DE SUBPRODUCTOS DE LA INDUSTRIA AGROALIMENTARIA MEDIANTE TECNOLOGÍAS EMERGENTES (ALVALOR), financiado por la Junta de Castilla y León y el Fondo Europeo de Desarrollo Regional (BU301P18).

Agradezco a estas instituciones públicas el apoyo económico recibido.

Agradezco también a la Junta de Castilla y León y al Fondo Social Europeo por financiar mi contrato predoctoral: (EDU/556/2019).



## AGRADECIMIENTOS

---

*A mis directoras de Tesis Teresa y Sagrario. A Tere, por guiarme en este proyecto, por su inestimable apoyo y dedicación y por todo lo que he podido aprender de ella durante este tiempo. A Sagrario, por darme la oportunidad de introducirme en el mundo de la investigación y por su ayuda durante este periodo.*

*A todos mis compañeros del Área de Ingeniería Química que han contribuido a que este trabajo fuera posible. A Beti, por todo lo que me ha ayudado y enseñado en el laboratorio. A mis compañeras de Tesis, Esther y Mansoore, por haberme acompañado y apoyado en este camino. A Eli y a Almu, por su ayuda, pero sobre todo por su apoyo y compañía. A Cipri, por estar siempre dispuesto a ayudar y por hacer que lo difícil parezca fácil. En general, a todas las personas con las que he trabajado durante estos años y que han contribuido de una forma u otra en el desarrollo de mi Tesis. A Óscar, Alba, Rodrigo, Pedro, Cherif, Davinia, Daysi, Sarai, María...*

*A la Profesora Ana Xavier, de la Universidad de Aveiro, por darme la oportunidad de colaborar con su grupo y por acogerme durante mi estancia de investigación predoctoral. A Mariana por su ayuda en el laboratorio y su disposición a contribuir a mi formación investigadora.*

*A mi familia y amigos, por su comprensión y paciencia y por darme ánimos durante todo este tiempo. En especial a mis padres, por su infinito cariño.*

*A Miguel, por creer en mí, por su paciencia, comprensión y apoyo incondicional, por estar siempre a mi lado y darme fuerzas.*

*A todos, gracias.*





# **GENERAL INDEX**

---



## GENERAL INDEX

---

SUMMARY .....	1
INTRODUCTION .....	9
OBJECTIVES .....	73
RESULTS.....	77
Water ultrasound-assisted extraction of polyphenol compounds from brewer's spent grain: Kinetic study, extract characterization and concentration .....	81
Valorization of brewer's spent grain by consecutive supercritical carbon dioxide extraction and enzymatic hydrolysis .....	113
Subcritical water as hydrolytic medium to recover and fractionate the protein fraction and phenolic compounds from craft brewer's spent grain .....	155
Preliminary study of subcritical water treatment scale-up from laboratory to pilot system for brewer's spent grain valorization .....	195
Pervaporation behaviour of subcritical water hydrolysates of lignocellulosic biomass: brewer's spent grain .....	241
Second generation bioethanol production from subcritical water pretreated brewer's spent grain within a biorefinery concept .....	271
CONCLUSIONS .....	307







# SUMMARY

---



## SUMMARY OF THE THESIS

---

The development of new strategies in the bioeconomy field aims to find alternatives to fossil-based feedstocks for the production of fuels and chemicals, since the availability of fossil resources is limited, and their use is associated with the global climate change. Furthermore, waste generation is increasing exponentially, as consequence of the growing population and higher quality of life. One of the most attractive alternatives to deal with both problems is the development of sustainable biorefineries for processing biomass into different products and energy, being key in the context of circular economy, closing loops of streams, and valorizing multiple outputs, considering both, environmental and economic aspects. In this sense, the integral conversion of lignocellulosic agro-industrial residual biomass (second-generation biomass) into high value-added products minimizes environmental impacts and maximizes the use of renewable resources.

In this work, an integral valorization of brewer's spent grain (BSG) by using clean and environmentally friendly technologies has been proposed. BSG is the main byproduct of the brewing industry (85%). It is a lignocellulosic biomass with high protein content (10 - 30%, w/w) and around 6% of lipids, being also a valuable source of phenolic compounds that have demonstrated antioxidant effects. Based on its chemical composition, the integration of BSG within a biorefinery concept is of great interest to obtain different high-value biocompounds. However, due to the recalcitrant structure of lignocellulosic biomass, the fractionation of these byproducts into their individual building blocks remains a challenge for the optimal development of second-generation biorefineries.

The integral valorization of BSG involves the recovery of all its valuable extractable components, and fractionation and recovery of its cell-wall components, cellulose, hemicellulose, lignin, and protein. This Thesis proposes the use of different green and efficient technologies for the recovery of bioactive compounds from BSG, such as supercritical fluid extraction (EFSC), and ultrasound-assisted extraction (UAE). In addition, the use of subcritical water (subW) has been proposed as an eco-friendly approach to hydrolyze and fractionate the BSG structural components (lignocellulose and protein fractions), recovering also different bioactive compounds, such as phenolic compounds,

biopeptides, and amino acids, which may improve the feasibility of the biomass processing within a biorefinery concept.

The results obtained with these technologies have been compared with those obtained with conventional extraction/hydrolytic methods, such as conventional extraction with water and hydroalcoholic mixtures, acid, and alkali hydrolysis as well as enzymatic hydrolysis with different enzyme types. Among this techniques, subW treatment was the most efficient extraction/hydrolysis method to recover the protein fraction from the BSG, yielding about 78% of the total protein content, being also an efficient technology to release the phenolic compounds from the BSG lignocellulosic matrix.

The incorporation of lignocellulosic biomass into a biorefinery concept also involves the separation and recovery of the valuable compounds generated during the treatment. In this Thesis, pervaporation has been proposed as a promising membrane separation process to remove and recover the furfural generated during the subW treatment, achieving a furfural recovery of about 94%, with 16-fold- higher concentration in the permeate than in the initial feed, which leads to a partial detoxification of the subW hydrolysates.

In addition, the effect of subW and supercritical CO<sub>2</sub> (sc-CO<sub>2</sub>) on the residual BSG after treatment has been evaluated, obtaining with both treatments an increase in the pretreated BSG digestibility, although this effect was more remarkable for subW treatment. The remained solids after subW treatment were subjected to enzymatic hydrolysis and a complete conversion of cellulose into glucose was achieved. Sequential and simultaneous saccharification and fermentation (SSF) processes with subW pretreated solids yielded second generation bioethanol with good results in terms of ethanol concentration (32 g/L) and ethanol productivity (1.07 g·L<sup>-1</sup>·h<sup>-1</sup>).

---

## RESUMEN DE LA TESIS

---

Actualmente, el desarrollo de nuevas estrategias en el campo de la bioeconomía trata de encontrar alternativas a las materias primas de origen fósil para la producción de combustibles y compuestos químicos, ya que la disponibilidad de recursos fósiles es limitada y su uso está asociado al cambio climático. Además, la generación de residuos está aumentando exponencialmente como consecuencia del incremento de la población y de la calidad de vida.

Una de las alternativas más atractivas para hacer frente a ambos problemas es el desarrollo de biorrefinerías sostenibles para la transformación de biomasa en diferentes productos y energía. En un contexto de economía circular, las corrientes secundarias de un proceso se convierten en la alimentación de un nuevo proceso, minimizando los residuos generados y obteniendo múltiples compuestos de alto valor, que se generan durante el procesamiento de la biomasa. Considerando tanto los aspectos ambientales como los económicos, una completa valorización de residuos procedentes de la industria agroalimentaria (biomasas de segunda generación) para convertirlos en productos de alto valor añadido, minimiza los impactos ambientales y maximiza el uso de recursos renovables.

En este trabajo se ha propuesto una valorización integral del bagazo de cerveza (BSG) mediante el uso de tecnologías limpias y respetuosas con el medio ambiente. El BSG es el principal subproducto de la industria cervecera (85%). Se trata de una biomasa lignocelulósica con alto contenido en proteínas (10 - 30%, p/p) y alrededor de un 6% de lípidos, siendo además una valiosa fuente de compuestos fenólicos que han demostrado tener efectos antioxidantes. En base a su composición química, la integración del BSG dentro de un concepto de biorrefinería es de gran interés para obtener diferentes biocompuestos de alto valor. Sin embargo, debido a la estructura recalcitrante de las biomasas lignocelulósicas, el fraccionamiento de estos subproductos en sus componentes individuales sigue siendo un reto para el desarrollo óptimo de biorrefinerías de segunda generación.

La valorización integral del BSG implica la recuperación de todos sus componentes extractables valiosos y el fraccionamiento y recuperación de sus componentes

estructurales, celulosa, hemicelulosa, lignina y proteínas. Este trabajo propone el uso de diferentes tecnologías verdes y eficientes para la recuperación de los compuestos bioactivos del BSG, tales como la extracción con fluidos supercríticos y la extracción asistida por ultrasonidos (UAE). Además, se ha propuesto el uso de agua subcrítica (subW) como una tecnología respetuosa con el medioambiente para hidrolizar y fraccionar los componentes estructurales del BSG (fracciones de lignocelulosa y proteínas), recuperando al mismo tiempo diferentes compuestos bioactivos, como compuestos fenólicos, biopéptidos y aminoácidos, que pueden mejorar la viabilidad del procesamiento de la biomasa dentro de un concepto de biorrefinería integrada.

Los resultados obtenidos con estas tecnologías se han comparado con los obtenidos con métodos convencionales de extracción o hidrólisis como son, la extracción convencional con agua y mezclas hidroalcohólicas, la hidrólisis ácida y alcalina, así como la hidrólisis enzimática con diferentes tipos de enzimas. Entre estas técnicas, el tratamiento con agua subcrítica fue el método de extracción/hidrólisis más eficiente para recuperar la fracción proteica del bagazo de cerveza, con un rendimiento de hasta el 78% del contenido proteico total, siendo también una tecnología eficaz para liberar los compuestos fenólicos de la matriz lignocelulósica del bagazo.

En una biorrefinería integrada, la valoración de la biomasa también implica la separación y recuperación de los compuestos valiosos generados durante el tratamiento de esta. En este trabajo se ha propuesto la pervaporación como un proceso prometedor de separación de membranas para eliminar y/o recuperar el furfural generado durante el tratamiento con agua subcrítica, consiguiendo una recuperación del furfural de alrededor del 94%, con una concentración 16 veces superior en el permeado que en la alimentación inicial, lo que conlleva también a una detoxificación parcial de los hidrolizados.

Asimismo, se ha evaluado el efecto que causa el tratamiento con agua subcrítica y con CO<sub>2</sub> supercrítico (sc-CO<sub>2</sub>) sobre el sólido que permanece después del tratamiento, obteniendo con ambos tratamientos un aumento de la digestibilidad enzimática del BSG pretratado, aunque este efecto fue más notable para el tratamiento con subW. El bagazo pretratado con agua subcrítica se sometió a hidrólisis enzimática y se consiguió una completa conversión de la celulosa en glucosa. Los procesos de sacarificación y fermentación (SSF) secuenciales y simultáneos con el bagazo pretratados con subW

*RESUMEN DE LA TESIS*

*Valorización integral del bagazo de cerveza mediante tecnologías emergentes*

---

produjeron bioetanol de segunda generación con buenos resultados en términos de concentración y productividad de etanol.

---







# INTRODUCTION

---



## Table of Contents

---

### INTRODUCTION

1.	Brewer's spent grain.....	13
1.1.	Brewer's spent grain generation.....	13
1.2.	BSG composition .....	15
1.2.1.	Carbohydrates.....	17
1.2.2.	Lignin.....	20
1.2.3.	Protein content and amino acids.....	20
1.2.4.	Phenolic compounds.....	22
1.2.5.	Lipids .....	23
1.3.	Integral valorization of brewer's spent grain .....	24
1.3.1.	Valorization of extractives .....	25
1.3.2.	Protein valorization.....	27
1.3.3.	Phenolic compounds valorization .....	28
1.3.4.	Lignocellulose fractionation.....	29
2.	Supercritical Carbon Dioxide.....	34
2.1.	Sc-CO <sub>2</sub> treatment of BSG from a biorefinery perspective .....	35
2.2.	Parameters affecting treatment with sc-CO <sub>2</sub> .....	36
3.	Subcritical water extraction/hydrolysis .....	39
3.1.	Physical and chemical properties of subcritical water .....	40
3.2.	Operational modes in subcritical water .....	42
3.3.	Valorization of BSG by hydrothermal treatment.....	44
3.3.1.	Lignocellulose fractionation by subcritical water treatment .....	44
3.3.2.	SubW extraction of phenolic compounds from BSG.....	52
3.3.3.	Protein extraction/hydrolysis by subcritical water treatment.....	54
4.	Detoxification of the subcritical water hydrolysates .....	56
4.1.	Membrane separation process: Pervaporation .....	58
	References.....	61

---



## 1. Brewer's spent grain

Brewer's spent grain (BSG) is the main solid by-product of the brewing industry, representing around 85% of the total by-products generated. It accounts for around 20 kg per 100 L of beer produced [1]. It represents up to 30% of the starting malted grain [2]. BSG is essentially composed of the malted barley seed coats, pericarp, and husks that cover the original cereal, endosperm fragments, and other residual compounds that are not converted to fermentable sugars through the brewing process [3]. **Figure I.1** shows the cross-section of a barley kernel, where the main components of barley that remain in BSG after the brewing process have been underlined.

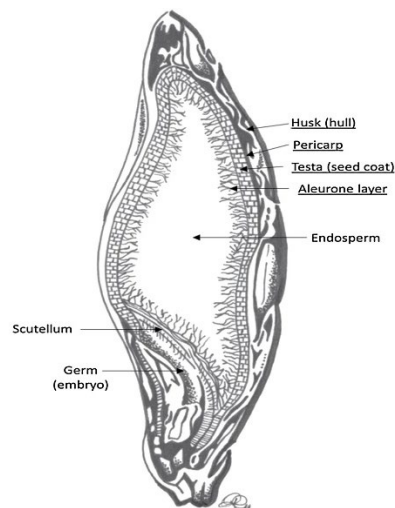


**Figure I.1.** Cross-section of a barley kernel showing the grain coverings (underlined) that constitute BSG. Adapted from [4].

### 1.1. Brewer's spent grain generation

**Figure I.2** shows a diagram of the beer production process from barley, although other grains may be malted and subsequently used in brewing. The first step in the brewing process is malting, consisting of three different unit operations: steeping, germination, and drying. During the second step, milling, the malt is coarsely milled and sieved into three fractions, namely husk, grits, and flour. Although the smaller the particle size, the greater

the extract and the lower the filtration rate, in traditional brewing, the husk must be kept as intact as possible to form porous filter beds.

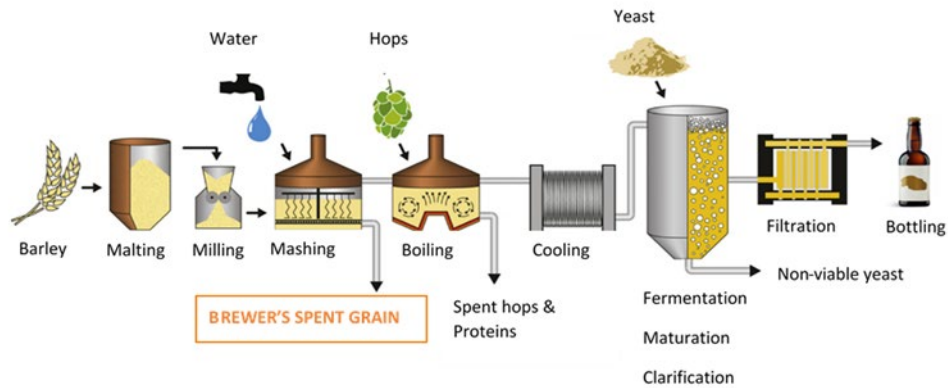


**Figure I.2.** Schematic of the beer production process. Adapted from [5].

Currently, craft breweries still use this method of mash filtration, while many larger breweries employ a mash filter, so malt can be milled more extensively [4]. **Figure I.3.** shows two samples of BSG, one from a craft brewery and other from an industrial brewery.

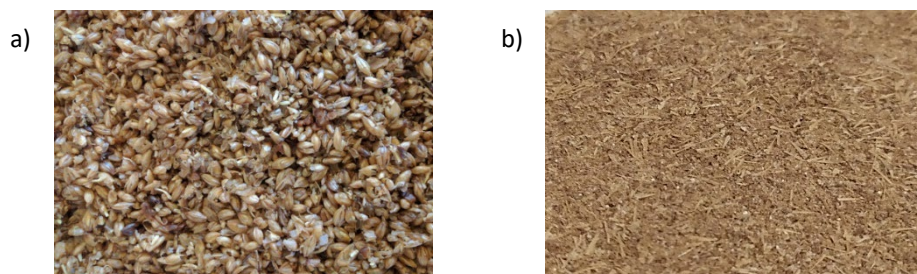


**Figure I.3.** Brewer's spent grain from **a)** local craft brewery (Brebajes del Norte S.L.) and **b)** industrial brewery (San Miguel S.A.).

During the mashing step, the grit is suspended into hot water and the temperature slowly increased (from 37 to 78 °C) to promote enzymatic hydrolysis of malt constituents, primarily starch, but also other components such as proteins, (1/3, 1/4)- $\beta$ -glucans and arabinoxylans, and to solubilize their breakdown products. The starch is converted to fermentable sugars (mainly maltose, and maltotriose) and non-fermentable sugars

(dextrins) [6]. The starch hydrolysis is conducted by the enzymes naturally present in the malt,  $\beta$ - and  $\alpha$ -amylases.  $\beta$ -amylase hydrolyses the second  $\alpha$ -1,4-glycosidic linkages from the non-reducing end of the amylose chains in starch, while  $\alpha$ -amylase randomly hydrolyses the  $\alpha$ -1,4 glycosidic linkages [7].

The fourth step is lautering, which involves separating the mash into the clear liquid wort and the residual grain, the so-called brewer's spent grains (**BSG**). This is followed by wort boiling in the brewing pan and wort clarification in a whirlpool separator.

After cooling, the wort is submitted to fermentation by brewer's yeast and fermentable sugars are converted into ethanol, carbon dioxide, and several other metabolic byproducts. After that, the freshly brewed liquid undergoes the second fermentation during the maturation step for a time range from 3 weeks to 3 months depending on the type of beer being produced. The next step in the beer brewing process is beer clarification and stabilization and finally, filling beer in trading units (glass bottles, PET-bottles, cans or kegs).

## 1.2. BSG composition

The chemical composition of BSG reported in different works has been collected in **Table I.1**. The values of each component in BSG are the following: protein (14.2 – 31%), cellulose (0.3 – 33%), hemicellulose (19.2 – 41.9%), lignin (11.5 – 27.8%), lipids (3 – 13%), extractives (5.8 – 10.7%) and ashes (1.11 – 4.6%), expressed on a dry weight basis.

**Extractives** in biomass refer to the non-structural components that are easily extracted by solvents (i.e., water, ethanol, acetone, hexane, etc) comprising several compounds such as fats, soluble proteins, terpenes, simple sugars, starches, phenolics, essential oils, pectins, fatty acids, sterols, and flavonoids, among others [8].

As can be seen in **Table I.1**, the values reported of each BSG component show considerable variability. BSG composition varies as a consequence of different factors, such as the cereal variety, time of harvesting, the malting and mashing regime, and the adjuncts employed (or not) during brewing [4].

**Table I.1.** Chemical composition of BSG collected from the literature.

Component (dw%)	Reference			
	Mussato [3]	Lynch et al. [4]	Meneses et al. [11]	Mussato & Roberto [6]
Protein	15.3 – 24.7	14.2 – 31	24.7	15.25
Cellulose	16.8 – 26	0.3 – 33	21.7	16.78
Starch	NR	1-12	NR	NR
Hemicellulose	19.2 – 41.9	19.2 – 41.9	19.3	28.4
Xylan	13.6 – 20.6	NR	NR	19.9
Arabinan	5.6 – 9.0	NR	NR	8.48
Acetyl groups	1.1 – 1.4	NR	NR	1.35
Lignin	11.9 – 27.8	11.5 – 27.8	19.4	27.78
Acid Soluble lignin	NR	NR	1.86	4.82
Acid Insoluble lignin	NR	NR	17.5	22.96
Lipids	NR	3 – 13	NR	NR
Ash	1.1 – 4.6	1.1 – 4.6	4.18	4.6
Extractives	5.8 – 10.7	NR	NR	5.8

“NR” stands for not reported.

However, Santos et al. [9], studied the variability of BSG within the same brewery and they found relatively homogeneity of samples, with slight variations for ash and phenolics. On the other hand, Robertson et al. [10] found noticeable differences in BSG composition between different breweries due to the use of distinct mashing technology or to variations in malt source among breweries. Specifically, these authors found that non-starch polysaccharides, lignin, and bound phenolics in BSG did not vary significantly between breweries, but BSG from lager brewing showed a higher protein content and lower residual starch content than BSG from ale brewing.

In addition, the chemical composition of craft BSG is significantly different from that of large brewing companies. Jin et al. [12] compared the composition of BSG from different craft breweries with that of BSG reported previously in the literature [6], [13], [14], as represented in **Figure I.4**. It should be noted that the proportions of protein, lipid, ash, and phenolic acids were comparable, while the contents of starch and fiber were remarkably different. The starch content varied from 1 to 12% in conventional BSG, which was in



## INTRODUCTION

### *Integral valorization of brewer's spent grain by emerging technologies*

---

contrast to 19–48% in the craft BSGs. The fiber content in BSG previously reported in the literature ranged from 50 to 80% compared to (32–49%) determined in that study for craft BSG.

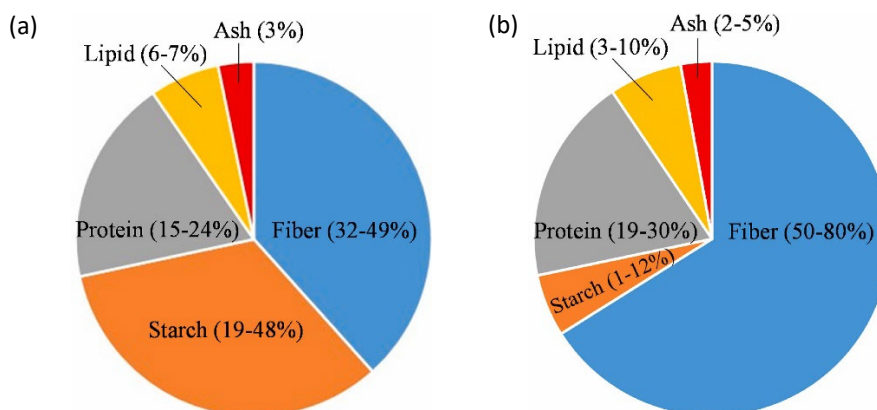


**Figure 1.4.** Comparison of chemical composition of BSG from craft and large brewing companies, expressed on a dry basis. **(a)** craft BSG reported by Jin et al. [12], **(b)** large brewing BSGs as reported in other studies [4], [6], [13], [15] and collected in [12].

Despite the different values reported for the chemical composition of BSG, it is mainly a lignocellulosic material composed of cellulose, hemicellulose, and lignin polymers that are associated with each other constituting the cellular complex of the biomass, besides an important content of protein and minor amount of lipids and phenolic compounds. A brief description of these components are collected in the following paragraphs.

#### 1.2.1. Carbohydrates

Carbohydrates constitute up to 50% of the BSG composition on a dry weight basis. Most of the carbohydrates in BSG exist as polysaccharides, although fermentable sugars, including maltose, glucose, maltotriose, and fructose may be also present [12], [16]. BSG polysaccharides are mainly composed of cellulose and arabinoxylan and variable amounts of non-cellulosic glucans such as starch, and a minor amount of (1–3,1–4)- $\beta$ -D-glucan (~1%) [4]. Glucan is an expression covering all glucose polymers, frequently used to describe cellulose-like compounds that are not cellulose [17]. That includes starch and  $\beta$ -glucans

which can be found in biomass such as BSG. Thus, the most abundant monosaccharides that make up the BSG polysaccharides are glucose, xylose, and arabinose.

**Cellulose** is the most abundant polymer on Earth. Cellulose is a  $\beta$ -1,4-polyacetal of cellobiose (4-O- $\beta$ -D-glucopyranosyl-D-glucose). It is a polysaccharide consisting of a linear chain of several hundred to many thousands of  $\beta$  (1-4) linked D-glucopyranose units. Cellulose chains are linked together by hydrogen bonds. **Figure I.5** represents the cellulose structure and the hydrogen bonding that allows the parallel arrangement of the cellulose polymer chains.

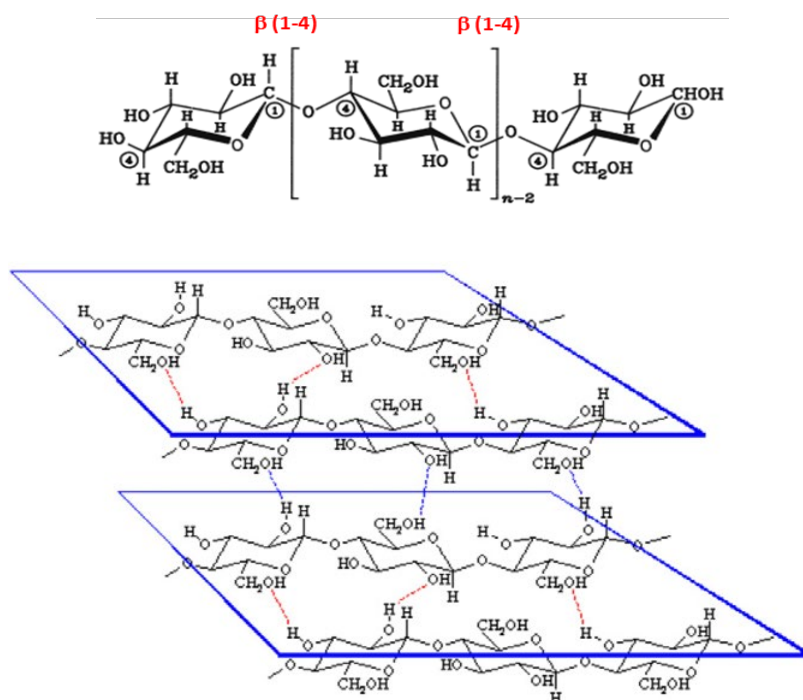


**Figure I.5.** Structure of cellulose illustrating the  $\beta$ -1,4-glycosidic bonds as well as intramolecular hydrogen bonds [18].

Natural cellulose exists in the form of a group of interconnected parallel fibers (microfibrils) linked to hemicelluloses and lignin polymers. In plants, cellulose is mainly present in crystalline form with a minor fraction existing in amorphous form [19]. Due to its crystallinity, cellulose is insoluble in water, dilute acid solutions and in most solvents at

## INTRODUCTION

### *Integral valorization of brewer's spent grain by emerging technologies*

---

ambient temperature. Cellulose is soluble in concentrated acids, but severe degradation of the polymer by hydrolysis is caused [18], [20].

**Starch** represents the major polysaccharide reserve of plants, made up of glucose polymers with  $\alpha$ -1-4-glycosidic bonds. Starch is mainly composed of amylose (18-35%) and amylopectin (65-82%). Amylose is a linear molecule of (1-4)-linked  $\alpha$ -D-glucopyranosyl units, whereas amylopectins have branch points formed from  $\alpha$ -1-6-glycosidic linkages [21].

The BSG starch content is determined by the effectiveness of the mashing process to hydrolyze starch polymers and it is associated with the milling step. As mentioned above, in larger breweries usually grains are milled more extensively than in craft breweries (see **Figure I.3**). Consequently, the starch content in craft BSG is often higher than in BSG from larger breweries. Besides cellulose and starch, small amounts of (1-3,1-4)- $\beta$ -D-glucan (~1 dw%), usually called  $\beta$ -glucan, may be also present in BSG [4].

**Hemicellulose** content in BSG ranges from 19 to up to 40% of its dry weight and is mainly composed of arabinoxylans (AXs). AXs are hydrogen-bonded to cellulose fibrils and have a backbone of (1,4)-linked xylose residues that can be substituted with arabinose residues. Ferulic acid can be esterified to the arabinose residue [4]. **Figure I.6** illustrates the structure of an AX chain. According to Coelho et al. [22], BSG AXs mostly contain terminally linked arabinose residues and additional substituted groups may be present such as hexose, uronic acid, methylated uronic acid, and acetyl groups. Acetyl groups are the main acid substituted groups present in the BSG hemicellulose.

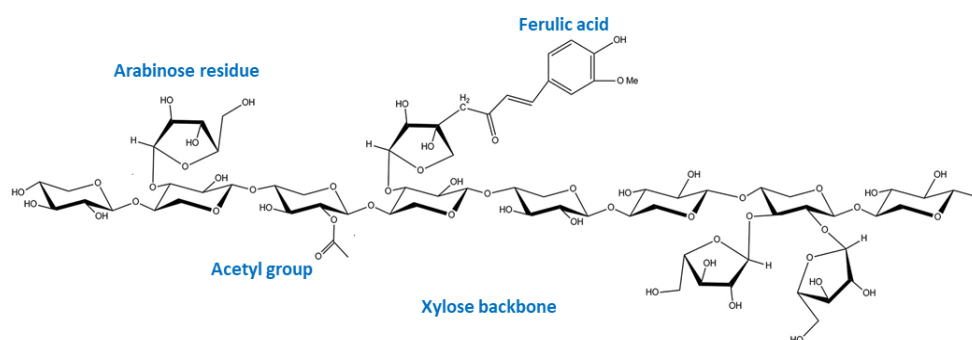


**Figure I.6.** Structure of arabinoxylan illustrating the main-chain xylose backbone, arabinose residues, acetyl group, and linked ferulic acid. Adapted from [4]

### **1.2.2. Lignin**

Lignin is a complex polyphenolic macromolecule that provides rigidity and cohesion to the material cell wall, forming a physic-chemical barrier against microbial attack [23]. Lignin is linked to cellulose and hemicelluloses by ether and ester bonds and forms a matrix in which the hemicelluloses and cellulose are connected by hydrogen bonds.

Lignin is formed from phenolic units or monolignols, p-coumaryl alcohol, coniferyl alcohol and sinapyl alcohol, which in lignin exists as p-hydroxyphenyl, guaiacyl and syringyl units, respectively. However, the composition of lignin widely varies from different biomasses. In BSG, lignin is mainly composed of guaiacyl units, and between 25 and 30% syringyl units that are linked with hydroxycinnamic acids, mainly ferulic and p-coumaric acids [24].

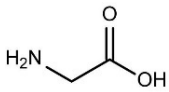
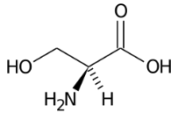
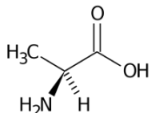
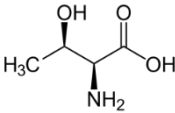
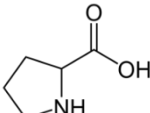
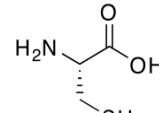
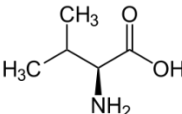
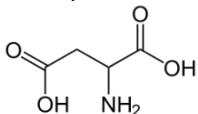
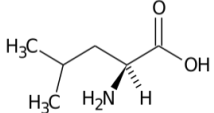
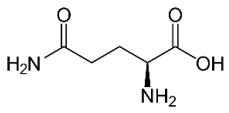
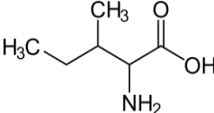
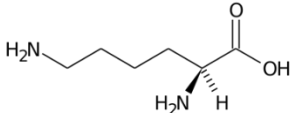
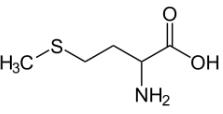
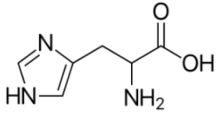
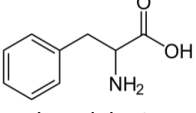
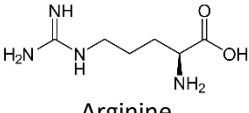
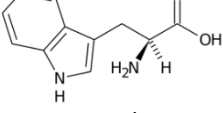
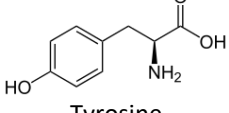
### **1.2.3. Protein content and amino acids**

The protein content in BSG (14-30 dw%) is higher than those reported for other lignocellulosic materials such as barley, oats, rice, and wheat straws, as consequence of the malt starch removal during the beer production process [6].

The main proteins in BSG are hordeins (alcohol soluble) and glutelins (acid/alkali-soluble). Albumins (water-soluble) and globulins (salt-soluble) represent only around 20% of the total protein content in BSG as a result of their unavoidable extraction during brewing process [25]. However, BSG may contain some precipitated protein from wort boiling [24].

Around 30% of the protein content of BSG is composed of essential amino acids, including lysine (14.3%), leucine (6.12%), phenylalanine (4.64%), isoleucine (3.31%), threonine (0.71%), and tryptophan (0.14%). The non-essential amino acids in BSG comprise histidine (26.27%), glutamic acid (16.59%), aspartic acid (4.81%), valine (4.61%), arginine (4.51%), alanine (4.12%), serine (3.77%), tyrosine (2.57%), glycine (1.74%), asparagine (1.47%),  $\gamma$ -aminobutyric acid (0.26%) and glutamine (0.07%) [16]. The amino acids can be also classified according to their polar or non-polar character, as has been collected in **Table I.2.**

**Table I.2.** Chemical structure of amino acids grouped into non-polar and polar.

Non-polar amino acids	Polar amino acids
 Glycine	 Serine
 Alanine	 Threonine
 Proline	 Cysteine
 Valine	 Aspartic acid
 Leucine	 Glutamine
 Isoleucine	 Lysine
 Methionine	 Histidine
 Phenylalanine	 Arginine
 Tryptophan	 Tyrosine

### 1.2.4. Phenolic compounds

BSG is also rich in phenolic compounds since most of the phenolic compounds of the barley grain are contained in the coat-pericarp-husk layer [2].

Phenolic compounds can be classified into different groups according to their chemical structure: phenolic acids, flavonoids, stilbenes, and lignans. The chemical structure of these phenolic compounds is represented in **Figure I.7**.

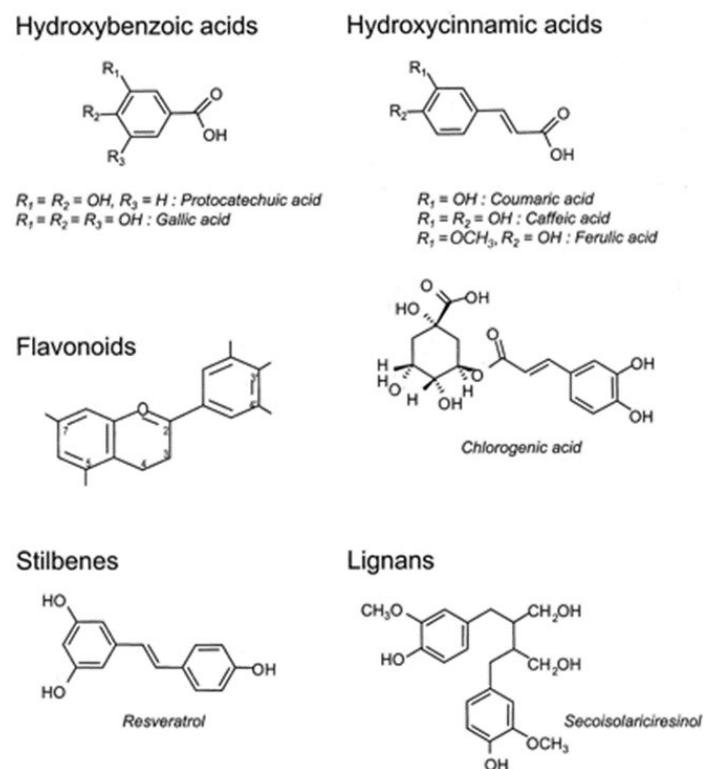


**Figure I.7.** Chemical structure of polyphenols [26].

Most of the phenolic compounds present in cereals are phenolic acids, which can be divided into two subgroups: hydroxybenzoic acid derivatives, including vanillic, syringic, p-hydroxybenzoic, and gallic acids; and hydroxycinnamic acid derivatives comprising ferulic, p-coumaric, caffeic, and sinapic acids.

## INTRODUCTION

### *Integral valorization of brewer's spent grain by emerging technologies*

---

In lignocellulosic materials, phenolic acids are present in three forms: soluble-free, soluble-conjugated, and insoluble-bound. Conjugated phenolic form soluble complex through ester and ether linkages with sugars, lipids, proteins, amino acids, and other phenolic compounds. Whereas insoluble phenolic acids are covalently bonded through ester and ether linkages with cell wall components, such as polysaccharides (e.g., arabinoxylans), lignin, protein, and pectin, forming insoluble complexes [27], [28].

The most abundant phenolic compounds found in BSG are the hydroxycinnamic acids ferulic acid (359 – 624 µg/g) and p-coumaric acid (79 – 260 µg/g) and in lesser extent sinapic, caffeic, and syringic acids [28], [29].

Most of the phenolic acids in BSG exist in a bound insoluble form. The total phenolic acid content in BSG ranges from 3 to 5 mg/g, whereas <0.5 mg/g occurs in soluble free forms [27]. It was reported that BSG exhibits 5-fold higher levels of p-coumaric and ferulic acids, as well as, ferulic acid dehydrodimers than barley grains, being the p-coumaric acid/ferulic acid ratio (0.30-0.40) similar in both, barley and BSG [29]. In the same study, the dehydrodimer/ferulic acid ratio found in BSG (> 0.48) was higher than in barley grains, suggesting that a higher amount of monomeric ferulic acid is solubilized during the mashing step compared to dimeric ferulic acid. In the same study, it was found a higher dehydrodimer/ferulic acid ratio in BSG (> 0.48) than the one found for barley grains, suggesting that a higher amount of monomeric ferulic acid is solubilized during the mashing step compared to dimeric ferulic acid.

#### **1.2.5. Lipids**

BSG lipids are mostly composed of triglycerides (55%) but also of a significant amount of free fatty acids (30%) and a minor content of phospholipids (9.1%) and diglycerides (5.7%) [24]. BSG fatty acids mainly comprise linoleic (18:2 n 6), palmitic (16:0), oleic (18:1 n 9), and linolenic acid (10:3 n 3), and a small amount of stearic acid (18:0) [24], [30].

The lipid content in BSG (5.8 – 11%) is higher than in barley (1.0 – 2.6%) even though lipids are located in barley's endosperm and embryo [24]. Therefore, although endosperm is almost hydrolyzed during the brewing process, barley's lipids remain in the spent grains.

### **1.3. Integral valorization of brewer's spent grain**

Currently, BSG is mainly used for animal feed (70%), biogas production (10%), or disposed of in landfills [31]. However, due to the large BSG availability and its high value as a source of bioactive products, the use of this by-product as a value-added resource offers opportunities from an economic and environmental point of view [15]. The use of BSG as a source of bioactive compounds such as phenolic acids, carbohydrates, or proteins has gained attention in the last years, with a particular interest in the food industry and the elaboration of added-value products [4], [7], [31]–[37].

Nowadays, it is well known that the availability of fossil resources is limited, and their use is associated with global climate change. One of the most attractive alternatives to fossil-based feedstocks for the production of fuels and chemicals is the use of biomass within a biorefinery concept. The biorefinery concept refers to the transformation of a raw material (biomass) into energy (heat, electricity, and biofuels) and several products, such as chemicals and biomaterials, by fractionation or conversion processes [38]. For this purpose, finding sources of valuable compounds, considering both, environmental and economic aspects is crucial.

Biorefineries are classified according to feedstock nature: classical agricultural biomass (first generation), lignocellulosic biomass (second generation), or feedstocks of algae (third generation) [39]. Through the biorefinery concept, the integral conversion of agro-industrial residual biomass into high value-added products minimizes environmental impacts and maximizes the use of renewable resources [40]. The development of sustainable biorefineries will contribute to the transition from an economy based on fossil feedstocks to a biobased economy.

In this sense, BSG is second-generation biomass based on non-food lignocellulosic biomass [39], generated in large quantities by the brewing industry. Around  $38.6 \cdot 10^6$  tons of BSG are annually globally generated from the brewing industry of which  $3.4 \cdot 10^6$  tons are produced in Europe [31]. Furthermore, BSG is generated in large, but also small companies [1]. For instance, the size of the European craft beer market was worth US\$ 42.52 million in 2020 and it is expected to grow up to 91.26 million by the end of 2025 [41].



However, due to the high BSG humidity content (~ 80%), together with the presence of fermentable sugars, BSG is strongly susceptible to degradation. Thus, a reduction of its moisture content to around 10% is necessary to be safely stored [1]. Santos et al. [9] studied different BSG preservation methods, such as oven drying, freeze-drying, and freezing, and concluded that oven drying was the most suitable method since its effect on BSG composition was lower than freezing wet, but it was similar to freeze-drying, being oven drying cheaper. In addition, drying allows reducing the BSG volume and, therefore, decreases transport and storage costs [6].

According to Pabbathi et al. [7], having a BSG treatment plant adjacent to or within the breweries may easily allow solving the drying and transport cost. In this way, the heat produced in the brewing process can be used to reduce the BSG moisture content, and transportation costs can also be significantly reduced or eliminated, making the process more feasible. In addition, BSG drying can be avoided in hydrothermal processes if the treatment is performed just following the brewing process.

For the development of advanced biorefineries, in a context of a circular economy, closing loops of streams and valorizing multiple outputs is very important. The valorization of different biomass components, in addition to fermentable carbohydrates, constitutes a significant advance that could enhance the feasibility of the industrial implementation of lignocellulosic biomass-based biorefineries [40]. Integral valorization of biomass involves extraction and fractionation of its individual building blocks including extractives, lipids, proteins, and structural components of the biomass (cellulose, hemicellulose, and lignin). Some of the technologies able to release them from the biomass and some applications of these components or their derivatives are briefly summarized in the following subsections.

### **1.3.1. Valorization of extractives**

A complete BSG valorization should first include extractives valorization towards the development of a biorefinery. Especially, considering the high extractives content in BSG (5.8 – 10.7 dw%) and the presence of important bioactive compounds, such as hydroxycinnamic acids that have demonstrated antioxidant effects [42].

In this sense, different technologies that meet the objective of a sustainable and green extraction process can be applied in the extraction of biomass extractives. Among them, **ultrasound-assisted extraction** (UAE), as an intensification process, is well known to have a significant effect on the rate of extraction of bioactive compounds compared to conventional extraction and it is easy to handle [43]. The mechanisms involved in the improvement of the extraction process by using UAE, namely fragmentation of the raw material, erosion, sonocapillary, sonoporation, shear stress, and detexturation, among others, have been reviewed in the literature [43]. Ultrasounds cause pressure fluctuations that form microscopic bubbles that collapse almost as soon as formed. As the bubbles collapse, the shear forces created act on whatever is nearby, causing a temperature rise. The ultrasonic waves and resulting cavitation break the cell walls and, as a result, the content of the cell wall is released from the matrix to the extraction medium. UAEs need less time, use smaller quantity of solvents, and lower extraction temperatures compared to conventional extraction methods. These advantages result in higher extraction yields and higher productivity [43]–[45].

**Hydrophobic compounds** have been traditionally extracted from biomass employing organic solvents. However, the use of organic solvents to recover the lipophilic extractives possess some environmental concerns. As an alternative, instead of traditional organic solvents, **supercritical CO<sub>2</sub>** (sc-CO<sub>2</sub>) is an attractive intensification technology for the extraction of non-polar components. In the literature, sc-CO<sub>2</sub> has been extensively studied as a green extracting agent over traditional organic extraction solvents to valorize different biomass components [46].

The recovery of water insoluble components such as fats and oils from renewable biomass could become one of the major keys in biorefineries. As they are chemically similar to some petroleum fractions, lipids are attractive for numerous commercial applications, such as their conversion into fuels and chemicals with bigger added value [47]. In this sense, the high triglycerides content in the lipidic fraction of BSG makes BSG a good source of these compounds, which can be used for instance for biodiesel production by transesterification of triglycerides by alkali and acid catalysis [48].

### **1.3.2. Protein valorization**

The valorization of the protein fraction of lignocellulosic materials with high protein content, such as BSG, may be key to the development of advanced sustainable integrated biorefineries [40]. On one hand, when high protein content materials are used in biorefineries focused on sugar-derived products, large amounts of nitrogenous waste streams are generated. On the other hand, proteins are high valuable biocompounds with several applications which can contribute to the overall economy of the biorefinery system [3], [49]–[51].

BSG proteins can be used in food and feed applications [4] to produce bioactive peptides, in the synthesis of protein biofilms with antioxidant properties [52], etcetera. Furthermore, proteins have recently been considered as potential sources of free amino acids, which can be used as precursors to high-priced chemicals [40].

Most of the BSG proteins are connected within a matrix of cell wall polysaccharides. Therefore, it is necessary the use of a hydrolytic medium to achieve high protein yield. In the literature, different techniques have been employed to extract/hydrolyze proteins from BSG, comprising alkaline extraction, enzymatic hydrolysis, hydrothermal treatment, and ultrasound-assisted extraction, among others [50], [53]–[55]. Among these, the most common method used is alkali hydrolysis followed by acid precipitation. However, at high pH conditions, proteins are susceptible to degradation, which results in the production of some toxic substances and the need of large amounts of water to remove the alkali from the solution [32]. Alternatively, enzymatic hydrolysis does not generate toxic products but requires long times and large amounts of enzyme, or a combination of various enzymes (mainly proteases and carbohydrases).

Hydrothermal pretreatments include the use of subcritical water (subW). SubW treatment, as alternative technology for protein recovery, instead of chemical or enzymatic hydrolysis, have the advantages of needing shorter times and avoiding the use of enzymes and chemicals. The efficacy of subcritical water to hydrolyze deoiled rice bran to produce protein and amino acids has been previously shown, achieving higher yields by subW treatment than by conventional alkali hydrolysis [56].

The use of subW to release the protein fraction together with the hemicellulose fraction from BSG, while maintaining a high amount of lignin and cellulose available for further valorization, can maximize the utilization of this biomass.

### **1.3.3. Phenolic compounds valorization**

Phenolic compounds have been recognized as added-value products due to their antioxidant properties with several applications in the food, cosmetic, and pharmaceutical industries [57], [58]. The hydroxycinnamic acids, such as *p*-coumaric and ferulic acid, the most important phenolic acids in BSG, have demonstrated antioxidant effects [42].

Ferulic acid, the most abundant phenolic compound in BSG, is considered as one of the most important phenolic acids, since it exhibits many physiological functions, such as antioxidant, anti-microbial, anti-inflammatory, anti-thrombosis, and anti-cancer activities [59]. Furthermore, ferulic acid is used to produce vanillin, which is priced at about \$1000/kg when it comes from plant sources [60].

Conventional extraction techniques to recover the BSG phenolic compounds have been widely reported in the literature, such as mechanical agitation solvent extraction, Soxhlet extraction with different solvents, enzymatic and alkaline hydrolysis assisted extractions [11], [61]–[63].

Solvent extraction is the primary and essential step to recover the bioactive compounds from the raw material. The extraction efficiency is determined by different factors such as type of solvent, temperature, pH, solvent to solid ratio, particle size, and extraction method.

Several solvents such as methanol, ethanol, water, acetone, and mixtures, as well as pure hexane and ethyl acetate, have been used to study the influence of solvent extraction on the recovery of phenolic compounds from BSG [11]. Ultrasound-assisted extraction (UAE) is an extractive technique with reduced use of solvents and higher extraction yields compared with conventional extraction processes [64].

In lignocellulosic biomass, most of the phenolic acids are bounded to the lignocellulosic matrix by ester and ether linkages, as described above. For this reason, hydrolytic

techniques are needed to release these compounds from the biomass. Alkaline hydrolysis is frequently used to recover phenolic acids while degrading lignin and hemicelluloses [61]

Karlen et al.[65] have recently published a work evaluating the viability of recovering p-coumaric and ferulic acids produced by alkaline pretreatment of grass in the context of lignocellulosic biorefineries. In that study, the techno-economic analysis revealed that the minimum product selling price of ferulic and p-coumaric would be ~\$5.05/kg while the market selling price of these compounds was \$1/kg. These authors concluded that extracting only these compounds is not viable. The recovery of different bioactive compounds must be carried out simultaneously for a biorefinery to generate income.

Alternatively, subcritical water has been successfully used to extract different phenolic compounds from defatted rice bran, since it provides the temperature and the acidic conditions necessary for the hydrolysis reaction [66]. These authors observed a maximum extraction in the temperature range from 155 to 300 °C depending on the phenolic compound (from p-coumaric acid to vanillic acid). Phenolic compounds can be selectively extracted in short reaction times (residence time = 10 min) offering several advantages over conventional extraction methods.

#### **1.3.4. Lignocellulose fractionation**

The building molecules of the lignocellulosic biomass (cellulose, hemicellulose, and lignin) are connected by intra and interpolymer linkages. **Figure I.8** illustrates the typical structure of a lignocellulosic material like BSG.

Biomass fractionation is the process in which the biomass is separated into its constitutive biopolymers. Due to the recalcitrant structure of the lignocellulosic biomass, fractionation is the most limiting step for their conversion into its individual building blocks [20]. Conventional hydrolytic methods require long reaction times (24 – 70 h for enzymatic hydrolysis) or the use of strong reagents such as acids and alkalis [20].

The development of sustainable and green technologies is an important step in biomass valorization to convert lignocellulosic biomass into valuable bioproducts. In the literature, different research articles review different methods and technologies to optimize the pretreatment of the biomass to further obtain the derived building blocks from

## INTRODUCTION

### *Integral valorization of brewer's spent grain by emerging technologies*

lignocellulosic materials. The choice of the optimum treatment will mainly depend on the final objective; nevertheless, the economic and environmental impact should be considered [18].

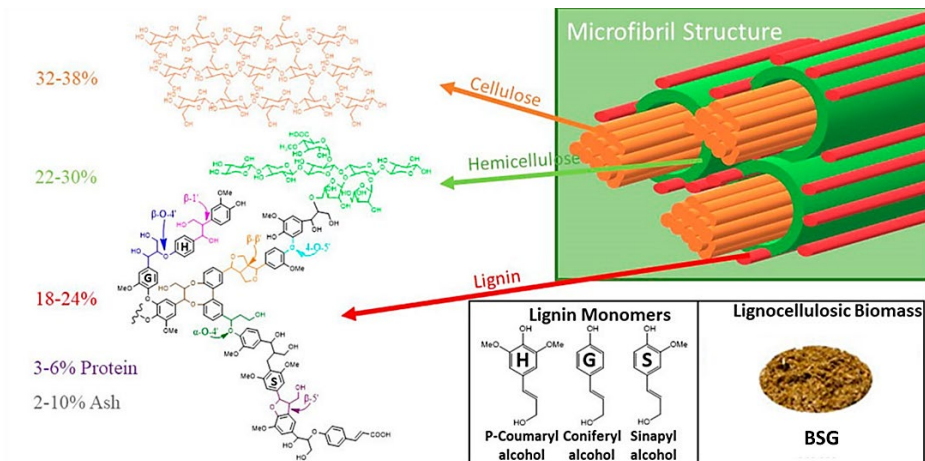


**Figure 1.8.** Ultrastructure of plant cell wall comprising cellulose, hemicellulose, lignin, protein, and ash in different ratios. Adapted from [67].

The pretreatment methods can be classified as biological, mechanical (milling), chemical (hot pressurized water, weak and strong acid hydrolysis, alkaline hydrolysis, organosolv process, oxidative delignification) and combined methods (steam explosion, CO<sub>2</sub> explosion, ammonia fibre explosion).

Different pretreatments have been applied in BSG, such as acid, alkali, acid-alkali, supercritical, pulsed electric, hydrothermal, and enzymatic hydrolysis, as reviewed by Sganzerla et al. [51]. Based on these studies, a general scheme to propose a biorefinery using BSG as raw material to obtain several valuable compounds, such as arabinoxylans, proteins, ferulic acid, xylitol, xylose, lactic acid, butanol, biogas, fertilizer, and ethanol, was performed by these authors, as can be seen in **Figure 1.9**.

INTRODUCTION

Integral valorization of brewer's spent grain by emerging technologies

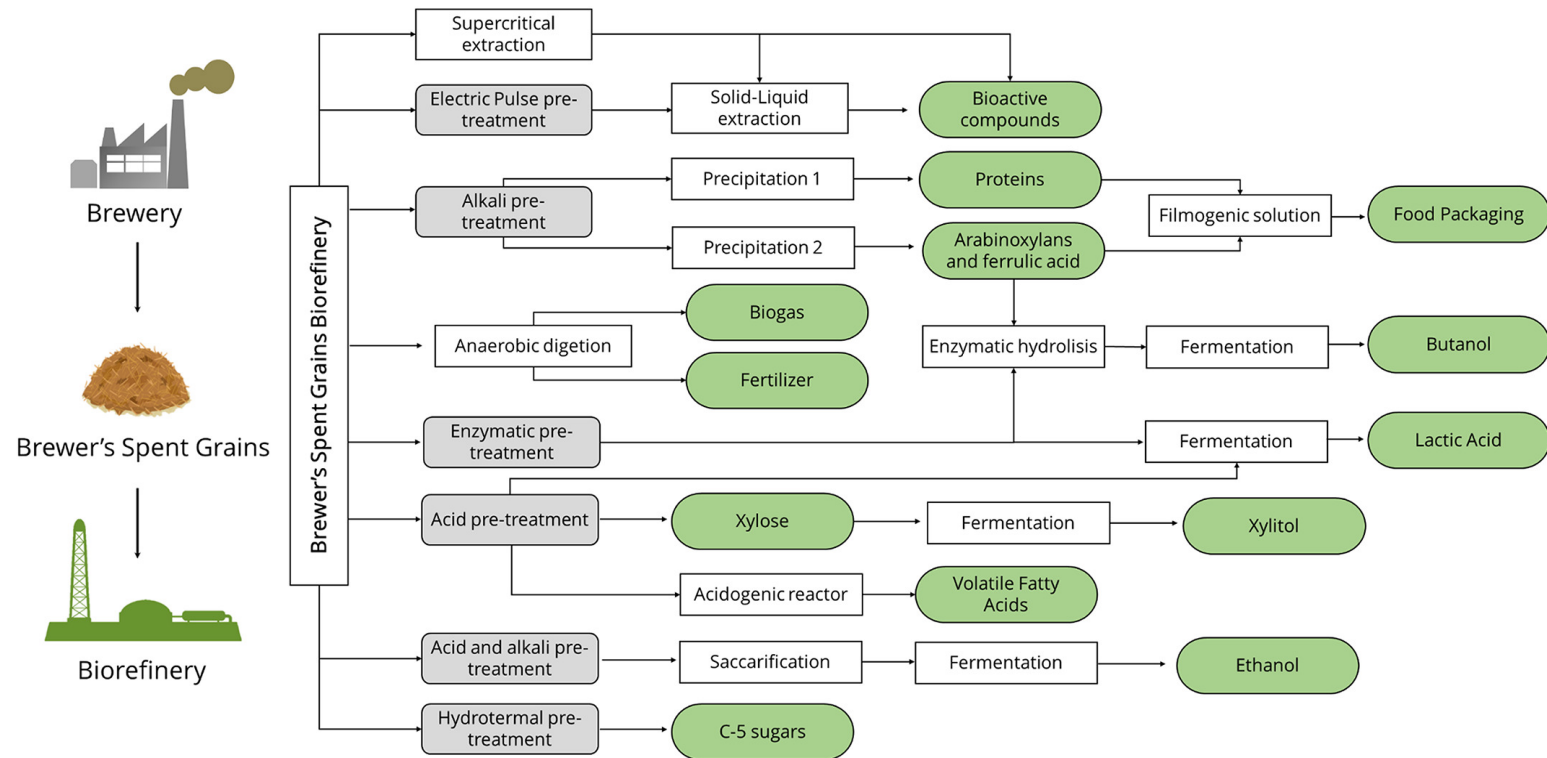


Figure I.9. The overall scheme of the technological routes for a biorefinery on the valorization of BSG and possible value-added products generated [51].

## INTRODUCTION

### *Integral valorization of brewer's spent grain by emerging technologies*

---

After the pretreatment, the cellulose fraction can be effectively converted into glucose, usually by enzymatic hydrolysis. It has been found that the lower the hemicellulose and lignin content in the sample, the higher the efficiency of cellulose hydrolysis [68]. Glucose (C6) is the sugar platform element for the generation of 5-hydroxymethylfurfural (HMF), lactic and succinic acids, and biofuels, such as bioethanol and biobutanol through various biological pathways or chemical processing [69].

Lignin is composed of a variety of aromatic units, which can be extracted to produce aromatic compounds derived from its depolymerization. However, the complex structure and low reactivity of lignin limits its further applications and currently, most of the lignin is burned for generating energy. Therefore, lignin is still considered a waste in the lignocellulosic processing industry, although high-quality lignin in abundance should be used to produce fuels or chemicals. For instance, after bioethanol production from lignocellulosic materials, the remaining solid present high content of lignin [70]. The valorization of the recovered lignin is one of the most interesting challenges in the second generation biorefineries [71].

From the BSG hemicellulose fraction, xylose and arabinose (C5) can be obtained as monomers or as oligomers. Xylose and arabinose can be also used to obtain xylitol and arabitol, respectively, after fermentation [72], [73]. Furan derivatives such as furfural, obtained from dehydration of pentoses can be used to produce more than 1600 kinds of chemical products [74]–[76]. **Figure I.10** shows the chemical structure of the sugars-derived compounds mentioned, together with some examples of furfural-derived compounds and their applications.



## INTRODUCTION

### *Integral valorization of brewer's spent grain by emerging technologies*

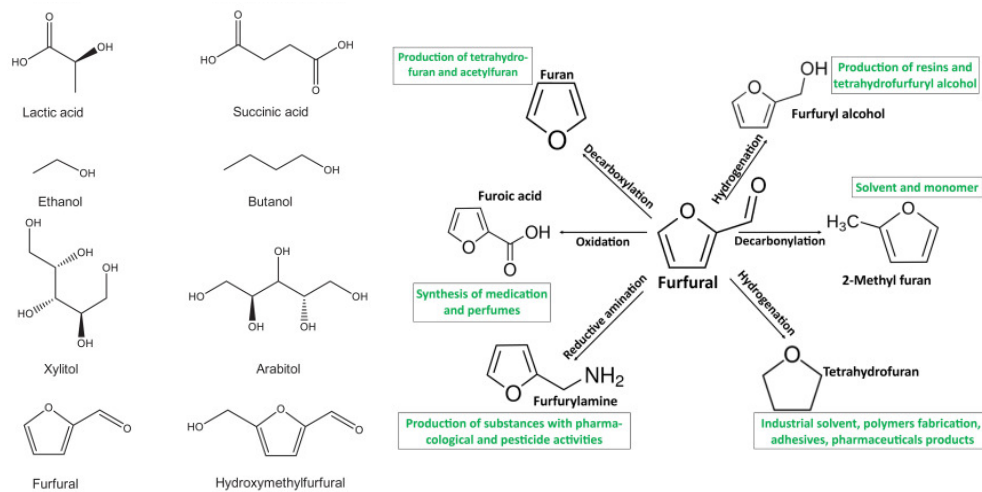


**Figure I.10.** Chemical structure of some compounds derived from C5 and C6 sugars and specific examples of furfural derivatives and their applications [69].

Likewise, oligosaccharides are gaining attention, as they can be used in the food industry as precursors of food-grade chemicals, or as energy sources in microbial fermentations [63]. Xylooligosaccharides (XOS) and arabinoxylooligosaccharides (AXOS) obtained from BSG exhibit higher prebiotic potential *in vitro* than that of fructooligosaccharides [4].

Traditionally, AX from BSG has been extracted by alkali extraction. Alternatively, Reis et al. [45] performed UAE with alkali to extract AX from BSG and achieved a yield of 60% in 25 min. In that study, conventional alkaline extraction yielded a similar AX level in 7 h.

Alternatively, the use of high-pressure fluids for biomass processing offers a great possibility to extract and valorize the different bioactive components. The use of pressurized water and supercritical CO<sub>2</sub> presents a great attraction, since they are green solvents. When exploring sc-CO<sub>2</sub> and subW treatments of biomass, the focus must be, not only on extract valorization, but also on the effect of these treatments on the remaining solid after extraction. At its supercritical conditions, CO<sub>2</sub> can penetrate into the small pores of the lignocellulosic biomass resulting in structural modifications of the biomass. Some

studies have demonstrated the ability of sc-CO<sub>2</sub> to increase the digestibility of lignocellulosic materials in subsequent enzymatic processes [77].

According to Cocero et al. [20] hydrothermal extraction at mild conditions (160–210 °C) is a promising technique for hemicellulose hydrolysis without chemical addition. During the subW pretreatment, the hemicellulose fraction is mostly hydrolyzed/solubilized. This way, the sugars present in the hemicellulose fraction are released (as oligomers and/or monomers) and also the cellulose and lignin fractions of the raw material are exposed [79]. SubW treatment of BSG has been reported in the literature as a suitable technique for selective hemicellulose solubilization from BSG, releasing mainly oligomers [72].

The use of subcritical water (subW) as an eco-friendly pretreatment to improve the conversion of cellulose into glucose from lignocellulosic biomass has been proposed in recent studies [79]–[81]. In addition, the valorization of different bioactive compounds, such as phenolic compounds, protein, and amino acids, released during the subW treatment, may improve the feasibility of the process within a biorefinery concept [40].

The use of sc-CO<sub>2</sub> and subW as emerging technologies to perform an integral valorization of the BSG will be widely described in the next sections, as the study of green emerging technologies constitutes one of the main objectives of this PhD thesis.

## 2. Supercritical Carbon Dioxide

A supercritical fluid is the state of a compound, mixture, or element above its critical temperature and pressure but below the critical pressure required to condense it into a solid [82]. Several fluids can be used as supercritical solvents, being carbon dioxide the most widely used. Supercritical carbon dioxide (sc-CO<sub>2</sub>) is considered a green solvent, as it is inert, non-toxic, and non-flammable. The carbon dioxide critical point is 304.15 K and 7.38 MPa, as can be seen in **Figure I.11**. In its supercritical region, CO<sub>2</sub> presents intermediate properties between a gas and a liquid, gas-like (high diffusivities), and liquid-like (good solvation power) properties, reason for which, sc-CO<sub>2</sub> has good solvent power and good transport properties [83]. The use of CO<sub>2</sub> as a solvent presents several advantages: it is widely available, harmless, non-flammable, and low-cost. Moreover, its moderate critical

properties allow the extraction of thermolabile compounds. Furthermore, CO<sub>2</sub> separation from the solid matrices is achieved easily by depressurization because CO<sub>2</sub> is a gas at ambient conditions.[84].

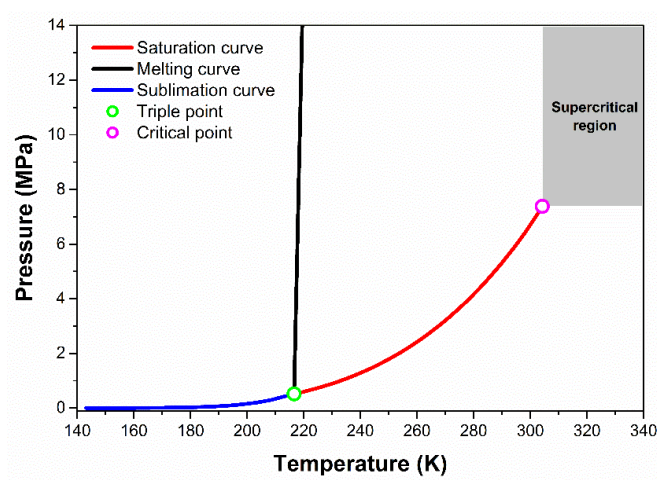


**Figure I.11.** Phase diagram of carbon dioxide illustrating the supercritical region above the critical temperature and pressure. Data taken from [85].

## 2.1. Sc-CO<sub>2</sub> treatment of BSG from a biorefinery perspective

The first stage in the BSG valorization within a biorefinery concept is the extraction of the valuable hydrophilic and lipophilic fractions of the BSG. As CO<sub>2</sub> has lower polarity than water, it is able to extract water-insoluble compounds, such as lipids. sc-CO<sub>2</sub> has been extensively studied as a green extracting agent as an alternative to traditional organic extraction solvents to valorize different biomass components [46]. Moreover, the sc-CO<sub>2</sub> extraction of BSG has been previously explored in the literature [86]–[88]. Fernández et al. [88] studied the sc-CO<sub>2</sub> extraction from conditions from milled and raw BSG (mean particle size of 0.85 mm and 3.00 mm, respectively and 58% moisture in both cases) at different temperatures (40, 60, and 80 °C) and pressures from 10 to 35 MPa, for 5 h. Considering the criterion of maximum yield (3.5 g/100 g<sub>BSG</sub>), the optimum conditions resulted to be 40 °C, 35 MPa and milled BSG. A higher amount of lipids (5.49 g/100 g<sub>dry-BSG</sub>) was reported by Kitrytė et al. [86], who studied the sc-CO<sub>2</sub> extraction at 40 °C, and 35 MPa for 70 min from dry BSG (0.2 mm particle size). Furthermore, these authors also evaluated the antioxidant

capacity of BSG sc-CO<sub>2</sub> extracts, and remaining solid, and concluded that, although the sc-CO<sub>2</sub> extracts showed an antioxidant activity of 212.36 mg Trolox equivalents per g extract, as measured in lipophilic-oxygen radical absorbance capacity (L-ORAC assay), a considerable fraction of BSG compounds with particular antioxidant capacity remained in the solid residue. Therefore, under a biorefinery concept, the solid stream generated after the sc-CO<sub>2</sub> extraction of the lipidic fraction of BSG should be also valorized, as it may constitute the feedstock of other processes to obtain valuable compounds.

In this sense, sc-CO<sub>2</sub> has been considered not only a good extraction solvent but also an agent to pretreat the biomass for subsequent enzymatic hydrolysis of the polysaccharides [77]. After sc-CO<sub>2</sub> treatment, an increase in the digestibility of lignocellulosic materials in subsequent enzymatic processes has been found in some studies [46], [77]. This fact could be attributed to different factors:

- (1) The removal of the lipid fraction could influence the susceptibility of carbohydrates to enzymes [89].
- (2) sc-CO<sub>2</sub> can penetrate into the small pores of the lignocellulosic biomass resulting in structural modifications.
- (3) CO<sub>2</sub> is quickly released during the depressurization process, promoting the disruption of the cellulose and decreasing its crystallinity. These structural changes result in a larger exposed surface area of the polymers such as glucans and xylans to the hydrolytic enzymes.

## **2.2. Parameters affecting treatment with sc-CO<sub>2</sub>**

The two main parameters affecting sc-CO<sub>2</sub> processes are temperature and pressure, since both of them affect the main properties of sc-CO<sub>2</sub>, such as density, diffusivity, viscosity, dielectric constant, etc., which in turn affect the solubility of solutes in sc-CO<sub>2</sub> and mass transfer, the two main mechanisms involved in sc-CO<sub>2</sub> processes.

Mass transfer is usually enhanced by increasing temperatures although it might be negatively influenced by too high pressures.

Regarding solutes solubility in sc-CO<sub>2</sub>, the effect of pressure is usually quite straightforward, since pressure increases the density of the solvent, which in turn increases the

## INTRODUCTION

### *Integral valorization of brewer's spent grain by emerging technologies*

---

solubility of the solutes in sc-CO<sub>2</sub>; however, the effect of temperature is some more complex since a temperature increase decreases the density of the solvent, which would cause a decreasing solubility power, but also increases the vapor pressure of the solute, which would increase its solubility in CO<sub>2</sub>. This opposite effect of temperature on solubility often causes a crossover behaviour among the isothermal solubility versus pressure curves. This variability of solutes solubility in sc-CO<sub>2</sub>, provides this solvent with an interesting tunability that allow it to behave as a good or poor solvent just by adjusting pressure and temperature [90].

This behaviour was reported in research of the use of sc-CO<sub>2</sub> for the valorization of BSG [88] when the effect of pressure (10 – 35 MPa) on the extraction yield at constant temperature (313 K) was investigated.

In addition, other parameters influence the extraction yield of objective compounds, such as particle size or flow rate. These parameters are also associated with the thermodynamics (solubility) and the kinetics of the extraction process in the specific raw matter (mass transfer resistances). The extraction rate is determined by the slowest mechanism that controls the process. If the process is controlled by an external mass transfer resistance or by equilibrium, the **flow rate** determines the extraction rate, as a higher flow rate involves a greater solvent:solute ratio. If the extraction process is controlled by internal mass transfer resistances, the particle size plays an important role since, the smaller the **particle size**, the higher the amount of compounds accessible for extraction, which would reduce the importance of diffusion compared to convection [91].

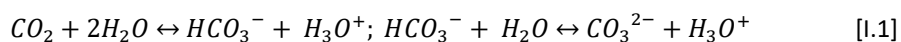
The use of optimum conditions for each variable is one of the main processing aspects, as it could significantly enhance the recovery of the target compound [90]. However, when sc-CO<sub>2</sub> treatment is proposed not only as an extraction process but also as a pretreatment technique to improve the enzymatic digestibility in subsequent enzymatic hydrolysis of the polysaccharides within a biorefinery concept, the effect of the operating conditions in the pretreated solid should be also considered.

Evaluating the use of sc-CO<sub>2</sub> as **pretreatment**, the **pressure** is in some cases a critical parameter in improving the glucose yield of further enzymatic hydrolysis. An increase in the glucose yield with increasing sc-CO<sub>2</sub> pretreatment pressure was observed in the literature for different materials, such as Avicel, recycled paper mix, and sugarcane bagasse [92] as

well as rice straw [93]. Conversely, an increase of the CO<sub>2</sub> pressure from 21.4 to 27.6 MPa did not improve the enzymatic yield of sc-CO<sub>2</sub> pretreated aspen and southern yellow pine (SYP) [94]. According to these studies, the pretreatment **temperature** appears to considerably affect the enzymatic digestibility of pretreated lignocellulose material. In this regard, a moderate increase of the glucose yield of rice straw with increasing pretreatment temperature was achieved, from 27.6% for untreated material to 29 and 32.4% for pretreated rice straw with sc-CO<sub>2</sub> at 40 and 110 °C, respectively [93]. The effect of temperature on the sc-CO<sub>2</sub> pretreatment of aspen and SYP was also noticeable, as a significant increase of reducing sugar yield from enzymatic hydrolysis of the pretreated materials was only obtained at 165 °C, being negligible at 112 and 138 °C [94]. However, the latest only observed effectiveness in the sc-CO<sub>2</sub> pretreatment when aspen and SYP contained a certain amount of **moisture** before the pretreatment. When the initial moisture content of lignocellulose was 73% (w/w), the sugar yields from the enzymatic hydrolysis of aspen and southern yellow pine pretreated with sc-CO<sub>2</sub> at 21.37 MPa and 165 °C for 30 min were 84.7 and 27.3%, respectively. Similarly, Narayanaswamy et al. [95] observed that when using pretreated wet corn stover (humidity content of 75%) with sc-CO<sub>2</sub> at 240 bar, 120 °C for 60 min, they obtained double glucose yield than the obtained from pretreated dry raw material at the same conditions.

The presence of water in sc-CO<sub>2</sub> pretreatments can exert a double effect [92], [77].

- (1) The carbonic acid formed when carbon dioxide is dissolved in water and dissociated in two stages according to Equation I.1, causes a similar effect as dilute-acid hydrolysis.



- (2) Water facilitates a swelling effect on biomass.

However, if water is co-extracted with biomass oil, the extraction would be not so efficient. According to Alonso [60], the water content in the matrix must be reduced before the extraction process by sc-CO<sub>2</sub> as it interferes in the vitamin and oil extraction yields of wheat bran, reaching its maximums when the moisture content in the matrix was below 3%. In addition, water coextraction led to milky droplets in the oil when the initial moisture

content in cooked and preheated canola samples was higher than 12% and the cloudiness of the extracts obtained could be correlated with moisture loss from feed material [96].

In any case, the **composition of the feedstock** influences the enzymatic digestibility of a given biomass, as the recalcitrant structure of the biomass is influenced by inherent properties, such as the lignin content, the cellulose crystallinity and degree of polymerization, and the cellulose accessibility to enzymes due to the sheathing of cellulose by hemicellulose and lignin [77].

### 3. Subcritical water extraction/hydrolysis

The use of subcritical water is an alternative technology to traditional methods for dissolution/hydrolysis of biomass, being a low-cost and environmentally friendly process, as no chemicals are involved.

The use of water under subcritical conditions is also known in the literature as hydrothermal treatment. The use of subW at moderate temperatures (140 – 250 °C) is often called Pressurized Hot Water (PHW) or Hot Compressed Water (HCW) [60]. Moreover, when subW is used as pretreatment of lignocellulosic material is usually named autohydrolysis pretreatment. Throughout this PhD thesis, the term subcritical water (subW) will be used to refer to pressurized hot water in the temperature range from 100 °C to 374 °C. The terms subW treatment, hydrothermal treatment, and autohydrolysis pretreatment will be also used to refer to the use of pressurized hot water at subW temperatures and at a pressure enough to keep water in its liquid state. The water phase diagram can be seen in **Figure I.12**.

As mentioned in Section 1, subcritical water extraction/hydrolysis has been employed in the literature to achieve successful recovery of different high-value biocompounds from lignocellulosic materials such as phenolic compounds with antioxidant capacity, proteins, and amino acids. This technique has been also employed to hydrolyze the hemicellulose fraction of different lignocellulosic biomass releasing oligosaccharides and monosaccharides. In addition, hydrothermal pretreatment has been shown to be effective in improving the enzymatic digestibility of the cellulose fraction remaining after hemicellulose solubilization.

In this section, the fundamentals of the extraction and fractionation with subcritical water are described considering both, the variation of the physical and chemical properties of water with temperature under subcritical conditions, and the parameters affecting the extraction/hydrolysis of the main components of lignocellulosic biomass, in order to select the operating conditions to incorporate the subcritical water technology in a biorefinery based on lignocellulosic biomass.

### 3.1. Physical and chemical properties of subcritical water

Water is the greenest of all solvents according to the principles of green chemistry. SubW is pressurized water in the temperature range from 100 °C (boiling point) to 374 °C (critical point) at a pressure high enough to maintain its liquid state and under subcritical conditions (critical point: 373 °C and 22.1 MPa) (**Figure I.12**).

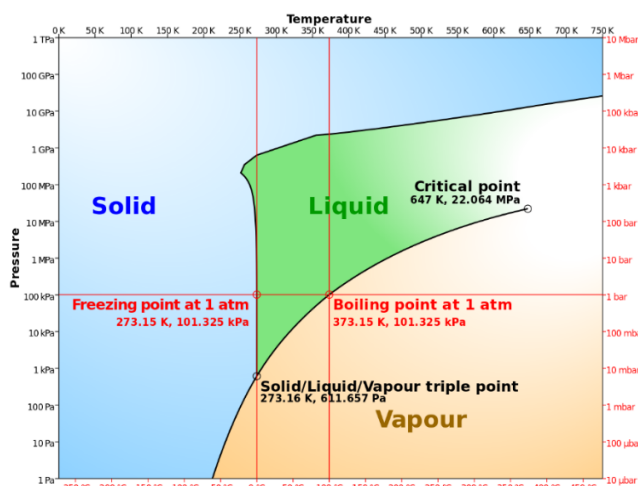


**Figure I.12.** Water phase diagram. Adapted from [97]

The physical properties of water, including its dielectric constant, density, and ionic product, can be modified by varying temperature and pressure [20]. Under subcritical conditions, the physical and chemical properties of water as a solvent are modified and provide water with unique properties as a solvent, such as high diffusivity, low viscosity, low surface tension, and higher polarizability [98].



**Figure I.13** shows the variation of the water properties with temperature at 25 MPa. Water density, and dielectric constant ( $\epsilon$ ) of water decrease with increasing temperature in its subcritical region, while pKw decreases with increasing temperature up to 250 °C.

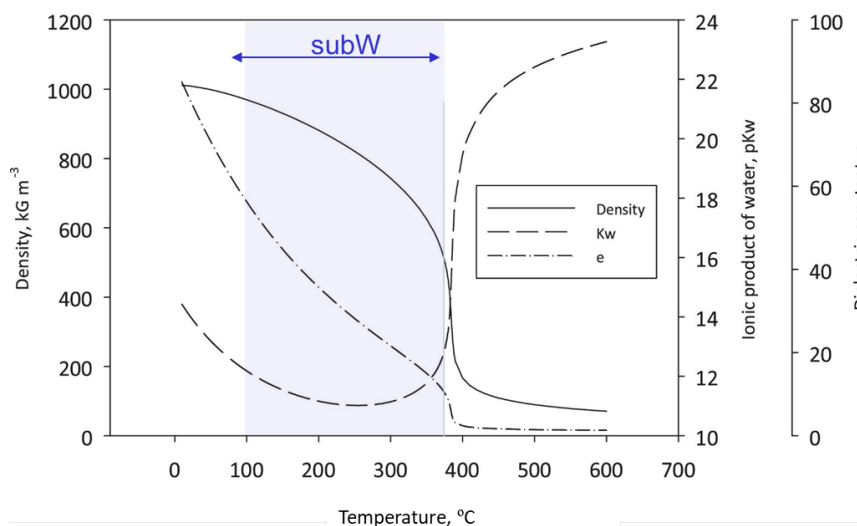


**Figure I.13.** Properties of subcritical water (shaded region) and supercritical water as a function of temperature at 25 MPa. Adapted from [20].

Water is a polar solvent at ambient temperature with a relatively high **dielectric constant** at 20 °C ( $\epsilon = 80.103$ ) [99], although it can acquire similar values to organic solvents because of dielectric constant modulation with temperature, such as methanol ( $\epsilon = 32.6$ ), ethanol ( $\epsilon = 24.3$ ) and acetone ( $\epsilon = 20.7$ ) at ambient temperature, making water an effective solvent for extraction of polar and non-polar organic compounds [100], [101].

When temperature increases under subW conditions, the **ionization constant** gradually increases (pKw decreases). The hydrogen bonds of subW gradually weaken with temperature, producing more acidic hydronium ions ( $\text{H}_3\text{O}^+$ ) and alkaline hydroxide ions ( $\text{OH}^-$ ) [20]. The dissociation constant of water ( $K_w$ ) at ambient conditions is  $10^{-14}$  and increases with temperature, reaching a maximum value of  $4.9 \times 10^{-12}$  at 250 °C. As a consequence, the pH changes from around 7.0 to 5.5, promoting hydrolysis reactions, and the catalytic effect of hydronium ions [97]. **Figure I.14a** shows this pH changes in the subW region.

Furthermore, the mass-transfer properties in liquid water such as viscosity, diffusivity, and surface tension also change with the temperature of water [97]. **Figure I.14b** shows the variation of the mass-transfer properties of water with temperature. Water viscosity and surface tension decrease with temperature, while water self-diffusivity increase with increasing temperature. Therefore, subW enables faster mass transfer and enhanced wetting of the sample due to the higher diffusivity and lower viscosity and surface tension of water at subW conditions than at ambient conditions [97].

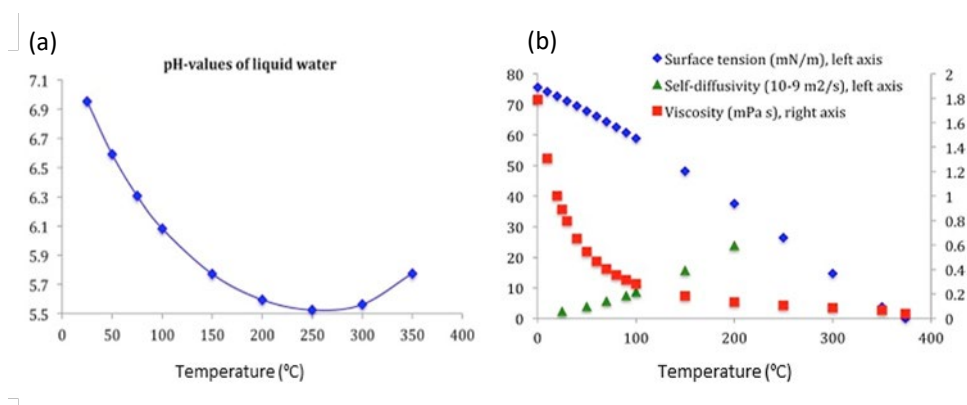


**Figure I.14.** Properties of water as a function of temperature, **(a)** pH values at 25 MPa, **(b)** Mass mass-transfer properties: viscosity, self-diffusivity, and surface tension of liquid water, at saturation pressure [97].

### 3.2. Operational modes in subcritical water

In subcritical water treatment, three different operational modes have been widely used, depending on the direction of the water and biomass flow into the reactor: static or discontinuous, dynamic or continuous, and static-dynamic or semicontinuous mode.

In static or discontinuous mode, a certain amount of biomass is loaded into the reactor (batch reactor) with a determined volume of water, while in dynamic or continuous mode water and a biomass suspension are continuously pumped through the reactor. Static-dynamic or semicontinuous mode is a combination of the other two modes. In this case, the solid remains in the reactor during the extraction process while water is

continuously pumped to the reactor. **Figure I.15** shows a diagram of the different operational modes in subW systems.

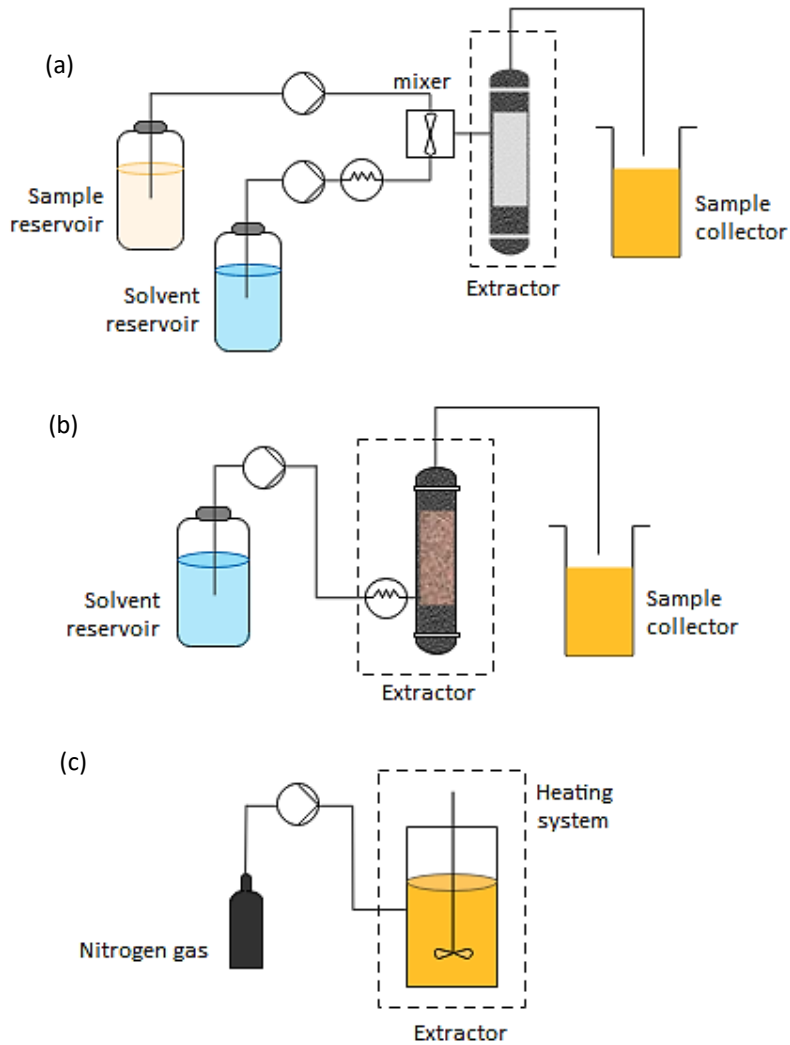


**Figure I.15.** Different operational modes in subcritical water extraction systems.

(a) continuous (dynamic), (b) semicontinuous (static-dynamic), (c) discontinuous mode (static).

In discontinuous mode, the treatment time is the same for the liquid and the solid, while in continuous, and semicontinuous modes the residence time ( $\tau$ ) for the liquid in the reactor is determined by the volume of the reactor and the flow rate according to

Equation 1.2, while the treatment time for the solid is the time that the solid is being treated with the liquid into the reactor [20].

$$\tau = \frac{V}{F_v} = \frac{V}{F_{v,o}} \frac{\rho_r}{\rho_o} \quad [1.2]$$

where  $V$  is the reactor volume in  $\text{m}^3$ ,  $F_{v,o}$  the flow rate measured at ambient conditions, in  $\text{m}^3/\text{s}$ ,  $\rho_o$  is the water density at ambient conditions and  $\rho_r$  the water density at the reaction conditions.

In discontinuous mode, the different solutes are hydrolysed/extracted along time until equilibrium is reached under the conditions established. In continuous or semicontinuous mode, the equilibrium is continuously displaced because fresh water is renewed continuously, which stimulates mass transfer of the analytes from the matrix to the aqueous medium [102]. As consequence, the continuous and semicontinuous modes are usually faster than the discontinuous mode. However, a larger amount of water is often used in the continuous and semicontinuous modes, which results in the dilution of target compounds [101].

The principal advantage of discontinuous mode is that the dilution of the analytes is avoided, but decomposition reactions, due to the long exposure time of the sample to water, may occur at high temperature [101]. On the other hand, in continuous and semicontinuous modes, the solute is pumped out of the reactor once it is dissolved, thus, it is exposed to the high temperatures a shorter time than in discontinuous mode; and as a consequence, thermal degradation is reduced [60].

### **3.3. Valorization of BSG by hydrothermal treatment**

#### **3.3.1. Lignocellulose fractionation by subcritical water treatment**

Subcritical water treatment at mild conditions (160 – 210 °C) is a promising technique for selective hemicellulose hydrolysis [51], [72], [103]–[107]. Hemicellulose, being an amorph heteropolymer, is more susceptible to hydrothermal extraction and hydrolysis under mild temperatures than crystalline cellulose. According to Bobleter [17], hemicellulose is easily dissolved in water at temperatures of about 180 °C. This fact allows

selective depolymerization and solubilization of the hemicellulosic fraction, while cellulose and acid-insoluble lignin remain in the solid fraction [108]. After subW pretreatment of the biomass, the products can be separated into solid and liquid fractions. Due to the hydrolysis and solubilization of hemicellulose and other compounds by subW treatment, the percentage of cellulose and lignin in the solid fraction increase, and the cellulose becomes more available to be converted into glucose monomers [79]–[81]. Therefore, the pretreated solid can be subjected to further processing for cellulose conversion into glucose by enzymatic hydrolysis leading to a lignin-rich remaining solid, which also addresses the opportunity of a further lignin valorization. As an example, **Figure I.16.** shows a biorefinery approach proposed by Ruiz et al. [107], where lignocellulosic biomass is milled and treated with subW, leading to a liquid stream with fermentable sugars, oligomers, and furans, while the solid stream contains cellulose and lignin. Then, the remaining solid is subjected to enzymatic hydrolysis to obtain fermentable sugars, mainly glucose from the cellulose fraction.

The subW liquid fraction mainly contains dissolved hemicelluloses as well as bioactive compounds such as phenolic compounds, protein/peptides, and a minor amount of free amino acids, besides sugar degradation products. If subW technology is used as lignocellulosic pretreatment to produce fermentable sugars, particular attention must be paid to the formation of fermentation inhibitors. Those include acetic acid, furfural, and HMF, as well as phenolic compounds. On the other hand, the degradation products can be also the target compounds. Considering all of the above, the operating conditions should be chosen focusing on the target compound/effect:

- Hemicellulosic oligosaccharides, which have important applications in the pharmaceutical and food industries as described previously.
- Monomeric sugars, mainly formed by arabinose and xylose to be used as platform compounds for chemicals and fuels.
- Degradation products such as furfural to be converted into chemicals.
- To enhance the digestibility of the pretreated solids for a further cellulose conversion into glucose units.

## INTRODUCTION

### *Integral valorization of brewer's spent grain by emerging technologies*

---

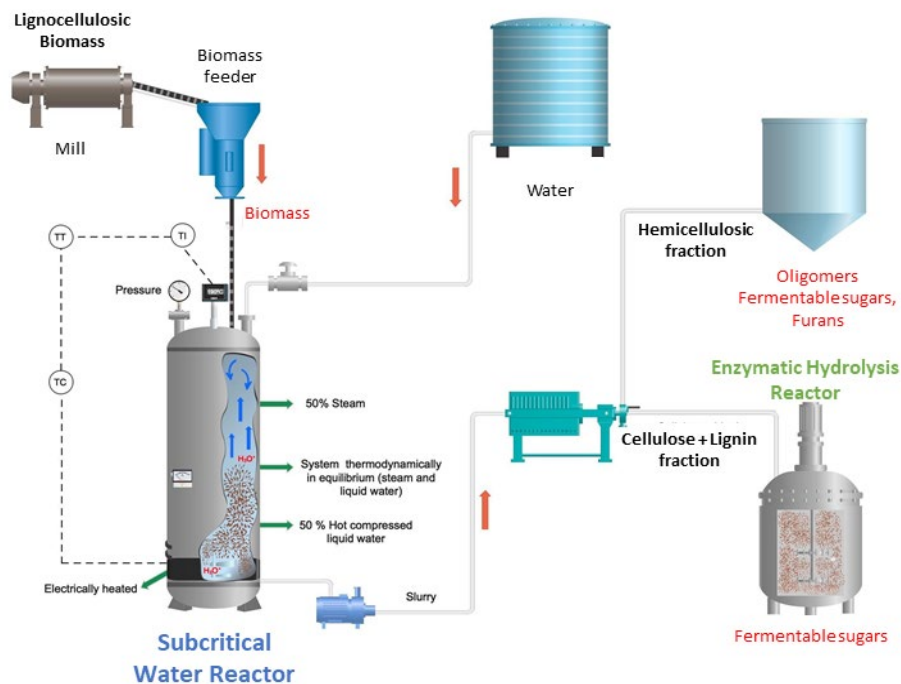


**Figure I.16.** Flowsheet of a biorefinery for lignocellulosic biomass fractionation using subcritical water reactor. Adapted from [107].

Hemicellulose hydrothermal fractionation comprises numerous physical phenomena such as hemicellulose cleaving into decreasing molecular weight oligomers, hemicellulose deacetylation, hemicelluloses dissolution, and mass transfer between the solid and the liquid, production of sugars and sugars degradation into furfural or other compounds, as well as porosity changes in the solid matrix: extraction, swelling and biomass compaction [20]. Thus, a clearer understanding of this phenomena is the key to selecting subW operating conditions and achieving the desired treatment effects.

Under subcritical conditions, water can act as a catalytic agent due to the weak acid properties of water at elevated temperatures. As described above, an increase in the subW temperature promotes hydrolysis reactions by the catalytic effect of hydronium ions generated in situ by water ionization. The hydronium ions generated lead to the release of the acetyl groups from hemicelluloses, producing acetic acid. Then, the resulting acetic acid molecules cause cleavage of hemicellulosic glycosidic bonds and reduce their degree of

polymerization to enhance hemicelluloses solubilization [20]. Along this reaction, high-molecular weight hemicellulosic polymers are progressively broken down into smaller molecules until reaching a length low enough to be extracted from the solid by solubilization or dragging [20], [38], [109]. Longer reaction times and higher temperatures lead to higher xylan solubilization from the solid phase, and higher fragmentation of the polymeric and oligomeric xylan-derived compounds already present in the liquid phase [103]. Then, monosaccharides are released, and the sugar-dehydration reactions arise, particularly, the formation of furfural from pentoses and 5-hydroxymethylfurfural from hexoses. Levulinic acid can also be generated from the dehydration of HMF. A simplified scheme of these reactions is shown in **Figure I.17**. It should be noted that low-molecular weight xylooligosaccharides can also produce furfural [110].

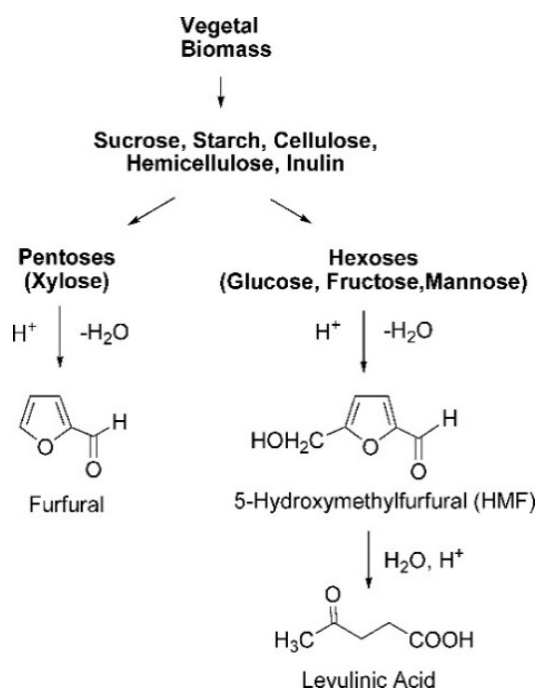


**Figure I.17.** Products obtained by dehydration of monosaccharides under subW.

As this technique does not use any added reagents, it is known as autohydrolysis or autocatalytic hydrothermal treatment. Furthermore, the decrease of viscosity of subW with temperature enhances its fluidity, providing a higher mass transfer than water at ambient conditions and promoting hemicellulose hydrolysis and solubilization.

## INTRODUCTION

### *Integral valorization of brewer's spent grain by emerging technologies*

---

Temperature and reaction time are the most important parameters to be optimized when dealing with subW. The combined effect of temperature and reaction time during hydrothermal processes can be considered in a single parameter, the severity factor ( $R_o$ ). The severity factor was proposed by Overend and Chornet [111] to predict the solubilization of xylan in hydrothermal processes.

$$R_o = t \cdot \exp\left(\frac{T-100}{14.75}\right) \quad [1.2.]$$

where  $R_o$  is the severity factor,  $t$  is the treatment time (min),  $T$  is the operating temperature (°C),  $T_{ref}$  is 100 °C since under this temperature practically no depolymerization of the hemicellulose takes place, and the value 14.75 is a typical activation energy for glycosidic bond cleavage of carbohydrates under hydrothermal treatment assuming conversion is first order.

In batch reactors, the time needed to reach the desired temperature (heating time) and the time spent to decrease the temperature inside the reactor after the fixed reaction time is finished (cooling time), can influence the results. This periods (no-isothermal stages) has been represented in **Figure I.18**. The severity factor can be modified to incorporate the effect of non-isothermal stages by integrating the temperature vs time profile at heating, isothermal, and cooling periods [107], [112], according to Equation [1.3]. These periods should be taken into consideration to study the effect of the severity factor in the extraction/hydrolysis of target compounds but, especially, when performing studies to scaling-up processes [106].

$$\begin{aligned} R_o &= R_{o,Heating} + R_{o,Isothermal} + R_{o,Cooling} \\ &= \int_{t_0}^{t_H} \exp\left(\frac{T(t)-100}{14.75}\right) \cdot dt + t \cdot \exp\left(\frac{T-100}{14.75}\right) + \int_{t_F}^{t_C} \exp\left(\frac{T(t)-100}{14.75}\right) \cdot dt \end{aligned} \quad [1.3]$$

where  $T(t)$  is a function of the temperature vs time,  $t_0-t_H$  is the time range to reach the work temperature ( $T$ ),  $t$  is the isothermal time and  $t_F-t_C$  is the time range to decrease temperature from  $T$  to 100 °C after the isothermal period.



## INTRODUCTION

### *Integral valorization of brewer's spent grain by emerging technologies*

---

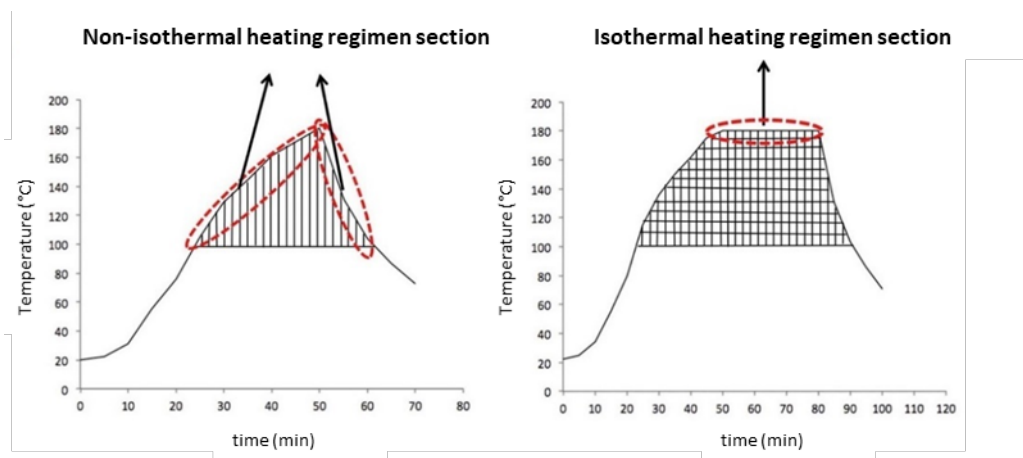


**Figure I.18.** Diagram representing non-isothermal and isothermal regimes in hydrothermal treatments [107].

Higher temperatures and reaction times, usually lead to higher hemicellulose release, but also higher degradation and decomposition reactions occur when the temperature is too high [20]. Moreover, the combination of time and temperature exerts a powerful effect upon the selectivity of the subW process to produce oligomers or monomers from hemicelluloses hydrolysis. For instance, Wang et al. [112] found that temperatures between 175 to 190 °C and times from 15 to 60 min enhanced the production of oligosaccharides during the hydrothermal treatment of rapeseed straw, while longer treatment times (60–120 min) and lower temperature (160–175 °C) resulted in higher yields of monosaccharides. These authors obtained the highest oligosaccharide content (99.94 g/kg<sub>raw material</sub>) at 190 °C for 15 min and the maximum monosaccharide content (30.43 g/kg<sub>raw material</sub>) at 170 °C for 120 min. Carvalho et al. [72] studied the use of subW to produce XOS from BSG at different temperatures (150 – 190 °C), obtaining the maximal XOS yield (61%) at 190 °C after 5 min of reaction. The molecular weight distribution of the oligosaccharide mixtures obtained in this study varied with both, temperature, and reaction time. In general, high molecular weight oligomers were obtained at a high temperature for a short reaction time.

It should be considered that extracted oligomers with a high degree of polymerization may precipitate after cooling. In this sense, Gray et al. [113] found that, although the solubility of the polymers extracted was not a limiting factor in the conditions studied (18%

## INTRODUCTION

### *Integral valorization of brewer's spent grain by emerging technologies*

---

solids at 180 °C), the higher degree of polymerization oligomers precipitate when subW hydrolysates from birchwood and oat spelt xylan were cooled from 80 to 26 °C. Therefore, when subW is performed in batch mode, and the hydrolysates are separated from the solid after cooling down the reactor below 80 °C, as it is typically reported, the oligomer yields from xylan hydrolysis could be underestimated.

Particle size has also an important effect on the subW process. Smaller particle sizes increase the contact area between the sample matrix and the subW, so reducing extraction time and increasing extraction efficiency [32]. The particle size has also an influence on the degree of polymerization of the xylan-derivates. Smaller particle sizes produce higher molecular weights polymers/oligomers as the rate of extraction is higher. On the other hand, subW penetrates into the matrix of higher particle size enhancing the hydrolysis of the hemicellulose [20].

To sum up, reaction time and temperature are the key factors affecting the effectiveness and selectivity of subW treatments [20]. The yield of polymers, oligomers, monomers, and degradation products as a function of time/temperature in subW treatments, expected from the previous discussion, is shown in **Figure I.19**. This behaviour has been discussed for subW hydrolysis of hemicelluloses, but it is also applicable to the protein fraction, as will be briefly commented later.

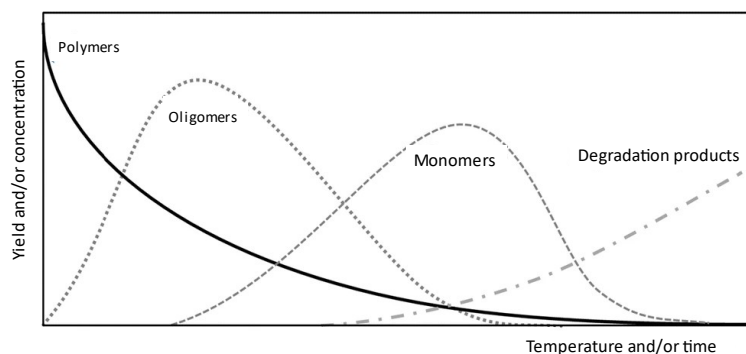


**Figure I.19.** Simplified scheme illustrating the effect of time and/or temperature on the yield of oligomers, monomers, and degradation products by depolymerization of the target fractions [70].

Regarding **cellulose**, most of it remains in the solid stream after subW treatment at the temperature generally used to release hemicelluloses, below 200 °C [60]. At higher temperature, cellulose becomes soluble in water, as the energy provided is enough to break the hydrogen bonds that keep the crystalline structure of the molecule [18]. Cellulose conversion in supercritical water has been proposed by Sasaki et al. [114]. These authors performed experiments in a flow type reactor, specially designed to achieve a very rapid heating of the cellulose slurry by mixing it with a preheated water stream. The results show that the hydrolysis rate of cellulose and the hydrolysis products change dramatically with temperature. Residence time and temperature were the most important parameters affecting the yield and selectivity of the process. These authors proposed that, below 350 °C, oligomers and monomers decomposition rate is faster than the hydrolysis rate of cellulose. In contrast, cellulose hydrolysis is faster than decomposition of the hydrolysis products at higher temperatures, 400 °C, and very short residence times (50 ms). Under these conditions, nearly 100% of cellulose conversion was achieved, obtaining mainly hydrolysis products. This fact was associated with the transformation of the cellulose structure from crystalline to amorphous under the conditions studied.

As amorphous and semi-crystalline zones are easier to be hydrolyzed than crystalline regions, the behaviour of the cellulosic fraction of different biomasses considerably depends on their chemical and physical properties (crystallinity). Moreover, milling produces an amorphous structure in cellulose by cleavage of the hydrogen bonds thus generating amorphous zones that facilitates the action of water [20].

Unlike cellulose, starch is semi-crystalline at ambient temperature and undergoes crystalline-to-amorphous transformation when it is heated in water to 60–70 °C (gelatinization). Deguchi et al. [115] compared the behaviour of cellulose and starch in water at high temperatures and high pressures by in situ high-resolution optical microscopy. The results can be seen in **Figure 1.20**. They found that the starch granules swelled considerably from 80 to 90 °C and the texture of the starch granules gradually became weaker with increasing temperature, being completely lost at 200 °C. On the other hand, the crystalline structure of cellulose is retained up to 320 °C. From 320 to 330 °C the increase of the transparency of crystalline cellulose was related to crystalline-to-amorphous transformation. Cellulose fibres were completely broken at 340 °C.

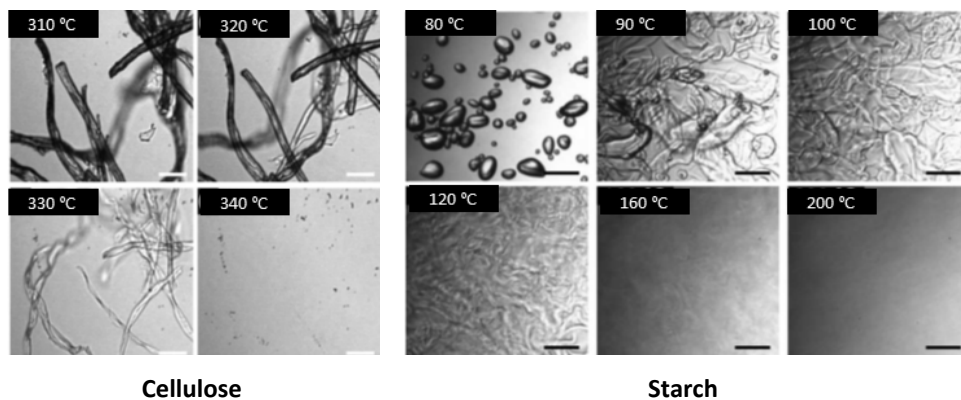


**Figure I.20.** Behaviour of cellulose and starch in water with temperature at 25 MPa. In situ optical microscopic images [115].

On the other hand,  $\beta$ -glucans has been effectively recovered from waxy barley by subW at 155 °C, in a fixed-bed reactor, obtaining high extraction yield (53.7%) and high molecular weight oligomers (200 kDa), without formation of degradation products such as HMF [116].

### 3.3.2. SubW extraction of phenolic compounds from BSG

Subcritical water has been widely used for the extraction of phenolic compounds from different biomasses [57], [66], [117], [118]. As mentioned in Section 1, phenolic acids are bounded to the lignocellulosic matrix by ester and ether linkages, being necessary a hydrolytic method to release them from the lignocellulosic biomass. They are bounded with lignin through their hydroxyl groups in the aromatic ring by ether linkages and with structural carbohydrates and proteins through their carboxylic group by ester linkages. Due to the properties of subW described above, subW is appropriate for hydrolysis reactions. Since ester linkages are labile at 170 °C, working with subW at temperatures above 170 °C allows the release of phenolic acids from the lignocellulosic matrix. **Figure I.21.** represents the release of ferulic acid from a typical lignin/phenolics-carbohydrate complex using subW.

## INTRODUCTION

### *Integral valorization of brewer's spent grain by emerging technologies*

---

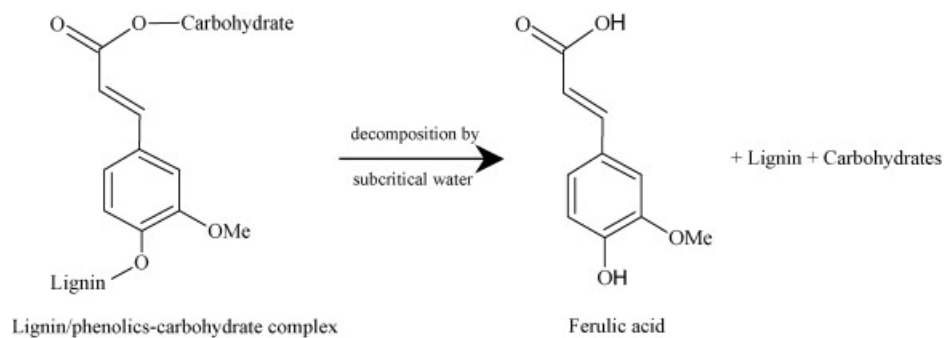


**Figure I.21.** Proposed hydrothermal degradation of a typical lignin/phenolics-carbohydrate complex under subcritical water conditions [66].

From the physical and chemical properties of water at high temperatures under subcritical conditions, it can be assumed that the higher the temperature, the higher the extraction and hydrolysis ability of subW. As described above, with the increase of temperature, subW dielectric constant, viscosity, and surface tension gradually decrease, and its diffusion coefficient is improved. The increase of the ionic product of water with temperature improves the subW ability for promoting hydrolysis reactions. However, under certain temperatures and reaction times, phenolic compounds may undergo degradation.

Pourali et al. [66] examined the effect of the subW temperature (100 – 360 °C) on the release and decomposition of individual phenolic compounds from rice bran in a batch stainless steel reactor. These authors found that the total phenolic content and antioxidant activity increased with temperature, while different optimum temperatures were obtained for each compound. Among the phenolic compounds identified, vanillin and p-coumaric showed a peak at lower temperatures (< 200 °C). On the other hand, Doctor et al.[119] found that vanillin was stable under subW conditions at temperatures up to 200 °C.

Fabian et al. [117] suggest that, at temperatures above 175 °C, phenolic acids may be damaged, or they may be involved in Maillard reactions. In their study of the release of phenolic acids from defatted rice bran by subW treatment at different temperatures (125 – 200 °C), they found that the amount of ferulic and p-coumaric acids extracted decreased from 175 °C. These authors also examined the thermal degradation of phenolic acids and found that decomposition of ferulic and coumaric acids started at about 172 °C.

Kawamura et al. [120] reported that the subW extraction yield of p-coumaric and ferulic acids from oil palm biomass reached a maximum at 160 °C and decreased at 180 °C and 200 °C, respectively; while gallic acid concentration declined from 100°C and completely disappeared at 180 °C.

Therefore, selecting the appropriate subW conditions is key to maximize the recovery of phenolic compounds.

### 3.3.3. Protein extraction/hydrolysis by subcritical water treatment

Subcritical water treatment may improve the protein yield when comparing with traditional methods. On the one hand, the dielectric constant of water decreases with increasing temperature, thus the polarity of subW decreases and becomes similar to methanol and ethanol at ambient conditions [100], [101], making subW an effective solvent for extraction of the protein fraction insoluble at ambient conditions (e.g., alcohol soluble proteins). On the other hand, the high levels of hydronium ( $\text{H}_3\text{O}^+$ ) and hydroxide ( $\text{OH}^-$ ) ions derived from autoionization of water under subW conditions, together with the presence of acids released mainly from the hemicellulose fraction, promotes peptide bond hydrolysis. At these conditions, the protein fraction would be probably hydrolyzed into valuable peptides and free amino acids [56], [121]–[123]. **Figure I.22** represents the hydrolysis of the peptide bond in water catalysed by hydronium ions. Furthermore, the low viscosity and high diffusivity of subW facilitate water to diffuse into the matrix [124].

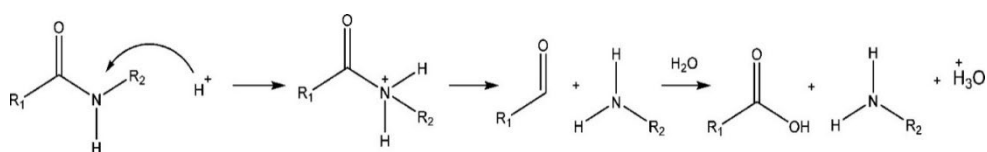


**Figure I.22.** Hydrolysis of the peptide bond in water

Hydrothermal treatments have been employed for a successful protein recovery from different materials. For instance, Lamp et al. [125] reported a protein yield as high as 75% from the insoluble fraction of bioethanol stillage with subW at 170 °C and 20 min. Sereewatthanawut et al. [56] studied the effect of temperature on the extraction of protein from deoiled rice bran between 100 and 220 °C, extracting almost 100% of the protein

## INTRODUCTION

### *Integral valorization of brewer's spent grain by emerging technologies*

---

present in the original bran at 200 °C. Trigueros et al. [124] achieved 70% recovery of the protein fraction from an industrial seaweed waste by subW treatment in a fix-bed reactor. In this study several experiments were performed at different temperatures (129 – 200 °C) and flow rates (2 and 6 mL min<sup>-1</sup>) for a total treatment time of 240 min. The best operating conditions in that work resulted to be 200 °C and 6 mL min<sup>-1</sup>, obtaining extracts with high antioxidant activity containing also free amino acids. However, it was found that when working at constant flow rate of 2 mL min<sup>-1</sup>, a maximum in the protein extraction was achieved at 185 °C and higher temperatures led to degradation of protein or its hydrolysis products due to high residence times.

On the other hand, the use of subW to release the protein fraction of BSG was shown as a noneffective treatment in a study found in the literature [53]. In that study a low protein extraction yield of 6.7% was obtained from BSG by subW treatment at 200 °C (F = 6 mL min<sup>-1</sup>), but only 20 min of extraction time was reported. The authors concluded that time is a crucial factor to obtain high protein extraction yields.

Besides reaction time, temperature is also a key parameter affecting the protein extraction/hydrolysis in subW treatment. A temperature increase, associated to a decrease in the subW polarity, could lead to an increase in protein solubility. Moreover, the activity energies of hydrolysis vary between different peptide bonds and some of them require elevated temperatures to be broken [125].

However, some compounds start degradation and decomposition reactions when temperature is too high and/or longer reaction times are used [126]. The primary mechanisms of degradation of the amino acids in subW are decarboxylation and deamination [127]. Rogalinski et al. [128] studied the production and decomposition of amino acids from bovine serum albumin (BSA) by continuous subW. The main degradation products of BSA found were carboxylic acids such as acetic acid, propionic acid, n-butyric acid, isobutyric acid and isovaleric acid, with only two nitrogen containing compounds, ethanolamine and the non-proteinogenic amino acid ornithine.

In addition, above 160 °C, amino acids can react by nucleophilic addition with the carbonyl groups of released sugars and be involved in Maillard reactions [125].

Therefore, the effect of temperature and reaction time in subW extraction/hydrolysis must be studied for target components, although it is no easy as there are several aspects to be considered.

- A high dependence on the protein source. Higher temperatures and/or longer reaction times are required to hydrolyze proteins from animal wastes than from vegetable wastes [121]. Furthermore, biomass is often generated as by-products of industrial processes. Therefore, the effect of the raw material treatment on the structure of the resulting biomass must be considered.
- Different behaviour of polar and non-polar amino acids. The constant rate of degradation for the polar amino acids was about one order of magnitude higher than for the non-polar amino acids [125].
- Thermal stability varies between different amino acids. Serine and aspartic and glutamic acids have been reported as some of the most temperature-sensitive amino acids [129].
- The trend to be involved in Maillard reactions is different for each amino acid. All polar amino acid side groups are reported to be involved in Maillard reactions. Among them, lysine has a high tendency to be involved in these reactions [125].

#### 4. Detoxification of the subcritical water hydrolysates

When processing lignocellulosic materials with high protein content, like BSG, by subcritical water treatment, it is expected to obtain hydrolysates with high protein and sugar content, mainly pentoses released as monomers and as oligomers, from the hydrolysis of the hemicellulose, besides other bioactive compounds, such as amino acids and phenolic compounds with high antioxidant capacity.

However, using subcritical water at high temperatures or during high reaction times lead to the degradation of these sugars. As an example, **Figure I.23** shows a scheme of the degradation of xylose in pressurized water, where furfural, as pentose dehydration product, and hydrolysis products, such as various organic acids can be formed.



INTRODUCTION

Integral valorization of brewer's spent grain by emerging technologies

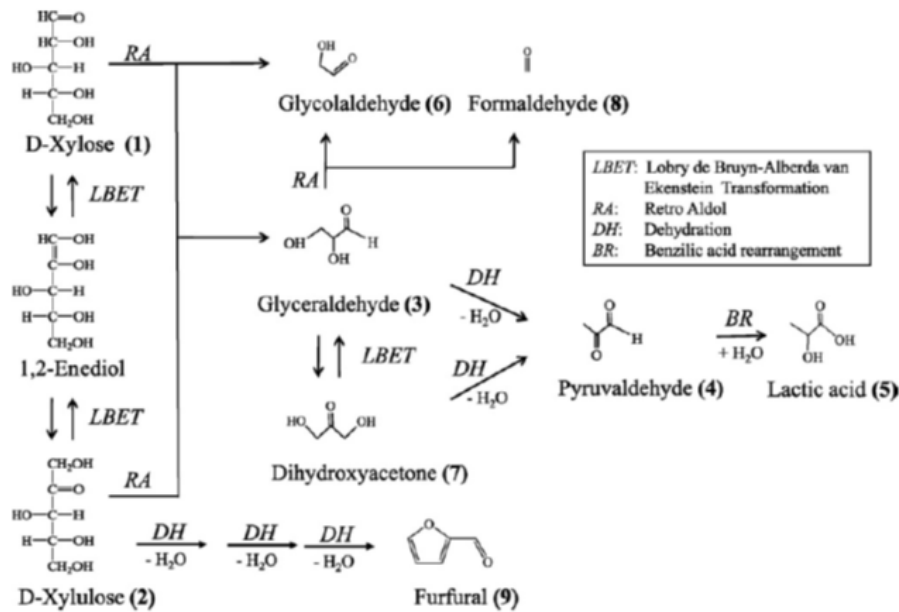


Figure I.23. Xylose degradation pathways in pressurized water at high temperature [47].

These hydrolysates, as mentioned above, may have protein and sugar content, hydrolyzed monomeric products from the partial hydrolysis of the polysaccharides of the raw material, so that, they have good characteristics to be used as fermentation broths. However, the mentioned degradation products may inhibit the fermentation process. The relative toxicity of the mayor types of fermentation inhibitors that could be formed by the subW hydrolysis of hemicelluloses are furfural > HMF > acetic acid [130]. According to Klinke et al. [131] the maximum tolerable concentration for ethanol fermentation of each compound is 3g/L of acetic acid, less than 0.25 g/L of furfural, and about 0.25 g/L of HMF.

The formation of acetic acid is unavoidable during the hemicellulose hydrolysis due to the release of the acetyl groups present in this fraction. The generation of HMF comes from hexoses and, as has been reviewed, BSG hemicelluloses are mainly composed of pentoses (xylose and arabinose) and cellulose is not hydrolyzed under subW at mild temperatures (~180 °C). Therefore, the most important inhibitor expected to be generated during subW processing of BSG is furfural, which is also the strongest inhibitor of ethanol fermentation.

Furthermore, the use of furfural to produce chemicals and fuels has gained attention in the last years, as has been mentioned in Section 1.3.4. Therefore, the detoxification of the subW hydrolysate through selective membrane removal processes, allows the separation and recovery of this valuable compound generated during the pretreatment of lignocellulosic biomass under a biorefinery concept.

#### **4.1. Membrane separation process: Pervaporation**

Membrane technologies have been proven to be environmentally friendly, low energy consuming and easy to scale up alternative for separation processes in bioenergy and biomaterial production [132].

Pervaporation (PV) is a membrane process in which the permeation of certain components from a liquid feed mixture through a selective membrane, into a vapor phase, is combined with the evaporation of such components. Transport through the membranes is induced by maintaining the vapor pressure of the permeating components on the permeate side of the membrane lower than the vapor pressure on the feed side of the membrane. This pressure difference can be achieved by means of a vacuum pump on the permeate side of the membrane or by using a sweeping gas. Then, the permeate condenses, while the retentate is thus enriched in the preferentially non-permeating component. Since only a fraction of the feed has to be evaporated, the energy consumption is lower than in distillation process.

The mass transport through the membrane involves three steps: sorption of the molecules on the membrane surface, diffusion of the components through the non-porous membrane, and desorption by evaporation at the permeate side. **Figure 1.24** shows a simplified diagram of the mass transport steps in pervaporation.

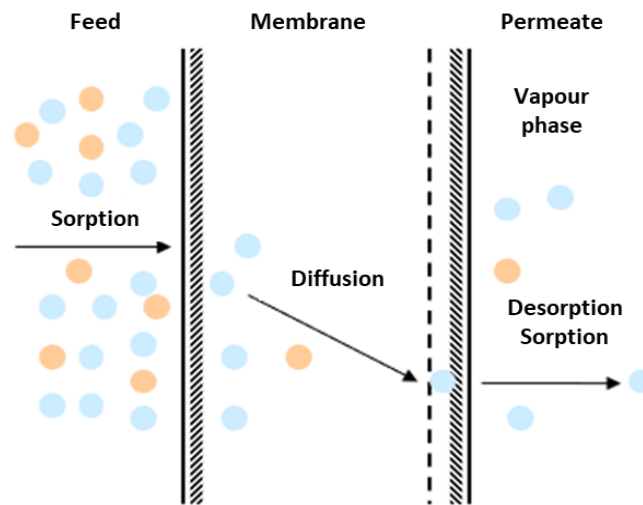


**Figure I24.** Simplified diagram illustrating the pervaporation fundamentals.

The selectivity of the process is determined by the type of membranes used in PV process. Thus, hydrophilic membranes are selective towards polar compounds such as water and are successfully used in the dehydration of organic compounds. On the other hand, PV with hydrophobic membranes has emerged in recent years as an efficient alternative to classical distillation or solvent extraction processes for the separation and concentration of dilute organic compounds in aqueous media [132].

The selectivity of PV membranes offers great advantages in the detoxification of the subW hydrolysates considering a double goal:

- Removal of inhibitors such as furan derivatives or some organic acids from the subW hydrolysates to be used as fermentation broths.
- Separation and purification of these bio-based chemical compounds with enough purity.

The use of PV as an eco-friendly separation technology to remove and recover some of the compounds that can be generated during the subW hydrolysis of lignocellulosic biomass has been proposed in the literature [133], [134]. However, the use of PV to achieve a selective recovery of furfural has been barely reported [76]. Some studies have been found in the literature regarding the use of this technology in hydrolysates obtained after acid

## *INTRODUCTION*

### *Integral valorization of brewer's spent grain by emerging technologies*

---

hydrolysis of different biomasses with dilute acetic acid [134], [135], obtaining good furfural removal. However, no previous studies have been found in the literature to remove some of the organic components generated during the hydrolysis of biomass by subW, by using organophilic membranes.

## References

- [1] S. I. Mussatto, G. Dragone, and I. C. Roberto, "Brewers' spent grain: Generation, characteristics and potential applications," *Journal of Cereal Science*, vol. 43, no. 1, pp. 1–14, 2006, doi: 10.1016/j.jcs.2005.06.001.
- [2] S. A. Socaci, A. C. Fărcaș, Z. M. Diaconeasa, D. C. Vodnar, B. Rusu, and M. Tofană, "Influence of the extraction solvent on phenolic content, antioxidant, antimicrobial and antimutagenic activities of brewers' spent grain," *Journal of Cereal Science*, vol. 80, pp. 180–187, 2018, doi: 10.1016/j.jcs.2018.03.006.
- [3] S. I. Mussatto, "Brewer's spent grain: a valuable feedstock for industrial applications," *Journal of the Science of Food and Agriculture*, vol. 94, no. 7, pp. 1264–1275, May 2014, doi: 10.1002/jsfa.6486.
- [4] K. M. Lynch, E. J. Steffen, and E. K. Arendt, "Brewers' spent grain: a review with an emphasis on food and health," *Journal of the Institute of Brewing*, vol. 122, no. 4, pp. 553–568, 2016, doi: 10.1002/jib.363.
- [5] J. U. Fangel, J. Eiken, A. Sierksma, H. A. Schols, W. G. T. Willats, and J. Harholt, "Tracking polysaccharides through the brewing process," *Carbohydrate Polymers*, vol. 196, pp. 465–473, Sep. 2018, doi: 10.1016/j.CARBPOL.2018.05.053.
- [6] S. I. Mussatto and I. C. Roberto, "Chemical characterization and liberation of pentose sugars from brewer's spent grain," *Journal of Chemical Technology and Biotechnology*, vol. 81, no. 3, pp. 268–274, Mar. 2006, doi: 10.1002/jctb.1374.
- [7] N. P. P. Pabbathi *et al.*, "Brewer's spent grains-based biorefineries: A critical review," *Fuel*, vol. 317, p. 123435, Jun. 2022, doi: 10.1016/j.fuel.2022.123435.
- [8] A. Pattiya, "1 - Fast pyrolysis," in *Direct Thermochemical Liquefaction for Energy Applications*, Elsevier, 2018, pp. 3–28. doi: 10.1016/B978-0-08-101029-7.00001-1.
- [9] M. Santos, J. J. Jiménez, B. Bartolomé, C. Gómez-Cordovés, and M. J. del Nozal, "Variability of brewer's spent grain within a brewery," *Food Chemistry*, vol. 80, no. 1, pp. 17–21, Jan. 2003, doi: 10.1016/S0308-8146(02)00229-7.
- [10] J. A. Robertson *et al.*, "Profiling brewers' spent grain for composition and microbial ecology at the site of production," *LWT - Food Science and Technology*, vol. 43, no. 6, pp. 890–896, 2010, doi: 10.1016/j.lwt.2010.01.019.
- [11] N. G. T. Meneses, S. Martins, J. A. Teixeira, and S. I. Mussatto, "Influence of extraction solvents on the recovery of antioxidant phenolic compounds from brewer's spent grains," *Separation and Purification Technology*, vol. 108, pp. 152–158, 2013, doi: 10.1016/j.seppur.2013.02.015.
- [12] Z. Jin, Y. Lan, J.-B. Ohm, J. Gillespie, P. Schwarz, and B. Chen, "Physicochemical composition, fermentable sugars, free amino acids, phenolics, and minerals in brewers' spent grains obtained from craft brewing operations," *Journal of Cereal Science*, vol. 104, p. 103413, Mar. 2022, doi: 10.1016/j.jcs.2022.103413.
- [13] S. Ikram, L. Huang, H. Zhang, J. Wang, and M. Yin, "Composition and Nutrient Value Proposition of Brewers Spent Grain.," *Journal of food science*, vol. 82, no. 10, pp. 2232–2242, Oct. 2017, doi: 10.1111/1750-3841.13794.

## INTRODUCTION

### *Integral valorization of brewer's spent grain by emerging technologies*

---

- [14] A. J. Jay *et al.*, "A systematic micro-dissection of brewers' spent grain," *Journal of Cereal Science*, vol. 47, no. 2, pp. 357–364, Mar. 2008, doi: 10.1016/j.jcs.2007.05.006.
- [15] T. Bonifácio-Lopes, J. A. Teixeira, and M. Pintado, "Current extraction techniques towards bioactive compounds from brewer's spent grain—A review," *Critical Reviews in Food Science and Nutrition*, vol. 60, no. 16. Taylor and Francis Inc., pp. 2730–2741, Sep. 07, 2020. doi: 10.1080/10408398.2019.1655632.
- [16] D. M. Waters, F. Jacob, J. Titze, E. K. Arendt, and E. Zannini, "Fibre, protein and mineral fortification of wheat bread through milled and fermented brewer's spent grain enrichment," *European Food Research and Technology*, vol. 235, no. 5, pp. 767–778, 2012, doi: 10.1007/s00217-012-1805-9.
- [17] O. Bobleter, "HYDROTHERMAL DEGRADATION OF POLYMERS DERIVED FROM PLANTS," 1994.
- [18] P. Harmsen, W. Huijgen, L. Bermudez, and R. Bakker, *Literature Review of Physical and Chemical Pretreatment Processes for Lignocellulosic Biomass*. 2010.
- [19] P. Ning *et al.*, "Recent advances in the valorization of plant biomass," *Biotechnology for Biofuels*, vol. 14, no. 1. BioMed Central Ltd, Dec. 01, 2021. doi: 10.1186/s13068-021-01949-3.
- [20] M. J. Cocero *et al.*, "Understanding biomass fractionation in subcritical & supercritical water," *The Journal of Supercritical Fluids*, vol. 133, no. August 2017, pp. 550–565, Mar. 2018, doi: 10.1016/j.supflu.2017.08.012.
- [21] A. Buleon and P. Colonna, "Physicochemical Behaviour of Starch in Food Applications," in *The Chemical Physics of Food*, Oxford, UK: Blackwell Science Ltd, 2007, pp. 20–67. doi: 10.1002/9780470995792.ch2.
- [22] E. Coelho, M. A. M. Rocha, A. S. P. Moreira, M. R. M. Domingues, and M. A. Coimbra, "Revisiting the structural features of arabinoxylans from brewers' spent grain," *Carbohydrate Polymers*, vol. 139, pp. 167–176, Mar. 2016, doi: 10.1016/j.carbpol.2015.12.006.
- [23] S. I. Mussatto, M. Fernandes, and I. C. Roberto, "Lignin recovery from brewer's spent grain black liquor," *Carbohydrate Polymers*, vol. 70, no. 2, pp. 218–223, 2007, doi: 10.1016/j.carbpol.2007.03.021.
- [24] P. Niemi *et al.*, "Characterization of Lipids and Lignans in Brewer's Spent Grain and Its Enzymatically Extracted Fraction," 2012, doi: 10.1021/jf302684x.
- [25] P. J. Arauzo, L. Du, M. P. Olszewski, M. F. Meza Zavala, M. J. Alhnidi, and A. Kruse, "Effect of protein during hydrothermal carbonization of brewer's spent grain," *Bioresource Technology*, vol. 293, no. July, p. 122117, Dec. 2019, doi: 10.1016/j.biortech.2019.122117.
- [26] C. Manach, A. Scalbert, C. Morand, C. Rémésy, and L. Jiménez, "Polyphenols: food sources and bioavailability," *The American Journal of Clinical Nutrition*, vol. 79, no. 5, pp. 727–747, May 2004, doi: 10.1093/ajcn/79.5.727.
- [27] Md. J. Rahman, L. N. Malunga, M. Eskin, P. Eck, S. J. Thandapilly, and U. Thiyam-Hollander, "Valorization of Heat-Treated Brewers' Spent Grain Through the

- Identification of Bioactive Phenolics by UPLC-PDA and Evaluation of Their Antioxidant Activities," *Frontiers in Nutrition*, vol. 8, p. 634519, Apr. 2021, doi: 10.3389/fnut.2021.634519.
- [28] S. Ikram, H. Zhang, H. Ming, and J. Wang, "Recovery of major phenolic acids and antioxidant activity of highland barley brewer's spent grains extracts," *Journal of Food Processing and Preservation*, vol. 44, no. 1, p. e14308, Jan. 2020, doi: 10.1111/JFPP.14308.
- [29] D. Hernanz *et al.*, "Hydroxycinnamic Acids and Ferulic Acid Dehydrodimers in Barley and Processed Barley," *Journal of Agricultural and Food Chemistry*, vol. 49, no. 10, pp. 4884–4888, Oct. 2001, doi: 10.1021/jf010530u.
- [30] C. Severini, D. Azzollini, K. Jouppila, L. Jussi, A. Derossi, and T. de Pilli, "Effect of enzymatic and technological treatments on solubilisation of arabinoxylans from brewer's spent grain," 2015, doi: 10.1016/j.jcs.2015.07.006.
- [31] M. Kavalopoulos *et al.*, "Sustainable valorisation pathways mitigating environmental pollution from brewers' spent grains," *Environmental Pollution*, vol. 270, p. 116069, Feb. 2021, doi: 10.1016/j.envpol.2020.116069.
- [32] J. Zhang, C. Wen, H. Zhang, Y. Duan, and H. Ma, "Recent advances in the extraction of bioactive compounds with subcritical water: A review," *Trends in Food Science & Technology*, vol. 95, pp. 183–195, Jan. 2020, doi: 10.1016/j.tifs.2019.11.018.
- [33] J. A. Rojas-Chamorro, I. Romero, J. C. López-Linares, and E. Castro, "Brewer's spent grain as a source of renewable fuel through optimized dilute acid pretreatment," *Renewable Energy*, vol. 148, pp. 81–90, Apr. 2020, doi: 10.1016/j.renene.2019.12.030.
- [34] S. A. L. Bachmann, T. Calvete, and L. A. Féris, "Potential applications of brewery spent grain: Critical an overview," *Journal of Environmental Chemical Engineering*, vol. 10, no. 1. Elsevier Ltd, Feb. 01, 2022. doi: 10.1016/j.jece.2021.106951.
- [35] E. Vieira, J. Teixeira, and I. M. P. L. V. O. Ferreira, "Valorization of brewers' spent grain and spent yeast through protein hydrolysates with antioxidant properties," *European Food Research and Technology*, vol. 242, no. 11, pp. 1975–1984, 2016, doi: 10.1007/s00217-016-2696-y.
- [36] P. Puligundla and C. Mok, "Recent advances in biotechnological valorization of brewers' spent grain," *Food Science and Biotechnology*, vol. 30, no. 3. The Korean Society of Food Science and Technology, pp. 341–353, Mar. 01, 2021. doi: 10.1007/s10068-021-00900-4.
- [37] A. B. de Camargos *et al.*, "Production of biogas and fermentable sugars from spent brewery grains: Evaluation of one- and two-stage thermal pretreatment in an integrated biorefinery," *Journal of Environmental Chemical Engineering*, vol. 9, no. 5, Oct. 2021, doi: 10.1016/j.jece.2021.105960.
- [38] A. Cabeza, C. M. Piqueras, F. Sobrón, and J. García-Serna, "Modeling of biomass fractionation in a lab-scale biorefinery: Solubilization of hemicellulose and cellulose from holm oak wood using subcritical water," *Bioresource Technology*, vol. 200, pp. 90–102, Jan. 2016, doi: 10.1016/J.BIORTECH.2015.09.063.

- [39] S. S. Hassan, G. A. Williams, and A. K. Jaiswal, "Moving towards the second generation of lignocellulosic biorefineries in the EU: Drivers, challenges, and opportunities," *Renewable and Sustainable Energy Reviews*, vol. 101, pp. 590–599, Mar. 2019, doi: 10.1016/J.RSER.2018.11.041.
- [40] G. Dragone, A. A. J. Kerssemakers, J. L. S. P. Driessen, C. K. Yamakawa, L. P. Brumano, and S. I. Mussatto, "Innovation and strategic orientations for the development of advanced biorefineries," *Bioresource Technology*, vol. 302, no. January, p. 122847, 2020, doi: 10.1016/j.biortech.2020.122847.
- [41] Market Data Forecast, "marketdataforecast.com/market-reports/europe-craft-beer-market," *Europe Craft Beer Market by Product Type (Ale and Lager), Distribution Channel (On-Trade and Off-Trade), and By Segments (Brewpubs, Microbreweries, Regional Craft Breweries and Contract Brewing Companies), and By Country (UK, France, Spain, Germany, Italy, 2020.* <https://www.marketdataforecast.com/market-reports/europe-craft-beer-market> (accessed Dec. 21, 2020).
- [42] A. L. McCarthy *et al.*, "The hydroxycinnamic acid content of barley and brewers' spent grain (BSG) and the potential to incorporate phenolic extracts of BSG as antioxidants into fruit beverages," *Food Chemistry*, vol. 141, no. 3, pp. 2567–2574, 2013, doi: 10.1016/j.foodchem.2013.05.048.
- [43] F. Chemat, N. Rombaut, A. G. Sicaire, A. Meullemiestre, A. S. Fabiano-Tixier, and M. Abert-Vian, "Ultrasound assisted extraction of food and natural products. Mechanisms, techniques, combinations, protocols and applications. A review," *Ultrasonics Sonochemistry*, vol. 34. Elsevier B.V., pp. 540–560, Jan. 01, 2017. doi: 10.1016/j.ultsonch.2016.06.035.
- [44] H. Wu, J. Zhu, W. Diao, and C. Wang, "Ultrasound-assisted enzymatic extraction and antioxidant activity of polysaccharides from pumpkin (*Cucurbita moschata*)," *Carbohydrate Polymers*, vol. 113, pp. 314–324, 2014, doi: 10.1016/j.carbpol.2014.07.025.
- [45] S. F. Reis, E. Coelho, M. A. Coimbra, and N. Abu-Ghannam, "Improved efficiency of brewer's spent grain arabinoxylans by ultrasound-assisted extraction," *Ultrasonics Sonochemistry*, vol. 24, pp. 155–164, 2015, doi: 10.1016/j.ultsonch.2014.10.010.
- [46] M. Arshadi *et al.*, "Pre-treatment and extraction techniques for recovery of added value compounds from wastes throughout the agri-food chain," *Green Chemistry*, vol. 18, no. 23, pp. 6160–6204, 2016, doi: 10.1039/C6GC01389A.
- [47] A. Corma Canos, S. Iborra, and A. Velty, "Chemical routes for the transformation of biomass into chemicals," *Chemical Reviews*, vol. 107, no. 6. pp. 2411–2502, Jun. 2007. doi: 10.1021/cr050989d.
- [48] P. Verma and M. P. Sharma, "Review of process parameters for biodiesel production from different feedstocks," *Renewable and Sustainable Energy Reviews*, vol. 62, pp. 1063–1071, Sep. 2016, doi: 10.1016/J.RSER.2016.04.054.
- [49] Z. Solati, K. Manevski, U. Jørgensen, R. Labouriau, S. Shahbazi, and P. E. Lærke, "Crude protein yield and theoretical extractable true protein of potential



- biorefinery feedstocks," *Industrial Crops and Products*, vol. 115, pp. 214–226, May 2018, doi: 10.1016/j.indcrop.2018.02.010.
- [50] F. Qin, A. Z. Johansen, and S. I. Mussatto, "Evaluation of different pretreatment strategies for protein extraction from brewer's spent grains," *Industrial Crops and Products*, vol. 125, no. June, pp. 443–453, 2018, doi: 10.1016/j.indcrop.2018.09.017.
- [51] W. G. Sganzerla, L. C. Ampese, S. I. Mussatto, and T. Forster-Carneiro, "A bibliometric analysis on potential uses of brewer's spent grains in a biorefinery for the circular economy transition of the beer industry," *Biofuels, Bioproducts and Biorefining*, p. bbb.2290, Sep. 2021, doi: 10.1002/bbb.2290.
- [52] J. L. Proaño, P. R. Salgado, R. E. Cian, A. N. Mauri, and S. R. Drago, "Physical, structural and antioxidant properties of brewer's spent grain protein films," *Journal of the Science of Food and Agriculture*, vol. 100, no. 15, pp. 5458–5465, Dec. 2020, doi: 10.1002/jsfa.10597.
- [53] L. Du, P. J. Arauzo, M. F. Meza Zavala, Z. Cao, M. P. Olszewski, and A. Kruse, "Towards the properties of different biomass-derived proteins via various extraction methods," *Molecules*, vol. 25, no. 3, 2020, doi: 10.3390/molecules25030488.
- [54] D. S. Tang, Y. J. Tian, Y. Z. He, L. Li, S. Q. Hu, and B. Li, "Optimisation of ultrasonic-assisted protein extraction from brewer's spent grain," *Czech Journal of Food Sciences*, vol. 28, no. 1, pp. 9–17, 2010.
- [55] A. Connolly, C. O. Piggott, and R. J. Fitzgerald, "Characterisation of protein-rich isolates and antioxidative phenolic extracts from pale and black brewers' spent grain," *International Journal of Food Science and Technology*, vol. 48, no. 8, pp. 1670–1681, 2013, doi: 10.1111/ijfs.12137.
- [56] I. Sereewatthanawut, S. Prapintip, K. Watchirarujj, M. Goto, M. Sasaki, and A. Shotipruk, "Extraction of protein and amino acids from deoiled rice bran by subcritical water hydrolysis," *Bioresource Technology*, vol. 99, no. 3, pp. 555–561, 2008, doi: 10.1016/j.biortech.2006.12.030.
- [57] R. Macias-Garbett, S. O. Serna-Hernández, J. E. Sosa-Hernández, and R. Parra-Saldívar, "Phenolic Compounds From Brewer's Spent Grains: Toward Green Recovery Methods and Applications in the Cosmetic Industry," *Frontiers in Sustainable Food Systems*, vol. 5, p. 196, Jun. 2021, doi: 10.3389/FSUFS.2021.681684/BIBTEX.
- [58] G. Virginia Nevárez-Moorillón *et al.*, "Sustainable Food Processing, a section of the journal *Frontiers in Sustainable Food Systems* Phenolic Compounds From Brewer's Spent Grains: Toward Green Recovery Methods and Applications in the Cosmetic Industry," vol. 5, p. 681684, 2021, doi: 10.3389/fsufs.2021.681684.
- [59] S. I. Mussatto, G. Dragone, and I. C. Roberto, "Ferulic and p-coumaric acids extraction by alkaline hydrolysis of brewer's spent grain," *Industrial Crops and Products*, vol. 25, no. 2, pp. 231–237, Feb. 2007, doi: 10.1016/J.INDCROP.2006.11.001.

- [60] E. Alonso, "The role of supercritical fluids in the fractionation pretreatments of a wheat bran-based biorefinery," *The Journal of Supercritical Fluids*, vol. 133, pp. 603–614, 2018, doi: 10.1016/j.supflu.2017.09.010.
- [61] S. Wilkinson, K. A. Smart, and D. J. Cook, "Optimisation of alkaline reagent based chemical pre-treatment of Brewers spent grains for bioethanol production," *Industrial Crops and Products*, vol. 62, pp. 219–227, 2014, doi: 10.1016/j.indcrop.2014.08.036.
- [62] O. Gligor, A. Mocan, C. Moldovan, M. Locatelli, G. Crişan, and I. C. F. R. Ferreira, "Enzyme-assisted extractions of polyphenols – A comprehensive review," *Trends in Food Science and Technology*, vol. 88. Elsevier Ltd, pp. 302–315, Jun. 01, 2019. doi: 10.1016/j.tifs.2019.03.029.
- [63] L. F. Guido and M. M. Moreira, "Techniques for Extraction of Brewer's Spent Grain Polyphenols: a Review," *Food and Bioprocess Technology*, vol. 10, no. 7. Springer New York LLC, pp. 1192–1209, Jul. 01, 2017. doi: 10.1007/s11947-017-1913-4.
- [64] R. Carciochi, C. Sologubik, M. Fernández, G. Manrique, and L. D'Alessandro, "Extraction of Antioxidant Phenolic Compounds from Brewer's Spent Grain: Optimization and Kinetics Modeling," *Antioxidants*, vol. 7, no. 4, p. 45, Mar. 2018, doi: 10.3390/antiox7040045.
- [65] S. D. Karlen *et al.*, "Assessing the Viability of Recovery of Hydroxycinnamic Acids from Lignocellulosic Biorefinery Alkaline Pretreatment Waste Streams," *ChemSusChem*, vol. 13, no. 8, pp. 2012–2024, Apr. 2020, doi: 10.1002/CSSC.201903345.
- [66] O. Purali, F. S. Asghari, and H. Yoshida, "Production of phenolic compounds from rice bran biomass under subcritical water conditions," *Chemical Engineering Journal*, vol. 160, no. 1, pp. 259–266, 2010, doi: 10.1016/j.cej.2010.02.057.
- [67] H. Dong, L. da C. Sousa, B. Ubanwa, A. D. Jones, and V. Balan, "A New Method to Overcome Carboxamide Formation During AFEX Pretreatment of Lignocellulosic Biomass," *Frontiers in Chemistry*, vol. 9, Jan. 2022, doi: 10.3389/fchem.2021.826625.
- [68] S. I. Mussatto, M. Fernandes, A. M. F. Milagres, and I. C. Roberto, "Effect of hemicellulose and lignin on enzymatic hydrolysis of cellulose from brewer's spent grain," *Enzyme and Microbial Technology*, vol. 43, pp. 124–129, 2008, doi: 10.1016/j.enzmictec.2007.11.006.
- [69] M. del M. Contreras, A. Lama-Muñoz, J. M. Romero-García, M. García-Vargas, I. Romero, and E. Castro, "Production of renewable products from brewery spent grains," *Waste Biorefinery*, pp. 305–347, Jan. 2021, doi: 10.1016/B978-0-12-821879-2.00011-9.
- [70] M. Álvarez-Viñas *et al.*, "Subcritical Water for the Extraction and Hydrolysis of Protein and Other Fractions in Biorefineries from Agro-food Wastes and Algae: a Review," *Food and Bioprocess Technology*, vol. 14, no. 3, pp. 373–387, Mar. 2021, doi: 10.1007/s11947-020-02536-4.

- [71] S. Xie, A. J. Ragauskas, and J. S. Yuan, "Lignin Conversion: Opportunities and Challenges for the Integrated Biorefinery," *Industrial Biotechnology*, vol. 12, no. 3, pp. 161–167, Jun. 2016, doi: 10.1089/ind.2016.0007.
- [72] F. Carvalheiro, M. P. Esteves, J. C. Parajó, H. Pereira, and F. M. Gírio, "Production of oligosaccharides by autohydrolysis of brewery's spent grain," *Bioresource Technology*, vol. 91, no. 1, pp. 93–100, 2004, doi: 10.1016/S0960-8524(03)00148-2.
- [73] L. J. Swart, S. P. Johann, F. Görgens, and E. van Rensburg, "Techno-economic analysis of the valorisation of brewers spent grains: Production of xylitol and xylo-oligosaccharides," 2020. [Online]. Available: <https://scholar.sun.ac.za>
- [74] R. Mariscal, P. Maireles-Torres, M. Ojeda, I. Sádaba, and M. López Granados, "Furfural: A renewable and versatile platform molecule for the synthesis of chemicals and fuels," *Energy and Environmental Science*, vol. 9, no. 4, pp. 1144–1189, 2016, doi: 10.1039/c5ee02666k.
- [75] F. Qin, S. Li, P. Qin, M. N. Karim, and T. Tan, "A PDMS membrane with high pervaporation performance for the separation of furfural and its potential in industrial application," *Green Chemistry*, vol. 16, no. 3, pp. 1262–1273, 2014, doi: 10.1039/c3gc41867g.
- [76] H. Shan *et al.*, "Molecular dynamics simulation and preparation of vinyl modified polydimethylsiloxane membrane for pervaporation recovery of furfural," *Separation and Purification Technology*, vol. 258, no. P2, p. 118006, 2021, doi: 10.1016/j.seppur.2020.118006.
- [77] A. R. C. Morais, A. M. da Costa Lopes, and R. Bogel-Lukasik, "Carbon dioxide in biomass processing: Contributions to the green biorefinery concept," *Chemical Reviews*, vol. 115, no. 1. American Chemical Society, pp. 3–27, Jan. 14, 2015. doi: 10.1021/cr500330z.
- [78] W. G. Sganzerla, G. L. Zabot, P. C. Torres-Mayanga, L. S. Buller, S. I. Mussatto, and T. Forster-Carneiro, "Techno-economic assessment of subcritical water hydrolysis process for sugars production from brewer's spent grains," *Industrial Crops and Products*, vol. 171, Nov. 2021, doi: 10.1016/j.indcrop.2021.113836.
- [79] D. G. Gomes, M. Michelin, A. Romani, L. Domingues, and J. A. Teixeira, "Co-production of biofuels and value-added compounds from industrial Eucalyptus globulus bark residues using hydrothermal treatment," *Fuel*, vol. 285, Feb. 2021, doi: 10.1016/j.fuel.2020.119265.
- [80] A. B. de Camargos *et al.*, "Production of biogas and fermentable sugars from spent brewery grains: Evaluation of one- and two-stage thermal pretreatment in an integrated biorefinery," *Journal of Environmental Chemical Engineering*, vol. 9, no. 5, Oct. 2021, doi: 10.1016/j.jece.2021.105960.
- [81] J. Chen *et al.*, "Integrating enzymatic hydrolysis into subcritical water pretreatment optimization for bioethanol production from wheat straw," *Science of the Total Environment*, vol. 770, May 2021, doi: 10.1016/j.scitotenv.2021.145321.
- [82] P. G. Jessop and W. Leitner, "Supercritical Fluids as Media for Chemical Reactions," in *Chemical Synthesis Using Supercritical Fluids*, P. G. Jessop and W. Leitner, Eds. John Wiley & Sons, Ltd, 1999, pp. 1–36. doi: 10.1002/9783527613687.CH1.

- [83] G. Brunner, *Gas Extraction: an Introduction to Fundamentals of Supercritical Fluids and the Application to Separation Processes*. New York: Springer, 1994.
- [84] M. O. Balaban, "Effects of DPCD on Enzymes," in *Dense Phase Carbon Dioxide: Food and Pharmaceutical Applications*, M. O. Balaban and G. Ferrentino, Eds. Blackwell, 2012, pp. 113–134.
- [85] S. Angus, B. Armstrong, and K. M. de Reuck, *International Thermodynamic Tables of the Fluid State*. Pergamon Press, 1976.
- [86] V. Kitryte, A. Šaduikis, and P. R. Venskutonis, "Assessment of antioxidant capacity of brewer's spent grain and its supercritical carbon dioxide extract as sources of valuable dietary ingredients," *Journal of Food Engineering*, vol. 167, pp. 18–24, Dec. 2015, doi: 10.1016/J.JFOODENG.2014.12.005.
- [87] S. Spinelli, A. Conte, L. Lecce, L. Padalino, and M. A. del Nobile, "Supercritical carbon dioxide extraction of brewer's spent grain," *Journal of Supercritical Fluids*, vol. 107, pp. 69–74, 2016, doi: 10.1016/j.supflu.2015.08.017.
- [88] M. P. Fernández, J. F. Rodríguez, M. T. García, A. de Lucas, and I. Gracia, "Application of Supercritical Fluid Extraction to Brewer's Spent Grain Management," *Industrial & Engineering Chemistry Research*, vol. 47, no. 5, pp. 1614–1619, Mar. 2008, doi: 10.1021/ie0708529.
- [89] M. E. Taheri *et al.*, "Effect of pretreatment techniques on enzymatic hydrolysis of food waste," *Biomass Conversion and Biorefinery*, vol. 11, no. 2, pp. 219–226, Apr. 2021, doi: 10.1007/s13399-020-00729-7.
- [90] J. Shi, S. J. Xue, Y. Ma, Y. Jiang, X. Ye, and D. Yu, "Green separation technologies in food processing: supercritical-CO<sub>2</sub> fluid and subcritical water extraction," *Food Engineering Series*, pp. 273–294, 2012, doi: 10.1007/978-1-4614-1587-9\_11.
- [91] S. Rebolleda, S. Beltrán, M. T. Sanz, M. L. González-Sanjosé, and Á. G. Solaesa, "Extraction of alkylresorcinols from wheat bran with supercritical CO<sub>2</sub>," *Journal of Food Engineering*, vol. 119, no. 4, pp. 814–821, 2013, doi: 10.1016/j.jfoodeng.2013.07.008.
- [92] Y. Zheng, H. M. Lin, and G. T. Tsao, "Pretreatment for cellulose hydrolysis by carbon dioxide explosion," *Biotechnology Progress*, vol. 14, no. 6, pp. 890–896, 1998, doi: 10.1021/BP980087G.
- [93] M. Gao, F. Xu, S. Li, X. Ji, S. Chen, and D. Zhang, "Effect of SC-CO<sub>2</sub> pretreatment in increasing rice straw biomass conversion," *Biosystems Engineering*, vol. 106, no. 4, pp. 470–475, 2010, doi: 10.1016/j.biosystemseng.2010.05.011.
- [94] K. H. Kim and J. Hong, "Supercritical CO<sub>2</sub> pretreatment of lignocellulose enhances enzymatic cellulose hydrolysis," *Bioresource Technology*, vol. 77, no. 2, pp. 139–144, 2001, doi: 10.1016/S0960-8524(00)00147-4.
- [95] N. Narayanaswamy, A. Faik, D. J. Goetz, and T. Gu, "Supercritical carbon dioxide pretreatment of corn stover and switchgrass for lignocellulosic ethanol production," *Bioresource Technology*, vol. 102, no. 13, pp. 6995–7000, Jul. 2011, doi: 10.1016/j.biortech.2011.04.052.

## INTRODUCTION

### *Integral valorization of brewer's spent grain by emerging technologies*

---

- [96] N. T. Dunford and F. Temelli, "Extraction Conditions and Moisture Content of Canola Flakes as Related to Lipid Composition of Supercritical CO<sub>2</sub> Extracts," 1997.
- [97] M. Plaza and C. Turner, "Pressurized hot water extraction of bioactives," *TrAC - Trends in Analytical Chemistry*, vol. 71, pp. 39–54, 2015, doi: 10.1016/j.trac.2015.02.022.
- [98] C. M. Martínez, D. A. Cantero, and M. J. Cocero, "Production of saccharides from sugar beet pulp by ultrafast hydrolysis in supercritical water," *Journal of Cleaner Production*, vol. 204, pp. 888–895, 2018, doi: 10.1016/j.jclepro.2018.09.066.
- [99] C. G. Malmberg and A. A. Maryott, "Dielectric Constant of Water from 0 to 100 °C," *Journal of Research of the National Bureau of Standards*, vol. 56, no. 1, 1956.
- [100] J. Park, Y. Jeong, and B. Chun, "The Journal of Supercritical Fluids Physiological activities and bioactive compound from laver ( *Pyropia yezoensis* ) hydrolysates by using subcritical water hydrolysis," *The Journal of Supercritical Fluids*, vol. 148, no. January, pp. 130–136, 2019, doi: 10.1016/j.supflu.2019.03.004.
- [101] A. G. Carr, R. Mammucari, and N. R. Foster, "A review of subcritical water as a solvent and its utilisation for the processing of hydrophobic organic compounds," *Chemical Engineering Journal*, vol. 172, no. 1, pp. 1–17, Aug. 2011, doi: 10.1016/J.CEJ.2011.06.007.
- [102] C. C. Teo, S. N. Tan, J. W. H. Yong, C. S. Hew, and E. S. Ong, "Pressurized hot water extraction (PHWE)," *Journal of Chromatography A*, vol. 1217, no. 16, pp. 2484–2494, Apr. 2010, doi: 10.1016/j.chroma.2009.12.050.
- [103] P. Yue, Y. Hu, R. Tian, J. Bian, and F. Peng, "Hydrothermal pretreatment for the production of oligosaccharides: A review," *Bioresource Technology*, vol. 343. Elsevier Ltd, Jan. 01, 2022. doi: 10.1016/j.biortech.2021.126075.
- [104] T. Scapini *et al.*, "Hydrothermal pretreatment of lignocellulosic biomass for hemicellulose recovery," *Bioresource Technology*, vol. 342, p. 126033, Dec. 2021, doi: 10.1016/J.BIORTECH.2021.126033.
- [105] C. R. M. Monteiro, L. G. G. Rodrigues, K. Cesca, and P. Poletto, "Evaluation of hydrothermal sugarcane bagasse treatment for the production of xylooligosaccharides in different pressures," *Journal of Food Process Engineering*, no. October 2021, 2022, doi: 10.1111/jfpe.13965.
- [106] F. Rodríguez, E. Aguilar-Garnica, A. Santiago-Toribio, and A. Sánchez, "Polysaccharides Release in a Laboratory-Scale Batch Hydrothermal Pretreatment of Wheat Straw under Rigorous Isothermal Operation," *Molecules*, vol. 27, no. 1, p. 26, Dec. 2021, doi: 10.3390/molecules27010026.
- [107] H. A. Ruiz *et al.*, "Severity factor kinetic model as a strategic parameter of hydrothermal processing (steam explosion and liquid hot water) for biomass fractionation under biorefinery concept," *Bioresource Technology*, vol. 342. Elsevier Ltd, Dec. 01, 2021. doi: 10.1016/j.biortech.2021.125961.
- [108] G. Garrote, R. Yáñez, J. L. Alonso, and J. C. Parajó, "Coproduction of Oligosaccharides and Glucose from Corncobs by Hydrothermal Processing and Enzymatic Hydrolysis,"

- Industrial & Engineering Chemistry Research*, vol. 47, no. 4, pp. 1336–1345, Feb. 2008, doi: 10.1021/ie071201f.
- [109] A. Mittal, S. G. Chatterjee, G. M. Scott, and T. E. Amidon, “Modeling xylan solubilization during autohydrolysis of sugar maple and aspen wood chips: Reaction kinetics and mass transfer,” *Chemical Engineering Science*, vol. 64, no. 13, pp. 3031–3041, 2009, doi: 10.1016/j.ces.2009.03.011.
- [110] G. Garrote, H. Domínguez, and J. C. Parajó, “Kinetic modelling of corncob autohydrolysis,” *Process Biochemistry*, vol. 36, no. 6, pp. 571–578, 2001, doi: 10.1016/S0032-9592(00)00253-3.
- [111] R. P. Overend, E. Chornet, J. A. Gascoigne, B. S. Hartley, P. M. A. Broda, and P. J. Senior, “Fractionation of lignocellulosics by steam-aqueous pretreatments,” *Philosophical Transactions of the Royal Society of London. Series A, Mathematical and Physical Sciences*, vol. 321, no. 1561, pp. 523–536, Apr. 1987, doi: 10.1098/rsta.1987.0029.
- [112] Z.-W. Wang, M.-Q. Zhu, M.-F. Li, J.-Q. Wang, Q. Wei, and R.-C. Sun, “Comprehensive evaluation of the liquid fraction during the hydrothermal treatment of rapeseed straw,” *Biotechnol Biofuels*, vol. 9, p. 142, 2016, doi: 10.1186/s13068-016-0552-8.
- [113] M. C. Gray, A. O. Converse, and C. E. Wyman, “Solubilities of Oligomer Mixtures Produced by the Hydrolysis of Xylans and Corn Stover in Water at 180 °C,” 2007, doi: 10.1021/ie060325.
- [114] M. Sasaki, Z. Fang, Y. Fukushima, T. Adschiri, and K. Arai, “Dissolution and Hydrolysis of Cellulose in Subcritical and Supercritical Water,” 2000, doi: 10.1021/ie990690j.
- [115] S. Deguchi, K. Tsujii, and K. Horikoshi, “Crystalline-to-amorphous transformation of cellulose in hot and compressed water and its implications for hydrothermal conversion,” *Green Chemistry*, vol. 10, no. 2, pp. 191–19, Feb. 2008, doi: 10.1039/b713655b.
- [116] Benito-Román, E. Alonso, and M. J. Cocero, “Pressurized hot water extraction of B-glucans from waxy barley,” *Journal of Supercritical Fluids*, vol. 73, pp. 120–125, Jan. 2013, doi: 10.1016/J.SUPFLU.2012.09.014.
- [117] C. Fabian, N. Y. Tran-Thi, N. S. Kasim, and Y. H. Ju, “Release of phenolic acids from defatted rice bran by subcritical water treatment,” *Journal of the Science of Food and Agriculture*, vol. 90, no. 15, pp. 2576–2581, 2010, doi: 10.1002/jsfa.4123.
- [118] P. C. Mayanga-Torres *et al.*, “Valorization of coffee industry residues by subcritical water hydrolysis: Recovery of sugars and phenolic compounds,” *Journal of Supercritical Fluids*, vol. 120, pp. 75–85, 2017, doi: 10.1016/j.supflu.2016.10.015.
- [119] N. Doctor, G. Parker, K. Vang, M. Smith, B. Kayan, and Y. Yang, “Stability and extraction of vanillin and coumarin under subcritical water conditions,” *Molecules*, vol. 25, no. 5, pp. 1–9, 2020, doi: 10.3390/molecules25051061.
- [120] F. Kawamura *et al.*, “Subcritical Water Extraction of Low-molecular-weight Phenolic Compounds from Oil Palm Biomass,” *JARQ*, vol. 48, no. 3, pp. 355–362, 2014, Accessed: Mar. 16, 2022. [Online]. Available: <http://www.jircas.affrc.go.jp>

- [121] I. Marcet, C. Álvarez, B. Paredes, and M. Díaz, "The use of sub-critical water hydrolysis for the recovery of peptides and free amino acids from food processing wastes. Review of sources and main parameters," *Waste Management*, vol. 49, pp. 364–371, 2016, doi: 10.1016/j.wasman.2016.01.009.
- [122] X. ZHU, C. ZHU, L. ZHAO, and H. CHENG, "Amino Acids Production from Fish Proteins Hydrolysis in Subcritical Water," *Chinese Journal of Chemical Engineering*, vol. 16, no. 3, pp. 456–460, Jun. 2008, doi: 10.1016/S1004-9541(08)60105-6.
- [123] M. B. Esteban, A. J. García, P. Ramos, and M. C. Márquez, "Sub-critical water hydrolysis of hog hair for amino acid production," *Bioresource Technology*, vol. 101, no. 7, pp. 2472–2476, 2010, doi: 10.1016/j.biortech.2009.11.054.
- [124] E. Trigueros, M. T. Sanz, P. Alonso-Riaño, S. Beltrán, C. Ramos, and R. Melgosa, "Recovery of the protein fraction with high antioxidant activity from red seaweed industrial solid residue after agar extraction by subcritical water treatment," *Journal of Applied Phycology*, vol. 33, no. 2, pp. 1181–1194, Apr. 2021, doi: 10.1007/s10811-020-02349-0.
- [125] A. Lamp, M. Kaltschmitt, and O. Lüdtke, "Protein recovery from bioethanol stillage by liquid hot water treatment," *Journal of Supercritical Fluids*, vol. 155, p. 104624, 2020, doi: 10.1016/j.supflu.2019.104624.
- [126] W. Abdelmoez, T. Nakahasi, and H. Yoshida, "Amino acid transformation and decomposition in saturated subcritical water conditions," *Industrial and Engineering Chemistry Research*, vol. 46, no. 16, pp. 5286–5294, 2007, doi: 10.1021/ie070151b.
- [127] N. Sato, A. T. Quitain, K. Kang, H. Daimon, and K. Fujie, "Reaction kinetics of amino acid decomposition in high-temperature and high-pressure water," *Industrial and Engineering Chemistry Research*, vol. 43, no. 13, pp. 3217–3222, 2004, doi: 10.1021/ie020733n.
- [128] T. Rogalinski, K. Liu, T. Albrecht, and G. Brunner, "Hydrolysis kinetics of biopolymers in subcritical water," *Journal of Supercritical Fluids*, vol. 46, no. 3, pp. 335–341, 2008, doi: 10.1016/j.supflu.2007.09.037.
- [129] R. Ahmed and B. S. Chun, "Subcritical water hydrolysis for the production of bioactive peptides from tuna skin collagen," *Journal of Supercritical Fluids*, vol. 141, no. March, pp. 88–96, 2018, doi: 10.1016/j.supflu.2018.03.006.
- [130] S. I. Mussatto and I. C. Roberto, "Alternatives for detoxification of diluted-acid lignocellulosic hydrolyzates for use in fermentative processes: a review," *Bioresource Technology*, vol. 93, no. 1, pp. 1–10, May 2004, doi: 10.1016/J.BIORTECH.2003.10.005.
- [131] H. B. Klinke A B Thomsen B K Ahring, "MINI-REVIEW Inhibition of ethanol-producing yeast and bacteria by degradation products produced during pre-treatment of biomass," *Appl Microbiol Biotechnol*, vol. 66, pp. 10–26, 2004, doi: 10.1007/s00253-004-1642-2.
- [132] A. Bokhary, L. Cui, H. J. Lin, and B. Q. Liao, "A review of membrane technologies for integrated forest biorefinery," *Journal of Membrane Science and Research*, vol. 3, no. 3, pp. 120–141, 2017, doi: 10.22079/jmsr.2016.22839.

## INTRODUCTION

### *Integral valorization of brewer's spent grain by emerging technologies*

---

- [133] D. R. Greer *et al.*, "Fermentation of hydrolysate detoxified by pervaporation through block copolymer membranes," *Green Chemistry*, vol. 16, no. 9, pp. 4206–4213, 2014, doi: 10.1039/c4gc00756e.
- [134] H. A. Terblanche, "Fractionation of an acidic hydrolysate from steam-treated wood using pervaporation," North-West University (South Africa), Potchefstroom Campus, May 2017, <https://repository.nwu.ac.za/handle/10394/25888>.
- [135] D. Cai *et al.*, "Biobutanol from sweet sorghum bagasse hydrolysate by a hybrid pervaporation process," *Bioresource Technology*, vol. 145, pp. 97–102, Oct. 2013, doi: 10.1016/j.biortech.2013.02.094.





# OBJECTIVES

---



## OBJECTIVES

---

The general objective of this PhD thesis is to achieve a complete valorization of the brewer's spent grain (BSG) under an integrated biorefinery concept by using sustainable emerging clean technologies. The integral valorization of biomass requires the extraction and fractionation of its different constituents, extractives, lipids, proteins, and structural components such as cellulose, hemicellulose and lignin.

To achieve this general objective, in this Thesis, a cascade approach has been proposed to recover and valorize the different chemical compounds of interest in the BSG.

For conversion of BSG into bioproducts, the first objective was to provide a detailed compositional analysis of this feedstock including structural and non-structural components. Compositional analysis will include carbohydrate, lignin, protein, ash and other non-structural materials.

In this Thesis valorization of the chemicals present in the BSG has been divided into two main objectives: (1) valorisation of hydrophilic and lipophilic extractives and (2) valorisation of protein and carbohydrate fraction of the BSG.

### **1. Valorization of hydrophilic and lipophilic extractives.**

Valorization of the easily BSG water and ethanol soluble material was carried out by using the intensification technology of ultrasound assisted extraction (UAE) by using water and hydroalcoholic mixtures as extracting agents. The effect of the main operating parameters (solvent polarity, particle size, solvent to solid ratio) was determined and results were compared with conventional extraction.

On the hand, sc-CO<sub>2</sub> technology was applied to obtain a lipophilic fraction of good quality. In both cases, hydroalcoholic and lipophilic extracts were characterized in terms of chemical composition and antioxidant capacity. Extraction kinetics were fitted to different empirical models.

Regarding the sc-CO<sub>2</sub> treatment, the effect of fat removal as well as physical changes after treatment on subsequent enzymatic hydrolysis was also explored.

The work performed to achieve this specific objective has been collected in Chapters 1 and 2

**2. Valorization of protein and carbohydrate fraction.**

In this Thesis, subcritical water (subW) was applied to hydrolyse and fractionate hemicellulose, proteins and phenolic compounds bound to structural components from BSG. Semi-continuous and discontinuous operation modes were performed. The effect of the main operating variables (temperature and time -residence time-) was considered on extraction/hydrolysis yields of these three components. One of the main goals of this Thesis was the scaling up study from the laboratory to pilot system in a discontinuous configuration. Results obtained to achieve this objective have been compiled in Chapters 3 and 4.

After subW treatment two streams were generated: a liquid and a solid stream.

2.1 *Valorization of the liquid hydrolysate.* In this Thesis, as a further step in the BSG valorisation removal of furfural, generated from pentoses dehydration, from the liquid hydrolysate was proposed by membrane technologies, specifically pervaporation. A permeate rich in furfural was obtained that could be used as a biomass-derived platform-chemical. Additionally, a detoxified fermentation broth was obtained. (Chapter 5)

2.2 *Valorization of the solid residue.* After hemicellulose removal from the BSG, the solid residue was rich in cellulose that could more easily hydrolysed by cellulases. The enzymatic hydrolysate from subW-pre-treated BSG was subjected to fermentation to obtain bioethanol. Simultaneous saccharification and fermentation (SSF) assays were also carried out. Second generation bioethanol was produced in this final objective. (Chapter 6)



# RESULTS

---



## RESULTS

---

The most outstanding results of this PhD Thesis are presented as different chapters, which correspond to the scientific publications detailed below. A brief summary in Spanish language of each publication is included at the beginning of each chapter.

**Chapter 1:** Water ultrasound-assisted extraction of polyphenol compounds from brewer's spent grain: Kinetic study, extract characterization and concentration

**Chapter 2:** Valorization of brewer's spent grain by consecutive supercritical carbon dioxide extraction and enzymatic hydrolysis

**Chapter 3:** Subcritical water as hydrolytic medium to recover and fractionate the protein fraction and phenolic compounds from craft brewer's spent grain.

**Chapter 4:** Preliminary study of subcritical water treatment scale-up from laboratory to pilot system for brewer's spent grain valorization

**Chapter 5:** Pervaporation behaviour of subcritical water hydrolysates of lignocellulosic biomass: brewer's spent grain.

**Chapter 6:** Second generation bioethanol production from subcritical water pretreated brewer's spent grain within a biorefinery concept





# CHAPTER 1

---

**Water ultrasound-assisted extraction of polyphenol compounds from brewer's spent grain: Kinetic study, extract characterization and concentration**

**Based on the article:**

P. Alonso-Riaño, M. T. Sanz, B. Blanco, S. Beltrán, E. Trigueros, O. Benito-Román (2020).

“Water Ultrasound-Assisted Extraction of Polyphenol Compounds from Brewer's Spent Grain: Kinetic Study, Extract Characterization and Concentration”.

Antioxidants, 9(3), 265 (2020)

DOI: <https://doi.org/10.3390/antiox9030265>



## Capítulo 1

### Extracción asistida por ultrasonidos de compuestos polifenólicos del bagazo de cerveza. Estudio cinético, caracterización y concentración de los extractos obtenidos

---

#### RESUMEN

En este capítulo se determinó la composición química del bagazo de cerveza generado en una cervecera artesanal, resultando en un 52,1% de hidratos de carbono, un 17,8% de proteínas, un 5,9% de lípidos, un 13,5% de lignina insoluble y un 24,3% de extractables solubles en agua.

Este capítulo se ha centrado en el estudio de la extracción de los polifenoles presentes en los extractables acuosos del bagazo de cerveza, mediante extracción asistida por ultrasonidos (EAU), utilizando agua como disolvente. Las condiciones de extracción seleccionadas fueron 47 °C y 21,7 mL de agua por gramo de bagazo seco. Se estudió el efecto de la polaridad del disolvente en la extracción de polifenoles utilizando mezclas hidroalcohólicas con distinto porcentaje de etanol, desde el 20% hasta el 100%. Las cinéticas de extracción de polifenoles se ajustaron a dos modelos cinéticos: la ley de potencias y el modelo de Weibull, obteniéndose valores medios de la desviación cuadrática media inferiores al 7,5%.

Se realizó una caracterización detallada de los extractos obtenidos. Los compuestos fenólicos individuales se identificaron y cuantificaron mediante cromatografía de líquidos de alto rendimiento con un detector de haz de diodos (HPLC-DAD). También se cuantificaron las proteínas solubles y los azúcares presentes en los extractos (glucosa, xilosa y arabinosa). El perfil de polifenoles obtenido se comparó con el obtenido empleando otras técnicas hidrolíticas: hidrólisis ácida, básica y enzimática. Se determinó que la UAE no fue tan eficaz como la hidrólisis básica para liberar los ácidos fenólicos esterificados a la pared celular.

Finalmente, se utilizó la ultrafiltración centrífuga para fraccionar y concentrar los extractos acuosos obtenidos por UAE. Mediante esta técnica, las proteínas presentes en el extracto se concentraron en el retenido, mientras que los compuestos fenólicos individuales se transfirieron principalmente al permeado.

CHAPTER 1

*Water ultrasound-assisted extraction of polyphenol compounds from brewer's spent grain: Kinetic study, extract characterization and concentration*

---

**Palabras clave:** bagazo de cerveza, extracción asistida por ultrasonidos, polifenoles, concentración de extractables.

## Abstract

---

Brewer's spent grain (BSG) was chemically characterized obtaining 52.1 % of carbohydrates, 17.8% protein, 5.9% lipids, 13.5% insoluble lignin and 24.3% of water-soluble extractives. This work has been focused on the study of polyphenol extraction of the extractive fraction by water ultrasound-assisted extraction. Selected extraction conditions were 47 °C and 21.7 mL water/g<sub>dry-BSG</sub>. The effect of solvent polarity on polyphenol extraction was studied by using ethanol aqueous mixtures, from 20% to 100% ethanol. The kinetics of polyphenol extraction have been fitted to the power law and the Weibull models yielding mean values of the root mean square deviation lower than 7.5%. Extracts have been characterized in terms of quantification of individual phenolic compounds by HPLC-DAD and protein and sugar soluble fractions (glucose, xylose, and arabinose). Polyphenol profile has been compared with other hydrolytic techniques, such as acid, basic and enzymatic hydrolysis, showing that ultrasound was not as effective as basic hydrolysis to release the phenolic acids esterified to the cell wall. A further centrifuge ultrafiltration concentration step was able to yield a retentate enriched in the protein fraction while individual phenolic compounds were mainly transferred to the permeate.

---

**Keywords:** brewer's spent grains; ultrasound assisted extraction; polyphenol compound; extractives concentration.



## 1. Introduction

Brewer's spent grain is the main by-product produced by breweries, accounting for 20 kg per 100 L of beer produced [1]. BSG represents up to 30% of the starting malted grain [2]. Currently, it is mostly used as animal feed, but its high moisture content results in an increased cost of transportation. Furthermore, the presence of fermentable sugars, reduces its shelf life. However, BSG is a lignocellulosic material rich in proteins, polysaccharides, and other bioactive compounds such as polyphenols. Therefore, BSG presents a great potential to obtain valuable products to be incorporated in the food and pharmaceutical industries. Specially, taking into account that European beer production reached nearly 39.7 billion litres in 2017 [3]. Furthermore, BSG valorization will contribute to reduce the percentage of BSG that is released in landfills yearly.

This work is mainly focused on the BSG extractives valorization by solvent extraction optimization and further centrifuge ultrafiltration concentration. According to the literature, the amount of extractives from different BSG sources were found to vary between 10.7 and 14.4 g/100 g in a dry basis [4], [5]. Valorization of phenolic compounds found in the extractive fraction, offers a great potential due to their antioxidant properties. Most of the phenolic compounds of the barley grain are contained in the coat-pericarp-husk layer [2]. Therefore, BSG can be regarded as a potentially valuable source of these compounds, mainly hydroxycinnamic acids [6].

Solvent extraction is the primary and essential step to recover the bioactive compounds from the raw material. Extraction efficiency is determined by different factors such as type of solvent, temperature, pH, solvent to solid ratio, particle size and extraction method. In this work, the potential of Ultrasound Assisted Extraction (UAE) was explored to obtain a rich fraction of polyphenol extractives and compared with other hydrolytic techniques. Ultrasound has been proposed as a key technology to reach higher extraction yields and faster extraction kinetics than conventional extraction processes. Chemat et al. [7] reviewed the mechanisms involved for an improved extraction process of natural products, namely fragmentation of the raw material, erosion, sonocapillary effects, sonoporation, shear stress, and detexturation among others.

The influence of the extraction solvent on the recovery of phenolic compounds from BSG has been reported in the literature [4]. Acetone aqueous mixtures (60% v/v acetone) at 60 °C (1 g BSG/20 mL solvent for 30 min) was the best solvent for phenolic compounds extraction with

$9.9 \pm 0.41$  mg gallic acid equivalent/ $g_{\text{dry BSG}}$ . By using water as extraction solvent ( $T = 80$  °C), these authors reported no statistically significant difference in the total phenolic compounds compared to methanol and ethanol aqueous mixtures (less than 20% and 60% v/v water content for ethanol and methanol aqueous mixtures respectively and extraction temperature of 60 °C).

Based on these results, one of the main objectives of this work was to provide a comprehensive study of total polyphenol content (TPC) extraction kinetics from BSG by using water as solvent, having the advantage of being “the greenest solvent”. Enhanced extraction kinetics have been explored by using UAE and results have been compared with mechanical stirring extraction. The effect of particle size, solvent to solid ratio and solvent polarity on the TPC extraction kinetics has been analyzed. TPC extraction kinetics were fitted to different empirical models as proposed by Kitanovic et al. [8]. Individual phenolic compounds were identified, quantified, and compared with other hydrolytic methods, such as enzymatic, basic, and acid hydrolysis. Other components present in the extracts such as soluble proteins were also measured. Finally, a further concentration step was performed by centrifuge ultrafiltration

## 2. Materials and methods

### 2.1. Raw material

BSG samples were obtained from Brebajes del Norte S.L. (Dolina, craft beer) a local brewery factory in Burgos (Spain) with an initial moisture content higher than 80% w/w. Samples were water washed and dried in an air convection oven at 45 °C until a final moisture content of 8% w/w. Dry BSG was stored at 4 °C until use and it was used in the extraction study. To study the effect of particle size on TPC extraction kinetics, dry samples were ground in a QILIVE, 5321 miller. Particle size distribution of the original and ground feedstock was determined by a vibratory sieve shaker (CISA, RP.09) and is presented in **Table 1.1**. A total of 65.9% w/w of ground BSG presented a particle size lower than 0.5 mm, while for the original feedstock, about 85% w/w of the particles presented a size between 2 and 4 mm.



**Table 1.1.** Particle size distribution of the original BSG and ground BSG

Original BSG		Ground BSG	
Size, mm	Mass percentage, %	Size, mm	Mass percentage, %
> 4	4.4	> 1	2.9
2 - 4	84.5	0.5 - 1	31.3
1 - 2	10.3	0.25 - 0.50	34.8
0.5 - 1	0.71	0.125 - 0.25	24.6
0.25 - 0.50	0.06	< 0.125	6.5

## 2.2. Biomass characterization

BSG chemical composition was determined according to the NREL standard protocols to determine structural carbohydrates (cellulose and hemicellulose), lignin, moisture, total solids, ash, total extractives, and protein [9].

Starch analysis was carried out using the "Total starch assay kit" (Megazyme, Wicklow, Ireland).

## 2.3. Mechanical stirring and ultrasound assisted extraction

For both extraction methods, a specific amount of dry BSG was suspended in the selected solvent and extraction was performed at the desired extraction temperature for 24 h and 1 h in a mechanical stirring system and in the UAE extraction equipment, respectively.

For UAE, a 750 W Sonics Material™ with a 13 mm probe was used. Samples were processed at a constant ultrasound frequency of 20 kHz. The extraction temperature was controlled by circulating water through the external jacket of the extraction vessel connected to a thermostat, which was fixed to different temperatures depending on the final working temperature. The BSG sample and the solvent were introduced in the thermostated vessel ( $\Phi = 4.8$  cm,  $V = 199$  cm<sup>3</sup>) and the probe was submerged in the mixture at a constant depth of 2 cm from the bottom of the vessel. The amplitude was fixed at 100% and the temperature and energy input were recorded along the extraction experiments. UAE was performed in pulse mode (5 s on and 5 s off). Total treatment time under pulsed conditions,  $t_p$ , was determined as:

$$t_p = t_c \left[ 1 + \left( \frac{1}{R} \right) \right] \quad [1.1]$$

where  $t_c$  is the corresponding time of exposure in a continuous experiment, 30 min, and  $R$  is the ratio on/off. The ultrasonic Power Density, PD (J/s·g), was evaluated as:

$$PD = \frac{E}{t \cdot m} = \frac{P}{m} \quad [1.2]$$

where  $E$ , is the energy input (J),  $t$  is the ultrasonication time (s),  $P$ , the ultrasonic power (J/s = W) and  $m$  is the BSG mass (g). Based on equation 1.2, by varying BSG mass, at fixed amplitude, the power density was also varied and its effect on polyphenol extraction was analyzed.

The effect of particle size on TPC extraction kinetics have been determined by mechanical stirring extraction and UAE by using deionized water as solvent. Other operating variables were also studied, such as the solvent volume to BSG mass ratio (v/w) in the range from 35.3 to 10.9 mL/g<sub>BSG, dry</sub>, temperature (39–58 °C) and solvent polarity by performing the UAE with different ethanolic aqueous mixtures as solvent.

Results were expressed as extraction yield, defined as mg of gallic acid equivalent (GAE)/g<sub>BSG, dry</sub>. Results were also compared in terms of productivity ( $Pr$ ), being the yield obtained in a certain range of time,  $\Delta t$ :

$$Productivity, Pr = \frac{mg \text{ GAE}}{g_{dry, BSG} \Delta t} \quad [1.3]$$

## 2.4. Hydrolysis treatments

The release of TPC by UAE has been compared with enzymatic, acid and basic hydrolysis. Acid hydrolysis was performed similar to Arranz and Saura Calixto [10]. Briefly, 200 mg of dry BSG were incubated with a mixture of 20 mL of methanol and 2 mL of concentrated sulfuric acid for 20 h at 85 °C. Basic hydrolysis was carried out as previously described by Benito-Román et al. [11]. Two grams of dry BSG was digested with 40 mL of NaOH 2 M for 4 h at 65 °C. The mixture was acidified to pH 2–3 by the addition of hydrochloric acid and centrifuged. Enzymatic hydrolysis was carried out by incubating the BSG with different amounts of the commercial preparation of xylanase from *Trichoderma Longibrachiatum* (Biocon Española, S.A.) at different concentrations 1%, 3%, and 6% w/w referred to the BSG mass for 24 h. Temperature and solvent to BSG mass

ratio (v/w) were fixed at 47 °C and 21.7 mL water:  $g_{BSG,dry}$ , respectively. Samples were collected and stored at -18 °C until analysis.

## 2.5. Total polyphenol content (TPC) and antioxidant capacity

TPC were determined by using the Folin–Ciocalteu reagent (VWR). One hundred microliters of the BSG extract were mixed with 2.8 mL of water, and subsequently with 100  $\mu$ L of the Folin–Ciocalteu reagent. After that, 2 mL of sodium carbonate 7.5% (w/v) were added and the reaction started. Absorbance was measured after 60 min of reaction at 750 nm. A blank was also prepared using water instead of the extract. A calibration curve was prepared with standard solutions of gallic acid by following the same colorimetric method and results were expressed as mg of GAE per gram of dry BSG.

The FRAP method was performed according to Benzie and Strain [12], 2850  $\mu$ L of the working FRAP reagent were added to 150  $\mu$ L of the extract and incubated at 37 °C for 30 min. Absorbance was read at 593 nm. As standard, a solution of  $FeSO_4 \cdot 7H_2O$  (0.1 M) was used. Results were expressed in  $\mu$ moles of  $Fe^{2+}$  per gram of dry BSG.

## 2.6. Identification and quantification of extracts components

Chromatographic separation was performed on HPLC/DAD Agilent 110 with a Kinetex® 5  $\mu$ m Biphenyl 100 Å, 250 × 4.6 mm column (Phenomenex). The mobile phase consisted of (A) ammonium acetate 5 mM with acetic acid (1%; v/v) in water and (B) ammonium acetate 5 mM with acetic acid (1%; v/v) in acetonitrile. The gradient profile was the following: from 0 to 7 min 2% of solvent B (isocratic), from 7 to 20 min from 2% to 8% solvent B, from 20 to 35 min from 8% to 10% solvent B and from 35 to 55 min 10% to 18% solvent B and post time of 10 min. The flow rate was set to 0.8 mL/min and temperature column was 25 °C. UV detection was done at 240, 280, 330, 340, 350, and 370 nm. Before injection, extracts were filtered through 0.45  $\mu$ m pore size. HP ChemStation software was employed to collect and analyze the chromatographic data delivered by the diode array detector and own library was used to identify the different polyphenols by comparing retention times and spectral data with those of authentic standards. p-Hydroxybenzoic acid, protocatechuic aldehyde, syringic aldehyde, vanillic acid, vanillin, syringic acid, p-coumaric acid, ferulic acid, and sinapic acid standards were purchased from Sigma-Aldrich. Standard solutions were prepared by dissolution of the compound in methanol.

Identification and quantification of glucose, xylose and arabinose were performed by HPLC-RID Agilent 1260 with an Aminex HPX-87H column (300 × 7.8 mm, Bio-Rad) using H<sub>2</sub>SO<sub>4</sub> 10 mM as mobile phase with a flow rate of 0.6 mL/min. The column and detector were maintained at 40 °C.

Protein content was determined by total nitrogen measured by a Shimadzu TOC-V-CSN analyzer with a conversion factor of 6.25.

## 2.7. Solvent extraction kinetics

TPC extraction kinetic curves for the different extraction methods and extraction conditions were fitted to different empirical models described and collected by Kitanovic et al. [8]. Among them, in this work, the power law model and the Weibull model were considered.

### 2.7.1. Power law model

The power law model has been proposed to describe the extraction mechanism of any compound through non-swelling material:

$$\text{Extraction yield, mg GAE/g}_{dry,BSG} = Bt^n \quad [1.4]$$

where  $t$  is extraction time,  $B$  is a constant incorporating the characteristics of the particle-active substance system and  $n$  is the diffusional exponent, with values lower than 1 for most vegetable materials. This model does not approach to a limit with time.

### 2.7.2. Weibull's model

The Weibull model was expressed as:

$$\text{Extraction yield, mg GAE/g}_{dry,BSG} = A(1 - \exp(-kt^n)) \quad [1.5]$$

where  $t$  is the extraction time,  $A$  is a kinetic parameter that represents the maximum extraction yield at infinite extraction time and  $k$  is a kind of extraction rate constant. The exponent  $n$  is the shape parameter of the extraction curve. If  $n > 1$ , the curve is sigmoidal with upward curvature, and if  $n < 1$ , the curve is parabolic with a high initial slope followed by an exponential shape.

To estimate the kinetic parameters, non-linear regression was performed by using the Marquardt algorithm (Statgraphics X64). Experimental results were then compared with those of the model prediction through the values of the Root Mean Square Deviation (RMSD) between experimental and calculated extraction yield:

$$RMSD = \sqrt{\frac{\sum_{i=1}^n (C_{p,exp} - C_{p,calc})^2}{n}} \cdot 100 \quad [1.6]$$

where  $n$  is the number of experimental data points in each extraction.

## 2.8. Centrifuge Ultrafiltration

Aqueous extracts obtained by UAE were treated by centrifuge ultrafiltration by using Amicon Ultra centrifugal filters with different Nominal Molecular Weight Limit (NMWL): 3000, 10,000, and 100,000 Dalton. The regenerate cellulose membrane of the filters allowed high recovery. A ratio of permeate: retentate volume of 3:1 mL was fixed. Protein, sugars, and polyphenols content was determined, and the retention ratio was evaluated as:

$$R = 1 - \frac{C_{i,p}}{C_{i,f}} \cdot 100 \quad [1.7]$$

where  $C_{i,p}$  and  $C_{i,f}$  are the concentrations in the permeate ( $p$ ) and initial extract ( $f$ ), respectively, and  $i$  refers to polyphenol compounds, protein or sugars. The yield ( $Y$ ) in the permeate and retentate ( $r$ ) was evaluated as a mass ( $m$ ) ratio [13]:

$$Y(\%) = \frac{m_{i,p-r}}{m_{i,f}} \cdot 100 \quad [1.8]$$

## 2.9. Statistical Analysis

Statistical difference and correlation coefficient between total polyphenol compounds and antioxidant capacity were obtained using the software Statgraphics X64. The results are presented as the mean  $\pm$  standard deviation of at least three replicates. The significance of the differences was determined based on an analysis of the variance with the Fisher's Least Significant Difference (LSD) method at  $p$ -value  $\leq 0.05$ .

### 3. Results and discussion

#### 3.1. Biomass characterization

**Table 1.2** lists the BSG composition according to the NREL protocols. The polysaccharide fraction (starch, cellulose and hemicellulose) accounts for  $52.1 \pm 3.6\%$  in a dry weight basis. The local BSG used in this work showed an important amount of starch,  $7.87\%$  w/w ( $78.7 \text{ mg}_{\text{starch}}/\text{g}_{\text{BSG,dry}}$ ), that can be associated with the source of the BSG. Robertson et al. [14] reported that the starch content of BSG from lager and ale producers shows significant differences. These authors reported medium values around  $97.6 \text{ mg}_{\text{starch}}/\text{g}_{\text{BSG,dry}}$  and  $35.8 \text{ mg}_{\text{starch}}/\text{g}_{\text{BSG,dry}}$  for ale and larger producers, respectively. According to the two-step extractives determination proposed in the NREL, extractives of BSG were found to be  $26.03 \pm 0.98\%$  (w/w) with a TPC of  $2.72 \pm 0.04$  and  $1.61 \pm 0.15 \text{ mg}_{\text{GAE}}/\text{g}_{\text{BSG,dry}}$  for water and ethanol extractives respectively.

**Table 1.2.** Chemical composition of BSG from a local Spanish brewery.

Component	g/100 g <sub>BSG,dry</sub>
Extractives in water	$24.25 \pm 0.64$
Extractives in ethanol	$1.78 \pm 0.15$
Starch	$7.87 \pm 0.20$
Cellulose	$18.18 \pm 1.64$
Hemicellulose	$26.05 \pm 1.79$
Insoluble Lignin	$13.53 \pm 0.45$
Soluble lignin	$4.33 \pm 0.06$
Proteins	$17.84 \pm 0.14$
Lipids	$5.9 \pm 0.002$
Ash	$2.92 \pm 0.02$

## 3.2. Kinetics of extraction of phenolic compounds from BSG

Taking into account the water extractive fraction of the BSG, valorization of its polyphenol fraction was studied by ultrasound assisted and conventional extraction by using water as solvent.

### 3.2.1. Comparison of UAE and mechanical stirring extraction

First, TPC extraction kinetics were determined by mechanical stirring extraction and UAE to assess the improvement of UAE (**Figure 1.1a** and **Figure 1.1b**, respectively). The temperature and solvent volume to dry BSG mass ratio (v/w) were fixed at 47 °C and 21 mL:g<sub>BSG,dry</sub>, respectively. **Figure 1.1b** also shows the temperature profile for a 30 min sonication time (60 min of total experiment) treatment in pulse mode at 100% amplitude (79 μm), for a temperature of the jacketed water of 30 °C. A sharp temperature increase was observed during the first three minutes of sonication, and then it reached a plateau with a mean value of 47 ± 1 °C. Similar temperature profiles have been reported in the literature for sonication treatments [15].

For both extraction methods, faster kinetics were obtained when using ground BSG due to enhanced internal mass transfer. Comparing UAE and mechanical stirring extraction, a significant improvement was observed by UAE observing much faster extraction kinetics, showing the effectiveness of UAE. For ground BSG, by mechanical stirring agitation, extraction was nearly completed after 24 h, but by UAE, extraction was completed after only 1200–1800 s. Comparing final extraction yields by the two extraction methods, an increase of 55% and 30% was observed for non-ground and ground BSG, respectively. It is clear that the improvement of UAE was less pronounced when using ground BSG particles. This fact was also observed by Galvan d'Alessandro [16] in the extraction of polyphenols from black chokeberry. These authors concluded that the positive effect of sonication was less evident, when the operating conditions were favorable for the extraction of polyphenols, as it has been also observed in this work.

Productivity at the final extraction time for both extraction methods was 0.109 mg<sub>GAE</sub>/g<sub>BSG,dry</sub>·min and 0.0078 mg<sub>GAE</sub>/g<sub>BSG,dry</sub>·min for UAE and conventional extraction, respectively. It is clear the higher productivity obtained by UAE. Furthermore, at 5 min of extraction time (300 s) 90% of the final extraction yield was already achieved by UAE, while only 65% by mechanical stirrer agitation.

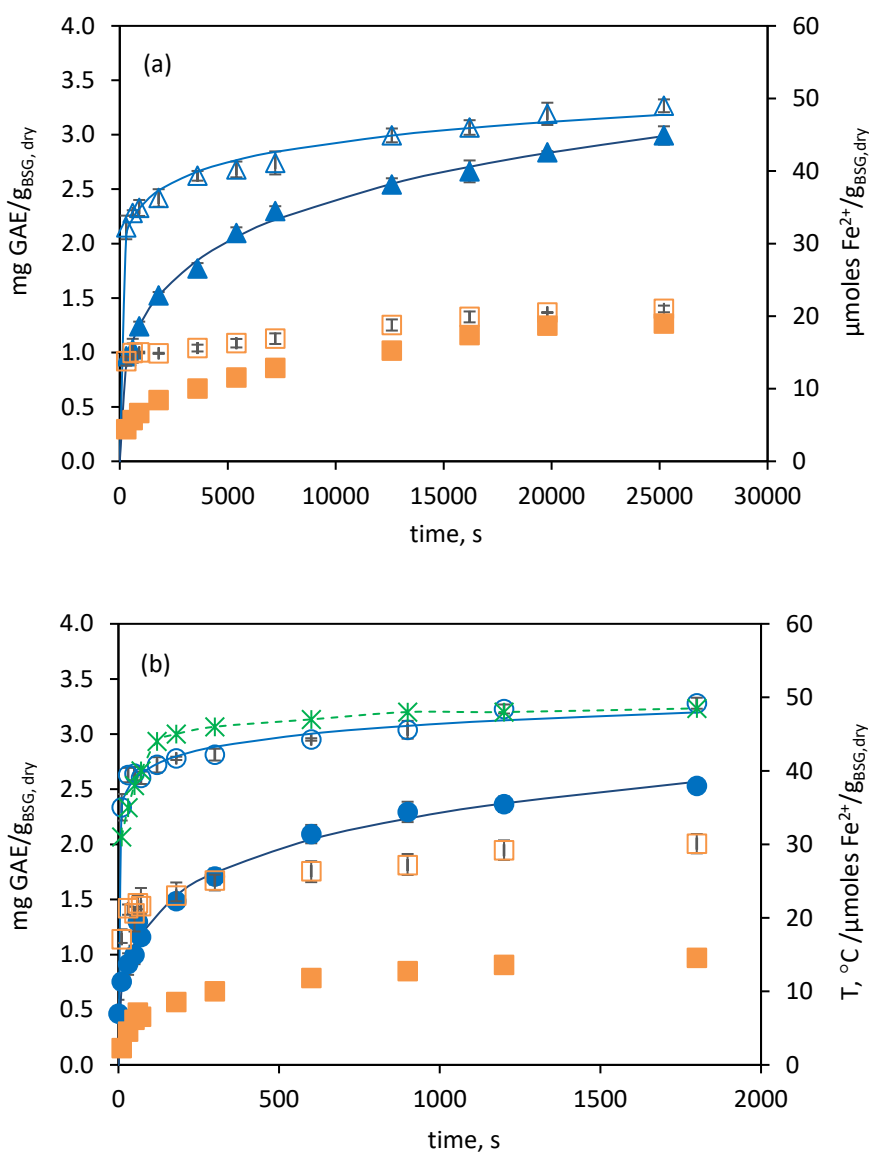


**Figure 1.1.** TPC water extraction kinetics at 47 °C and 21.7 mL:g<sub>BSG,dry</sub> (a) mechanical stirring extraction ( $\Delta$  ground,  $\blacktriangle$  non ground) (b) UAE ( $\circ$  ground,  $\bullet$  non ground). The secondary axis represents the reducing power of the extracts as determined by the FRAP assay ( $\square$  ground,  $\blacksquare$  non ground) and the temperature profile along UAE extraction ( $*$ ). Continuous lines represent the Weibull model.



**Figure 1.1 a,b** also show the antioxidant capacity along extraction time, as determined by the FRAP assay, observing in all cases an increase of the reducing power of the extract as the extraction yield of TPC increased. A multiple variable analysis was performed to determine the correlation between both variables yielding a positive correlation between them for p-values below 0.05 with a correlation coefficient of 0.9462.

### 3.2.2. Effect of Solvent to Mass Ratio by UAE

The effect of solvent to dry mass BSG ratio (v/w) on the extraction of TPC was studied at 47 °C in the range from 10.9 to 35.3 mL:g<sub>BSG,dry</sub>. The results are presented in **Figure 1.2 a,b** in terms of extract concentration, mg<sub>GAE</sub>/L, and extraction yield, mg<sub>GAE</sub>/g<sub>BSG,dry</sub>, respectively.

**Figure 1.2 a** shows that polyphenol concentration in the extract (mg<sub>GAE</sub>/L) increased as the ratio solvent: g<sub>BSG,dry</sub> decreased in the range from 35.3 to 10.9 mL:g<sub>BSG,dry</sub>. However, the extraction yield in terms of mg<sub>GAE</sub>/g<sub>BSG,dry</sub> reached a plateau from ratio values higher than 21.7 mL:g<sub>BSG,dry</sub>, while it decreased by using lower solvent:g<sub>BSG,dry</sub> ratios.

This can be also observed in **Figure 1.3**, where final extraction yield as mg<sub>GAE</sub>/g<sub>BSG,dry</sub> after 1800 s of extraction was plotted as a function of mL water: g<sub>BSG,dry</sub> ratio together with the specific power density, W/ g<sub>BSG,dry</sub>. By increasing the solvent: g<sub>BSG,dry</sub> ratio, the specific power density also increased, observing a linear dependence, PD (J/s·g) = 1.055 (mL: g<sub>BSG,dry</sub>) + 0.191, R<sup>2</sup> = 0.9983). Therefore, taking into account the TPC yield and the power density by UAE, the ratio 21.7 mL: g<sub>BSG,dry</sub> was fixed to study the effect of temperature and solvent type.

In the literature, an increase in extraction yield was also observed by solvent bath extraction (maceration) for 60 min when using a 70% ethanol aqueous mixture at 60 °C with values of 2.59, 2.74, and 3.07 mg<sub>GAE</sub>/g<sub>BSG,dry</sub> at 10, 20, and 30 mL<sub>solvent</sub>/g<sub>BSG,dry</sub>, respectively [17]. These authors explained that higher liquid/solid ratio implies higher concentration gradient between the solid and the bulk of the liquid, resulting in a greater driving force for diffusion of compounds to the solvent and higher extraction efficiency.

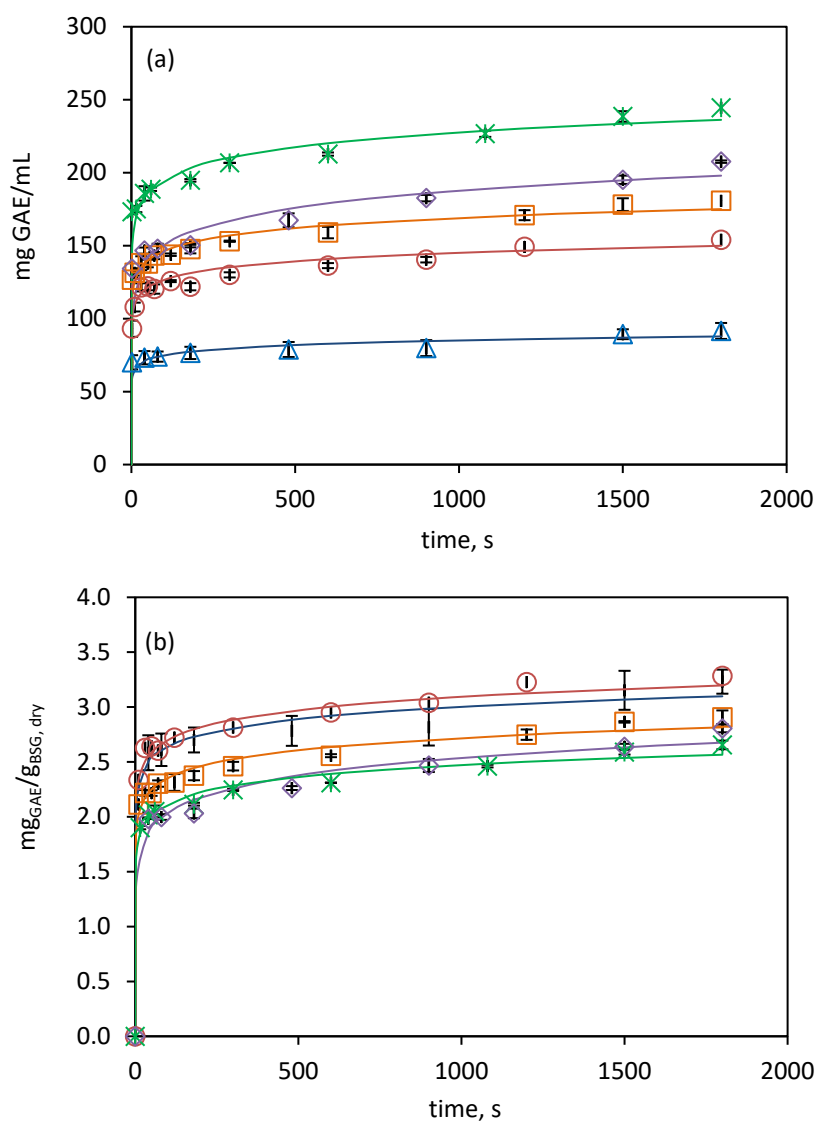


**Figure 1.2.** (a) Total polyphenol content in the water extracts as  $\text{mg}_{\text{GAE}}/\text{L}$  as a function of time  
(b) Extraction yield,  $\text{mg}_{\text{GAE}}/\text{g}_{\text{BSG, dry}}$  for UAE at 47 °C, at different solvent:mass ratios (mL:g<sub>BSG, dry</sub>)  
as a function of time: \* 10.9;  $\diamond$  13.6;  $\square$  18.1;  $\circ$  21.7;  $\triangle$  35.3. Continuous lines represent the  
Weibull model.

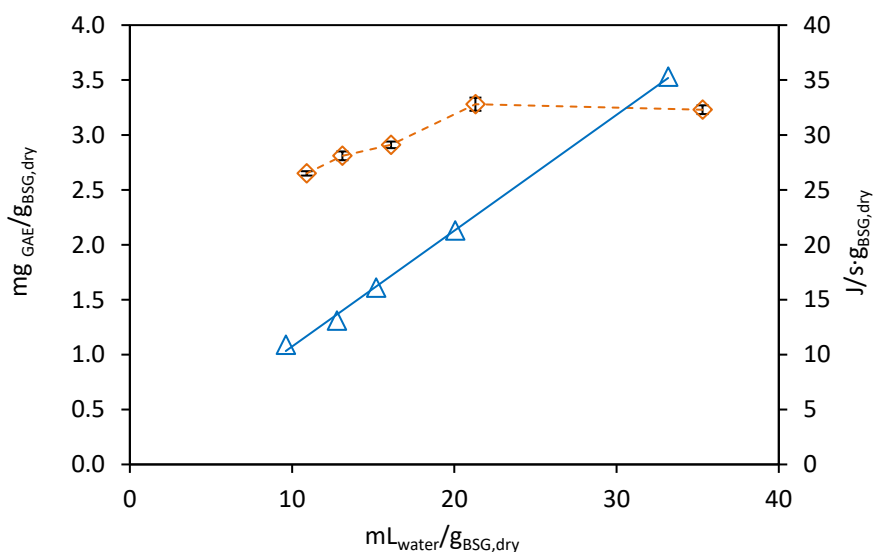


**Figure 1.3.** TPC water extraction yield, mg GAE/g<sub>BSG,dry</sub> (◇) and power density, (PD, J/s·g) (△) as a function of solvent:mass ratio after 1800 s of UAE at 47 °C. Continuous line represents the linear fitting of PD (PD = 1.0547 (mL:g) + 0.1905, R<sup>2</sup> = 0.9983).

### 3.2.3. Effect of temperature on polyphenol extraction kinetics by UAE

In this work, TPC extractions by UAE have been carried out at three different temperatures, 39, 47, and 58 °C (**Figure 1.4**) at a ratio of 21.7 mL:g<sub>BSG,dry</sub>. Temperature affected positively TPC extraction kinetics by increasing temperature from 39 to 47 °C. Further increase in the temperature did not bring a faster kinetic extraction or higher extraction yield. An increase of temperature results in an increase of diffusivity and a decrease of viscosity and surface tension of the solvent. Therefore, faster extraction rate might be expected by increasing temperature. However, an increase in temperature also results in an increase of solvent vapor pressure that made more solvent vapor enter the bubble and collapse less violently reducing the sonication effects [7]. In this work, this effect was observed at the highest temperature essayed. Lower water viscosity and higher diffusivity with temperature were compensated by the increase of the solvent vapor pressure.

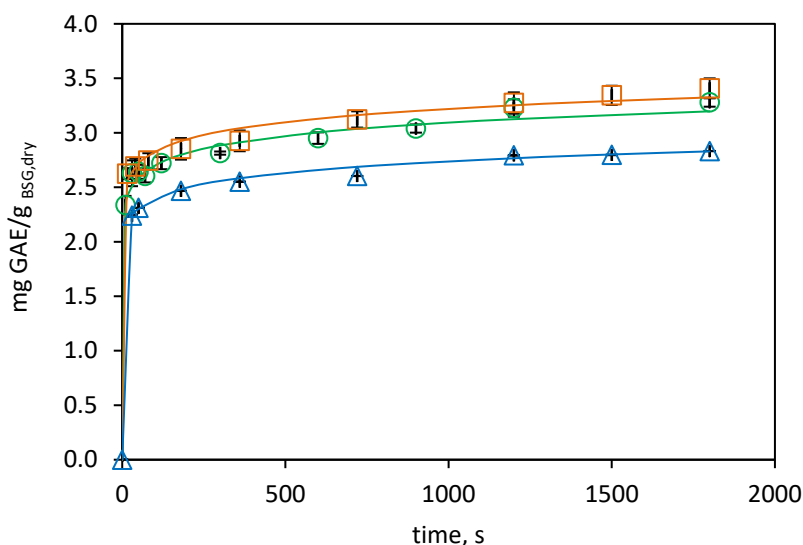


**Figure 1.4.** Effect of temperature on TPC extraction kinetics by UAE ( $\Delta$  39 °C,  $\circ$  47 °C;  $\square$  58 °C).

Continuous lines represent the Weibull model.

Other studies found in the literature reported temperature as one of the positive variables on the extraction of TPC from black chokeberry in the temperature range from 20 to 80 °C [16]. These authors also reported that the effect of temperature on kinetics of water extraction of TPC from black chokeberry was less significant for ground samples than for berries cut in half where extraction was not very efficient and solvent penetration and extraction were hampered [16].

### 3.2.4. Effect of ethanol concentration on polyphenol extraction kinetics by UAE

In the literature, other solvents such as ethanol, methanol and acetone and their corresponding aqueous mixtures have been used to extract polyphenols from plant matrixes. In this work, different ethanol aqueous mixtures were also explored to determine the effect of solvent polarity on TPC extraction kinetics. **Figure 1.5** shows the kinetics of TPC extraction from ground BSG using water, pure ethanol and different water-ethanol mixtures at 47°C and 21.7 mL:g<sub>BSG,dry</sub>.

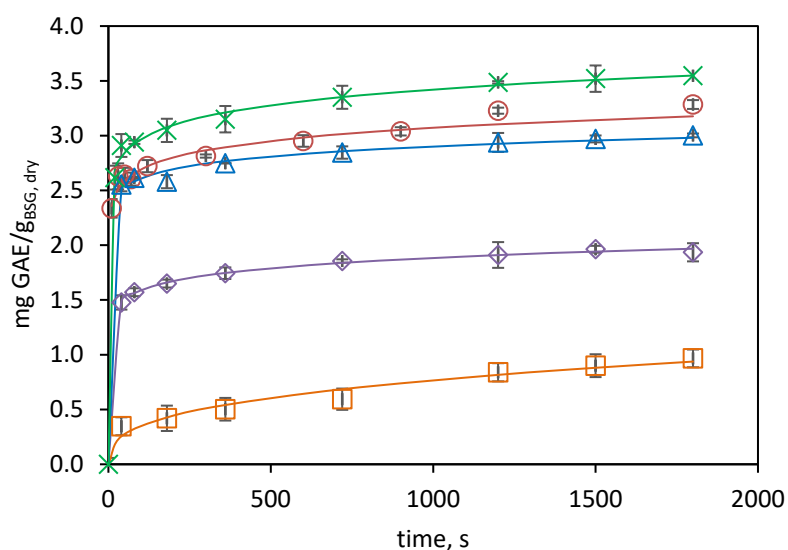


**Figure 1.5.** Effect of ethanol concentration on TPC extraction kinetics by UAE at 47 °C and 21.7

mL:  $g_{BSG,dry}$ : ○ water, \* 20% ethanol, △ 50% ethanol, ◇ 80% ethanol, □ 100% ethanol.

Continuous lines represent the Weibull model

TPC extraction was dependent on the type of solvent used and therefore on the polarity of the solvent. The best results were obtained for the hydroalcoholic mixture with 20% of ethanol. Pure water as solvent gave better extraction kinetics and higher extraction yields than pure ethanol or ethanol alcoholic mixtures with high ethanol percentage. Therefore, water could create a more polar medium that facilitates the extraction of phenolic compounds. Water and mixtures with low ethanol concentration could access to cells, but high concentration of ethanol could cause protein denaturation, preventing the dissolution of polyphenols, and then influencing the extraction [17]. Socaci et al. [2] found that an increase in ethanol concentration from 60% to about 68% increased TPC extraction while higher ethanol concentration led to a gradual decrease in TPC. The higher extraction efficiency for the 20:80 (EtOH:water) mixture could be attributed to the lower value of the dielectric constant for ethanol:water mixtures than the value for pure water that increases the solubility of phenolic compounds in hydroalcoholic mixtures with low ethanol content.

Dent et al. [18] carried out the study of TPC extraction from Dalmatian wild sage by conventional solvent extraction with ethanol and acetone aqueous mixtures and water as

solvent. These authors found a maximum of total polyphenol content with 30% ethanol or acetone. However, these authors, concluded, that the differences in TPC between 30% ethanol and 50% acetone aqueous extracts with water extracts were not significant. Therefore, in this work, taking into account the green chemistry principle, water was considered as an efficient solvent for TPC extraction from BSG.

### 3.2.5. Kinetic modelling

TPC extraction kinetics were fitted to different empirical models as described in **Section 2.7**. **Table 1.3** lists the parameter of the models essayed. Both models, the power law and the Weibull models, fitted the data quite well with a mean RMSD for all the kinetics of 7.45 and 7.50, respectively. For both models, the exponent of time,  $n$ , called the diffusion coefficient and the shape parameter for the power law and Weibull models, respectively, followed the same tendency. It presented low values for TPC extraction of ground BSG, with values lower than 0.1, except when using pure ethanol as solvent. The values of  $n$  of the power law model showed that Fickian diffusion controlled TPC extraction from BSG, while values of  $n < 1$  for the Weibull model described the parabolic shape of the extraction curves with a high initial slope.  $B$  and  $A$  parameters for the power law and the Weibull models, respectively, also followed the same tendency. These parameters presented a maximum at 20% w/w ethanol as solvent, increased with decreasing the particle size and decreased by decreasing the ratio solvent:BSG in the range covered in this work. Regarding  $k$  parameter for the Weibull model, it can be considered as the extraction rate constant having higher values for the fastest extraction kinetics. **Figures 1.1, 1.2, 1.4 and 1.5** include the Weibull model fitting, since it was considered a more realistic approach.

### 3.3. Determination of extract components

**Table 1.4** shows the total amount of individual phenolic compounds released by UAE at 47 °C, 21.7 mL solvent: $g_{BSG,dry}$  by using water and 20% ethanol aqueous mixture as extraction solvents that could be identified by HPLC/DAD. By using water as solvent, concentration of identified individual phenolic compounds was not very high with values of  $10.0 \pm 0.5 \mu\text{g}$  of *p*-hydroxybenzoic acid/ $g_{BSG,dry}$ ,  $10.7 \pm 0.3 \mu\text{g}$  of ferulic acid/ $g_{BSG,dry}$  and  $2.8 \pm 0.2 \mu\text{g}$  of sinapic acid/ $g_{BSG,dry}$ . When using 20% ethanol as extraction solvent, similar results were obtained, although higher values for sinapic acid were quantified,  $13.4 \pm 0.3 \mu\text{g}$  of sinapic acid/ $g_{BSG,dry}$ .

In this work, hydrolytic methods have been also carried out to compare the release of phenolic compounds (**Table 1.4**). The influence of the hydrolysis technique can be observed in the results of TPC and phenolic profile. As reported in **Table 1.2**, BSG used in this work contained 13.5% of insoluble lignin that it is connected to the cell wall polysaccharides by phenolic acids, being necessary a hydrolytic method to release them [19]. After acid hydrolysis, TPC was determined as  $30 \pm 5$  mg GAE/g<sub>BSG,dry</sub>. This value is higher than the value obtained for basic hydrolysis,  $16.2 \pm 0.2$  mg GAE/g<sub>BSG,dry</sub>. In the literature, it has been reported that acid hydrolysates of wheat flour and wheat bran yielded higher total phenolic content than the corresponding alkali hydrolysates[10], similar to the results obtained in this work.

Furthermore, the amount of individual phenolic compounds released in each extraction technique was different. For basic hydrolysis  $1305.7 \pm 0.5$  µg ferulic acid/g<sub>BSG,dry</sub> were released while only  $54.4 \pm 0.3$  by acid hydrolysis. The same trend was observed in the acid and basic hydrolysis of wheat bran by Arranz and Saura Calixto [10],  $219 \pm 5$  and  $60 \pm 2$  mg ferulic acid/100 g of fresh weight wheat bran by basic and acid hydrolysis, respectively. The p-coumaric acid/ferulic acid ratio (2.43) obtained for basic hydrolysis was consistent with the values reported in the literature (1.74–2.97) [20]. Phenolic acids esterified to the cell wall were more easily released under basic conditions, due the higher solubility of the lignin under basic conditions. HPLC chromatograms for phenolic standards and basic hydrolysis are presented in **Figure 1.6**. The percentage match obtained comparing the UV spectra of authentic standards with the UV spectra of the selected peaks were the following: p-hydroxybenzoic acid 95.8%, vanillic acid 98.83%, syringic acid 90.29%, p-coumaric acid 99.99%, vanillin 99.16%, ferulic acid 99.6%, and sinapic acid 90.21%. Protocatechuic aldehyde and syringic aldehyde were not identified in any of the extracts.

**Table 1.3.** Kinetic model parameters for TPC extraction from BSG

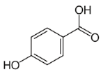
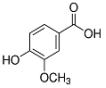
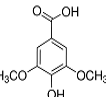
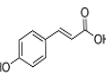
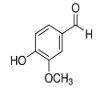
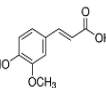
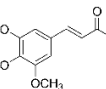
Extraction mode	Pre-treatment	T, °C	Solvent	mL: g <sub>BSG,dry</sub>	Power law model			Weibull model			
					B	n	RMS	A	k	n	RMS
MS	--	47	Water	21.7:1	0.208	0.264	5.74	5.2450	0.027	0.341	4.88
UAE	--	47	Water	21.7:1	0.431	0.241	7.32	4.1643	0.088	0.319	6.56
MS	ground	47	Water	21.7:1	1.197	0.097	5.23	6.133	0.197	0.127	6.37
UAE	ground	47	Water	21.7:1	2.066	0.057	6.47	5.895	0.415	0.084	6.80
UAE	ground	47	Water	35.3:1	2.027	0.0570	8.89	5.699	0.429	0.080	10.10
UAE	ground	47	Water	18.1:1	1.744	0.065	5.97	5.120	0.4070	0.090	6.52
UAE	ground	47	Water	13.6:1	1.297	0.097	8.94	5.796	0.244	0.125	9.40
UAE	ground	47	Water	10.8:1	1.438	0.084	9.22	4.643	0.391	0.096	5.92
UAE	ground	39	Water	21.7:1	1.837	0.057	20.68	6.664	0.316	0.075	21.82
UAE	ground	58	Water	21.7:1	2.159	0.058	9.66	6.418	0.403	0.079	9.93
UAE	ground	47	20% EtOH	21.7:1	2.229	0.062	4.92	8.144	0.314	0.080	4.97
UAE	ground	47	50% EtOH	21.7:1	2.110	0.046	4.37	4.830	0.559	0.072	4.59
UAE	ground	47	80% EtOH	21.7:1	1.130	0.074	1.59	3.458	0.376	0.107	1.52
UAE	ground	47	100% EtOH	21.7:1	0.073	0.342	5.35	3.491	0.019	0.372	5.68

MS: mechanical stirring, UAE: ultrasound assisted extraction.



## CHAPTER 1

*Water ultrasound-assisted extraction of polyphenol compounds from brewer's spent grain: Kinetic study, extract characterization and concentration***Table 1.4.** Individual phenolic compounds in the different extracts ( $\mu\text{g}/\text{g}_{\text{BSG,dry}}$ ).

Compounds	Formula	UAE-W	UAE-20EtOH	Acid-Hydrolysis	Alkaline-Hydrolysis	Xylanase 1%	Xylanase 3%	Xylanase 6%
p-hydroxybenzoic acid		$10.0 \pm 0.5^a$	$10.0 \pm 0.7^a$	n.d.	$59.3 \pm 2.2^b$	n.d.	n.d.	n.d.
Vanillic acid		n.d.	n.d.	n.d.	$48.8 \pm 1.5^c$	$17.9 \pm 1.1^a$	$42.6 \pm 2.3^b$	$61.2 \pm 3.3^d$
Syringic acid		n.d.	n.d.	n.d.	$106.1 \pm 5.7$	n.d.	n.d.	n.d.
p-Cumaric acid		n.d.	n.d.	n.d.	$538.2 \pm 4.4^b$	$5.9 \pm 1.4^a$	$5.3 \pm 1.7^a$	$5.3 \pm 0.4^a$
Vanillin		n.d.	n.d.	n.d.	$217.2 \pm 1.4^c$	$110.5 \pm 2.6^a$	$191.2 \pm 0.1^b$	$203.5 \pm 10^{b,c}$
Ferulic acid		$10.7 \pm 0.3^a$	$9.5 \pm 0.3^a$	$54.4 \pm 0.3^b$	$1305.7 \pm 0.5^e$	$52.4 \pm 0.9^b$	$185.8 \pm 4.5^c$	$292.4 \pm 2.6^d$
Sinapic acid		$2.8 \pm 0.2^a$	$13.5 \pm 0.3^{c,d}$	$31.1 \pm 0.5^f$	$27.2 \pm 1.2^e$	$7.5 \pm 0.2^b$	$12.9 \pm 0.6^c$	$14.9 \pm 1.2^d$
TPC (Folin-Ciocalteu) $\text{mg}_{\text{GAE}}/(\text{g}_{\text{BSG,dry}} \cdot \text{min})$		$3.28 \pm 0.12^{a_{0.5h}}$	$3.55 \pm 0.07^{a_{0.5h}}$	$30 \pm 5^{e_{24h}}$	$16.2 \pm 0.2^{c_{4h}}$	$7.2 \pm 0.2^{b_{24h}}$	$25.2 \pm 0.1^{d_{24h}}$	$42.0 \pm 0.4^{f_{24h}}$
Productivity, $\text{mg}_{\text{GAE}}/(\text{g}_{\text{BSG,dry}} \cdot \text{min})^*$		$0.109 \pm 0.002^{a,b}$	$0.118 \pm 0.004^b$	non-determined	$0.55 \pm 0.04^c$	$0.050 \pm 0.004^a$	$0.065 \pm 0.002^{a,b}$	$0.087 \pm 0.001^{a,b}$

n.d.: non detected. Values with different letters in each column are significantly different when applying the Fisher's least significant differences (LSD) method at  $p\text{-value} \leq 0.05$ .

\* Evaluated after 30 min of extraction

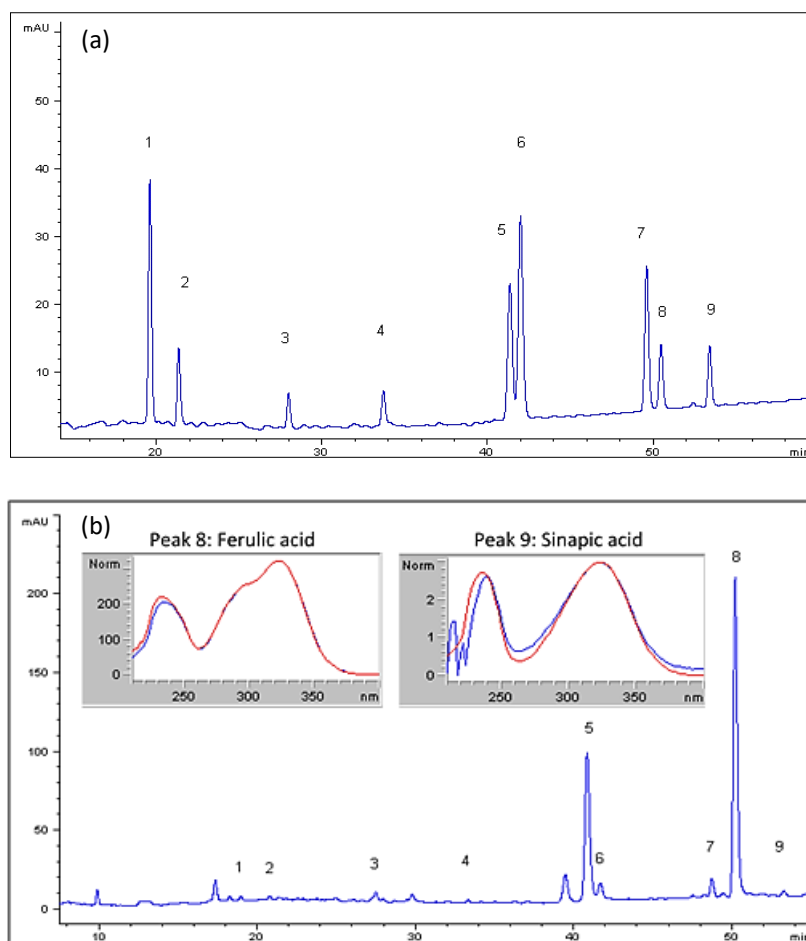


**Figure 1.6.** HPLC/DAD chromatograms at 280 nm of individual phenolic standards **(a)** and obtained after alkali hydrolysis of BSG **(b)**. 1, p-Hydroxybenzoic acid; 2, protocatechuic aldehyde; 3, vanillic acid; 4, syringic acid; 5, p-coumaric acid; 6, vanillin; 7, syringic aldehyde; 8, ferulic acid; and 9, sinapic acid.

Moreira et al. [21] determined the TPC of different types of BSG with a maximum content of  $20 \text{ mg}_{\text{GAE}}/\text{g}_{\text{BSG,dry}}$  as determined by Folin–Ciocalteu after microwave assisted extraction for 0.75% NaOH concentration. Total alkali-extractable ferulic acid and p-coumaric acid was reported as  $1.8 \text{ mg}_{\text{ferulic acid}}/\text{g}_{\text{BSG,dry}}$  and  $0.8 \text{ mg}_{\text{p-coumaric}}/\text{g}_{\text{BSG,dry}}$  from the BSG obtained from Mahou S.A[20]. Most of the literature studies have reported p-coumaric and ferulic acids as the most abundant hydroxycinnamic acids in BSG [6]. However, other authors found that the two main phenolic compounds were p-hydroxybenzoic and

protocatechuic acid, by using BSG as by product from the mashing process of dark larger beer [2]. As a general trend, lower amounts of hydroxycinnamic acids have been reported in different aqueous methanolic extract when comparing pale and black BSG [6]. In this work, p-hydroxybenzoic was determined, but protocatechuic acid was not detected.

**Table 1.4** also lists the TPC and the identified individual phenolic compounds obtained by enzymatic hydrolysis with a commercial xylanase. It can be observed that an increase in the xylanase concentration (w/w, referred to BSG), led to an increase of TPC extraction yield. However, at 6% w/w of xylanase, a release of 23% and 1% of total alkali-extractable ferulic acid p-coumaric acid, respectively, was only obtained. Bartolomé and Gómez-Cordovés [20] determined the release of ferulic and p-coumaric acid by different commercial enzyme preparations with ferulic acid esterase activity. These authors also found that for the most active enzyme preparation (Lallzyme preparation) the enzymatic release of these two hydroxycinnamic acids was lower than for the alkali extraction, especially for p-coumaric acid, reaching maximum values around 70% and 10% with respect to the basic hydrolysis for ferulic and p-coumaric, respectively. It can be concluded that basic conditions are needed to release the hydroxycinnamic acids.

Productivity of the different extraction or hydrolytic methods after 30 min of treatment has been listed in **Table 1.4**. Compared to xylanase hydrolysis, higher or similar values were obtained by UAE after 30 min of treatment. The highest productivity value at 30 min was obtained by alkali hydrolysis. However, the use of NaOH results in a more aggressive extraction medium.

For UAE water extracts individual sugars and soluble protein concentrations were also determined. Individual sugars concentrations were  $9.4 \text{ mg}_{\text{glucose}}/\text{g}_{\text{BSG,dry}}$ ,  $31.7 \text{ mg}_{\text{xylose}}/\text{g}_{\text{BSG,dry}}$  and  $21.8 \text{ mg}_{\text{arabinose}}/\text{g}_{\text{BSG,dry}}$ . Therefore, total arabinoxylans (AX) content in the extract was  $53.5 \text{ mg}_{\text{AX}}/\text{g}_{\text{BSG,dry}}$ , reaching 18% extraction yield of AX at the selected extraction conditions determined for TPC extraction. The efficiency of UAE in the production of AX-rich extracts from BSG was studied by Reis et al. [22] finding that a maximum of 4.8% yield could be achieved for water soluble AX for 12 min of ultrasound treatment, 92% maximum amplitude and 23 min of autoclave treatment at 120 °C after ultrasound treatment for a  $25 \text{ mL}_{\text{solvent}}/\text{g}_{\text{BSG,dry}}$  ratio. The higher yield obtained in the present work could be attributed to longer ultrasound treatment time, 30 min. In any case, these authors concluded that the

highest yield, 60%, was achieved, when alkaline ultrasound treatment was applied. The concentration of soluble protein in UAE water extracts was  $82 \pm 1 \text{ mg}_{\text{protein}}/\text{g}_{\text{BSG,dry}}$ . This value is of the same order as the one reported by Tang et al. [23] in the study of UAE of protein fraction from BSG, with an optimum yield value of  $104.2 \text{ mg}_{\text{protein}}/\text{g}_{\text{BSG}}$ . Total yield of UAE water extract was determined by weighting the extract after removing all the solvent by evaporation in an oven at  $105 \text{ }^\circ\text{C}$  until constant weight, a value of  $24 \text{ g}$  of dry extract/ $100 \text{ g}_{\text{BSG,dry}}$  was obtained. With this value, concentrations could be easily expressed in a dry extract basis instead of per gram of dry BSG, when needed.

### 3.4. Partial concentration by centrifuge ultrafiltration

The extract obtained by water solvent extraction by UAE at  $47 \text{ }^\circ\text{C}$  for a  $21.7 \text{ mL}:\text{g}_{\text{BSG,dry}}$  ratio was submitted to centrifuge ultrafiltration to partially concentrate the fraction of the total polyphenol compounds. **Figure 1.7a** shows that the TPC yield in the retentate slightly increased by decreasing the NMWL of the membrane from 31% to 41% for 100 and 3 kDa, respectively, and so it did the retention ratio. The regenerated cellulose membrane allowed a high recovery of TPC, not being adsorbed in the membrane, however, it can be observed an increase in the TPC adsorbed in the membrane (as recovered by MeOH after centrifuge ultrafiltration) by decreasing the NMWL of the membrane, reaching values up to 9% for 3 kDa. For the 10 kDa membrane, **Figure 1.7b** shows the permeate and retentate yield of the different phenolic compounds identified by HPLC DAD. Ferulic acid, sinapic acid and p-hydroxybenzoic acid preferably crossed the membrane and concentrated on the permeate, as can be also observed in the low values of the retention ratio.

The separation and concentration results of the co-extracted soluble protein fraction have been plotted in **Figure 1.7c**. The protein yield in the retentate increased by decreasing the NMWL of the membrane from 64% to 82% and a retention coefficient for protein from 53% to 76% for 100 and 3 kDa respectively. Tang et al. [13] in the study of protein concentration from BSG reported that more than 92% protein was retained by ultrafiltration membranes with molecular weight cut off of 5 and 30 kDa.

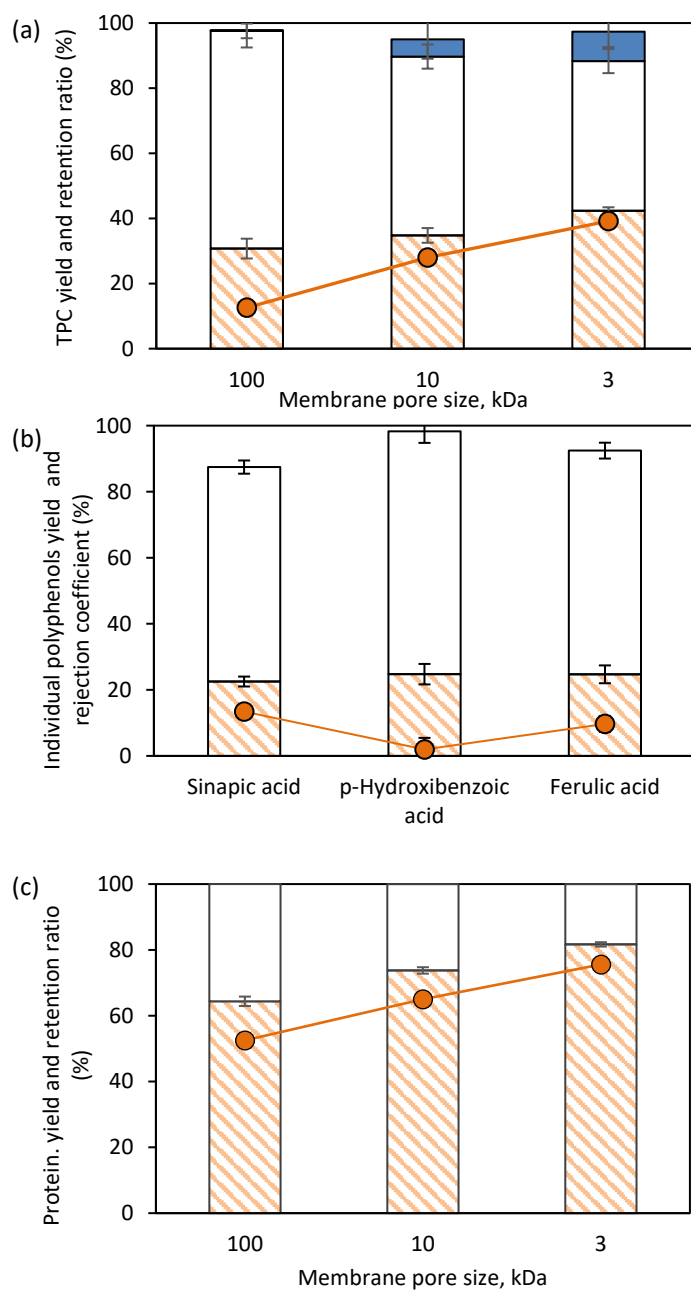


**Figure 1.7.** Permeate/retentate yield and retention ratio at different membrane NMWL (a) TPC (b) individual phenolic compounds at 10 kDa membrane size (c) protein. Columns represent the yield (▨ retentate yield, □ permeate yield, ■ TPC adsorbed in the membrane), ● retention ratio.

## 4. Conclusions

A complete brewery spent grains valorization should first include extractives valorization due to the important amount of these easily extractable compounds and the presence of important bioactive compounds, such as hydroxycinnamic acids. The analysis of the data led to the following conclusions. UAE has been shown to be more efficient in the total polyphenol extraction than conventional extraction. The most significant operating parameters were particle size and type of solvent. Water has been proved as a good solvent for total polyphenol extraction meeting the principle of green extraction. The power law and the Weibull models fitted experimental data quite well. Compared to other hydrolytic extraction methods, UAE productivity after 30 min of treatment yielded similar values as enzyme hydrolysis. However, UAE has been shown to be not as effective as basic hydrolysis to release the phenolic compounds esterified to the cell wall. By a further concentration step via centrifuge ultrafiltration a retentate rich in the soluble protein fraction can be obtained while low retention ratios were obtained for the individual phenolic compounds and sugars identified in the extracts. The results obtained in this work are useful as a preliminary step in the industrial design of a complete valorization of the BSG since large-scale ultrasonic equipment is available.

## References

- [1] S. I. Mussatto, G. Dragone, and I. C. Roberto, "Brewers' spent grain: Generation, characteristics and potential applications," *Journal of Cereal Science*, vol. 43, no. 1, pp. 1–14, 2006, doi: 10.1016/j.jcs.2005.06.001.
- [2] S. A. Socaci, A. C. Fărcaș, Z. M. Diaconeasa, D. C. Vodnar, B. Rusu, and M. Tofană, "Influence of the extraction solvent on phenolic content, antioxidant, antimicrobial and antimutagenic activities of brewers' spent grain," *Journal of Cereal Science*, vol. 80, pp. 180–187, 2018, doi: 10.1016/j.jcs.2018.03.006.
- [3] The Brewers of Europe, "Beer statistics 2018 edition," 2018.
- [4] N. G. T. Meneses, S. Martins, J. A. Teixeira, and S. I. Mussatto, "Influence of extraction solvents on the recovery of antioxidant phenolic compounds from brewer's spent grains," *Separation and Purification Technology*, vol. 108, pp. 152–158, 2013, doi: 10.1016/j.seppur.2013.02.015.
- [5] A. Paz, D. Outeiriño, N. Pérez Guerra, and J. M. Domínguez, "Enzymatic hydrolysis of brewer's spent grain to obtain fermentable sugars," *Bioresource Technology*, vol. 275, no. December 2018, pp. 402–409, 2019, doi: 10.1016/j.biortech.2018.12.082.
- [6] A. L. McCarthy *et al.*, "The hydroxycinnamic acid content of barley and brewers' spent grain (BSG) and the potential to incorporate phenolic extracts of BSG as antioxidants into fruit beverages," *Food Chemistry*, vol. 141, no. 3, pp. 2567–2574, 2013, doi: 10.1016/j.foodchem.2013.05.048.
- [7] F. Chemat, N. Rombaut, A. G. Sicaire, A. Meullemiestre, A. S. Fabiano-Tixier, and M. Abert-Vian, "Ultrasound assisted extraction of food and natural products. Mechanisms, techniques, combinations, protocols and applications. A review," *Ultrasonics Sonochemistry*, vol. 34, pp. 540–560, 2017, doi: 10.1016/j.ultsonch.2016.06.035.
- [8] S. Kitanović, D. Milenović, and V. B. Veljković, "Empirical kinetic models for the resinoid extraction from aerial parts of St. John's wort (*Hypericum perforatum* L.)," *Biochemical Engineering Journal*, vol. 41, no. 1, pp. 1–11, 2008, doi: 10.1016/j.bej.2008.02.010.
- [9] J. B. Sluiter, R. O. Ruiz, C. J. Scarlata, A. D. Sluiter, and D. W. Templeton, "Compositional analysis of lignocellulosic feedstocks. 1. Review and description of methods," *Journal of Agricultural and Food Chemistry*, vol. 58, no. 16, pp. 9043–9053, 2010, doi: 10.1021/jf1008023.
- [10] S. Arranz and F. Saura Calixto, "Analysis of polyphenols in cereals may be improved performing acidic hydrolysis: A study in wheat flour and wheat bran and cereals of the diet," *Journal of Cereal Science*, vol. 51, no. 3, pp. 313–318, 2010, doi: 10.1016/j.jcs.2010.01.006.
- [11] Ó. Benito-Román, V. H. Alvarez, E. Alonso, M. J. Cocero, and M. D. A. Saldaña, "Pressurized aqueous ethanol extraction of  $\beta$ -glucans and phenolic compounds from waxy barley," *Food Research International*, vol. 75, pp. 252–259, 2015, doi: 10.1016/j.foodres.2015.06.006.

- [12] I. F. F. Benzie and J. J. Strain, "The ferric reducing ability of plasma (FRAP) as a measure of 'antioxidant power': The FRAP assay," *Analytical Biochemistry*, vol. 239, no. 1, pp. 70–76, 1996, doi: 10.1006/abio.1996.0292.
- [13] D. S. Tang *et al.*, "Recovery of protein from brewer's spent grain by ultrafiltration," *Biochemical Engineering Journal*, vol. 48, no. 1, pp. 1–5, 2009, doi: 10.1016/j.bej.2009.05.019.
- [14] J. A. Robertson *et al.*, "Profiling brewers' spent grain for composition and microbial ecology at the site of production," *LWT - Food Science and Technology*, vol. 43, no. 6, pp. 890–896, 2010, doi: 10.1016/j.lwt.2010.01.019.
- [15] A. E. Illera *et al.*, "Effect of thermosonication batch treatment on enzyme inactivation kinetics and other quality parameters of cloudy apple juice," *Innovative Food Science and Emerging Technologies*, vol. 47, 2018, doi: 10.1016/j.ifset.2018.02.001.
- [16] L. Galvan D'Alessandro, K. Kriaa, I. Nikov, and K. Dimitrov, "Ultrasound assisted extraction of polyphenols from black chokeberry," *Separation and Purification Technology*, vol. 93, pp. 42–47, 2012, doi: 10.1016/j.seppur.2012.03.024.
- [17] R. A. Carciochi, C. A. Sologubik, M. B. Fernández, G. D. Manrique, and L. G. D'Alessandro, "Extraction of antioxidant phenolic compounds from brewer's spent grain: Optimization and kinetics modeling," *Antioxidants*, vol. 7, no. 4, 2018, doi: 10.3390/antiox7040045.
- [18] M. Dent, V. Dragović-Uzelac, M. Penić, M. Brčić, T. Bosiljkov, and B. Levaj, "The effect of extraction solvents, temperature and time on the composition and mass fraction of polyphenols in dalmatian wild sage (*Salvia officinalis* L.) extracts," *Food Technology and Biotechnology*, vol. 51, no. 1, pp. 84–91, 2013.
- [19] R. I. Birsan, P. Wilde, K. W. Waldron, and D. K. Rai, "Recovery of polyphenols from brewer's spent grains," *Antioxidants*, vol. 8, no. 9, pp. 1–12, 2019, doi: 10.3390/antiox8090380.
- [20] B. Bartolomé and C. Gómez-Cordovés, "Barley spent grain: release of hydroxycinnamic acids (ferulic and p-coumaric acids) by commercial enzyme preparations," *Journal of the Science of Food and Agriculture*, vol. 79, no. 3, pp. 435–439, 1999, doi: 10.1002/(sici)1097-0010(19990301)79:3<435::aid-jsfa272>3.3.co;2-j.
- [21] M. M. Moreira, S. Morais, D. O. Carvalho, A. A. Barros, C. Delerue-Matos, and L. F. Guido, "Brewer's spent grain from different types of malt: Evaluation of the antioxidant activity and identification of the major phenolic compounds," *Food Research International*, vol. 54, no. 1, pp. 382–388, 2013, doi: 10.1016/j.foodres.2013.07.023.
- [22] S. F. Reis, E. Coelho, M. A. Coimbra, and N. Abu-Ghannam, "Improved efficiency of brewer's spent grain arabinoxylans by ultrasound-assisted extraction," *Ultrasonics Sonochemistry*, vol. 24, pp. 155–164, 2015, doi: 10.1016/j.ultsonch.2014.10.010.
- [23] D. S. Tang, Y. J. Tian, Y. Z. He, L. Li, S. Q. Hu, and B. Li, "Optimisation of ultrasonic-assisted protein extraction from brewer's spent grain," *Czech Journal of Food Sciences*, vol. 28, no. 1, pp. 9–17, 2010, doi: 10.17221/178/2009-cjfs.



# CHAPTER 2

---

**Valorization of brewer's spent grain by consecutive supercritical carbon dioxide extraction and enzymatic hydrolysis**

**Based on the article:**

P. Alonso-Riaño, R. Melgosa, E. Trigueros, S. Beltrán, M. T. Sanz

“Valorization of brewer's spent grain by consecutive supercritical carbon dioxide extraction and enzymatic hydrolysis”.



## Capítulo 2

### Valorización del bagazo de cerveza mediante extracción con dióxido de carbono supercrítico y posterior hidrólisis enzimática

---

#### Resumen

En este capítulo se evaluó el efecto doble ejercido por el dióxido de carbono en condiciones supercríticas (sc-CO<sub>2</sub>) sobre el sólido residual tras la extracción, aplicado sobre el bagazo de cerveza, en un contexto de biorrefinería. Se estudiaron las condiciones de extracción para eliminar y valorizar la fracción lipofílica del bagazo, a distintas presiones y temperaturas (20 - 40 MPa y 313 - 353 K), obteniendo un rendimiento máximo de  $5,70 \pm 0,07$  g /100 g<sub>bagazo</sub> a 353 K y 40 MPa, a partir de bagazo de cerveza con un tamaño de partícula < 500 µm. Las presiones y temperaturas más altas dieron lugar a un mayor contenido de compuestos fenólicos y flavonoides totales, así como a una mayor capacidad antioxidante de los extractos. Se observó un incremento del rendimiento de la hidrólisis enzimática utilizando celulasa en el bagazo tratado con sc-CO<sub>2</sub>, en comparación con el obtenido para el bagazo no tratado. Esta mejora podría atribuirse, en parte, a la eliminación de la fracción lipídica y a los cambios estructurales del bagazo de cerveza que se observaron tras el tratamiento con sc-CO<sub>2</sub>. En base a este doble efecto, el sc-CO<sub>2</sub> puede desempeñar un papel importante en la valorización de la biomasa.

---

**Palabras clave:** biorrefinería, bagazo de cerveza, extracción con fluidos supercríticos, hidrólisis enzimática.



## Abstract

---

The double effect of supercritical carbon dioxide, sc-CO<sub>2</sub>, in a biorefinery concept applied to brewer's spent grain (BSG) was assessed in this work. Extraction conditions to remove and valorize the lipophilic fraction were studied (20 – 40 MPa and 313 - 353 K) obtaining a maximum yield of  $5.70 \pm 0.07$  g /100 g<sub>BSG</sub> at 353 K and 40 MPa, with particle size < 500 μm. High pressures and temperatures resulted in higher content of total phenolic and flavonoids compounds, as well as higher antioxidant capacity. It was observed an improvement of the enzymatic hydrolysis yield by cellulase in the sc-CO<sub>2</sub> treated BSG compared to the non-treated. This improvement could be partially attributed to the removal of the lipid fraction and to morphological changes of BSG after sc-CO<sub>2</sub>. Based on this double benefit, sc-CO<sub>2</sub> can play an important role on biomass valorization.

---

**Keywords:** biorefinery, brewer's spent grain, supercritical fluid extraction, enzymatic hydrolysis.



## 1. Introduction

Renewable resources constitute the basis of the development of a bioeconomy-based society. The implementation of a bioeconomy involves strategies based on biorefinery technologies to improve the use of these biological resources. Therefore, biorefineries constitutes a key pillar to close material loops offering a wide variety of products from different types of biomasses to boost emerging circular economy extending the life cycle of a product [1]

Currently, there is a low recycling rate of raw materials that made necessary to push development of holistic approaches to reach the transition towards a more circular economy through innovation creating closed-loop systems [2]. Integration of waste material flows as raw material to another industrial process is one of the main principles of the circular economy to reach the zero-waste objective.

The selection of the raw material is one of the basis for the technology and economic successful implementation of the bio-economy. In this regard, lignocellulosic biomass is the renewable resource that can be considered the pillar for a sustainable development. The brewing industry generates different solid by-products during processing, being the most important the brewer's spent grains (BSG). BSG is the solid residue generated after the mashing and wort filtration process. It accounts to about 85 % of the total byproducts, being generated approximately 20 kg per 100 L [3]. BSG is mainly used for animal feed (70 %), biogas production (10 %), or disposed of in landfills. However, BSG presents a valuable chemical composition with a high content of protein and carbohydrates and an important source of phenolic compounds. BSG also contains an important amount of lipids (5 %) with more than 50 % of linoleic acid [4]. The integration of BSG within a holistic approach to produce different bioproducts will have a great social and economic impact also at local level [1] due to the expansion and growth of craft and microbreweries at local and regional level in the last decades.

Biorefinery development also involves new and optimized technologies for the conversion of biomass materials into bio-based commodities [1]. Due to the chemical composition of the BSG, different techniques have been proposed to valorize this

lignocellulosic biomass, such as enzymatic, acid and basic hydrolysis, ultrasound assisted extraction or microwave assisted extraction [5].

High pressure processing of biomass offers a great possibility to extract and valorize the different bioactive components. Among the different high pressure processes, the use of supercritical CO<sub>2</sub> (sc-CO<sub>2</sub>) has become a promising technology to process biomass. At supercritical conditions ( $T_c = 31.1\text{ °C}$   $p_c = 7.39\text{ MPa}$ ), CO<sub>2</sub> presents gas-like (high diffusivities) and liquid-like (good solvation power) properties. sc-CO<sub>2</sub> has been extensively studied as green extracting agent over traditional organic extraction solvents to valorize different biomass components [6].

When dealing with sc-CO<sub>2</sub> treatment of biomass from a biorefinery perspective, the focus must be not only on extraction but also on the effect of sc-CO<sub>2</sub> on the residual biomass after extraction. CO<sub>2</sub> at supercritical conditions can penetrate into the small pores of the lignocellulosic biomass resulting in structural modifications. Furthermore, CO<sub>2</sub> can be quickly released during the depressurization process, leading to explosion decompression of the feedstock promoting a decrease in its crystallinity. These structural changes result in a larger exposure surface area of the polymers such as glucans and xylans to hydrolytic enzymes [7]. In this regard, a future perspective of advanced biorefinery systems must consider the combination of one or more of different approaches and technologies [2]. In this work, the combination of sc-CO<sub>2</sub> treatment with a subsequent enzymatic hydrolysis step is proposed to achieve a more complete approach for BSG valorization.

In the literature, it is also reported that CO<sub>2</sub> can be also solubilize in the moisture content of the biomass leading to the formation of carbonic acid promoting hydrolysis of biomass polymers such as hemicelluloses [6], [7]. However, these studies were carried out under more severe conditions of temperature (120-180 °C) where dissolved CO<sub>2</sub> improves the autocatalytic effect of water in subcritical conditions. These studies concluded that temperature, moisture and the presence of CO<sub>2</sub> were the most important processing parameters to obtain a high yield of hemicellulose removal [8]–[10] that has been demonstrated to lead to high enzymatic saccharification yield of the remaining cellulose in the biomass [8]. However, the focus of this work is to check if common temperatures used in sc-CO<sub>2</sub> extraction (lower than 100 °C) and low moisture content in the feedstock



somewhat enhances glucose yield by enzymatic hydrolysis after sc-CO<sub>2</sub> extraction of the oily fraction of BSG, which up to the authors' knowledge, has not been reported in the literature.

The enzymatic hydrolysis of the remaining polysaccharide fraction after sc-CO<sub>2</sub> treatment, into monomeric sugars will be monitored by comparing the sugar yields of untreated and sc-CO<sub>2</sub> treated BSG. Due to the properties of sc-CO<sub>2</sub> as green solvent for natural compounds, a complete study of the extraction of BSG lipophilic fraction by sc-CO<sub>2</sub> was also carried out.

Regarding the extraction of lipophilic components from BSG by sc-CO<sub>2</sub>, some previous studies can be found in the literature [11] [3][12] [5]. These works covered a maximum operating pressure of 300 – 350 bar. At this maximum pressure level, an increase in temperature resulted in a decrease in the extraction yield due to dominant effect of decreasing sc-CO<sub>2</sub> density with temperature over an increase of solute vapor pressure. Therefore, in this work, higher extraction pressures were explored to check a crossover point with pressure previously reported for other oil vegetable at pressures higher than 40 MPa where solute vapor pressure increase with temperature is the dominant effect [13]. In this work, extraction kinetics at different pressures, temperatures and milling degree were performed to determine the optimum operating conditions, covering a wider pressure and temperature range than the extraction conditions previously reported in literature. Extraction kinetics were conveniently modelled by Sovova's model [14]. Mathematical modelling is of great importance in modern food engineering. Knowledge of dependence of model parameters on process conditions helps to optimization, simulation design and control of process [15]. Characterization of the oily fraction in terms of fatty acid profile and bioactive compounds composition for the different extracts was also done. To analyze the effect of the sc-CO<sub>2</sub> treatment on sugar yield after enzymatic hydrolysis of sc-CO<sub>2</sub> treated BSG, changes were assessed by X-ray diffraction, chemical composition, and surface structures analysis. Therefore, valorization of BSG is presented under a biorefinery integration concept.

## 2. Experimental section

### 2.1. Materials

The raw material used in this work was the brewer's spent grain supplied by Brebajes del Norte, S.L. (Dolina craft beer, Burgos, Spain) with an average moisture content of 70-80% (w/w). This raw material was first preconditioned, as soon as obtained, by washing and drying it in an air convection oven (45 °C) until reaching a final moisture content of 8.5% (w/w). Dehydration is necessary to reduce the storage and transportation costs as well as to reduce the microbial spoilage.

Biomass characterization was performed according to the NREL protocols. Previous details about BSG chemical characterization can be found elsewhere [16]. Carbohydrates were quantified by high-performance liquid chromatography (HPLC) with a Bio-Rad Aminex-HPX-87 H column, a variable wavelength detector (VWD) and a refractive index detector (RID) using a mobile phase constituted by 0.005M sulfuric acid. The column detector was maintained at 40 °C. The oil content of the BSG was determined by Soxhlet extraction (Buchi B-8111) using hexane as solvent, resulting to be  $5.92 \pm 0.01$  (w/w, %) in a dry basis. The dry BSG was milled in a Retsch SM100 mill to get two types of final fineness by using bottom sieves with apertures sizes of 500  $\mu\text{m}$  and 1000  $\mu\text{m}$ . Particle size distribution for each of the aperture sizes of the sieves was determined by a vibratory sieve shaker (CISA, RP.09) presenting the following distribution in percentage (w/w):

(1) fineness of 1000  $\mu\text{m}$ : > 1000  $\mu\text{m}$ , 14.2%; 1000-500  $\mu\text{m}$ , 58.1%; 500-250  $\mu\text{m}$ , 17.4%; 250-125  $\mu\text{m}$ , 6.5% and < 125  $\mu\text{m}$ , 3.9%

(2) fineness of 500  $\mu\text{m}$ : > 1000  $\mu\text{m}$ , 0%; 1000-500  $\mu\text{m}$ , 2.9%; 500-250  $\mu\text{m}$ , 70.4%; 250-125  $\mu\text{m}$ , 21.0% and < 125  $\mu\text{m}$ , 5.7%

The hydrolytic enzyme used in this work was a cellulase, 1,4-(1,3:1,4)- $\beta$ -D-Glucan 4-glucanohydrolase, EC 3.2.1.4, from *Aspergillus niger* provided by Sigma-Aldrich. The enzyme units, as reported by the supplier was 1.18 U/mg, being 1 U the corresponding amount of enzyme that liberates 1  $\mu\text{mol}$  of glucose from carboxymethyl cellulose per minute at pH of 5.0 and 37 °C.

## 2.2. Supercritical fluid extraction equipment and procedure

The sc-CO<sub>2</sub> extraction experiments were carried out in a laboratory supercritical fluid extraction (SFE) plant, whose P&I diagram is shown in **Figure 2.1** and has been previously described [13], [17], [18]. In a SFE experiment, 8.5 g of dry BSG were loaded in the extractor (26.5 mL capacity, with ½" internal diameter). Two syringe pumps (ISCO 260 DM), that work alternatively, provide an uninterrupted flow of CO<sub>2</sub> (*Carburos metálicos*, liquid CO<sub>2</sub> ≥ 99.9%) compressed up to the desired operating working pressure. The pressurized solvent was pre-heated up to the desired extraction temperature before entering the extractor. The extractor was held in an oven whose temperature is controlled within an accuracy of ± 0.5 °C. The extraction yield was determined gravimetrically by measuring the extract weight at different time intervals.

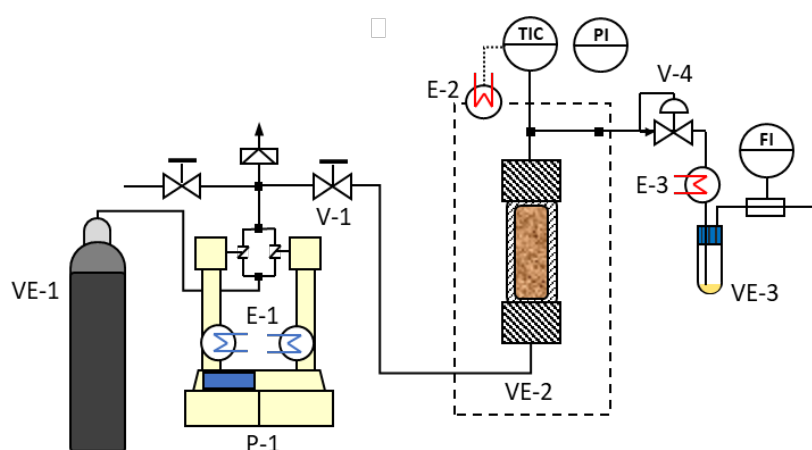


**Figure 2.1.** Schematic representation of the SFE-plant. VE-1: CO<sub>2</sub> reservoir; VE-2: extractor; VE-3: separator, VE-3: separator, VE-4: Back-pressure valve: extract; P-1: CO<sub>2</sub> pump; E-1: cryostat, E-2: oven, E-3: heating resistance; TIC and PI: temperature and pressure indicators and controllers.

The first group of SFE experiments were carried out to determine the effect of particle size at constant operation pressure and temperature of 20 MPa and 313 K, respectively. First, whole BSG was used. Subsequently, different particle size fractions were studied, according to the fineness particle distribution obtained by milling and sieving, by using bottom sieves with aperture sizes of 1000 and 500 µm. The BSG was charged in the extractor

according to the percentage and particle size distribution found for each type of final fineness reported in section 2.1. This way, the effect of particle size was studied, avoiding the effect of chemical composition of each particle size fraction. Once the final fineness was selected, the effect of pressure, from 20 to 40 MPa, and temperature, from 313 to 353 K, was assessed.

### **2.3. Enzymatic hydrolysis**

Enzymatic hydrolysis was performed on samples after sc-CO<sub>2</sub> treatment and non-treated BSG samples. Enzymatic hydrolysis was carried out at 323 K in an acetate buffer at pH = 5. Assays were performed at different cellulase concentrations, 0.25%, 0.5% and 1% expressed as enzyme: BSG ratio (*w/w*), which means 2.95, 5.9 and 11.8 IU/g<sub>solid</sub>, respectively, expressed as IU per mass unit of solid. Samples were withdrawn at regular time intervals to plot the corresponding hydrolysis curves. To stop the hydrolytic reaction, the enzyme was inactivated by heating the withdrawn samples at 373 K for 5 min and immediately cooling in ice and kept in the refrigerator until analysis.

Liquid samples were analyzed by HPLC for determination of monomeric sugar concentration (glucose, xylose, and arabinose). Liquid samples were analyzed by HPLC for determination of monomeric sugar concentration (glucose, xylose and arabinose) according to the method described in section 2.1 for carbohydrate identification in the raw material.

### **2.4. Analytical methods**

#### **2.4.1. Determination and quantification of fatty acids profile**

The fatty acids profile was determined by the AOAC method [19]. The fatty acid methyl esters were firstly prepared and then analyzed by gas chromatography (GC) in a Hewlett Packard gas chromatograph (6890N Network GC System) equipped with an auto-sampler (7683B series) and a flame ionization detector (FID). The method has been previously described in detail [9], [16]. Fatty acid methyl esters were identified by comparison of their retention times with those of chromatographic standards (Sigma Chemical Co.). Their quantification was made by relating the peaks area to the area of an internal standard (methyl tricosanoate). Calibration curves were made for several pairs formed by the internal

standard plus several representative chromatographic standards to find the corresponding response factors. Results were expressed as mg of fatty acid per g of extract and as fatty acid percentage.

#### **2.4.2. Determination of total phenolic compounds**

The total phenolic content (TPC) of sc-CO<sub>2</sub> extracts was determined by the Folin-Ciocalteu method [20]. The sc-CO<sub>2</sub> extract was diluted in ethanol (5 mg/mL). 500 µL of the diluted extract were mixed with 5.0 mL of water and then, 500 µL of the Folin-Ciocalteu reagent. After that, 1 mL of sodium carbonate 7.5% (w/v) were added to the mixture. Sample was filtered and centrifuged, and the absorbance of optically clear supernatant was measured at 725 nm after 60 min of reaction in darkness (spectrophotometer V-750, Jasco, Japan). A calibration curve was prepared with standard solutions of gallic acid and results were expressed as mg of gallic acid equivalent (GAE)/g extract (mg<sub>GAE</sub>/g<sub>E</sub>).

#### **2.4.3. Determination of total flavonoid compounds**

The total flavonoids content (TFC) was determined by the aluminum trichloride method as described by Spinelli et al. [12] with slight modifications. An ethanolic solution was prepared by dissolving 5 mg of the sc-CO<sub>2</sub> extract in 1 mL of ethanol. 0.5 mL of this solution were mixed with 2.0 mL of distilled water and 0.15 mL of NaNO<sub>2</sub> (5% w/v). Subsequently (after 6 min), 0.15 mL of AlCl<sub>3</sub> solution (10%, w/v) were added. Finally, after 5 min reaction, 1 mL of NaOH (1M) and 1.2 mL of ethanol were added to the mixture. After 30 minutes in darkness, sample was filtered and centrifuged, and the absorbance of optically clear supernatant was measured at 415 nm. A quercetin standard curve was constructed to express the results as mg of Quercetin Equivalent per gram of extract, mg QE/g<sub>E</sub>.

#### **2.4.4. Determination of antioxidant capacity**

The antioxidant activity (AA) of the sc-CO<sub>2</sub> extracts was assessed by the ABTS method. This method is based on the decolorization of the radical cation 2,2'-azinobis-(3-ethylbenzothiazoline-6-sulfonic acid) (ABTS<sup>+</sup>) prepared according to Re et al. [21]. Briefly, 3 mL of the ABTS<sup>+</sup> solution were mixed with 1 mL of the BSG oil diluted in ethanol (10 mg/mL). After 1 h in the dark, sample was filtered and centrifuged, and the

absorbance of optically clear supernatant was measured in a spectrophotometer (Jasco V-750) at 734 nm and 25 °C using ethanol as a blank. A Trolox standard curve in ethanol was used to express the antioxidant capacity of the samples as mg of Trolox Equivalent (TE) per g of extract (mg TE/g<sub>E</sub>).

#### **2.4.5. X-Ray diffraction (XRD)**

An X-ray diffractometer (Bruker D8 Discover, Davinci Design) was used to determine the crystallinity of the different BSG samples: untreated BSG, sc-CO<sub>2</sub>-treated BSG and after enzymatic hydrolysis of the BSG samples. A scan type of theta-2-theta with a step size of 0.05 was carried out at 0.05/min. The scattering angle ( $2\theta$ ) was varied from 5 to 70°.

#### **2.4.6. Scanning electron microscopy (SEM)**

The surface morphology of the different samples was examined in a Scanning Electron Microscope JEOL JSM-6460LV with Energy Dispersive X-ray (JEOL Ltd. Japan) operating at 20 kV. Samples were gold-sputtered and observed at different magnifications.

### **2.5. Modelling**

#### **2.5.1. Supercritical fluid extraction modelling**

The model proposed by Sovová was used to fit the experimental extraction curves [14]. This type of model has been successfully used to describe the extractive curves of different seed oils [13], [18], [22]. In the model of Sovová the extraction yield is expressed as:

$$e = \frac{E}{N_m} \quad [2.1]$$

where  $E$  is the amount of extract (kg) and  $N_m$  the amount of insoluble solid (kg) loaded in the extractor. The amount of solvent consumed is obtained by:

$$q = \frac{Qt}{N_m} \quad [2.2]$$

where  $Q$  is the solvent flow rate (kg/h) and  $t$  the extraction time (h). This model considers that the extraction curves consist of two parts. First, the easily accessible solute from broken cells is transferred directly to the fluid phase and in the second part of the extraction curve, the solute from intact cells diffuses first to broken cells and then to the fluid phase. For vegetable oil extraction, Sovová found that extraction curves are initially linear with a slope close to the value of oil solubility in CO<sub>2</sub> [10]. Assuming an initial solubility control in the first part of the extraction curve, Sovová proposed equations 2.3 and 2.4 to evaluate the first and second part of the extraction curve, respectively:

$$e = qy_s, \text{ for } 0 \leq q \leq q_c \quad [2.3]$$

$$e = x_u[1 - C_1 \exp(C_2 q)], \text{ for } q > q_c \quad [2.4]$$

$C_1$  and  $C_2$  are adjustable parameters,  $y_s$  is the experimental solubility datum,  $q_c$  the crossing point and  $x_u$  is the solute concentration in the BSG (kg<sub>solute</sub>/kg<sub>insoluble solid</sub>). The adjustable parameters of the model were calculated by using the software Statgraphics Centurion XVI X64 and the Marquardt's algorithm. From constants  $C_1$ ,  $C_2$  and co-ordinate  $q_c$  at the crossing point, the volumetric fraction of broken cells in the particles, called grinding efficiency,  $r$ , and the solid-phase mass transfer coefficient,  $k_s a_s$ , can be estimated [10]:

$$r = 1 - C_1 \exp(-C_2 q_c / 2) \quad [2.5]$$

$$k_s a_s = (1 - r)(1 - \varepsilon) \dot{Q} C_2 / N_m \quad [2.6]$$

### 2.5.2. Enzymatic hydrolysis modelling

The experimental enzymatic hydrolysis data were fitted to the hyperbolic correlation of Holtzapfle, which involves two kinetic parameters ( $C_{i,max}$  and  $t_{1/2}$ ) [23], [24]:

$$C_i = \frac{C_{i,max} \cdot t}{t_{1/2} + t} \quad [2.7]$$

where  $C_i$  is the concentration of each monomeric sugar (glucose, xylose or arabinose),  $C_{i,max}$  is the maximum concentration of the monomeric sugar that could be achieved at the working experimental conditions,  $t_{1/2}$  is the time required to achieved 50 % of  $C_{i,max}$  and  $t$  is

the enzymatic hydrolysis time (min). To estimate the kinetic parameters, non-linear regression was performed by using the Marquardt algorithm (Statgraphics Centurion XVI X64).

## **2.6. Statistical analysis**

Statistical analyses were conducted using the software Statgraphics Centurion XVI X64. The results were presented as a mean  $\pm$  standard deviation of at least three replicates. To confirm significant differences, the Fisher's least significant differences method at p-value  $\leq 0.05$  was applied.

## **3. Results and discussion**

### **3.1. Supercritical extraction of the lipophilic fraction of BSG**

The first step in the BSG valorization within a biorefinery concept was the extraction of the valuable lipophilic fraction of the BSG. Extraction curves were obtained, and the optimal conditions required to achieve the maximum extraction yield were determined.

#### **3.1.1. Influence of process parameters**

**Figure 2.2** shows the extraction curves at 30 MPa and 313 K obtained for non-grounded BSG and two final fineness obtained for 1000 and 500  $\mu\text{m}$  sieve sizes in the mill. From the extraction curves it can be observed that the initial extraction rate increased by decreasing the particle size. This could be due to the higher amount of compounds that can be easily extracted outside the particle size at smaller particle sizes that would reduce the importance of diffusion compared to convection [13]. Furthermore, lower extraction yields, for a given extraction time, were obtained with larger particle size distribution, since only part of the oil contained in the largest particles seems to be accessible to sc-CO<sub>2</sub> as a result of internal diffusional limitations. Therefore, for further experiments, BSG was charged in the extraction according to the particle size distribution obtained for a fineness obtained with the 500  $\mu\text{m}$  sieve size in the mill to study the effect of pressure and temperature.



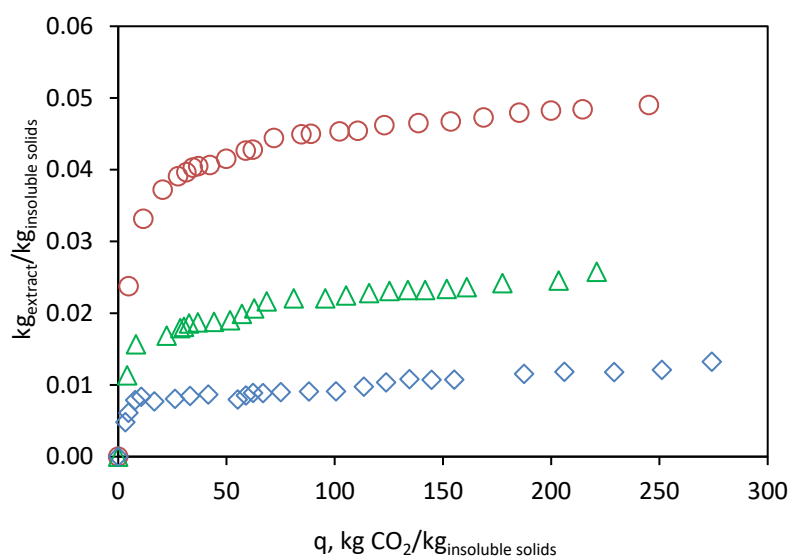


**Figure 2.2.** Effect of the particle size on the extraction kinetics of oil from BSG at 30 MPa and 313 K:  $\diamond$  original BSG and different PSD for fineness obtained with different sieve size in the mill:  $\triangle$  1000  $\mu\text{m}$  and  $\circ$  500  $\mu\text{m}$ .

The effect of extraction temperature was studied at 313, 333 and 353 K, at three different pressures, 20, 30 and 40 MPa. At any of the operating temperatures, an increase in the extraction rate was observed when pressure was increased (see **Figure 2.3**).

This behaviour can be attributed to the higher solvating power associated to the higher CO<sub>2</sub> density. Fernandez et al. [11] observed also an increase in the extraction rate with pressure from 10 to 35 MPa, at a constant temperature of 313 K. However, these authors reported lower extraction yields with a highest value of 3.5 g extract per 100 g of BSG, probably due to the use of partially dried BSG by vacuum drying, with a moisture content of 58 % (w/w) and a larger mean particle size of 0.85 mm of the BSG. At the best extraction conditions reported by Fernandez et al. (313 K and 35 MPa), Kitryté [3] reported a similar extraction yield as the one obtained in this work ( $5.49 \pm 0.07$  g /100 g<sub>BSG</sub>) by using freeze-dried BSG samples of 0.2 mm mean particle size. In the present work a maximum extraction yield of  $5.70 \pm 0.07$  g /100 g<sub>BSG</sub> at 353 K and 40 MPa was obtained.

Regarding the effect of temperature at constant pressure, different behaviour was observed at the different pressures studied in this work. At the lowest pressure, 20 MPa, an

increase in temperature resulted in a decrease in the extraction rate. This trend was also observed by Fernandez et al. [11] in the pressure range from 10 to 30 MPa and the temperature range from 313 to 353 K. However, at the highest pressure essayed in this work, 40 MPa, an increase in temperature led to an increase in the extraction rate. As it is well described in literature [13], temperature has two opposite effects that influence sc-CO<sub>2</sub> extraction. As temperature increases, the solute vapor pressure of the extract increases, increasing its solubility, but the solvent density decreases, decreasing the solvent power of sc-CO<sub>2</sub>. The results obtained in this work indicated that the first effect prevails at high pressures and the second at low pressures. At 40 MPa, the increase of vapor pressure with temperature compensates the effect of a lower sc-CO<sub>2</sub> density in the extraction rate. These results agree with literature [22] that reported an increase of seed oil solubility with temperature when extraction was carried out at pressures higher than 40 MPa, pressure at which a crossover behaviour is usually observed in vegetable oils. This crossover point has been reported for the first time for BSG oily fraction extraction by sc-CO<sub>2</sub>, according to the authors's knowledge.

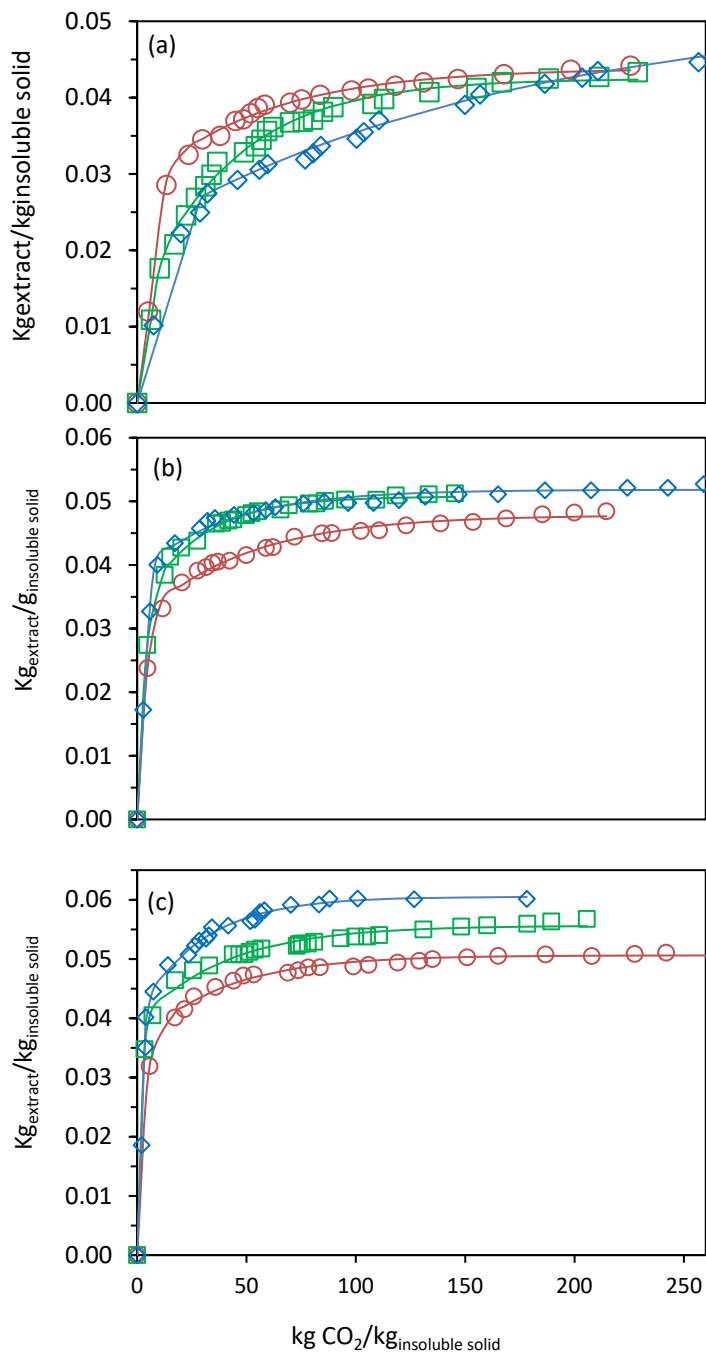


**Figure 2.3.** Effect of operating temperature and pressure on extraction kinetics of oil from BSG: (a) 20 MPa (b) 30 MPa (c) 40 MPa: (○) 313 K (□) 333 K (◇) 353 K. Continuous lines represent the Sovová's model.

**3.1.2. Modeling of the supercritical fluid extraction**

According to the model proposed by Sovová et al. [14] and described in Section 2.5.1, for many vegetable oils, the extraction curves are initially linear with a slope close to the value of oil solubility in sc-CO<sub>2</sub> at the working conditions. To check if the initial slopes of the extraction curves are within the range of previously reported vegetable oil solubility, the initial slope was evaluated and compared with the general equation (Equation 2.8) proposed by del Valle et al. [25] to predict the solubility of vegetable oils in high-pressure CO<sub>2</sub> (within ± of experimental values) as a function of CO<sub>2</sub> density and temperature:

$$c_{sat} (g \cdot kg^{-1}) = 8.07 \left( \frac{\rho}{910} \right)^{\left[ 9.59 - 8.45 \left( \frac{\rho}{910} - 1 \right) - 23.0 \left( \frac{\rho}{910} - 1 \right)^2 \right]} \exp \left\{ -4182 \left[ 1 - 259 \left( \frac{1}{T} - \frac{1}{313} \right) \right] \left( \frac{1}{T} - \frac{1}{313} \right) \right\} \quad [2.8]$$

According to Del Valle et al. [25], Equation 2.8 can be applied to systems composed by pure oil and high-pressure CO<sub>2</sub>, as well as to oil contained in different vegetable substrates, since the initial stages of the extraction process are typically solubility-controlled. To correct the values obtained at temperatures different from 313.15 K, the initial slopes were divided by the temperature-correction term (TCT) [25]:

$$TCT = \exp \left\{ -4182 \left[ 1 - 259 \left( \frac{1}{T} - \frac{1}{313} \right) \right] \left( \frac{1}{T} - \frac{1}{313} \right) \right\} \quad [2.9]$$

The corrected initial extraction slopes have been plotted in **Figure 2.4** as a function of pure CO<sub>2</sub> density, together with the prediction of the oil solubility and the error limit from the General Model. It can be concluded that the values of the slope of the first part of the extraction curves are within the error limits for solubility of vegetable oils in CO<sub>2</sub>. Therefore, it can be assumed that the initial part of the extraction curves is solubility-controlled and Equations 3 and 4 can be used to fit the extractive curves.

Fernández et al. [11] reported solubility data for BSG extraction by sc-CO<sub>2</sub> based on the dynamic flow criteria. These values have not been plotted in Figure 2.4 since they are much lower than the values obtained in the present work. For instance, at 30 MPa and 313 K, these authors reported values of 0.4581 mg/g CO<sub>2</sub> (or g/kg CO<sub>2</sub>), while in this work the solubility value determined according to the initial slope of the extraction curve was one order of magnitude higher which agrees with previous solubility data of vegetable oils in sc-CO<sub>2</sub>.

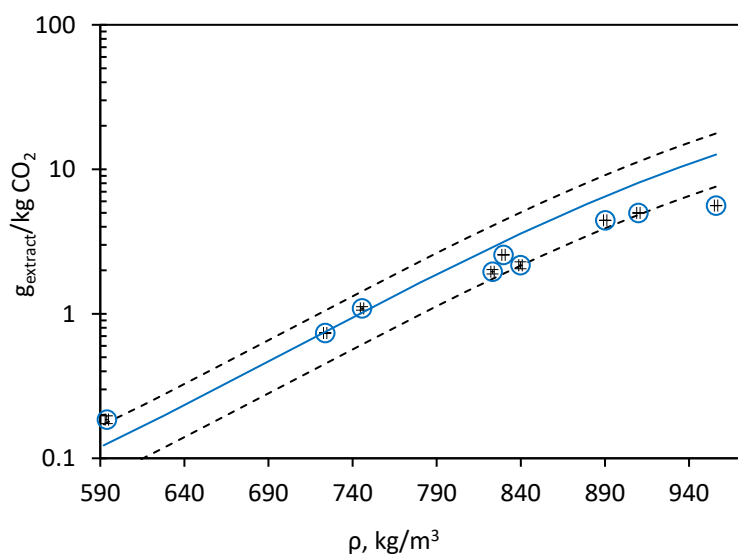


**Figure 2.4.** Corrected (at 313 K) experimental solubility values of BSG oil as function of pure CO<sub>2</sub> density. (○) experimental data points; (—) prediction of del Valle et al. General Model [25]; (---) error limits of the General Model.

The adjustable parameters of Sovova's model have been listed in **Table 2.1** together with the volumetric fraction of broken cells in the particles,  $r$ , and the solid-phase mass transfer coefficient,  $k_{s,a_s}$ , evaluated from the model parameters (Equations 2.5 and 2.6). The calculated extraction curves were plotted in **Figure 2.3** and a good agreement can be observed between experimental data and model fitting. The quality of the fitting has been evaluated through the values of the Root Mean Square Deviation (RMSD) between experimental and calculated extraction yields:

$$RMSD = \sqrt{\frac{\sum_{i=1}^n (e_{exp} - e_{calc})^2}{n}} \cdot 100 \quad [2.10]$$

The volumetric fraction of broken cells in the BSG,  $r$ , was above 0.65 for nearly all of the experiments, except for the lowest pressure at the highest temperatures. The values obtained for the solid-phase mass transfer coefficients,  $k_{s,a_s}$ , are of the same order than those obtained by Benito-Román et al. [18] when correlating supercritical extraction data of quinoa oil. The crossing point,  $q_c$ , was found to increase with a decrease in the solubility value, specially at the lowest operating pressure.

**Table 2.1.** Extraction conditions, values of the experimental solubility,  $y_s$ , and adjusting Sovová model parameters,  $C_1$ ,  $C_2$ ,  $x_u$  and  $q_c$ . Estimated grinding efficiency  $r$ , solid-phase mass transfer coefficient,  $k_{s,a_s}$  and RMSD

T, K	p, MPa	$y_s$ , kg/kg CO <sub>2</sub>	$q_c$ , kg CO <sub>2</sub> /kgIS	$x_u$	$C_1$	$C_2$	$r$	$k_{s,a_s}$	RMSD
313	20	0.0022	13.4	0.0438	0.3618	0.0181	0.68	4.8·10 <sup>-5</sup>	5.2·10 <sup>-4</sup>
333	20	0.0017	10.3	0.0425	0.7021	0.0236	0.38	9.5·10 <sup>-5</sup>	6.8·10 <sup>-4</sup>
353	20	0.0009	32.1	0.0520	0.5695	0.0058	0.48	3.4·10 <sup>-5</sup>	1.2·10 <sup>-3</sup>
313	30	0.0050	4.77	0.0478	0.3534	0.0209	0.66	3.9·10 <sup>-5</sup>	5.4·10 <sup>-4</sup>
333	30	0.0059	4.62	0.0508	0.3666	0.0379	0.66	6.5·10 <sup>-5</sup>	4.0·10 <sup>-4</sup>
353	30	0.0057	5.8	0.0518	0.2566	0.0251	0.76	4.6·10 <sup>-5</sup>	7.2·10 <sup>-4</sup>
313	40	0.0056	5.7	0.0506	0.3024	0.0266	0.72	5.7·10 <sup>-5</sup>	5.2·10 <sup>-4</sup>
333	40	0.0103	3.4	0.0556	0.3004	0.0257	0.71	4.5·10 <sup>-5</sup>	6.9·10 <sup>-4</sup>
353	40	0.0102	3.8	0.0605	0.3347	0.0347	0.69	4.3·10 <sup>-5</sup>	5.2·10 <sup>-4</sup>

### 3.1.3. Characterization of sc-CO<sub>2</sub> extracts

Characterization of the sc-CO<sub>2</sub> extracts have been carried out by determining their fatty acid profile, total phenolic and flavonoid content, and antioxidant capacity.

A total of 16 fatty acids were identified and quantified in the different sc-CO<sub>2</sub> extracts. The results are collected in **Table 2.2** and represented in **Figure 2.5**. No trend in the fatty acid percentage profile was observed neither with the extraction pressure nor with extraction temperature. In all the extracts, linoleic acid was the major fatty acid (more than 50%), followed by palmitic and oleic acid. **Table 2.2** also includes the fatty acid profile for BSG oil obtained by Soxhlet extraction. Farcas et al. [4] reported similar fatty acid composition of BSG by extracting the total lipids using a chloroform: methanol mixture.

The sc-CO<sub>2</sub> extracts were also analyzed in terms of total phenolic and flavonoid compounds and antioxidant capacity, and the results are plotted in **Figure 2.6**.

Temperature and pressure significantly affect the three parameters. Extracts obtained at higher pressures resulted in higher content of TPC, TFC and antioxidant activity, although the effect of pressure was less significant than the effect of temperature. The results of the statistical analysis are also presented in **Figure 2.6**. Temperature presented the main effect, specially at the highest pressure studied in this work. In literature, the effect of temperature on the solubility of some phenolic compounds was reported to be negative at low pressure, between 10 and 15 MPa [17]. However, at higher pressures (> 15 MPa), the temperature had a positive effect on the solubility of the hydroxycinnamic acids, as it has been also observed in this work. This behaviour was due to the increase in vapour pressure of the solute with temperature that compensate the decrease in CO<sub>2</sub> density with temperature. The positive effect of temperature in the pressure range covered in this work was observed for both, TPC and TFC. The increase observed in TPC and TFC led to an increase of the antioxidant capacity of the extracts. It must be highlighted that different crossover point was observed for the bioactive compounds and for the extracted oil, where the crossover point was around 400 bar.

**Table 2.2.** Fatty acid (FA) profile, mg/g<sub>extract</sub>, of the lipid fractions extracted with sc-CO<sub>2</sub> at different operating pressure and temperature

FA	20/313	20/333	20/353	30/313	30/333	30/353	40/313	40/333	40/353	Soxhlet
C14:0	1.7 ± 0.2	2.21 ± 0.01	2.0 ± 0.1	1.61 ± 0.01	1.99 ± 0.01	2.12 ± 0.01	2.18 ± 0.07	2.11 ± 0.09	1.6 ± 0.1	1.41 ± 0.02
C15:0	0.78 ± 0.08	1.00 ± 0.01	0.95 ± 0.04	0.85 ± 0.01	0.94 ± 0.01	0.96 ± 0.01	1.02 ± 0.05	0.99 ± 0.03	0.78 ± 0.08	0.82 ± 0.01
C16:0	150 ± 12	187.5 ± 0.1	180 ± 5	161.1 ± 0.1	176.8 ± 0.5	185.0 ± 0.6	196 ± 11	190 ± 4	151 ± 12	138 ± 20
C16:1n-7	1.3 ± 0.1	0.94 ± 0.01	1.61 ± 0.08	1.30 ± 0.01	1.57 ± 0.04	1.93 ± 0.07	1.9 ± 0.2	2.0 ± 0.1	1.30 ± 0.07	1.21 ± 0.02
C18:0	11.0 ± 0.8	14.3 ± 0.1	12.8 ± 0.2	12.8 ± 0.1	13.3 ± 0.5	13.7 ± 0.1	14.4 ± 0.7	13.9 ± 0.4	11 ± 1	11 ± 1
C18:1n-7	5.8 ± 0.5	7.8 ± 0.1	7.2 ± 0.3	6.8 ± 0.1	7.1 ± 0.1	7.9 ± 0.3	8.2 ± 0.8	8.5 ± 0.3	6.1 ± 0.1	6 ± 1
C18:1n-9	84 ± 6	115.1 ± 0.1	100.8 ± 0.7	104.1 ± 0.1	104 ± 4	102.8 ± 0.4	112 ± 5	108 ± 2	86 ± 8	79 ± 10
C18:2n-6	313 ± 22	428.8 ± 0.1	375 ± 4	369.3 ± 0.1	383 ± 12	380 ± 2	417 ± 21	398 ± 6	310 ± 29	288 ± 38
C18:3n-3	26 ± 2	35.5 ± 0.1	30.9 ± 0.2	32.3 ± 0.1	32 ± 2	31.0 ± 0.3	35 ± 2	32.9 ± 0.3	25 ± 2	26 ± 3
C20:0	1.9 ± 0.1	2.58 ± 0.01	2.23 ± 0.02	2.72 ± 0.01	2.5 ± 0.3	2.47 ± 0.04	2.59 ± 0.09	2.5 ± 0.1	2.1 ± 0.2	2.03 ± 0.01
C20:1n-9	5.8 ± 0.5	7.71 ± 0.01	6.51 ± 0.01	8.48 ± 0.01	7.3 ± 0.6	7.2 ± 0.1	7.7 ± 0.3	7.4 ± 0.2	6.0 ± 0.6	6 ± 1
C20:2n-6	0.88 ± 0.08	1.26 ± 0.01	1.08 ± 0.01	1.17 ± 0.01	1.13 ± 0.08	1.12 ± 0.02	1.1 ± 0.3	1.17 ± 0.04	0.90 ± 0.09	0.92 ± 0.01
C22:0	1.84 ± 0.09	2.13 ± 0.01	1.85 ± 0.01	2.37 ± 0.01	2.1 ± 0.1	2.18 ± 0.06	2.13 ± 0.06	2.09 ± 0.05	1.8 ± 0.2	2.11 ± 0.03
C22:1n-11	4.1 ± 0.2	5.46 ± 0.01	4.4 ± 0.2	5.65 ± 0.01	5.2 ± 0.7	5.5 ± 0.6	5.4 ± 0.3	5.19 ± 0.02	4.2 ± 0.3	4 ± 1
C22:1n-9	1.27 ± 0.08	1.49 ± 0.01	1.27 ± 0.05	1.89 ± 0.01	1.53 ± 0.09	1.48 ± 0.02	1.57 ± 0.09	1.52 ± 0.01	1.3 ± 0.1	1.4 ± 0.1
C24:0	1.24 ± 0.07	1.60 ± 0.01	1.47 ± 0.03	1.85 ± 0.01	1.6 ± 0.2	1.71 ± 0.06	1.63 ± 0.07	1.4 ± 0.1	1.4 ± 0.1	1.4 ± 0.1
SFA	168 ± 13	211.3 ± 0.1	201 ± 5	183.3 ± 0.1	199 ± 2	208.2 ± 0.8	219 ± 12	213 ± 5	170 ± 14	157 ± 21
MFA	102 ± 7	138.4 ± 0.1	122 ± 1	128.3 ± 0.1	126 ± 5	127 ± 1	137 ± 7	132 ± 3	104 ± 9	98 ± 13
168 ± 13	340 ± 24	465.6 ± 0.01	407 ± 4	402.8 ± 0.1	416 ± 13	412 ± 2	453 ± 23	432 ± 6	336 ± 31	315 ± 41

SFA: saturated fatty acids, MFA: monounsaturated fatty acids, PUFA: polyunsaturated fatty acid



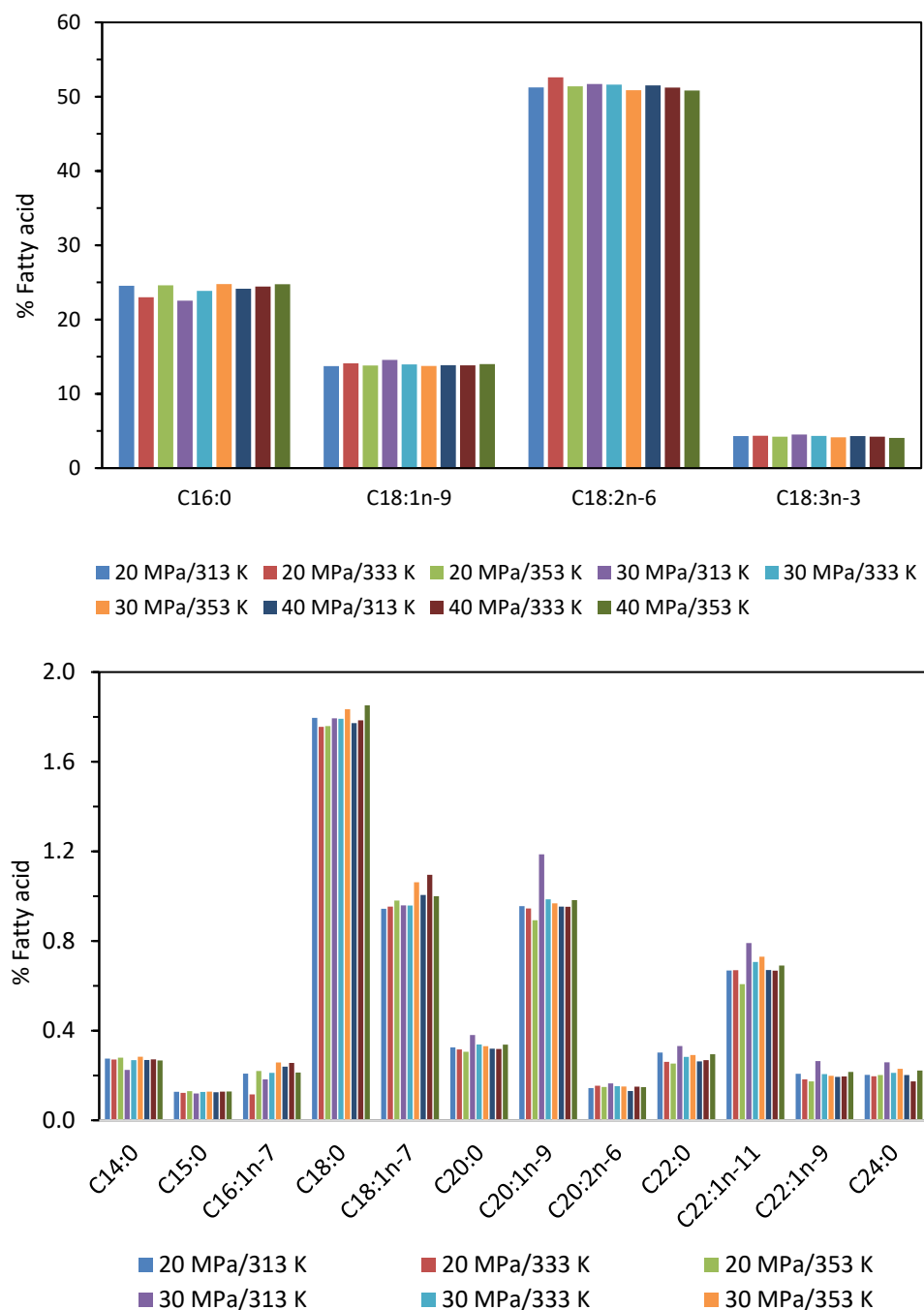


**Figure 2.5** Percentage of fatty acids of the lipid fraction extracted with sc-CO<sub>2</sub> at different operating pressure and temperature, p(MPa)/T(K).

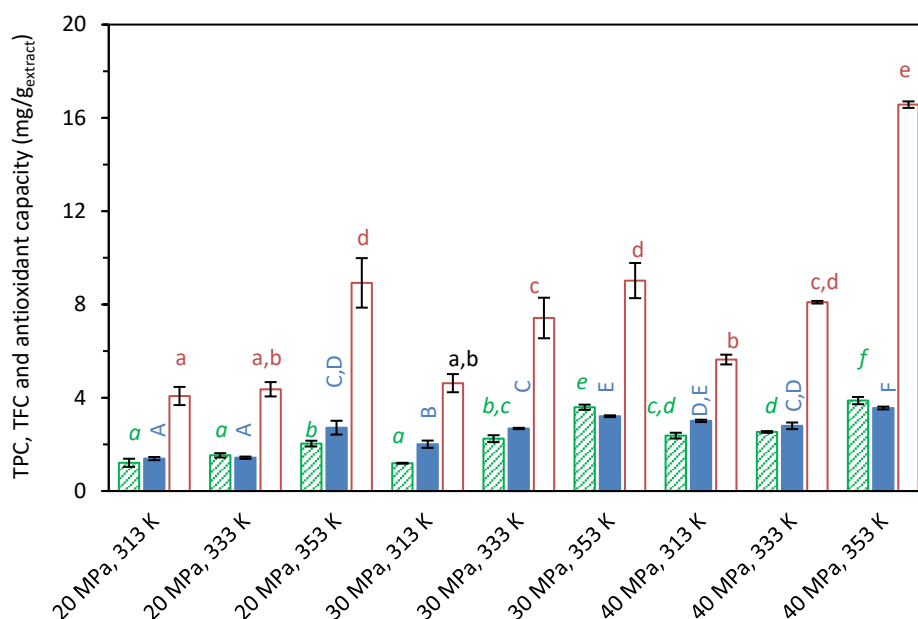


**Figure 2.6.** Characterization of sc-CO<sub>2</sub> extracts of BSG at different operating conditions: (▨) total flavonoids compounds, TFC, mg<sub>QE</sub>/g<sub>extract</sub>; (■) antioxidant capacity, mg<sub>TE</sub>/g<sub>extract</sub>; (□) total phenolic compounds, TPC, mg<sub>GAE</sub>/g<sub>extract</sub>. Values with different letters for each type of measurement (TPC, TFD and antioxidant capacity) are significantly different when applying the Fisher's least significant differences (LSD) method at p-value ≤ 0.05.

Ferrentino et al. [5] reported the TPC content and the antioxidant capacity, evaluated through the DPPH test, at two levels of pressure and temperature (20/30 MPa and 313/323 K), with maximum values of  $8.4 \pm 0.1$  mg<sub>GAE</sub>/g<sub>sample</sub> and  $4.3 \pm 0.1$  mg<sub>Trolox</sub>/g<sub>sample</sub> at 30 MPa and 323 K, similar to the values plotted in **Figure 2.6**. These authors also reported composition data when using ethanol as co-solvent, 4 and 8%, with maximum values of bioactive compounds of  $26.2 \pm 0.3$  mg<sub>GAE</sub>/g<sub>sample</sub> and  $14.2 \pm 0.1$  mg<sub>Trolox</sub>/g<sub>sample</sub> at 30 MPa, 323 K and 8% ethanol. Spinelli et al. [12] studied the influence of the sc-CO<sub>2</sub> operating conditions on the TPC, TFC and the AA, determined as the inhibition percentage of the DPPH radical of the sc-CO<sub>2</sub> extracts, focusing on the addition of ethanol as cosolvent. These authors concluded that, in the case of sc-CO<sub>2</sub> without co-solvent, the pressure barely had an effect on the chemical composition in the temperature and pressure range from 313 to 333 K and 15 to 35 MPa, respectively. According to these authors the BSG contain many

polar substances with low solubility in pure sc-CO<sub>2</sub>, concluding that it is necessary to add ethanol to increase the polarity of the extraction solvent. They found that the best operating conditions were 313 K, 35 MPa and 60% ethanol as co-solvent (v/v) with values of  $0.35 \pm 0.01 \text{ mg}_{\text{GAE}}/\text{g}_{\text{BSG}}$  ( $4.3 \text{ mg}_{\text{GAE}}/\text{g}_{\text{extract}}$ ),  $0.22 \pm 0.01 \text{ mg}_{\text{QE}}/\text{g}_{\text{BSG}}$  ( $2.7 \text{ mg}_{\text{QE}}/\text{g}_{\text{extract}}$ ) and  $2.09 \pm 0.04\%$  of DPPH inhibition. It must be highlighted that in the work of Spinelli et al. [12] the ethanol concentration is much higher than the concentration usually employed of ethanol as modifier in sc-CO<sub>2</sub> extraction [5]. As 60% of ethanol concentration would be similar to an ethanolic extraction that should have reached higher TPC yield according to pervious literature data on TPC extraction by ethanolic mixtures [26]. In the present, the best conditions in terms of chemical composition were 353 K and 40 MPa with values of  $16.6 \text{ mg}_{\text{GAE}}/\text{g}_{\text{extract}}$  ( $0.94 \pm 0.01 \text{ mg}_{\text{GAE}}/\text{g}_{\text{BSG}}$ ),  $3.88 \text{ mg}_{\text{QE}}/\text{g}_{\text{extract}}$  ( $0.219 \pm 0.009 \text{ mg}_{\text{QE}}/\text{g}_{\text{BSG}}$ ) and  $3.56 \text{ mg}_{\text{TE}}/\text{g}_{\text{extract}}$  ( $0.201 \pm 0.003 \text{ mg}_{\text{Trolox}}/\text{g}_{\text{BSG}}$ ). The results of bioactive compounds reported in this work, as well as those reported in literature, should be considered with skepticism, as suggested by Guido and Moreira [27], since conclusions are obtained from spectrophotometric analysis and individual bioactive compounds were not determined. Futhermore, analysis protocols for TPC, TFC and AA were different in previous reported works. Kitryté et al. [3] redissolve the sc-CO<sub>2</sub> in n-hexane, while Spinelli et al. [12] and Ferrantino et al. [5] dissolved the sc-CO<sub>2</sub> extract in ethanol, but at concentrations higher than in this work and higher than the usual solubility oil range in ethanol.

Regarding chemical composition of the lipid fraction of BSG, Guido and Moreira [27] concluded that typical hydroxycannamic acids present in the BSG, such as ferulic and p-coumaric acids were almost negligible in the extracts obtained by sc-CO<sub>2</sub> and ethanol as co-solvent, concluding that essential oils accounted for 13 % of oil fraction that contribute for its antioxidant activity. Bohnsack et al. [28] found tocotrienols and tocopherols in the extracting oil from BSG, especially in the sieving fraction of particle sizes < 500 µm. Series of 5-n-alkylresorcinols, as well as different classes of steroid compounds have been also identified among the lipids in BSG with antioxidant activity [29].

### **3.2. Enzymatic hydrolysis**

After sc-CO<sub>2</sub> treatment, the raffinate obtained at 40 MPa and 353 K (80 °C) was subjected to enzymatic hydrolysis by cellulase at different enzyme doses. As control, the

non-sc-CO<sub>2</sub> treated BSG was also hydrolyzed at the same conditions. At the sc-CO<sub>2</sub> extraction conditions studied in this work, the weight loss of the initial raw material, corresponds to the lipophilic fraction extracted by the sc-CO<sub>2</sub> (a medium value of 5.7% of weight loss), and the content of other components was not affected after the sc-CO<sub>2</sub> extraction conditions. Therefore, the carbohydrate fraction remained in the raffinate phase after extraction. Carbohydrate content in BSG and raffinate is collected in **Table 2.3**. A similar finding was obtained by Taheri et al. [30] in the study of the effect of the pretreatment technique on enzymatic hydrolysis of food wastes after Soxhlet solid-liquid fat extraction.

**Table 2.3.** Carbohydrate composition of the untreated and sc-CO<sub>2</sub> treated BSG obtained at 40 MPa and 353 K in a dry and free-fat basis (g/100 g BSG) .

Carbohydrate	non-treated BSG	sc-CO <sub>2</sub> treated BSG (40 MPa/353 K)
Glucans	42 ± 2	43 ± 1
Xylans	15 ± 1	15.2 ± 0.1
Arabinans	8 ± 1	7.5 ± 0.5

**Figure 2.7a** represents the glucose concentration along enzymatic hydrolysis for sc-CO<sub>2</sub> treated BSG and non-treated at different enzyme concentrations. This figure also shows the glucose concentration in the liquid extract carried out at the same conditions (acetate buffer and 323 K), but with no enzyme addition. It is clear that glucose was not released to the medium in the absence of enzyme. Comparison of enzymatic performance for sc-CO<sub>2</sub> treated and non-treated BSG was done at different cellulose doses in a BSG basis. However, after removal of the fat content, the percentage of glucan content in the sc-CO<sub>2</sub> treated in a dry basis was higher than in the untreated BSG what means slightly lower enzyme:glucans ratios for the sc-CO<sub>2</sub> treated BSG. To better compare results in terms of enzyme dose in a glucan basis, initial reaction rate for all the experiments was evaluated and plotted as a function of the enzyme concentration in a glucan basis (**Figure 2.7b**). Higher values of the slope indicate a higher initial reaction rate for sc-CO<sub>2</sub> treated BSG than for untreated. An ANOVA confirmed statistically significant differences among the slopes at the 95 % confidence level and among the intercepts at the 99 % confidence level.

At the end of the enzymatic hydrolysis, statistically significant higher glucose concentration in the medium was obtained for sc-CO<sub>2</sub> treated compared to non-treated sc-CO<sub>2</sub> for all the enzymes concentrations. The percentage increase in glucose concentration evaluated at the end of the experimental extraction curves, for sc-CO<sub>2</sub> treated and non-treated BSG was 20, 18 and 17% for the three cellulase concentrations essayed in this work, 0.25, 0.5 and 1%, respectively. This percentage increase was similar to the value reported by Gao et al. [31] for the enzymatic hydrolysis of sc-CO<sub>2</sub> treated and non-treated rice straw with a mixture of cellulase and β-glucosidase. These authors obtained a final glucose yield of 32.4% for sc-CO<sub>2</sub> pretreated rice straw at 30 MPa and 110 °C during 30 min compared with 27.7% of glucose yield for non-pretreated rice straw, after 48 h of enzymatic treatment. That meant a percentage increase of about 17%.

Morais et al. [7] reviewed the use of carbon dioxide in biomass processing by considering the sc-CO<sub>2</sub> not only as an extraction medium but also as an agent to pretreat the biomass for subsequent enzymatic hydrolysis of the polysaccharides. According to different studies, it was shown that to obtain high yield of reducing sugars, the most important parameters were the temperature and the moisture content. For instance, Narayanaswamy et al. [32] observed that for wet corn stover (75%, w/w) at 240 bar, 120 °C for 60 min, the glucose yield was double compared to dry raw material. Kim & Hong [32] also reported that a certain content of moisture was needed in treated hardwood and softwood lignocellulosic materials to observe an improvement in enzymatic hydrolysis after sc-CO<sub>2</sub> biomass pretreatment. A 57% moisture content resulted in a 77 ± 3 and 37 ± 2 reducing sugar yield for aspen and southern yellow pine, respectively, compared to 15 ± 2 and 13 ± 3 for untreated biomass. As reported by Morais et al. [7] water can exert a double effect; on one hand, water facilitates a swelling effect on biomass, but also the presence of CO<sub>2</sub> acidifies the aqueous medium, causing a similar effect to a dilute-acid hydrolysis. In any case, physical properties of pressurized water at the operating conditions in previous reported studies play an important role in the improvement of enzymatic digestibility after treatment of the biomass in pressurized water-CO<sub>2</sub> systems. In fact, as reported by Morais et al. [9] after treatment at 130 °C with CO<sub>2</sub> in the medium (up to 3 MPa), the subsequent glucose yield after enzymatic hydrolysis was 39.97% after 96 h, only slightly higher than for untreated material that yielded 34.31% (around 17% increase, similar to the enhancement

obtained in this study). On the contrary, in presence of only pressurized water, with no CO<sub>2</sub> in the medium, 75% of the hemicellulose from wheat straw was removed at 180 °C. And, according to Aguirre-Fiero et al. [8] improvement of enzymatic saccharification of cellulose after treatment in pressurized systems water- CO<sub>2</sub> was due to an effective hemicellulose removal. In this regard, hemicellulose extraction by hydrothermal treatments is one of the most promising options since relative mild temperatures (160-210 °C) are required due to the properties of pressurized water under these conditions such as an increase in the ionic product that favours ionic reactions.

Therefore, it can be clearly observed that more severe conditions were employed in these previous works than the usual temperature range employed for sc-CO<sub>2</sub> extraction of the oil fraction from different vegetables matrix. Although water and high temperatures are encouraged to improve the subsequent enzymatic yield, in this work BSG was dried before sc-CO<sub>2</sub> extraction and the maximum operating temperature was 353 K. Higher temperature would led to oxidation of the extracted oil. Furthermore, by increasing water content in the feedstock, some water will be co-extracted with BSG oil, and the extraction would be not so efficient. As described in literature [34] for cooked and preheated canola samples, water coextraction led to milky droplets in the oil when the initial moisture content was higher than 12% and the cloudiness of extracts could be correlated with moisture loss from feed material. Therefore, drying of the BSG was carried out before sc-CO<sub>2</sub> extraction to obtain an oily fraction of good quality. This way, the sc-CO<sub>2</sub> treatment carried out in this work, offers the advantage of obtaining an added-value product as extract in addition to the improvement of subsequent enzymatic hydrolysis. Furthermore, the presence of lipids during enzymatic hydrolysis could cause different problems such as clogging, flotation, and mass transfer issues inside the reactor [30]. In any case, the improvement of enzymatic digestibility would also depend on biomass composition.

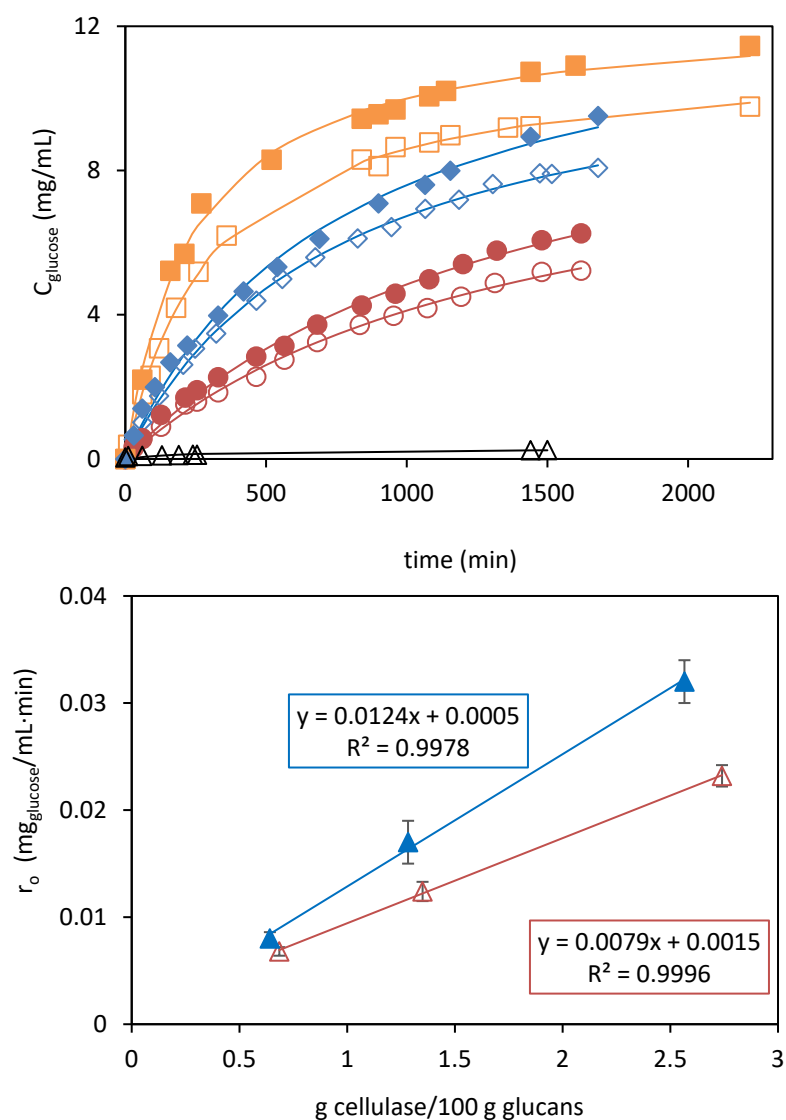


**Figure 2.7.** Results of enzymatic hydrolysis at 323 K (a) Glucose monomer concentration by using different cellulase dose on a BSG dry basis: ( $\Delta$ ) no cellulase; ( $\circ$ ,  $\bullet$ ) 0.25%, ( $\diamond$ ,  $\diamond$ ) 0.5%, ( $\square$ ,  $\blacksquare$ ) 1% cellulase. (b) Initial reaction rate for glucose release at different cellulase dose in a substrate (glucan) base ( $\Delta$ ,  $\blacktriangle$ ). Open symbols: untreated BSG. Filled symbols: sc-CO<sub>2</sub> treated BSG. Continuous lines: in (a) represent the Holtzapfle model in (b) the linear regression: for sc-CO<sub>2</sub> treated BSG,  $r_0 = 0.0124 E + 0.0005$   $R^2 = 0.9978$ ; for untreated BSG,  $r_0 = 0.0079 E + 0.0015$   $R^2 = 0.9996$  ( $E$  = cellulase dose on a glucan basis).

At 1% of cellulase dose, the hydrolysis kinetics for xylose and arabinose have been also determined for non-treated and sc-CO<sub>2</sub> treated BSG (**Figure 2.8**). Higher initial reaction rates were obtained for sc-CO<sub>2</sub>-treated BSG compared to non-treated. Although not big differences were observed in the final sugar concentration in the hydrolysates.

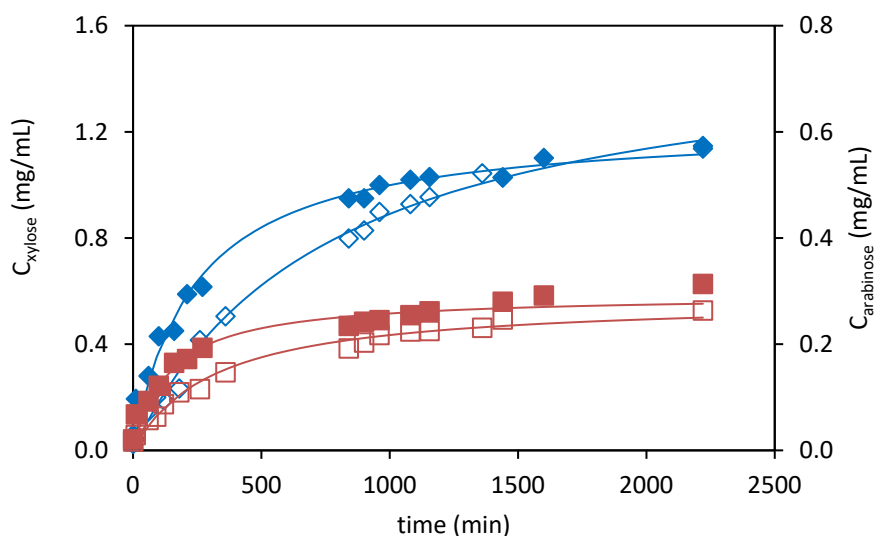


**Figure 2.8.** Results of enzymatic hydrolysis at 323 K and 1% of cellulase dose. (◆, ◇) xylose monomer concentration and (□, ■) arabinose monomer concentration. Open symbols: untreated BSG. Filled symbols: sc-CO<sub>2</sub> treated BSG. Continuous lines: represent the Holtzapfle model.

BSG is a lignocellulosic biomass, but it is also a valuable source of phenolic compounds, being hydroxycinnamic acids, such as ferulic and p-coumaric acids, the primary class of phenolic compounds. Enzyme assisted extraction of phenolic compounds is a suitable technology to achieve good extraction yields of these bioactive compounds. In this work, some phenolic compounds were determined in the enzymatic hydrolysates at the end of the hydrolysis by using 1% of cellulase. **Table 2.4** summarizes the values obtained in this work, together with other values previously reported by alkaline and enzymatic hydrolysis by using 1% xylanase and subcritical water hydrolysis [16], [26] (Chapter 1 and Chapter 3, respectively).



**Table 2.4.** Phenolic compounds release yield from BSG by different treatments

Treatment	Cumaric acid ( $\mu\text{g}/\text{g}_{\text{BSG}}$ )	Vanillin ( $\mu\text{g}/\text{g}_{\text{BSG}}$ )	Ferulic acid, ( $\mu\text{g}/\text{g}_{\text{BSG}}$ )	Reference
Celullase, 1%	$3.0 \pm 0.3$	$20 \pm 1$	$274 \pm 4$	This work
sc-CO <sub>2</sub> + Celullase, 1%	$3.9 \pm 0.3$	$21 \pm 2$	$341 \pm 6$	This work
Xylanase, 1%	$6 \pm 1$	$111 \pm 3$	$52.4 \pm 0.9$	
Alakaline hydrolysis	$538 \pm 4$	$217 \pm 1$	$1305.7 \pm 0.5$	[16], [26]
Subcritical water, 185 °C	$60 \pm 8$	$330 \pm 11$	$144 \pm 10$	

The concentration of p-coumaric and vanillin after cellulase hydrolysis was lower than the values previously reported for the same BSG by xylanase (1%), alkaline hydrolysis and subcritical water hydrolysis. However, for ferulic acid, only alkaline hydrolysis provided a higher value. Comparing the different results for cellulase treatment of non-treated and sc-CO<sub>2</sub> treated BSG, it can be observed that for vanillin similar concentration in the hydrolysates was obtained for both substrates. However, for p-coumaric acid and ferulic acid, a concentration 31% and 24% higher, respectively, was obtained in the BSG cellulase hydrolysates after sc-CO<sub>2</sub> treatment. That proves that sc-CO<sub>2</sub> treatment was also effective in the subsequent release of phenolic compounds.

The fitted parameters of Equation 7,  $C_{i,\text{max}}$  and  $t_{1/2}$  for non-treated and sc-CO<sub>2</sub> treated BSG are shown in **Table 2.5**. According to **Figure 2.7**, higher values of  $C_{i,\text{max}}$  for glucose were obtained for sc-CO<sub>2</sub> treated BSG. At the highest enzyme dose essayed in this work, the reduction in  $t_{1/2}$  was 23% for sc-CO<sub>2</sub>-treated BSG compared to non-treated-BSG. For xylose and arabinose, the final extraction yield was similar for non-treated, and sc-CO<sub>2</sub> treated BSG, but  $t_{1/2}$  decreased for the sc-CO<sub>2</sub> treated BSG (69 and 55% for xylose and arabinose, respectively). The calculated hydrolysis curves are plotted in **Figures 2.7a and 2.8** where a good agreement can be observed between experimental data and model.

**Table 2.5.** Fitted parameters of Equation 2.7 for enzymatic hydrolysis of non treated and sc-CO<sub>2</sub> treated BSG at different enzyme concentrations (C<sub>e</sub>% w/w).

C <sub>e</sub> (%)	Sugar	raw BSG			sc-CO <sub>2</sub> treated BSG		
		C <sub>i,max</sub>	t <sub>1/2</sub> (min)	RMSD	C <sub>i,max</sub>	t <sub>1/2</sub> (min)	RMSD
0	Glucose	0.29 ± 0.2	263 ± 99	0.03	<i>kinetics not performed</i>		
0.25	Glucose	9.8 ± 0.5	1385 ± 110	0.10	11.7 ± 0.6	1420 ± 119	0.12
0.5	Glucose	11.8 ± 0.2	743 ± 27	0.09	13.4 ± 0.6	758 ± 68	0.23
1	Glucose	11.3 ± 0.1	309 ± 10	0.11	12.4 ± 0.2	238 ± 14	0.23
1	Xylose	1.57 ± 0.06	774 ± 69	0.03	1.23 ± 0.04	234 ± 28	0.05
1	Arabinose	0.29 ± 0.01	342 ± 42	0.01	0.29 ± 0.01	143 ± 27	0.02

### 3.2.1. Mechanisms of enzymatic hydrolysis improvement after sc-CO<sub>2</sub> treatment

The higher enzymatic hydrolysis rate and yield obtained in the sc-CO<sub>2</sub> treated BSG compared with the untreated BSG could be partially attributed to the removal of the lipid fraction. As it has been described in literature [30], fats and oils could influence the susceptibility of carbohydrates to enzymes. Hu et al. [35] reported that the removal of lipids improved the enzymatic hydrolysis of starch by accelerating the penetration of enzymes into the starch granules and increasing the adsorption of enzymes to its substrate. Munira et al. [36] indicated that the lipid and protein, together with starch, might inhibit the enzymatic hydrolysis of starch as it was demonstrated by adding different fatty acids to starch and performing a subsequent enzymatic hydrolysis process by  $\alpha$ -amylase and amyloglycosidase enzymes. Therefore, it could be assumed an inhibition of cellulase enzymatic hydrolysis due to the presence of lipids. In this regard, Taheri et al. [30] concluded that the removal of fat by Soxhlet solid liquid extraction was the most appropriate pretreatment to increase the sugar yield by enzymatic hydrolysis for food waste collected from households, among different pretreatments essayed such as hydrothermolysis, sonolysis, electrocatalysis, electrolysis and sono-electrolysis.

The structural and chemical changes among untreated, sc-CO<sub>2</sub> treated and hydrolysed BSG were assessed by scanning electron microscopy and X-ray powder diffraction.

**Scanning electron microscope observation of BSG structure.**

The morphological changes of BSG after sc-CO<sub>2</sub> and enzymatic hydrolysis treatments were determined by scanning electron microscopy (SEM) (**Figure 2.9**).

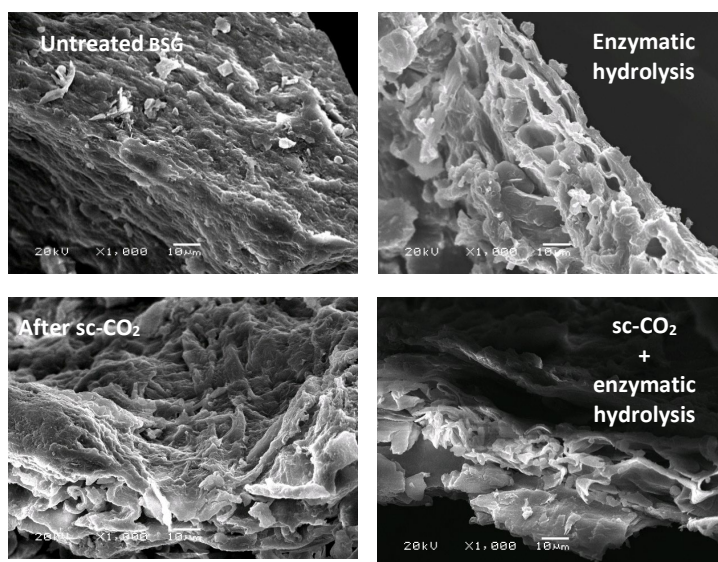


**Figure 2.9.** SEM micrographs (1000 x magnifications ) of the different BSG samples: untreated BSG, sc-CO<sub>2</sub> treated BSG and after enzymatic hydrolysis.

The untreated BSG presented a more rigid and continuous surface than after enzymatic and sc-CO<sub>2</sub> treatment at 40 MPa and 353 K (80 °C). After sc-CO<sub>2</sub> treatment, the BSG exhibited an irregular porosity and lamellar structure. sc-CO<sub>2</sub> breaks partially some structural barriers allowing a better enzyme access yielding higher hydrolysis yield. Gao et al. [31] also reported that microfibrils of rice straw were separated from the initial connected structure after sc-CO<sub>2</sub> at 30 MPa and 110 °C improving the enzyme access after treatment. From the micrographs of the enzymatic hydrolyzed BSG, it can be seen that the enzymatic hydrolysis left a swollen structure, with a porous and irregular structure, more disaggregated in the case of the previously sc-CO<sub>2</sub> treated BSG. This might be an indication of the intensity of the process and the removal of soluble and hydrolysable compounds.

**X-ray powder diffraction (XRD) analysis**

The XRD patterns of original BSG and the BSG after sc-CO<sub>2</sub> and enzymatic hydrolysis treatments is presented in **Figure 2.10**.

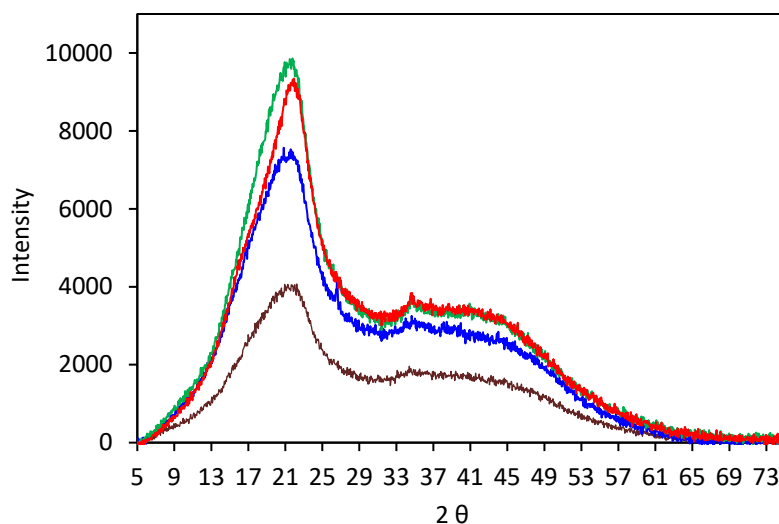


**Figure 2.10.** X-ray diffractograms of different BSG samples: (—) untreated BSG, (—) sc-CO<sub>2</sub> treated BSG, (—) BSG after enzymatic hydrolysis and (—) BSG after sc-CO<sub>2</sub> treatment and enzymatic hydrolysis.

The diffractogram for untreated BSG presented a broad peak at 21.6° and a small peak at 34.6°. A similar XRD pattern for raw BSG has been reported in literature [37]–[39]. Based on the XRD curve for BSG the crystallinity index as proposed by Segal et al. for native cellulose [40] was not evaluated in this work since the typical 002 lattice diffraction scattered intensity at the main peak around 22.5° for cellulose I was not observed. The lack of the typical crystalline and amorphous peaks at 22.5° and 18°, respectively was also indicated by Michelin and Teixeira [38] in the study of the degree of crystallinity of different bio-based materials. However, other authors [39] evaluated the crystallinity index for untreated BSG according to Segal et al. [40] obtaining a crystallinity index of 17.4% (in the present work a crystallinity index of 16.6% would have been obtained). The XRD pattern for BSG can be explained considering the BSG chemical composition with important amounts of different biopolymers, mainly proteins, hemicellulose, lignin, etc., which influenced the

XRD pattern [38]. Therefore, its structure is supposed to be semi-crystalline with broad bands and with a highly unclear crystallinity index as it can be observed in **Figure 2.10**.

After sc-CO<sub>2</sub> treatment a peak appeared at 26.6° and the peak at 34.7° was more remarkable. The XRD pattern after sc-CO<sub>2</sub> treatment indicated that the pretreatment was not strong enough to modify the BSG crystallinity. Narayanaswamy et al. [32] observed no change in crystallinity when comparing sc-CO<sub>2</sub> treated and untreated corn stover, probably due to the complex structure of corn stover where cellulose microfibrils are embedded in hemicellulose, lignin, and glycoproteins. Similar findings were reported by Liu et al. for cornstalk and rice straw [41]. These authors concluded that a change in biomass crystallinity might not be the only factor that could influence the enzymatic hydrolysis of the biomass. In any case, Park et al. [42] indicated that the interpretation of data on cellulose hydrolysis by enzymes in terms of crystallinity, assuming that the easily-accessible amorphous regions are more rapidly digested than the more difficult crystalline, is not straightforward based on several reasons, such as not a clear trend found in literature regarding the crystalline index and the hydrolysis degree, the effect of other components, such as particle size and porosity of the native cell wall sample must be considered.

After enzymatic hydrolysis, crystallinity seemed to increase based on the XRD plot with a sharper main peak and diffraction angles at around 34.7° for both untreated and sc-CO<sub>2</sub> treated BSG, probably due to the digestion of the amorphous cellulose fraction of the BSG during the enzymatic hydrolysis.

## 4. Conclusions

Sc-CO<sub>2</sub> has a double effect in a biorefinery context to include the BSG into a circular economy concept: (1) as green solvent for oil recovery obtaining an oily extract rich in linoleic acid with important amounts of bioactive compounds that provide good antioxidant properties (2) as pretreatment agent for further improvement of the enzymatic hydrolysis yield of the sc-CO<sub>2</sub> treated BSG. This improvement was mainly due to surface morphology modification and lipid fraction removal that facilitates the access of the

## CHAPTER 2

### *Valorization of brewer's spent grain by consecutive supercritical carbon dioxide extraction and enzymatic hydrolysis*

---

Therefore, in this work, low value BSG has been incorporated within a circular economy concept to obtain a valuable oil fraction and a useful residue for further hydrolytic enzyme process.

## 5. References

- [1] P. Manzanares, "The role of biorefining research in the development of a modern bioeconomy," *Acta Innovations*, no. 37, pp. 47–56, 2020.
- [2] P. Morone and G. Yilan, "A paradigm shift in sustainability: from lines to circles," *Acta Innovations*, no. 36, pp. 5–16, 2020.
- [3] V. Kitryte, A. Šaduikis, and P. R. Venskutonis, "Assessment of antioxidant capacity of brewer's spent grain and its supercritical carbon dioxide extract as sources of valuable dietary ingredients," *Journal of Food Engineering*, vol. 167, pp. 18–24, 2015, doi: 10.1016/j.jfoodeng.2014.12.005.
- [4] A. C. Fărcaș, S. A. Socaci, F. V. Dulf, M. Tofană, E. Mudura, and Z. Diaconeasa, "Volatile profile, fatty acids composition and total phenolics content of brewers' spent grain by-product with potential use in the development of new functional foods," *Journal of Cereal Science*, vol. 64, pp. 34–42, 2015, doi: 10.1016/j.jcs.2015.04.003.
- [5] G. Ferrentino, J. Ndayishimiye, N. Haman, and M. Scampicchio, "Functional Activity of Oils from Brewer's Spent Grain Extracted by Supercritical Carbon Dioxide," *Food and Bioprocess Technology*, vol. 12, no. 5, pp. 789–798, 2019, doi: 10.1007/s11947-019-02249-3.
- [6] M. Arshadi *et al.*, "Pre-treatment and extraction techniques for recovery of added value compounds from wastes throughout the agri-food chain," *Green Chemistry*, vol. 18, no. 23, pp. 6160–6204, 2016, doi: 10.1039/c6gc01389a.
- [7] A. R. C. Morais, A. M. Da Costa Lopes, and R. Bogel-Lukasik, "Carbon dioxide in biomass processing: Contributions to the green biorefinery concept," *Chemical Reviews*, vol. 115, no. 1, pp. 3–27, 2015, doi: 10.1021/cr500330z.
- [8] A. Aguirre-Fierro *et al.*, "Sustainable approach of high-pressure agave bagasse pretreatment for ethanol production," *Renewable Energy*, vol. 155, pp. 1347–1354, 2020, doi: 10.1016/j.renene.2020.04.055.
- [9] A. R. C. Morais, A. C. Mata, and R. Bogel-Lukasik, "Integrated conversion of agroindustrial residue with high pressure CO<sub>2</sub> within the biorefinery concept," *Green Chemistry*, vol. 16, no. 9, pp. 4312–4322, 2014, doi: 10.1039/c4gc01093k.
- [10] F. M. Relvas, A. R. C. Morais, and R. Bogel-Lukasik, "Kinetic modeling of hemicellulose-derived biomass hydrolysis under high pressure CO<sub>2</sub>-H<sub>2</sub>O mixture technology," *Journal of Supercritical Fluids*, vol. 99, pp. 95–102, 2015, doi: 10.1016/j.supflu.2015.01.022.
- [11] M. P. Fernández, J. F. Rodríguez, M. T. García, A. De Lucas, and I. Gracia, "Application of supercritical fluid extraction to brewer's spent grain management," *Industrial and Engineering Chemistry Research*, vol. 47, no. 5, pp. 1614–1619, 2008, doi: 10.1021/ie0708529.
- [12] S. Spinelli, A. Conte, L. Lecce, L. Padalino, and M. A. Del Nobile, "Supercritical carbon dioxide extraction of brewer's spent grain," *Journal of Supercritical Fluids*, vol. 107, pp. 69–74, 2016, doi: 10.1016/j.supflu.2015.08.017.

- [13] S. Rebolleda, S. Beltrán, M. T. Sanz, M. L. González-Sanjosé, and Á. G. Solaesa, "Extraction of alkylresorcinols from wheat bran with supercritical CO<sub>2</sub>," *Journal of Food Engineering*, vol. 119, no. 4, pp. 814–821, 2013, doi: 10.1016/j.jfoodeng.2013.07.008.
- [14] H. Sovová, "Mathematical model for supercritical fluid extraction of natural products and extraction curve evaluation," *Journal of Supercritical Fluids*, vol. 33, no. 1, pp. 35–52, 2005, doi: 10.1016/j.supflu.2004.03.005.
- [15] A. Bucić-Kojić, H. Sovová, M. Planinić, and S. Tomas, "Temperature-dependent kinetics of grape seed phenolic compounds extraction: Experiment and model," *Food Chemistry*, vol. 136, no. 3–4, pp. 1136–1140, 2013, doi: 10.1016/j.foodchem.2012.09.087.
- [16] P. Alonso-Riaño, M. T. Sanz, O. Benito-Román, S. Beltrán, and E. Trigueros, "Subcritical water as hydrolytic medium to recover and fractionate the protein fraction and phenolic compounds from craft brewer's spent grain," *Food Chemistry*, vol. 351, no. December 2020, 2021, doi: 10.1016/j.foodchem.2021.129264.
- [17] R. Murga, M. T. Sanz, S. Beltrán, and J. L. Cabezas, "Solubility of three hydroxycinnamic acids in supercritical carbon dioxide," *Journal of Supercritical Fluids*, vol. 27, no. 3, 2003, doi: 10.1016/S0896-8446(02)00265-6.
- [18] O. Benito-Román, M. Rodríguez-Perrino, M. T. Sanz, R. Melgosa, and S. Beltrán, "Supercritical carbon dioxide extraction of quinoa oil: Study of the influence of process parameters on the extraction yield and oil quality," *Journal of Supercritical Fluids*, vol. 139, no. May, pp. 62–71, 2018, doi: 10.1016/j.supflu.2018.05.009.
- [19] AOAC, "Tittle Fatty acids in oils and fats. Preparation of methyl esters boron trifluoride method AOAC 969.33-1969(1997), Fatty acids in oils and fats," vol. 1969, p. 1997, 1997.
- [20] V. L. Singleton, R. Orthofer, and R. M. Lamuela-Raventós, "Analysis of Total Phenols and Other Oxidation Substrates and Antioxidants by Means of Folin-Ciocalteu Reagent," *Methods in Enzymology*, vol. 299, pp. 152–178, 1999, doi: 10.1016/j.scienta.2016.11.004.
- [21] R. Re, N. Pellegrini, A. Proteggente, A. Pannala, M. Yang, and C. Rice-Evans, "Antioxidant Activity Applying an Improved Abts Radical Cation Decolorization Assay," *Free Radical Biology and Medicine*, vol. 26, no. 9, pp. 1231–1237, 1999, doi: 10.1016/S0891-5849(98)00315-3.
- [22] S. Rebolleda, N. Rubio, S. Beltrán, M. T. Sanz, and M. L. González-Sanjosé, "Supercritical fluid extraction of corn germ oil: Study of the influence of process parameters on the extraction yield and oil quality," *Journal of Supercritical Fluids*, vol. 72, pp. 270–277, 2012, doi: 10.1016/j.supflu.2012.10.001.
- [23] M. T. Holtzapple, H. S. Caram, and A. E. Humphrey, "A comparison of two empirical models for the enzymatic hydrolysis of pretreated poplar wood," *Biotechnology and Bioengineering*, vol. 26, no. 8, pp. 936–941, 1984, doi: 10.1002/bit.260260818.
- [24] D. P. Koullas, P. Christakopoulos, D. Kekos, B. J. Macris, and E. G. Koukios, "Correlating the effect of pretreatment on the enzymatic hydrolysis of straw,"



- Biotechnology and Bioengineering*, vol. 39, no. 1, pp. 113–116, 1992, doi: 10.1002/bit.260390116.
- [25] J. M. Del Valle, J. C. De La Fuente, and E. Uquiche, "A refined equation for predicting the solubility of vegetable oils in high-pressure CO<sub>2</sub>," *Journal of Supercritical Fluids*, vol. 67, pp. 60–70, 2012, doi: 10.1016/j.supflu.2012.02.004.
- [26] P. Alonso-Riaño, M. T. Sanz Diez, B. Blanco, S. Beltrán, E. Trigueros, and O. Benito-Román, "Water Ultrasound-Assisted Extraction of Polyphenol Compounds from Brewer's Spent Grain: Kinetic Study, Extract Characterization, and Concentration," *Antioxidants*, vol. 9, no. 3, p. 265, 2020, doi: 10.3390/antiox9030265.
- [27] L. F. Guido and M. M. Moreira, "Techniques for Extraction of Brewer's Spent Grain Polyphenols: a Review," *Food and Bioprocess Technology*, vol. 10, no. 7, pp. 1192–1209, 2017, doi: 10.1007/s11947-017-1913-4.
- [28] C. Bohnsack, W. Ternes, A. Büsing, and A. M. Drotleff, "Tocotrienol levels in sieving fraction extracts of brewer's spent grain," *European Food Research and Technology*, vol. 232, no. 4, pp. 563–573, 2011, doi: 10.1007/s00217-010-1419-z.
- [29] J. C. del Río, P. Prinsen, and A. Gutiérrez, "Chemical composition of lipids in brewer's spent grain: A promising source of valuable phytochemicals," *Journal of Cereal Science*, vol. 58, no. 2, pp. 248–254, 2013, doi: 10.1016/j.jcs.2013.07.001.
- [30] M. E. Taheri *et al.*, "Effect of pretreatment techniques on enzymatic hydrolysis of food waste," *Biomass Conversion and Biorefinery*, vol. 11, no. 2, pp. 219–226, 2021, doi: 10.1007/s13399-020-00729-7.
- [31] M. Gao, F. Xu, S. Li, X. Ji, S. Chen, and D. Zhang, "Effect of SC-CO<sub>2</sub> pretreatment in increasing rice straw biomass conversion," *Biosystems Engineering*, vol. 106, no. 4, pp. 470–475, 2010, doi: 10.1016/j.biosystemseng.2010.05.011.
- [32] N. Narayanaswamy, A. Faik, D. J. Goetz, and T. Gu, "Supercritical carbon dioxide pretreatment of corn stover and switchgrass for lignocellulosic ethanol production," *Bioresource Technology*, vol. 102, no. 13, pp. 6995–7000, 2011, doi: 10.1016/j.biortech.2011.04.052.
- [33] K. H. Kim and J. Hong, "Supercritical CO<sub>2</sub> pretreatment of lignocellulose enhances enzymatic cellulose hydrolysis," *Bioresource Technology*, vol. 77, no. 2, pp. 139–144, 2001, doi: 10.1016/S0960-8524(00)00147-4.
- [34] N. T. Dunford and F. Temelli, "Extraction conditions and moisture content of canola flakes as related to lipid composition of supercritical CO<sub>2</sub> extracts," *Journal of Food Science*, vol. 62, no. 1, pp. 155–159, 1997, doi: 10.1111/j.1365-2621.1997.tb04389.x.
- [35] P. Hu, X. Fan, L. Lin, J. Wang, L. Zhang, and C. Wei, "Effects of surface proteins and lipids on molecular structure, thermal properties, and enzymatic hydrolysis of rice starch," *Food Science and Technology*, vol. 38, no. 1, pp. 84–90, 2018, doi: 10.1080/10942912.2018.1561464.
- [36] Munira, Padil, Sarto, and M. Hidayat, "Inhibitor Effect (Lipid and Protein) in Starch Hydrolysis to Produce Glucose by using Amyloglucosidase," *IOP Conference Series*:

- Earth and Environmental Science*, vol. 175, no. 1, 2018, doi: 10.1088/1755-1315/175/1/012022.
- [37] D. M. Dos Santos, A. De Lacerda Bukzem, D. P. R. Ascheri, R. Signini, and G. L. B. De Aquino, "Microwave-assisted carboxymethylation of cellulose extracted from brewer's spent grain," *Carbohydrate Polymers*, vol. 131, pp. 125–133, 2015, doi: 10.1016/j.carbpol.2015.05.051.
- [38] M. Michelin and J. A. Teixeira, "Liquid hot water pretreatment of multi feedstocks and enzymatic hydrolysis of solids obtained thereof," *Bioresource Technology*, vol. 216, pp. 862–869, 2016, doi: 10.1016/j.biortech.2016.06.018.
- [39] P. K. Mishra, T. Gregor, and R. Wimmer, "Utilising brewer's spent grain as a source of cellulose nanofibres following separation of protein-based biomass," *BioResources*, vol. 12, no. 1, pp. 107–116, 2017, doi: 10.15376/biores.12.1.107-116.
- [40] L. Segal, J. J. Creely, A. E. Martin, and C. M. Conrad, "An Empirical Method for Estimating the Degree of Crystallinity of Native Cellulose Using the X-Ray Diffractometer," *Textile Research Journal*, vol. 29, no. 10, pp. 786–794, 1959, doi: 10.1177/004051755902901003.
- [41] Y. F. Liu, P. Luo, Q. Q. Xu, E. J. Wang, and J. Z. Yin, "Investigation of the effect of supercritical carbon dioxide pretreatment on reducing sugar yield of lignocellulose hydrolysis," *Cellulose Chemistry and Technology*, vol. 48, no. 1–2, pp. 89–95, 2014.
- [42] S. Park, J. O. Baker, M. E. Himmel, P. A. Parilla, and D. K. Johnson, "Cellulose crystallinity index: Measurement techniques and their impact on interpreting cellulase performance," *Biotechnology for Biofuels*, vol. 3, pp. 1–10, 2010, doi: 10.1186/1754-6834-3-10.

# CHAPTER 3

---

**Subcritical water as hydrolytic medium to recover and fractionate the protein fraction and phenolic compounds from craft brewer's spent grain**

**Based on the article:**

P. Alonso-Riaño, M. T. Sanz, B. Blanco, S. Beltrán, E. Trigueros and O. Benito-Román (2021).

“Subcritical water as hydrolytic medium to recover and fractionate the protein fraction and phenolic compounds from craft brewer's spent grain”.

Food Chemistry, 351, 129264

DOI: <https://doi.org/10.1016/j.foodchem.2021.129264>



## Capítulo 3

### Utilización de agua subcrítica para recuperar y fraccionar la fracción proteica y los compuestos fenólicos del bagazo de cerveza

---

#### Resumen

En este capítulo se ha estudiado la valorización del bagazo de cerveza (BSG) generado en una industria de cerveza artesanal mediante hidrólisis en agua subcrítica, utilizando un reactor semicontinuo de lecho fijo a escala de laboratorio. Se ha estudiado el efecto de la temperatura en un rango de 125 a 185 °C, a un flujo constante de 4 mL/min. La hidrólisis de esta biomasa proporcionó hasta un 78% de proteína solubilizada a 185 °C. Los aminoácidos libres presentaron un nivel máximo a 160 °C con un valor de 55 mg de aminoácidos libres/g<sub>proteína-bagazo</sub>. Los aminoácidos polares mostraron un rendimiento máximo a temperaturas más bajas que los aminoácidos no polares. El máximo contenido fenólico total se alcanzó a 185 °C. Los aldehídos fenólicos identificados, tanto en los extractos obtenidos a 160°C, como a 185 °C, fueron la vainillina, el aldehído siríngico y el aldehído protocatéquico, los cuales presentaron un nivel máximo a 185 °C. Sin embargo, los ácidos hidroxicinámicos, como el ferúlico y el p-cumárico, se obtuvieron en mayor concentración a 160 °C. Esto permite un fraccionamiento de los compuestos bioactivos. El agua subcrítica brinda nuevas oportunidades para que las pequeñas cerveceras se incorporen dentro del concepto de biorrefinería.

---

**Palabras clave:** extracción/hidrólisis con agua subcrítica, biorrefinería, bagazo de cerveza, proteínas, aminoácidos, compuestos fenólicos, capacidad antioxidante.



## Abstract

---

The valorization of the brewer's spent grain (BSG) generated in a craft beer industry was studied by subcritical water hydrolysis in a semi-continuous fixed-bed reactor. Temperature was varied from 125 to 185 °C at a constant flow rate of 4 mL/min. Biomass hydrolysis yielded a maximum of 78% of solubilized protein at 185 °C. Free amino acids presented a maximum level at 160 °C with a value of 55 mg free amino acids/g<sub>protein-BSG</sub>. Polar amino acid presented a maximum at lower temperatures than non-polar amino acids. The maximum in total phenolic compounds was reached at 185 °C. This maximum is the same for aldehyde phenolic compounds such as vanillin, syringic and protocatechuic aldehyde; however, for hydroxycinnamic acids, such as ferulic acid and p-coumaric, the maximum was obtained at 160 °C. This allows a fractionation of the bioactive compounds. Subcritical water addresses opportunities for small breweries to be incorporated within the biorefinery concept.

---

**Keywords:** subcritical water extraction, biorefinery, brewer's spent grain, protein, amino acids, individual phenolic compounds, antioxidant capacity.





## 1. Introduction

Currently, in the linear economic system most of the by-products or wastes generated in the food industry are usually discarded. Integration of these waste material flows as raw material to another industrial process constitutes the main principle of the circular economy concept to reach zero waste objective. Brewer's spent grain (BSG) is a lignocellulosic solid by-product generated in the brewing industry that remains after the mashing and wort filtration process. BSG is generated in large, but also small companies [1] Valorisation of the by-products generated by small local companies addresses also opportunities for small breweries to be incorporated within the biorefinery concept. Especially, taking into account that the size of the Europe craft beer market was worth US\$ 42.52 million in 2020 and it is expected to grow up to 91.26 million by the end of 2025 [2].

BSG accounts approximately for 20 kg per 100 L of beer produced [1]. BSG contains also a considerable amount of proteins, in the mass percent range from 10 to 30% and a small amount of lipids, around 5% [3]. BSG is also a valuable source of phenolic compounds, with approximately 1.2% of mono- and di-meric phenolic acids, being hydroxycinnamic acids, such as ferulic and p-coumaric acids, the primary class of phenolic compounds present in the BSG that have demonstrated antioxidant effects [4]. Therefore, based on the chemical composition of the BSG, integration of this by-product within a biorefinery concept is of great interest to obtain different high value biocompounds.

To convert BSG into valuable added products, the first step should be the extraction of the bioactive compounds. Different extraction techniques can be applied, being the most commonly used extraction system the solid-liquid extraction by maceration of the biomass in a solvent. However, long extraction times are needed and in most cases, low extraction yield is achieved. BSG as lignocellulosic biomass contains important amounts of insoluble lignin. This lignin is connected to the cell wall polysaccharides by phenolic acids, being necessary a hydrolytic method to release them [3], [5]. In a previous work, ultrasound assisted extraction (UAE) was compared with chemical/enzymatic hydrolysis to obtain extracts rich in hydroxycinnamic acids [6]. The best results were obtained by using alkaline hydrolysis in terms of productivity and final extraction yield due to higher solubility of the

lignin under basic conditions. Therefore, bioactive compounds extraction from biomass is still a major challenge to the biorefinery concept.

The use of subcritical water (subW) has been proposed in literature to fractionate and separate the different components of the lignocellulosic biomass [7]. subW is pressurized water in its liquid state in the temperature range from 100 °C to 374 °C. Under these conditions, water presents unique properties such as higher ionic product and lower dielectric constant than at ambient conditions [7]. Due to the tuneable properties with temperature, different selectivity can be achieved in the release of the bioactive compounds from the biomass. For instance, the different phenolic compounds obtained from decomposition of rice bran under subW treatment showed the maximum production of p-coumaric acid and vanillin at 165 °C and 190 °C, respectively, while protocatechuic acid and vanillic acid presented the highest level at 230 and 295 °C, respectively [8]. Therefore, the temperature in subW treatment is a critical parameter.

A few studies on subW have been conducted with BSG. [9] focused on the production of C-5 sugars observing that total carbohydrate yields were dependent of the hydrolysis temperature in the range from 160 to 210 C. On the other hand, [10] evaluated different pretreatment strategies for protein extraction from BSG including hydrothermal treatment, in the range from 30 up 135 °C at two different extraction times, 1 and 24 h. It must be notice that subW is water in its liquid state in the range from 100°C to 374 °C. These authors determined that the maximum extraction yield was obtained at 60 °C (ca 60%). This extraction yield was surprisingly higher, since, according to literature albumins (water-soluble), and globulins (salt-soluble) compose only around 20% of the total protein content in BSG as a result of their unavoidable extraction during brewing process [11], being hordeins (alcohol soluble) and glutelins (acid/alkali soluble) proteins the main proteins in BSG. Therefore, it is also worth exploring subW treatment further to produce hydrolysate from proteins from BSG, since by controlling temperature and reaction time it is possible to control the production of small peptides and free amino acids from different food wastes [12].

The aim of this work was to verify if subW treatment is a suitable technology to extract/hydrolyse the protein fraction from BSG. One of the main goals of this work is to perform a detail extract characterization considering also the release into the extraction

medium of the bound phenolic compounds of BSG. Antioxidant capacity of the subW extracts and the presence of inhibitors, such as furfural and hydroxymethyl furfural was also explored. The solid residue generated after subW treatment would be also characterized to check mass balance of the process.

## 2. Material and methods

### 2.1. Raw material

BSG was supplied by Brebajes del Norte S.L. (Dolina, craft beer), a local brewery located in Burgos (Spain). This raw material was first preconditioned by washing it with water (until neutral pH) and drying in an air convection oven (45 °C, 3 h) until a humidity value of 8 % (w/w) was reached. No size reduction was carried out.

### 2.2. Subcritical Water equipment

SubW experiments have been carried out in a semi-continuous fixed-bed reactor (see **Figure 3.1**) self-assembly by our research group [13].

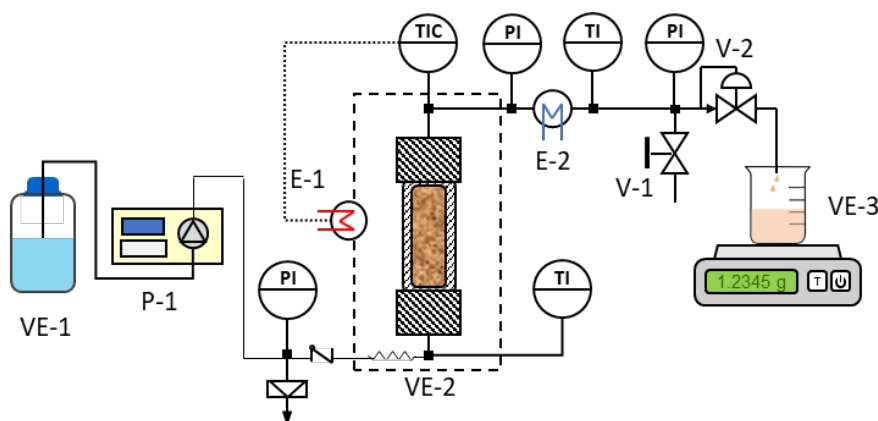


**Figure 3.1.** Continuous subW extraction equipment provided with a fixed-bed reactor.

Validated for temperatures up to 230 °C and volumetric flows up to 10 ml/min.

An HPLC pump (Gilson 305, SC-10 head with a maximum flow of 10 mL / min) was used for pressurization and water pumping. Water was heated up to the desired treatment

## CHAPTER 3

### Subcritical water as hydrolytic medium to recover and fractionate the protein fraction and phenolic compounds from craft brewer's spent grain

temperature by circulating it through a heat exchanger (60 cm of 0.317 cm AISI 316 piping) placed inside an oven (Selecta T 204A) together with the fixed bed reactor (length 20.6 cm and internal diameter of 2.8 cm). Two metallic filters (10  $\mu\text{m}$  pore size) were placed at the top and the bottom of the reactor to avoid loss of solid particles and clogging of the system. Pressure was controlled by a pressure regulating valve (pressure Tech 6784 V962 max 41.4 MPa).

subW experiments were performed at a fixed water flow rate of 4 mL/min and operating pressure of 5 MPa. Approximately 12 g of dry BSG were placed in the reactor and inserted in the oven. The experiments were performed in the temperature range from 125 to 185 °C. Temperature and pressure were steadily increasing up to the selected treatment conditions during a static holding time of 30 min, in order to have enough time to reach the operation temperature. The time zero was taken as the time at which liquid extract was obtained at the outlet pipe. Effluents were cooled and periodically collected for further characterization. The solid residue that remained in the reactor after subW treatment was washed, dried in an oven at 45 °C until constant weight, weighted and analyzed.

### **2.3. Enzymatic and basic hydrolysis**

Firstly, 7.5 g of the BSG were introduced into a 500 mL jacketed reactor provided with magnetic agitation together with 150 mL of the reaction medium. Enzymatic and basic hydrolysis were performed at 50 °C for 4 h. For basic hydrolysis, different concentrations of NaOH were assayed, 0.01 M, 0.1 M and 1 M. For enzymatic hydrolysis, the enzyme was added to the water medium in a mass percentage of 6% (enzyme:BSG ratio, w/w). Three different enzymes were used: protease, proteinase EC 3.2.1.6, from *Bacillus subtilis* (Biocon), xylanase, a mixture of xylanase endo-1,4 $\beta$  (EC 3.2.1.8) and xylanase endo-1,3 $\beta$  (EC 3.2.1.32) from *Trichoderma longibrachiatum* (Biocon) and cellulase, 1,4-(1,3:1,4)- $\beta$ -D-Glucan 4-glucanohydrolase, EC 3.2.1.4, from *Aspergillus niger* (Sigma-Aldrich). After 4 h, the enzyme was inactivated by heating the sample at 100 °C for 5 min and immediately cooled in ice and kept in the refrigerator until analysis.

## 2.4. Analytical methods

### 2.4.1. Brewer's spent grain characterization

A complete chemical characterization of BSG was performed according to the National Renewable Energy Laboratory standard protocols [14] to determine structural carbohydrates (cellulose and hemicellulose), lignin, moisture, total solids, ash, total extractives, and protein. Duplicate analysis was done for characterization of the composition of BSG. Detailed description can be found in the NREL protocols [14]. Extractives free BSG was subjected to two steps acid hydrolysis. Firstly, 0.3 g of dry BSG was mixed with 3.0 ml of 72% (w/w) H<sub>2</sub>SO<sub>4</sub> and incubated at 30 °C for 1 h. Then, the sample was diluted to 4% (w/w) H<sub>2</sub>SO<sub>4</sub> by adding 84 ml of deionized water and was autoclaved at 121 °C for 1 h. Then, the hydrolysate was cooled down to room temperature and vacuum filtered through a 0.7 µm pore size hydrophilic glass fiber filter (Millipore). The acid insoluble residue (AIR) was rinsed with 50 mL of deionized water, dry 4 h at 105 °C and weighed. Ash content was determined by weight difference after placing AIR in a muffle furnace at 575 °C for 24 hours. Klason lignin (KL) was calculated as the difference between AIR and ash. Acid soluble lignin in the hydrolysate was estimated by absorbance reading of the sample at 240 nm and using 25 L·g<sup>-1</sup>·cm<sup>-1</sup> as absorptivity constant.

For cellulose and hemicellulose determination, sugar recovery standards (SRSs) were used to account for sample sugar degradation during the dilute sulfuric acid step. SRSs and BSG hydrolysates were neutralized with CaCO<sub>3</sub> to pH 5–6 and filtered through a 0.2 µm syringe filters before HPLC determination.

Monosaccharides were determined by HPLC equipped with a Biorad Aminex-HPX-87 H column and its corresponding pre-column with two detectors, a variable wavelength detector (VWD) and a refractive index detector (RID) using 0.005 M sulfuric acid as mobile phase. The temperature of the column and the refractive index detector was 40 °C. The injected sample volume was 20 µL. Cellulose was estimated as the difference between glucose determined after hydrolysis and glucose due to starch and β-glucans. Hemicellulose was estimated from the xylan and arabinan content in the sample.

### CHAPTER 3

#### Subcritical water as hydrolytic medium to recover and fractionate the protein fraction and phenolic compounds from craft brewer's spent grain

*Ash content* was determined by weight difference after placing samples in a muffle furnace at 575 °C for 24 hours until constant weight.

*Starch and β-glucans.* Starch and β-Glucan content was determined by using the total starch (amyloglucosidase/α-amylase method) and the mixed linkage beta-glucan assay kit, according to the manufacturer's (Megazyme International Ltd.) instructions.

*Elemental composition.* Elemental composition (C, H, N, S, O) of the raw material was determined by an organic elemental micro-analyzer equipment (Thermo Scientific Model Flash 2000).

*Lipid fraction.* The oil content of the BSG was determined by Soxhlet extraction (Buchi B-811) using hexane as solvent.

*Protein content.* Protein in the raw material was estimated from the nitrogen content present in the samples as measured by the elemental analysis and verified by the Kjeldhal method. The N-factor was calculated from the amino acid profile and nitrogen data, according to the NREL standard protocols [14]. The N-factor of the sample was calculated as the average of the upper and lower limits,  $k_A$  and  $k_P$  respectively, according to the following equations:

$$k_A = \frac{\sum E_i}{\sum D_i} \quad [3.1a]$$

$$k_P = \frac{\sum E_i}{\sum N} \quad [3.1b]$$

where  $E_i$  are the grams of the  $i^{\text{th}}$  amino acid/100 g of dry sample;  $D_i$  are the grams of nitrogen of the  $i^{\text{th}}$  amino acid/100 g of dry sample and  $N$  are the grams of nitrogen/100 g of dry sample. A range of highest probability ( $k_1, k_2$ ) was calculated as follows:

$$k_1 = \text{avg}(k_A, k_P) + 0.25 (\text{avg}(k_A, k_P)) \quad [3.2a]$$

$$k_2 = \text{avg}(k_A, k_P) - 0.25 (\text{avg}(k_A, k_P)) \quad [3.2b]$$

*Amino acid profile.* The amino acid profile of BSG was obtained according to AOAC Official Method 982.30 [15] with some modifications. A sample of 100 mg of milled BSG

## CHAPTER 3

### Subcritical water as hydrolytic medium to recover and fractionate the protein fraction and phenolic compounds from craft brewer's spent grain

was hydrolyzed for 1 hour in a boiling water bath and then for 23 hours at 110 °C in an oven, in 1 mL of 6 N HCl, dissolved in 1 mL of 0.1 M HCl: EtOH (1:1, v: v) and neutralized with Na<sub>2</sub>CO<sub>3</sub> until the pH was greater than 1.5 but less than 5. Tryptophan and cysteine are lost by acid hydrolysis, and methionine can be partially destroyed by acid hydrolysis, so, an alkaline hydrolysis was performed to determine these amino acids. In this case, a sample of 100 mg of milled BSG was hydrolyzed for 1 hour in a boiling water bath and then for 23 hours at 110 °C in an oven, in 7 mL of 4.2 M NaOH, and neutralized with 6 N HCl until pH greater than 1.5 but less than 5. Final solutions were analyzed by gas chromatography after derivatization by using the EZ:faast™ kit (Phenomenex). The derivatized amino acids were analyzed using a GC-FID instrument (Hewlett Packard; HP, 5890 Series II) equipped with an auto-sampler (Avondale, PA, USA). Aliquots of the derivatized amino acids (4 µL) were injected at 1:15 split ratio at 250 °C into a Zebron column (ZB –AAA, 10 m and 0.25 mm in diameter) programmed from 110 to 320 °C at 32 °C/min. Helium was used as a carrier gas at 60 kPa and nitrogen was used as a make-up gas. The detector temperature was 320 °C. Amino acids were identified by standards includes in the mentioned kit. Norleucine was used as internal standard.

#### **2.4.2. Liquid and solid streams from subcritical water treatment characterization**

##### **2.4.2.1. Liquid extracts**

**Protein content.** Protein content in the subW extracts was quantitatively analyzed by two different methods: 1) from the nitrogen content by using a Shimadzu TOC-V CSN analyzer using KNO<sub>3</sub> as standard and a convenient NF and 2) by using the kit RC DCTM (Bio Rad Laboratories) based on the Lowry assay but modified to allow protein determination in the presence of reducing agents and detergents using bovine serum albumin as standard.

**Degree of hydrolysis.** Degree of hydrolysis (DH) is defined as the proportion of cleaved peptide bonds in a protein hydrolysate [16]:

$$DH = \frac{h}{h_{tot}} \cdot 100 \quad [3.3]$$

where  $h_{tot}$  is the sum of the millimoles of individual amino acids per gram in the unhydrolyzed protein that was calculated from the amino acid profile, and  $h$  is the free

### CHAPTER 3

#### Subcritical water as hydrolytic medium to recover and fractionate the protein fraction and phenolic compounds from craft brewer's spent grain

amino acid content in the subW extracts, expressed as meq/g protein and was determined by the ninhydrin assay. First, 2 mL of the sample were gently mixed with 1 mL of ninhydrin reagent solution and placed into a boiling water bath for 10 min. Samples were cooled and 5 mL of 95% ethanol were added. Absorbance was measured at 570 nm. Ninhydrin reagent solution was purchased from Sigma-Aldrich and leucine was used as standard.

*Free amino acids.* Free amino acids were analyzed by gas chromatography after derivatization by using the EZ:faast™ kit (Phenomenex) as described in section 2.4.1. Free amino acids yield of the aqueous extracts was obtained by the Equation 3.4.

$$\text{Yield}, i = \frac{E_i}{R_i} \cdot 100 \quad [3.4]$$

where  $E_i$  are the grams of the  $i^{\text{th}}$  amino acid/100 g<sub>dry-BSG</sub> in the subW extracts collected and  $R_i$  are the grams of the  $i^{\text{th}}$  amino acid/100 g<sub>dry-BSG</sub> in the raw material.

*Total organic carbon (TOC)* A Total Organic Carbon Analyzer Shimadzu (TOC-V CSN) was used to quantify the concentration of total carbon (TC) and inorganic carbon (IC). Potassium hydrogen phthalate and sodium hydrogen carbonate were used as standards. The TOC concentration was then calculated by subtracting the IC concentration from the obtained TC concentration.

*Total Polyphenols Content (TPC) and Antioxidant Activity.* TPC was determined by using the Folin–Ciocalteu reagent following the method described by [17]. A calibration curve was prepared with standard solutions of gallic acid by following the same colorimetric method and results were expressed as mg of gallic acid equivalent (GAE) per gram of dry BSG.

The FRAP method was performed according to [18]. Absorbance was read at 593 nm. As standard, a solution of FeSO<sub>4</sub>·7H<sub>2</sub>O (0.1 M) was used. Results were expressed in μmoles of Fe<sup>2+</sup> per gram of dry BSG.

*Individual phenolic compounds.* The identification and quantification of individual phenolic compounds was performed according to the method previously described by (Alonso-Riaño et al., 2020). This method was already applied to identify and quantify individual phenolic compounds from other raw materials such as olive leaves (Kashaninejad, Sanz, Blanco, Beltrán & Mehdi Niknam, 2020) and onion peels (Benito-Román, Blanco, Sanz



### CHAPTER 3

#### Subcritical water as hydrolytic medium to recover and fractionate the protein fraction and phenolic compounds from craft brewer's spent grain

& Beltrán, 2020). The sample was filtered through a 0.2 µm syringe filters. After that, 80 µl of sample were injected in the HPLC system. The separation was performed at 25 °C on a Kinetex® µm Biphenyl 100 Å, 250 × 4.6 mm column (Phenomenex). The mobile phase consisted of ammonium acetate 5 mM with acetic acid (1%; v/v) in water (solvent A) and ammonium acetate 5 mM with acetic acid (1%; v/v) in acetonitrile (solvent B). The composition of the mobile phase varied during the run according to a nonlinear gradient as follows: from 0 to 7 min 2% of solvent B (isocratic), from 7 to 20 min from 2% to 8% solvent B, from 20 to 35 min from 8% to 10% solvent B and from 35 to 55 min 10% to 18% solvent B and post time of 10 min at a flow rate of 0.8 ml/min. Detection and quantification was performed at 240, 280, 330, 340, 350, and 370 nm. The HP ChemStation software was employed to collect and analyse the chromatographic data delivered by the diode array detector and own library was used to identify the different phenolic compounds by comparing retention times and spectral data with those of authentic standards: syringic aldehyde, protocatechuic aldehyde, vanillin, p-coumaric acid, ferulic acid, catechin, vanillic acid, 4-vinylphenol and 4-vinylguaicol standards (Sigma-Aldrich). Peak purity was checked to exclude any contribution from interfering peaks. Individual stock solutions of the above phenolic compounds, and their mixtures, were prepared in methanol to plot the calibration curves.

*Furfural and hydroxymethylfurfural (HMF)* Furfural and HMF analysis were performed by HPLC-RID-VWD Agilent 1260 at 284 and 275 nm respectively, by using the same column and method as described in section 2.3.1. Calibration was performed with standards of 5-hydroxymethyl-2-furaldehyde (HMF), 97%, and furfural, 99%, purchased from Alfa Aesar and Sigma-Aldrich, respectively. The sample was filtered through a 0.2 µm syringe filters. After that, 20 µl of sample were injected in the HPLC system.

#### **2.4.2.2. Solid residues**

Solid residues after subW treatment were washed, dried for 24 h at 45 °C and weighted. Elemental composition (C, H, N, S, O) was determined. The high heating value (HHV) of the solid residue and raw material was evaluated by the following equation [19]

$$HHV (kJ/kg) = 3.55C^2 - 232C - 2230H + 51.2C \cdot H + 131N + 20600 \quad [3.5]$$

## 2.5. Statistical Analysis

All values were expressed as mean  $\pm$  standard deviation of at least three replicates. The significance of the differences was determined based on an analysis of the variance with the Fisher's Least Significant Difference (LSD) method at  $p$ -value  $\leq 0.05$ . Correlation between antioxidant activity and the different bio-compounds released in the medium, TPC, free amino acids and protein fraction, was determined using Person's Correlation Test. The software Statgraphics X64 was used.

## 3. Results and discussion

### 3.1. Brewer's spent grain characterization

Chemical composition of the BSG is showed in **Table 3.1**. The protein content was  $17.7 \pm 0.1\%$  (w/w). This value was within the range of other values found in the literature, from 10 to 31% (w/w) [1], [20], [21].

The protein content has been traditionally calculated by multiplying the total nitrogen determined by the Kjeldahl or Dumas methods by a standard nitrogen conversion factor of 6.25, which assumes that 1 kg of material contents 160 g of N. However, the relation between protein and nitrogen can vary depending on the amino acid composition and the presence of other nitrogenous organic compounds such as nucleic acids, urea, ammonia, phospholipids, nitrates, and purine derivatives [22]. In this work, the N:P conversion factor was calculated by using the amino acid profile showed in **Table 3.2**, yielding a value of 6.11. According to the Equations 3.2a and 3.2b, the range of highest probability ( $k_1$ ,  $k_2$ ) was 5.8-6.4. Since 6.25 was within the range of highest probability calculated and being the standard value widely used in the literature, this value was used as NF in this work. No conversion factor for BSG was found in the literature, although [23] reported a value of 5.83 as the specific factor for the conversion of nitrogen content to protein content for barley.

Extractives in water were 24.3% (w/w), which included 5.02 g/100 g<sub>dry-BSG</sub> of soluble proteins (28.4% of the total protein content). This result agrees with literature that reported around 20% of soluble proteins from the total protein content in BSG, being hordeins over 50% of the total amount of proteins, followed by glutelins [11]. Hordeins are rich in glutamic

### CHAPTER 3

#### *Subcritical water as hydrolytic medium to recover and fractionate the protein fraction and phenolic compounds from craft brewer's spent grain*

---

acid and proline and these amino acids constituted 24% of the BSG amino acids determined in this work,  $117 \pm 2$  and  $123 \pm 5$  mg aa/g<sub>prot-BSG</sub>, respectively (see **Table 3.2**). It was found that  $53 \pm 3\%$  of the total BSG amino acids were essential amino acids (EAA), being valine, leucine and lysine the three most abundant. These results agree with literature that also reported glutamine/glutamate, proline and leucine as the most abundant amino acids [10], [19], [23], [24].

**Table 3.1.** Chemical composition of BSG expressed in weight percentage in a dry basis

Component	g/100 g <sub>dry-BSG</sub>
Extractives in water	$24.3 \pm 0.6$
Water soluble protein	$5.02 \pm 0.08$
Water extractable polyphenols (mg <sub>GAE</sub> /g)	$2.72 \pm 0.04$
Extractives in ethanol	$1.8 \pm 0.2$
Ethanol extractable polyphenols (mg <sub>GAE</sub> /g)	$1.6 \pm 0.2$
Protein*	$17.7 \pm 0.1$
Cellulose	$18 \pm 2$
Hemicellulose	$26 \pm 2$
Xylan	$14.6 \pm 0.9$
Arabinan	$7.9 \pm 0.9$
Acetyl groups	$3.6 \pm 0.4$
Starch	$7.9 \pm 0.2$
β-Glucan	$0.62 \pm 0.02$
Soluble lignin	$4.30 \pm 0.06$
Insoluble lignin	$13.5 \pm 0.5$
Lipids	$5.90 \pm 0.01$
Ash	$2.90 \pm 0.02$

\*Protein includes the protein content in the extractives fraction (5.02%)

**Table 3.2.** Amino acid profile of BSG. Final accumulative free amino acid yields in the subW extracts obtained at different temperatures, expressed as mg aa/g<sub>protein</sub> and percent yield as the ratio of individual amino acids in the extracts and in the raw material, Eq 4). F = 4 mL/min. °°

Amino acid	BSG	SubW 125 °C		SubW 145 °C		SubW 160 °C		subW 185 °C	
	mg aa/g <sub>protein</sub>	mg aa/g <sub>protein</sub>	Yield, %	mg aa/g <sub>protein</sub>	Yield, %	mg aa/g <sub>protein</sub>	Yield, %	mg aa/g <sub>protein</sub>	Yield, %
Alanine	48.1 ± 0.2	2.46 ± 0.01 <sup>a</sup>	5.13 ± 0.03 <sup>a</sup>	3.08 ± 0.01 <sup>b</sup>	6.41 ± 0.01 <sup>b</sup>	3.29 ± 0.01 <sup>c</sup>	6.84 ± 0.01 <sup>c</sup>	3.62 ± 0.01 <sup>d</sup>	7.52 ± 0.02 <sup>d</sup>
Aspartic acid	69 ± 3	3.32 ± 0.01 <sup>a</sup>	4.8 ± 0.2 <sup>a</sup>	10.2 ± 0.1 <sup>c</sup>	15.6 ± 0.8 <sup>c</sup>	15.4 ± 0.2 <sup>d</sup>	22 ± 1 <sup>d</sup>	4.4 ± 0.1 <sup>b</sup>	6.3 ± 0.4 <sup>b</sup>
Cysteine	4.7 ± 0.2	n.d.	--	n.d.		0.33 ± 0.01 <sup>b</sup>	7.1 ± 0.4 <sup>b</sup>	0.22 ± 0.01 <sup>a</sup>	4.8 ± 0.3 <sup>a</sup>
Glutamic acid	117 ± 2	6.3 ± 0.1 <sup>c</sup>	5.4 ± 0.2 <sup>c</sup>	6.15 ± 0.02 <sup>c</sup>	5.3 ± 0.1 <sup>c</sup>	4.26 ± 0.09 <sup>b</sup>	3.65 ± 0.1 <sup>b</sup>	1.15 ± 0.06 <sup>a</sup>	0.98 ± 0.07 <sup>a</sup>
Glycine	42 ± 1	0.84 ± 0.01 <sup>a</sup>	2.01 ± 0.07 <sup>a</sup>	1.28 ± 0.01 <sup>b</sup>	3.1 ± 0.1 <sup>b</sup>	1.91 ± 0.01 <sup>c</sup>	4.6 ± 0.1 <sup>c</sup>	3.16 ± 0.01 <sup>d</sup>	7.6 ± 0.2 <sup>d</sup>
Histidine <sup>e</sup>	23 ± 2	1.47 ± 0.05 <sup>b</sup>	6.4 ± 0.8 <sup>b</sup>	1.92 ± 0.01 <sup>c</sup>	8.4 ± 0.8 <sup>c</sup>	1.9 ± 0.1 <sup>c</sup>	8 ± 1 <sup>c</sup>	1.08 ± 0.05 <sup>a</sup>	4.7 ± 0.6 <sup>a</sup>
Hydroxylysine	n.d.	n.d.		n.d.		5.0 ± 0.3 <sup>b</sup>		0.17 ± 0.01 <sup>a</sup>	
Hydroxyproline	4.3 ± 0.2	n.d.		0.14 ± 0.01 <sup>c</sup>	3.3 ± 0.2 <sup>c</sup>	0.09 ± 0.01 <sup>b</sup>	2.25 ± 0.3 <sup>b</sup>	0.023 ± 0.001 <sup>a</sup>	0.53 ± 0.03 <sup>a</sup>
Isoleucine <sup>e</sup>	69.4 ± 0.1	0.74 ± 0.01 <sup>a</sup>	1.07 ± 0.01 <sup>a</sup>	1.18 ± 0.01 <sup>b</sup>	1.69 ± 0.02 <sup>b</sup>	1.42 ± 0.01 <sup>d</sup>	2.04 ± 0.02 <sup>d</sup>	1.40 ± 0.01 <sup>c</sup>	2.01 ± 0.02 <sup>c</sup>
Leucine <sup>e</sup>	87 ± 2	1.39 ± 0.01 <sup>a</sup>	1.59 ± 0.05 <sup>a</sup>	2.13 ± 0.01 <sup>b</sup>	2.45 ± 0.08 <sup>b</sup>	2.35 ± 0.01 <sup>c</sup>	2.70 ± 0.08 <sup>c</sup>	2.43 ± 0.01 <sup>d</sup>	2.79 ± 0.08 <sup>d</sup>
Lysine <sup>e</sup>	83 ± 1	2.08 ± 0.01 <sup>a</sup>	2.51 ± 0.05 <sup>a</sup>	6.9 ± 0.3 <sup>c</sup>	8.4 ± 0.5 <sup>c</sup>	4.7 ± 0.3 <sup>b</sup>	5.7 ± 0.4 <sup>b</sup>	1.57 ± 0.03 <sup>a</sup>	1.90 ± 0.07 <sup>a</sup>
Methionine <sup>e</sup>	18.9 ± 0.8	0.24 ± 0.01 <sup>b</sup>	1.3 ± 0.1 <sup>b</sup>	0.85 ± 0.01 <sup>c</sup>	4.5 ± 0.2 <sup>c</sup>	1.25 ± 0.01 <sup>d</sup>	6.6 ± 0.3 <sup>d</sup>	0.17 ± 0.01 <sup>a</sup>	0.89 ± 0.9 <sup>a</sup>
Phenylalanine <sup>e</sup>	68 ± 3	1.46 ± 0.01 <sup>a</sup>	2.1 ± 0.1 <sup>a</sup>	1.83 ± 0.02 <sup>c</sup>	2.7 ± 0.2 <sup>c</sup>	1.61 ± 0.01 <sup>b</sup>	2.4 ± 0.1 <sup>b</sup>	1.37 ± 0.06 <sup>a</sup>	2.0 ± 0.2 <sup>a</sup>
Proline	123 ± 5	1.93 ± 0.01 <sup>a</sup>	1.56 ± 0.07 <sup>a</sup>	2.25 ± 0.01 <sup>c</sup>	1.83 ± 0.08 <sup>c</sup>	2.28 ± 0.01 <sup>d</sup>	1.85 ± 0.08 <sup>d</sup>	1.94 ± 0.01 <sup>b</sup>	1.57 ± 0.07 <sup>b</sup>
Serine	44.1 ± 0.6	1.96 ± 0.03 <sup>b</sup>	4.4 ± 0.1 <sup>b</sup>	2.86 ± 0.02 <sup>d</sup>	6.5 ± 0.1 <sup>d</sup>	2.43 ± 0.01 <sup>c</sup>	5.5 ± 0.1 <sup>c</sup>	1.21 ± 0.04 <sup>a</sup>	2.7 ± 0.1 <sup>a</sup>
Threonine <sup>e</sup>	41 ± 2	0.73 ± 0.01 <sup>a</sup>	1.8 ± 0.1 <sup>a</sup>	1.07 ± 0.01 <sup>b</sup>	2.6 ± 0.1 <sup>b</sup>	1.12 ± 0.01 <sup>c</sup>	2.7 ± 0.1 <sup>c</sup>	0.70 ± 0.03 <sup>a</sup>	1.7 ± 0.1 <sup>a</sup>
Tryptophan <sup>e</sup>	14.7 ± 0.2	0.26 ± 0.01 <sup>b</sup>	1.79 ± 0.07 <sup>b</sup>	0.40 ± 0.01 <sup>c</sup>	2.7 ± 0.1 <sup>c</sup>	0.67 ± 0.05 <sup>d</sup>	4.6 ± 0.4 <sup>d</sup>	0.016 ± 0.004 <sup>a</sup>	0.11 ± 0.03 <sup>a</sup>
Tyrosine	22.5 ± 0.6	2.20 ± 0.02 <sup>b</sup>	9.8 ± 0.3 <sup>b</sup>	2.80 ± 0.03 <sup>c</sup>	12.5 ± 0.4 <sup>c</sup>	1.85 ± 0.05 <sup>a</sup>	8.2 ± 0.4 <sup>a</sup>	2.4 ± 0.1 <sup>b</sup>	10.5 ± 0.8 <sup>b</sup>
Valine <sup>e</sup>	123 ± 6	1.56 ± 0.02 <sup>a</sup>	1.27 ± 0.07 <sup>a</sup>	2.30 ± 0.02 <sup>b</sup>	1.9 ± 0.1 <sup>b</sup>	3.25 ± 0.01 <sup>c</sup>	2.7 ± 0.1 <sup>c</sup>	4.76 ± 0.06 <sup>d</sup>	3.9 ± 0.2 <sup>d</sup>
TAA	1002 ± 31	28.9 ± 0.3 <sup>a</sup>	2.9 ± 0.1 <sup>a</sup>	47.4 ± 0.6 <sup>c</sup>	4.7 ± 0.2 <sup>c</sup>	55 ± 1 <sup>d</sup>	5.5 ± 0.3 <sup>d</sup>	31.7 ± 0.6 <sup>b</sup>	3.2 ± 0.2 <sup>b</sup>
TEAA	527 ± 17	9.9 ± 0.1 <sup>a</sup>	1.88 ± 0.09 <sup>a</sup>	18.6 ± 0.4 <sup>c</sup>	3.5 ± 0.2 <sup>c</sup>	18.3 ± 0.5 <sup>c</sup>	3.5 ± 0.2 <sup>c</sup>	13.5 ± 0.3 <sup>b</sup>	2.6 ± 0.1 <sup>b</sup>
TEAA/TAA (%)	53 ± 3 <sup>e</sup>	34.3 ± 0.8 <sup>b</sup>	--	39.4 ± 1 <sup>c</sup>		33 ± 2 <sup>a</sup>		43 ± 2 <sup>d</sup>	
non-P/TAA (molar ratio)	0.63 <sup>c</sup> ± 0.04	0.43 ± 0.01 <sup>b</sup>		0.37 ± 0.01 <sup>a</sup>		0.38 ± 0.01 <sup>a</sup>		0.66 ± 0.02 <sup>d</sup>	

n.d., not detected. Values are expressed as mean ± standard deviation from triplicate determination. Values with different letters in each row are significantly different when applying the Fisher's least significant differences (LSD) method at p-value ≤ 0.05 for mg aa/g<sub>protein</sub> and yield values. Aspartic acid includes asparagine. Glutamic acid includes glutamine. TAA, total amino acids. TEAA, total essential amino acids. TEAA/TAA: ratio essential amino acids to total amino acids. non-P/TAA: molar ratio of non-polar amino acids to total amino acids.

Elemental composition of the BSG is showed in **Table 3.3**, with a mass percent of C, H, N and O of  $47.0 \pm 0.2$ ,  $6.9 \pm 0.1$ ,  $2.8 \pm 0.1$  and  $39.5 \pm 0.1$ , respectively. The values obtained were similar to the values found in the literature that reported values of C (47.18-51.3%, w/w), H (6.02-8.20%, w/w), N (3.32-4.9%, w/w), O (32.9-41.04%, w/w) and S (0.26-0.45%, w/w) [26]–[29]. However, in this work, sulfur was not found. Elemental composition led to molar ratios H:C and O:C of  $1.75 \pm 0.04$  and  $0.63 \pm 0.01$ , respectively and an HHV of  $19.14 \pm 0.08$  MJ/kg.

**Table 3.3.** Elemental analysis and ash content (%w/w), H:C, O:C and N:C molar ratios and estimated heating value (HHV, MJ/kg) of BSG and the solid residues after subW treatment (SWR).

Sample	Raw material	SWR 125 °C	SWR 145 °C	SWR 160 °C	SWR 185 °C
C (%)	$47.0 \pm 0.2^a$	$52.3 \pm 0.9^b$	$53.7 \pm 0.2^c$	$54.8 \pm 0.9^c$	$60.3 \pm 0.5^d$
H (%)	$6.9 \pm 0.1^a$	$7.02 \pm 0.09^a$	$7.3 \pm 0.2^b$	$7.5 \pm 0.1^b$	$7.34 \pm 0.04^b$
N (%)	$2.8 \pm 0.1^b$	$3.33 \pm 0.05^c$	$2.45 \pm 0.02^b$	$1.67 \pm 0.01^a$	$1.79 \pm 0.01^a$
O (%)	$39.5 \pm 0.1^c$	$37 \pm 2^c$	$33.2 \pm 0.3^b$	$32 \pm 2^b$	$29 \pm 1^a$
Ash (%)	$2.92 \pm 0.02^d$	$1.62 \pm 0.01^b$	$1.67 \pm 0.01^b$	$1.26 \pm 0.09^a$	$2.41 \pm 0.04^c$
H:C	$1.75 \pm 0.04^c$	$1.61 \pm 0.01^b$	$1.63 \pm 0.05^b$	$1.65 \pm 0.05^b$	$1.46 \pm 0.02^a$
O:C	$0.63 \pm 0.01^d$	$0.54 \pm 0.04^c$	$0.468 \pm 0.003^b$	$0.46 \pm 0.02^b$	$0.37 \pm 0.02^a$
N:C	$0.052 \pm 0.002^c$	$0.055 \pm 0.005^c$	$0.039 \pm 0.006^b$	$0.026 \pm 0.004^a$	$0.0255 \pm 0.0003^a$
HHV	$19.14 \pm 0.08^a$	$21.7 \pm 0.5^b$	$22.5 \pm 0.2^c$	$23.1 \pm 0.5^d$	$26.0 \pm 0.3^e$

Values with different letters in each row are significantly different when applying the Fisher's least significant differences (LSD) method at p-value  $\leq 0.05$ .

### 3.2. Protein extraction

**Figure 3.2a** shows the accumulative total protein fraction obtained in the subW extracts, expressed as g protein/100 g<sub>dry-BSG</sub>, calculated by multiplying the total nitrogen determined by TOC-N by 6.25.

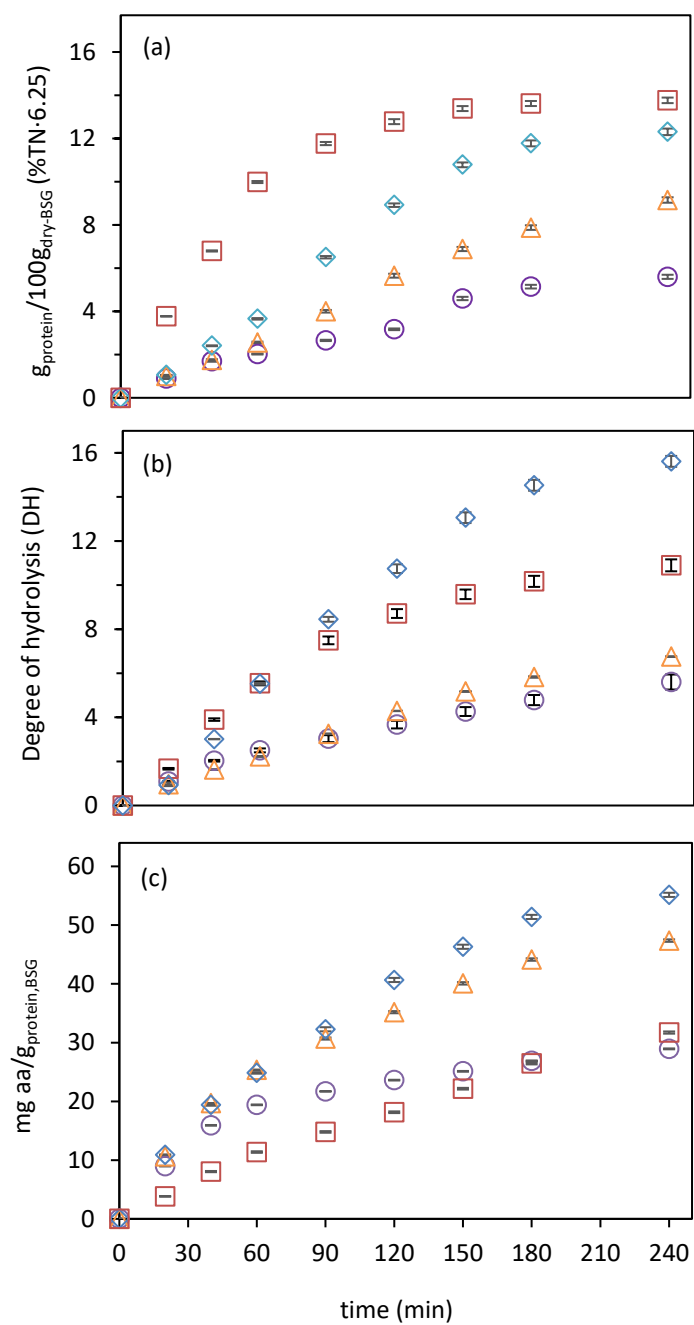


**Figure 3.2.** Accumulative profile in the subW extracts of (a) protein fraction,  $g_{\text{protein}}/100g_{\text{dry-BSG}}$  (b) degree of hydrolysis and (c) free amino acids ( $mg \text{ aa}/g_{\text{protein,BSG}}$ ) at different temperatures. ( $\circ$  125 °C,  $\triangle$  145 °C,  $\diamond$  160 °C and  $\square$  185 °C). ( $F = 4 \text{ mL/min}$ ).

The highest protein extraction level was 13.8 g/100 g<sub>dry-BSG</sub>, 78% of the total protein in the BSG, and it was achieved at the maximum temperature level covered in this work, 185 °C. At 185 °C a plateau was reached at 150 min of extraction, while longer times were needed at lower temperatures (see **Figure 3.2a**). [30] concluded that time was a crucial factor to obtain high protein extraction yields. These authors reported a low protein extraction yield of 6.7% from BSG by subW treatment at 200 °C (F = 6 mL/min), but only 20 min of extraction time. [31] studied the effect of temperature on the extraction of protein from deoiled rice bran between 100 and 220 °C by subW. These authors reached the highest protein yield at 200 °C, recovering nearly all the protein from the original bran.

Protein extraction by subW treatment was compared with other hydrolytic methods such as alkaline and enzymatic hydrolysis at the same treatment time, 4 h (**Table 3.4**). At the highest temperature levels essayed in this work, 160 and 185 °C, subW treatment achieved much higher extraction yields of the protein fraction than enzymatic treatment by protease ( $47.1 \pm 0.6\%$ , enzyme loading 6%) or basic hydrolysis ( $50.5 \pm 0.2\%$ , 0.1 M NaOH). **Table 3.4** also includes previous results obtained by ultrasound assisted extraction (UAE) of BSG that also yielded lower extraction yield than subW treatment,  $46.6 \pm 0.7\%$  [3]. Under subcritical conditions, the physical–chemical properties of water change drastically with temperature. The ionic product of water increases in the subcritical range increasing the concentration of H<sup>+</sup> and OH<sup>-</sup> that favors biomass hydrolysis. Moreover, the dielectric constant decreases allowing water to interact with non-polar substances, thus decreasing their binding force and dissolving them. Therefore, biopolymers, like proteins, are released from the matrix and broken down into valuable peptides and free amino acids.

**Table 3.4.** Protein extraction yield by different methods (protein content in the extracts/protein content in the raw material). Extraction time = 4 h

Extraction method	Protein yield, %
Subcritical water	
125 °C	31.7 ± 0.7 <sup>c</sup>
140 °C	51.8 ± 1.0 <sup>g</sup>
160 °C	69.6 ± 1.3 <sup>h</sup>
185 °C	77.8 ± 1.3 <sup>i</sup>
Enzyme (6%, T = 50 °C)	
Protease	47.1 ± 0.6 <sup>f</sup>
Xylanase	40.0 ± 0.1 <sup>d</sup>
Cellulase	10.7 ± 0.1 <sup>a</sup>
Basic hydrolysis (T = 50 °C)	
0.01 M NaOH	27.0 ± 0.1 <sup>b</sup>
0.1 M NaOH	50.5 ± 0.2 <sup>g</sup>
1 M NaOH	45.0 ± 0.4 <sup>e</sup>
UAE (T = 50 °C)*	46.6 ± 0.7 <sup>f</sup>

Values with different letters are significantly different when applying the Fisher's least significant differences (LSD) method at p-value ≤ 0.05. (\*) UAE =Ultrasound assisted extraction obtained from [3].

Total protein content was also determined by the kit RC DC™ and compared with the TOC-N method. The results obtained with the spectrophotometric method were around 30% higher than those obtained by nitrogen measurements. A linear correlation was established between the protein content determined by both methods:

$$\% \text{ Protein (kit RC DC}^{\text{TM}}) = 1.3735 \% \text{ Protein (\%TN} \cdot 6.25), R^2 = 0.9846 \quad [3.6]$$

The slope of this correlation shows the overestimation in the protein content by the spectrophotometric method. This overestimation can be also appreciated in literature. Sereewatthanawut et al. [31] reported a protein yield of 219 mg/g<sub>rice bran</sub> by subW as determined by the Lowry method, while the composition of the feedstock showed a mass percent of protein of 18.56%. In the literature, it is reported that the Cu<sup>2+</sup> ion present in the reagent is overly sensitive to some amino acids such as tryptophan and tyrosine [32]. The



different content of these amino acids in the BSG and in the BSA standard could be the reason that justify the difference in the protein fraction content by both methods. Furthermore, [33] studied the influence of 57 chemicals (mineral and organic acids, organic solvents, phenolic compounds, mineral and organic salts) on the efficiency of protein determination by the Lowry method. These authors found that the influence of phenolic compounds was governed by the structure of their molecules. This influence caused a high overestimation of the protein level.

### 3.3. Degree of hydrolysis and free amino acids

The degree of hydrolysis (DH) has been plotted in **Figure 3.2b**. The value of  $h_{\text{tot}}$ ,  $8.0 \pm 0.2$  mmol/g protein, was calculated using the amino acid profile of the BSG (see **Table 3.2**). The results show that the lowest DH was obtained at 125 °C ( $5.5 \pm 0.3$ ), and a maximum DH was reached at 160 °C ( $15.6 \pm 0.2$ ). This result correlated with the highest content of total free amino acids in the subW extracts, as determined by the sum of individual free amino acids determined by gas chromatography, with a maximum level at 160 °C (see **Figure 3.2c**). At 185 °C a significant decrease of the free amino acids content took place.

The lower DH and free amino acid content at 185 °C could be attributed to amino acid decomposition. According to literature, high temperatures and/or high residence time could cause amino acid degradation producing different carboxylic acids and other nitrogen containing compounds such as ethanolamine and the non-proteinogenic amino acid ornithine [34]. Furthermore, the temperature at which degradation of protein or its hydrolysis products take place depends on the protein source. For instance, animal wastes require higher temperatures or longer reaction times than vegetable wastes [12]. Considering the disrupted lignocellulosic structure during beer production, BSG protein could be even more accessible during extraction [30]. Other subW studies reported higher temperatures for the optimum amino acids release [12] but lower temperatures have been also observed in the literature for subW treatment of oysters at 150 °C [35]. In any case, it must be highlighted that the high residence time used in this work, around 28-29 min, could cause amino acid degradation even at not so high temperature.

Final free amino acid content of subW extracts is shown in **Table 3.2** together with the free amino acid yields evaluated according to Equation 3.4. The highest amino acid yield was obtained at 160°C with a value of  $55 \pm 1$  mg amino acid/  $g_{\text{protein-BSG}}$  ( $9.4 \pm 0.2$  mg amino acid/  $g_{\text{dry-BSG}}$ ) that corresponds to  $5.5 \pm 0.3\%$  of the total amino acids of the BSG. These values are comparable to the values reported for other authors for free amino acids release by subW treatment. [31] obtained  $8.0 \pm 1.6$  mg free amino acids/ $g_{\text{rice-bran}}$  while [36] recovered 5% of the total protein content as free amino acids from two different sources, deoiled rice bran and raw soybean.

Although, the concentration of total free amino acids at 160 °C was at maximum level, this maximum was achieved at different temperature for each individual amino acid. For a better understanding, the yields of the different amino acids have been plotted in **Figure 3.3**.

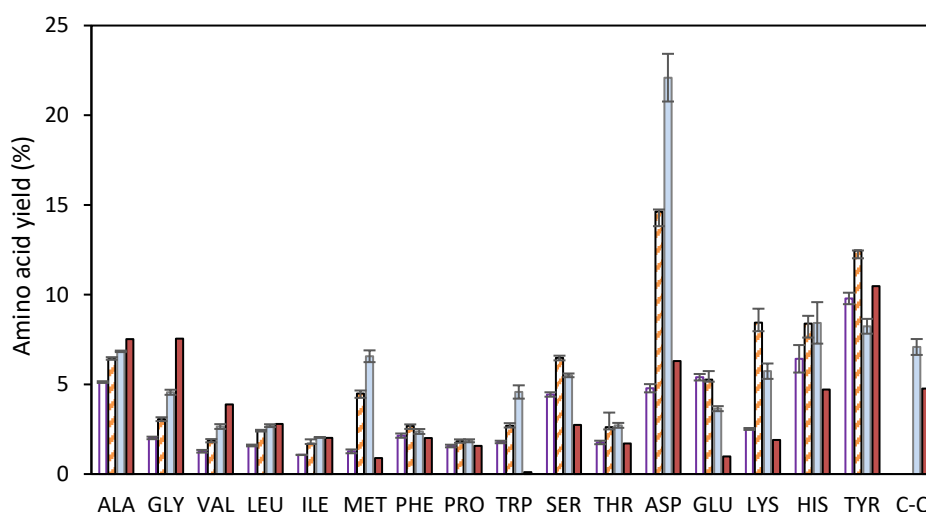


**Figure 3.3.** Final yield of individual amino acids as a function of temperature: □ 125 °C; ▨ 145 °C; ■ 160 °C, ■ 185°C.

It can be observed that polar amino acids (serine, threonine, aspartic and glutamic acids, lysine, histidine, tyrosine and cysteine) reached to the maximum level at lower temperatures with higher amino acid yields. Aspartic acid showed the highest yield at 160 °C but also a dramatic degradation at 185 °C. Glutamic acid yield continuously decreased by

increasing operating temperature. Both amino acids conform the negative charged amino acids group, the strong polar nature of their residues incomes that they are normally found on the surface of globular proteins and interact favourably with solvent molecules, nevertheless this fact also means that they are very labile [37]. Positive charged amino acid group includes lysine and histidine, which showed a maximum yield at 145-160 °C. These amino acids are highly hydrophilic and are usually involved in reactions with negatively charged groups. Furthermore, lysine has a high tendency to be involved in Maillard reactions with the carbonyl groups or reducing carbohydrates [38]. Serine, threonine, tyrosine and cysteine are hydrophilic neutral amino acids with an aliphatic chain. All of them presented the highest yield at 145-160 °C, except cysteine, which was found at negligible concentration due to its very low stability. On the other hand, for most of the non-polar amino acids, individual yields increased by increasing the operation temperature, except for methionine. Hydrophobic amino acids tend to reside in the interior of a protein to minimise contact with water, as this conformation stabilises the protein in the aqueous solution [39]. The decrease of the dielectric constant of subW with temperature may favour its affinity for these amino acids due to their hydrophobic character. In addition, small aliphatic amino acids could be formed during the decomposition of the other amino acids [40]. Similar trend in the extractability of amino acids has been reported by Abdelmoez & Yoshida [37].

The different behaviour of polar and non-polar amino acids with temperature was reflected in the selectivity value towards non-polar amino acids, defined as the amount of free non-polar amino acids released in the subW extracts relative to the total amount of free amino acids on a molar base, in a similar way as the hydrophobic selectivity defined by Widyarani et al. [39]. The non-polar selectivity remained constant in the temperature range from 125 to 160 °C, but it greatly increased at 185 °C. As an example, **Figure 3.4** shows the accumulative free amino acid content in the subW extracts collected at 160 °C.

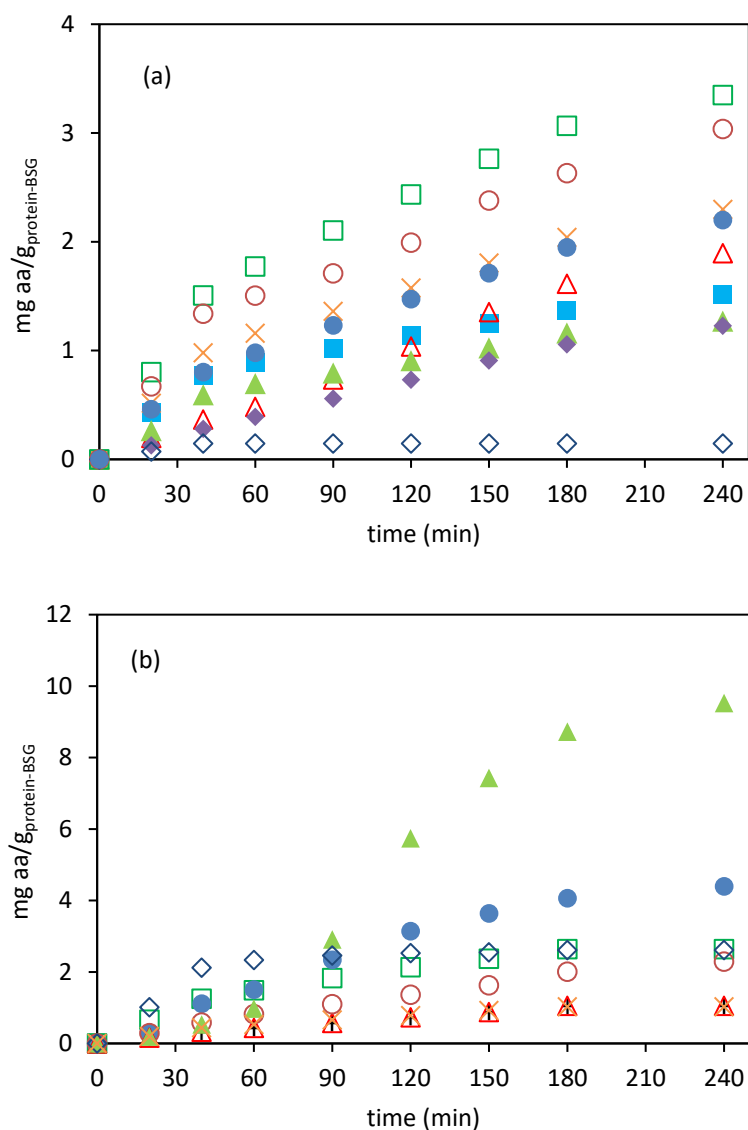


**Figure 3.4.** Accumulative release of individual amino acids at 160 °C (F = 4 mL/min)

(a) non polar amino acids (□ alanine, △ glycine, ○ valine, × leucine, ▲ isoleucine, ● proline, ■ phenylalanine, ◇ tryptophan, ◆ methionine) (b) polar amino acids (□ serine, ◇ glutamic acid, ● lysine, △ histidine, ○ tyrosine, × threonine, ▲ aspartic acid).

### 3.4. Total phenolic content and antioxidant activity of subW extracts

Figure 3.5 shows TPC release in the temperature range from 125 to 185 °C (F = 4 mL/min) as determined by the Folin Ciocalteu method.

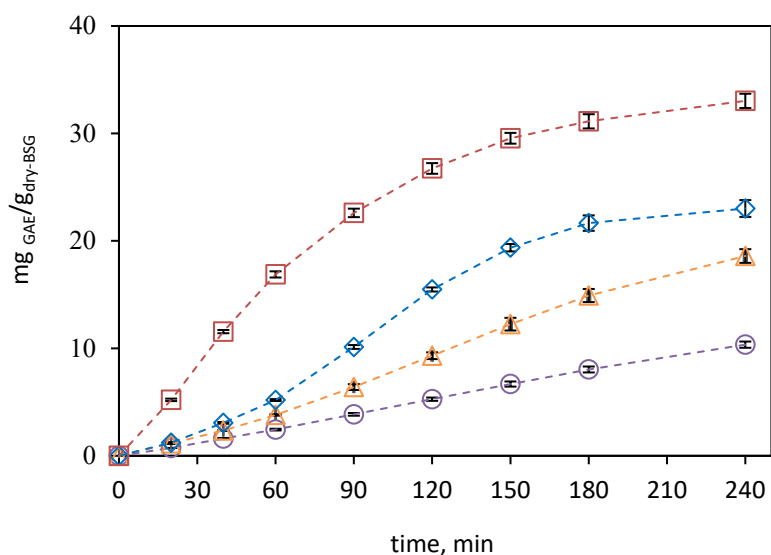
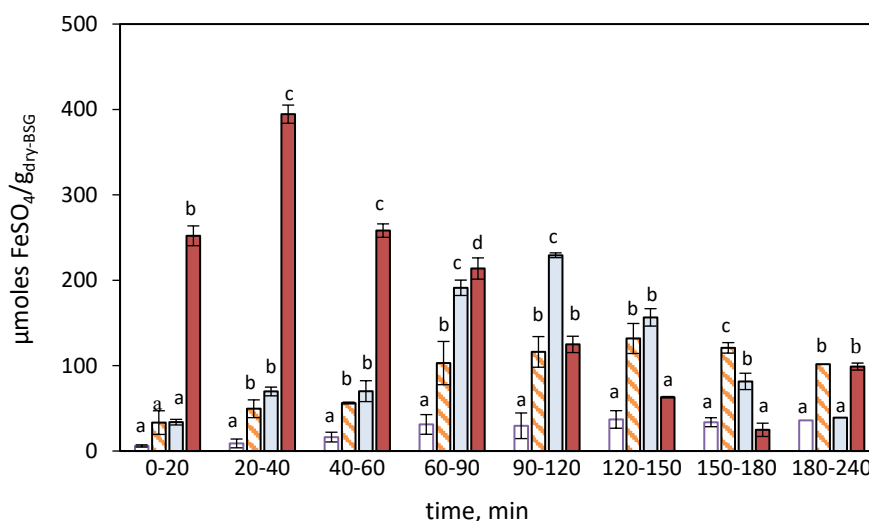


Figure 3.5. Accumulative TPC,  $\text{mg}_{\text{GAE}}/\text{g}_{\text{dry-BSG}}$ , at different temperatures ( $\circ$  125 °C,  $\triangle$  145 °C,  $\diamond$  160 °C and  $\square$  185 °C.)

An increase in the operating temperature led to an increase in TPC in the extraction medium, with values after 240 min of extraction, from  $10.3 \pm 0.3$  to  $33.0 \pm 0.3$   $\text{mg}_{\text{GAE}}/\text{g}_{\text{dry-BSG}}$  at 125 and 185 °C, respectively. SubW treatment resulted in higher amounts of TPC from BSG than the values obtained in previous studies by using other hydrolysis technics, such as UAE and acid/alkaline hydrolysis, with TPC values of  $3.3 \pm 0.1$ ,  $30 \pm 5$  and  $16.2 \pm 0.2$   $\text{mg}_{\text{GAE}}/\text{g}_{\text{dry-BSG}}$ , respectively [3]. In that work, a maximum TPC release of  $42.0 \pm 0.4$   $\text{mg}_{\text{GAE}}/\text{g}_{\text{dry-BSG}}$  was achieved by enzymatic hydrolysis with 6% (w/w) of xylanase for 24 h of incubation. However, productivity by enzymatic hydrolysis was lower,  $0.087$   $\text{mg}_{\text{GAE}}/(\text{g}_{\text{dry-BSG}} \cdot \text{min})$  than for subW,  $0.28$   $\text{mg}_{\text{GAE}}/(\text{g}_{\text{dry-BSG}} \cdot \text{min})$  at 185 °C, evaluated from the initial linear extraction curve.

**Figure 3.6** shows the results of the antioxidant capacity of the extracts collected at the different time intervals, as determined by the FRAP assay. The results showed that increasing the temperature up to 185 °C significantly increased the antioxidant activity ( $p < 0.05$ ). A positive correlation ( $R^2 = 0.9511$ ) between antioxidant activity and TPC was established according to the Pearson product moment correlation. According to Marcet et al. [12], antioxidant capacity increased when small peptides are obtained. In this work, it was also found a positive correlation ( $R^2 = 0.7629$ ) between antioxidant activity and the amount of protein in the subW extracts, while the amount of free amino acids was not significantly correlated with the antioxidant activity ( $R^2 = 0.1189$ ).



**Figure 3.6.** Antioxidant activity ( $\mu\text{m FeSO}_4/\text{g}_{\text{dry,BSG}}$ ) collected at the different time intervals at different temperatures:  $\square$  125 °C;  $\square$  145 °C,  $\square$  160 °C,  $\square$  185 °C. Values with different letters at each interval time are significantly different when applying the Fisher's least significant differences (LSD) method at  $p\text{-value} \leq 0.05$

The high TPC value and antioxidant capacity of the extracts obtained at the highest temperatures could be due to newly formed compounds related to Maillard reactions. The increase in browning is directly associated with advanced phases of the Maillard reaction. This browning was visually observed in the colour of the extracts from BSG since they become darker by increasing temperature (**Figure 3.7**). The colour change would indicate the increase of the amount of hydrolysis and decomposition products in the aqueous phase.

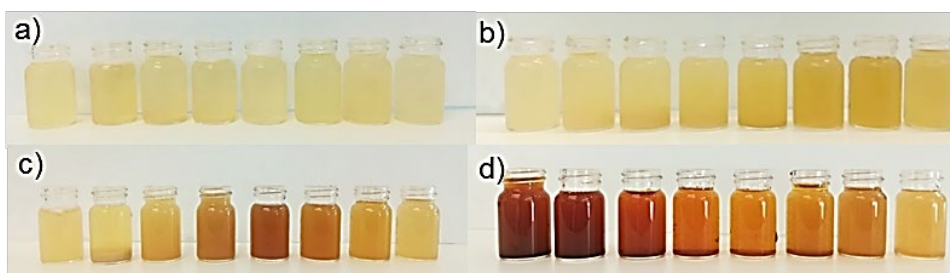


**Figure 3.7.** subW extracts collected at the different time intervals at different temperatures a) 125 °C, b) 145 °C, c) 160 °C and d) 185 °C.

The formation of hydroxymethyl furfural (HMF) and furfural can be also considered as indicators of Maillard reactions. It is well known that these compounds take part in reactions leading to the formation of melanoidins and other polymers and aromatic substances. The concentration of HMF and furfural in subW extracts has been reported in **Figure 3.8**. Both compounds significantly increased with temperature and showed a positive correlation with antioxidant activity ( $p < 0.05$ ) with Pearson's correlation coefficients of 0.6887 and 0.8091, respectively. In any case, it must be highlighted that synthetic aqueous dilutions of HMF and furfural standards, at similar concentrations to the concentrations found in the subW extracts, exhibited no response to the TPC and antioxidant activity assays.

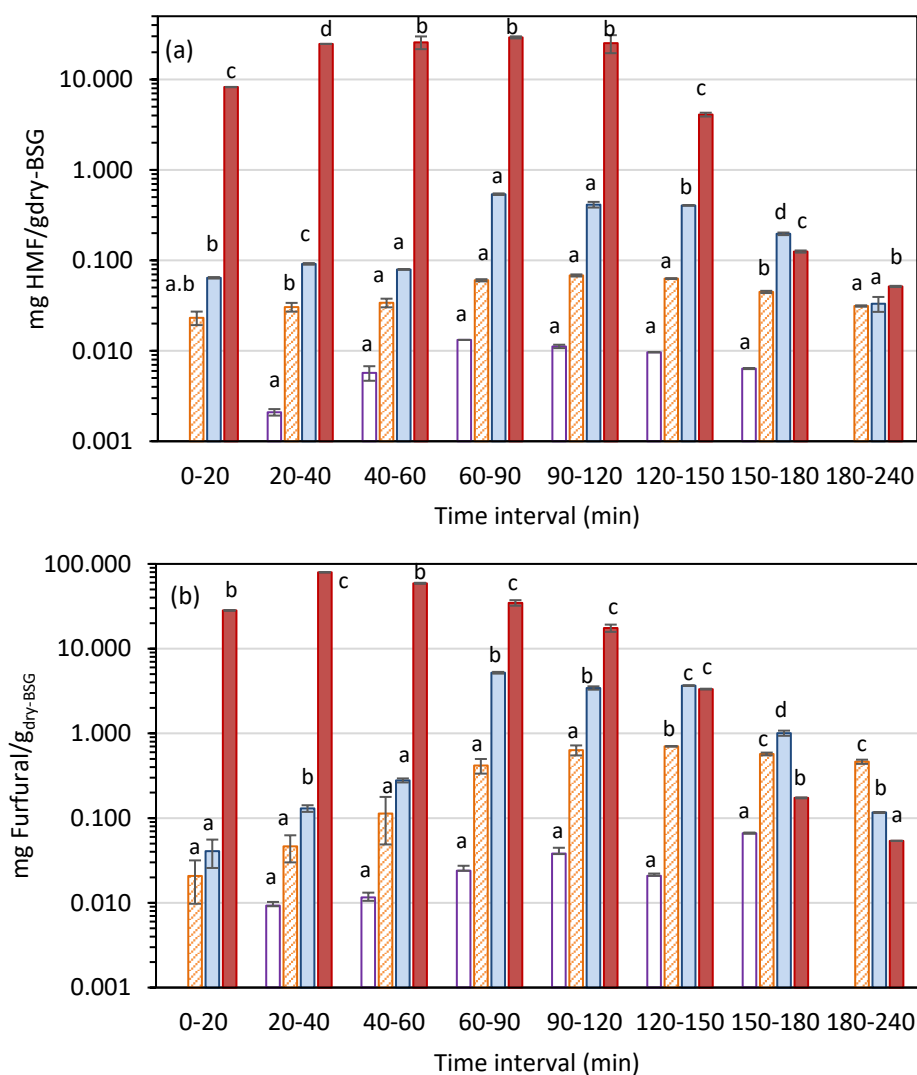


**Figure 3.8.** Concentration of a) HMF and b) furfural in the subW extracts collected at the different time intervals at different temperatures:  $\square$  125 °C;  $\square$  145 °C,  $\square$  160 °C,  $\blacksquare$  185 °C. Values with different letters at each interval time are significantly different when applying the Fisher's least significant differences (LSD) method at  $p$ -value  $\leq 0.05$ .

The effect of the Maillard reaction products on the response of the spectrophotometric methods used to determine the TPC and the antioxidant activity was determined by a simple experiment. A mixture of an amino acid, glutamine (0.05 M), and glucose (0.05 M)



was placed in a vessel immersed in a boiling water bath for 4 hours at a pH value of 5.8 adjusted with phosphate buffer. Aliquots were taken each hour and TPC and FRAP assays were performed (**Figure 3.9**). The TPC and FRAP responses increased with time proving that both measurements, TPC and antioxidant activity, in subW extracts could be influenced by the Maillard reaction products.

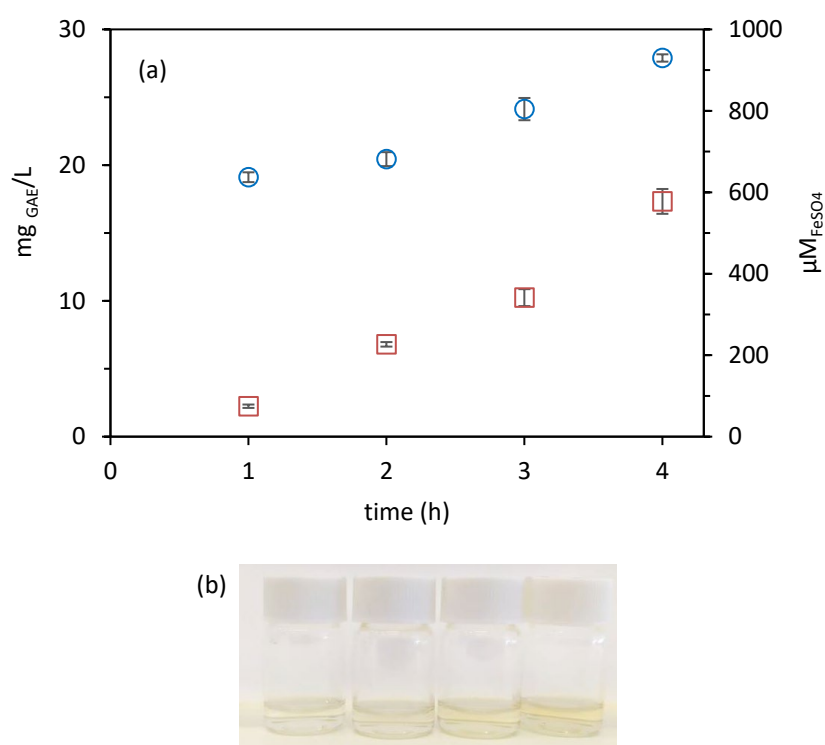


**Figure 3.9.** (a) TPC (mg<sub>GAE</sub>/L,  $\square$ ) and antioxidant activity (FRAP,  $\mu\text{M}_{\text{FeSO}_4}$ ,  $\circ$ ) from model Maillard reaction system at pH = 5.1; (b) visual aspect of model of Maillard reaction system collected each hour from left to right.

**Figure 3.10a** and **3.10b** show the accumulative release of the identified individual phenolic compounds in the subW extracts obtained at 160 °C and 185 °C, respectively. Five phenolic compounds were identified at both temperatures: two hydroxycinnamic acids, ferulic and p-coumaric acids, and three aldehydes, vanillin (4-hydroxy-3-methoxybenzaldehyde), protocatechuic aldehyde (3,4-dihydroxybenzaldehyde) and syringic aldehyde (4-hydroxy-3,5-dimethoxybenzaldehyde).

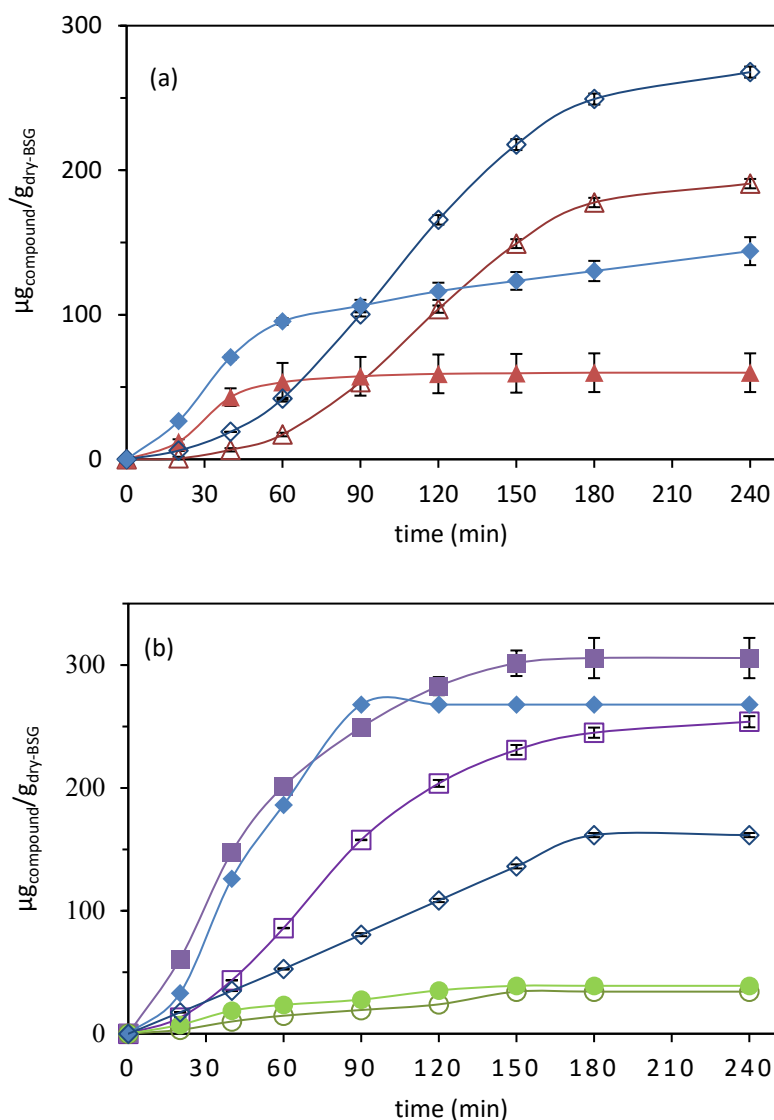


**Figure 3.10.** Accumulative individual phenolic compounds at 160 °C (open symbols) and 185 °C (filled symbols): (a)  $\triangle$   $\blacktriangle$  p-coumaric;  $\diamond$   $\blacklozenge$  ferulic acid (b)  $\square$   $\blacksquare$  vanillin;  $\circ$   $\bullet$  Syringic aldehyde;  $\diamond$   $\blacklozenge$  protocatechuic aldehyde. (F = 4 mL/min).

Other phenolic compounds were also identified in subW extracts at 160 °C, such as catechin ( $112 \pm 3 \mu\text{g/g dry-BSG}$ ), vanillic acid ( $443 \pm 12 \mu\text{g/g dry-BSG}$ ), 4-vinylphenol ( $19 \pm 5 \mu\text{g/g dry-BSG}$ ) and 4-vinylguaiacol ( $56 \pm 2 \mu\text{g/g dry-BSG}$ ), but they could not be determined at 185 °C. Higher release of hydroxycinnamic acids was found at 160 °C than at 185 °C. On

the contrary, the highest concentration of aldehydes was determined at 185 °C. In a previous work, the release of individual phenolic compounds was determined by UAE and chemical/enzymatic hydrolysis [3]. A comparison of these techniques with the results obtained by subW yielded the following conclusions. Among these techniques, the highest amount of vanillin was achieved by subW,  $306 \pm 16 \mu\text{g}/\text{g}_{\text{dry-BSG}}$  and  $254 \pm 5 \mu\text{g}/\text{g}_{\text{dry-BSG}}$ , at 185 °C and 160 °C respectively, followed by enzymatic hydrolysis with 6% of xylanase ( $\text{g enzyme}/\text{g}_{\text{dry-BSG}}$ ). [41] studied the stability of the vanillin under subW conditions and reported that no degradation of vanillin took place up to 200 °C. However, subW was not as effective as basic hydrolysis to release hydroxycinnamic acids at the operation conditions used in this work. By basic hydrolysis,  $1305.7 \pm 0.5 \mu\text{g}/\text{g}_{\text{dry-BSG}}$  and  $538 \pm 4 \mu\text{g}/\text{g}_{\text{dry-BSG}}$  of ferulic and p-coumaric were obtained, respectively. These values were higher than the highest level obtained at 160°C by subW (see **Figure 3.10a**). In any case, it must be highlighted, that neither chemicals nor enzymes are needed by subW treatment. At subW conditions, the ionic product of water increases making subW appropriate for hydrolysis reactions. Hydroxycinnamic acids are directly esterified or etherified to the lignin surface, so, higher temperatures could be necessary to improve the hydroxycinnamic acids extraction. However, higher temperatures could lead to degradation of these compounds. [42] reported that thermal decomposition of ferulic and coumaric acids started at about 172 °C and the amount extracted from defatted rice bran started to decrease at 175 °C in the study of the release of phenolic acids from defatted rice bran by subW treatment. In this work, a similar behaviour was observed since higher content of these two phenolic acids was determined at 160 °C than a 185 °C.

It must be highlighted that in the subW extracts from BSG, the total amount of individual phenolic compounds that could be successfully determined was  $1.64 \text{ mg}/\text{g}_{\text{dry-BSG}}$  and  $0.82 \text{ mg}/\text{g}_{\text{dry-BSG}}$  at 160 °C and 185 °C, respectively. On the other, hand,  $23.01 \text{ mg}_{\text{GAE}}/\text{g}_{\text{dry-BSG}}$  and  $33.03 \text{ mg}_{\text{GAE}}/\text{g}_{\text{dry-BSG}}$  were obtained by the Folin–Ciocalteu method, at 160 °C and 185 °C respectively. These differences could be attributed to the fact that some of the individual phenolic compounds could not be properly identified by our system due to lack of standards. Furthermore, subW extracts contain carbohydrates, proteins and amino acids, which are considered as interfering substances for TPC analysis. Additionally, Maillard reaction products showed signal at Folin–Ciocalteu analysis as previously shown.

This behaviour was also observed in other subW systems in the literature. [42] also reported a significant difference between TPC as determined by the Folin–Ciocalteu method (with the highest value of  $19.48 \text{ g}_{\text{GAE}} \text{ kg}^{-1} \text{ bran}$  at  $200 \text{ }^\circ\text{C}$ ) and by the HPLC analysis, showing also a different trend with temperature by both methods. The highest HPLC values reported by [42] was  $2 \text{ g kg}^{-1} \text{ bran}$  at  $175 \text{ }^\circ\text{C}$ , and an abrupt decrease at  $200 \text{ }^\circ\text{C}$ ,  $0.38 \text{ g (kg bran)}^{-1}$ , was observed.

### 3.5. Organic carbon in the subcritical water extracts

The total organic carbon (TOC) presented in the subW extracts has been plotted in **Figure 3.11**. TOC extraction rate and yield increased with temperature, although, at  $160 \text{ }^\circ\text{C}$  and  $185 \text{ }^\circ\text{C}$ , the same final TOC value was achieved. TOC would include monomers and oligomer carbohydrates, but also protein and amino acids and their degradation products, such as different organic acids [43]. Degradation of carbohydrates and proteins can release at high temperatures  $\text{NH}_3$  and  $\text{CO}_2$  or other gas products that would lead to similar TOC yield at  $185 \text{ }^\circ\text{C}$  and  $160 \text{ }^\circ\text{C}$ .

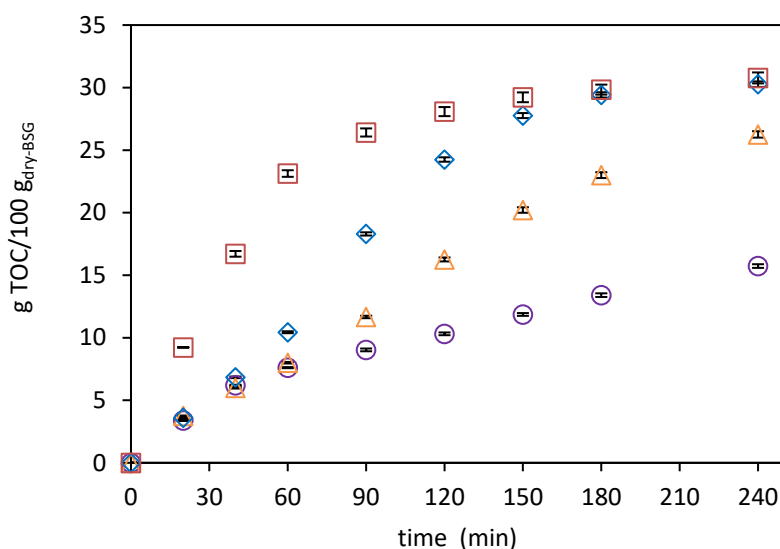


**Figure 3.11.** Accumulative total organic carbon ( $\text{g TOC}/100 \text{ g}_{\text{dry.BSG}}$ ) on subW extracts at different temperatures ( $\circ$   $125 \text{ }^\circ\text{C}$ ,  $\triangle$   $145 \text{ }^\circ\text{C}$ ,  $\diamond$   $160 \text{ }^\circ\text{C}$  and  $\square$   $185 \text{ }^\circ\text{C}$ ),  $F = 4 \text{ mL/min}$ .

### 3.6. Solid residue after subW treatment

The total extraction yield was evaluated according to Equation 3.7:

$$\text{Yield (\%)} = \frac{W - W_i}{W} \cdot 100 \quad [3.7]$$

where  $w$  is the weight of the dry BSG placed into the reactor and  $w_i$  is the weight of the dry solid residue remaining after the subW treatment.

The results are collected in **Table 3.5** and show significantly increasing values of the total extraction yield with temperature from 50% to 81% at 125 and 185 °C, respectively. This result agrees with the increase of TOC and the protein fraction in the subW extracts with temperature.

**Table 3.5.** Hydrolysis yield and mass balances (MB %) for C and N.

T.(°C)	Yield (%)	C <sub>outlet</sub> (g)	MB C (%)	N <sub>outlet</sub> (g)	MB. N (%)
125	50.4 ± 0.3 <sup>a</sup>	4.70 ± 0.08 <sup>a</sup>	90.8 ± 1.9	0.28 ± 0.02 <sup>a</sup>	90 ± 12
145	64.4 ± 0.2 <sup>b</sup>	5.12 ± 0.03 <sup>b</sup>	98.9 ± 1.1	0.26 ± 0.02 <sup>a</sup>	83 ± 13
165	73.5 ± 0.2 <sup>c</sup>	5.03 ± 0.05 <sup>b</sup>	97.3 ± 1.4	0.26 ± 0.01 <sup>a</sup>	85 ± 9
185	81.4 ± 0.1 <sup>d</sup>	4.61 ± 0.04 <sup>a</sup>	89.2 ± 1.1	0.28 ± 0.01 <sup>a</sup>	90 ± 9

C<sub>inlet</sub> = 5.17 ± 0.02 g, N<sub>inlet</sub> = 0.31 ± 0.01. Values with different letters in each column are significantly different when applying the Fisher's least significant differences (LSD) method at p-value ≤ 0.05. Error in mass balances (MB) was evaluated according to the error associated to the ratio of two variables, C(N)<sub>outlet</sub>/C(N)<sub>inlet</sub>·100).

The elemental composition of the solid residues after extraction was listed in **Table 3.3**. The C content in the solid residue increased with temperature, while the oxygen content decreased; therefore, the molar ratio O:C decreased from 0.63 to 0.37 by increasing temperature. The decrease of the O:C ratio is associated with a decrease in the amount of OH, carboxyl (COOH) and carbonyl (C=O) groups. According to Jackowski et al [28], hydrothermal carbonization (HTC) treatment made BSG much more similar to hard coal with higher HHV (26.5 MJ/kg) and C content (58.6% w/w), as well as lower O:C ratio, from 0.65 to 0.37, after HTC. In this work, HHV also increased by increasing temperature with a maximum value of 26.04 MJ/kg at 185°C. The values of both H:C and N:C ratios in the solid

residue decreased gradually with temperature. This trend suggests that carbon and nitrogen components of the solid have gradually moved to the aqueous phase in the form of their hydrolysis products or their decomposition products [37]

**Table 3.5** also shows the mass balance for C and N.  $C_{inlet}$  and  $N_{inlet}$  have been calculated from the elemental composition of the BSG and  $C_{outlet}$  and  $N_{outlet}$  from the C and N remaining in the solid residues (see **Table 3.3**) and the C and N present in the subW extracts (**Figures 3.2a** and **3.11**). The mass balance deviation for C and N was calculated according to the Equation 3.8:

$$C \text{ (or N) balance} = \frac{C \text{ (or N)}_{outlet}}{C \text{ (or N)}_{inlet}} \cdot 100 \quad [3.8]$$

In general, mass balances present deviations lower than 10% that can be considered acceptable mass balance errors in a semi-continuous system. It must be also highlighted that at severe operation conditions, high temperature and long residence time, part of the biomass may also be converted to volatile compounds that were not measured in this work.

## 4. Conclusions

SubW treatment was confirmed as an efficient extraction/hydrolysis method to recover the protein fraction of the BSG generated in a local brewery factory. Around of 78% of the protein fraction was recovered by working in a semi continuous fix-bed reactor at 185 °C and 4 mL/min. Polar amino acids showed a maximum at lower temperature level than non-polar amino acids. Therefore, fractionation of bioactive compounds can be achieved by working under different conditions. This fact was also observed for phenolic compounds. Hydroxycinnamic acids were more sensitive to temperature than aldehyde phenolic compounds. Subcritical water is a suitable technology to extract and fractionate the different biocompounds extracted from BSG allowing to incorporate this by-product within the biorefinery concept.

## References

- [1] S. I. Mussatto, G. Dragone, and I. C. Roberto, "Brewers' spent grain: Generation, characteristics and potential applications," *Journal of Cereal Science*, vol. 43, no. 1, pp. 1–14, 2006, doi: 10.1016/j.jcs.2005.06.001.
- [2] Market Data Forecast, "marketdataforecast.com/market-reports/europe-craft-beer-market," *Europe Craft Beer Market by Product Type (Ale and Lager), Distribution Channel (On-Trade and Off-Trade), and By Segments (Brewpubs, Microbreweries, Regional Craft Breweries and Contract Brewing Companies), and By Country (UK, France, Spain, Germany, Italy, 2020*. <https://www.marketdataforecast.com/market-reports/europe-craft-beer-market> (accessed Dec. 21, 2020).
- [3] P. Alonso-Riaño, M. T. S. Diez, B. Blanco, S. Beltrán, E. Trigueros, and O. Benito-Román, "Water ultrasound-assisted extraction of polyphenol compounds from brewer's spent grain: Kinetic study, extract characterization, and concentration," *Antioxidants*, vol. 9, no. 3, 2020, doi: 10.3390/antiox9030265.
- [4] A. L. McCarthy *et al.*, "The hydroxycinnamic acid content of barley and brewers' spent grain (BSG) and the potential to incorporate phenolic extracts of BSG as antioxidants into fruit beverages," *Food Chemistry*, vol. 141, no. 3, pp. 2567–2574, 2013, doi: 10.1016/j.foodchem.2013.05.048.
- [5] R. I. Birsan, P. Wilde, K. W. Waldron, and D. K. Rai, "Recovery of polyphenols from brewer's spent grains," *Antioxidants*, vol. 8, no. 9, pp. 1–12, 2019, doi: 10.3390/antiox8090380.
- [6] M. J. Cocero *et al.*, "Understanding biomass fractionation in subcritical & supercritical water," *Journal of Supercritical Fluids*, vol. 133, no. August 2017, pp. 550–565, 2018, doi: 10.1016/j.supflu.2017.08.012.
- [7] O. Pourali, F. S. Asghari, and H. Yoshida, "Production of phenolic compounds from rice bran biomass under subcritical water conditions," *Chemical Engineering Journal*, vol. 160, no. 1, pp. 259–266, 2010, doi: 10.1016/j.cej.2010.02.057.
- [8] P. C. Torres-Mayanga *et al.*, "Subcritical water hydrolysis of brewer's spent grains: Selective production of hemicellulosic sugars (C-5 sugars)," *Journal of Supercritical Fluids*, vol. 145, no. September 2018, pp. 19–30, 2019, doi: 10.1016/j.supflu.2018.11.019.
- [9] F. Qin, A. Z. Johansen, and S. I. Mussatto, "Evaluation of different pretreatment strategies for protein extraction from brewer's spent grains," *Industrial Crops and Products*, vol. 125, no. June, pp. 443–453, 2018, doi: 10.1016/j.indcrop.2018.09.017.
- [10] P. J. Arauzo, L. Du, M. P. Olszewski, M. F. Meza Zavala, M. J. Alhnidi, and A. Kruse, "Effect of protein during hydrothermal carbonization of brewer's spent grain," *Bioresource Technology*, vol. 293, no. July, 2019, doi: 10.1016/j.biortech.2019.122117.
- [11] I. Marcet, C. Álvarez, B. Paredes, and M. Díaz, "The use of sub-critical water hydrolysis for the recovery of peptides and free amino acids from food processing

- wastes. Review of sources and main parameters," *Waste Management*, vol. 49, pp. 364–371, 2016, doi: 10.1016/j.wasman.2016.01.009.
- [12] NREL Laboratory Analytical Procedures, "NREL." [gy/biomass-compositional-analysis.html](#) (accessed Dec. 21, 2020).
- [13] C. Method, "AOAC Official Method 982 . 30 Protein Efficiency Ratio Calculation Method First Action 1982," pp. 3–9, 2019.
- [14] J. Adler-Nissen, "Determination of the Degree of Hydrolysis of Food Protein Hydrolysates by Trinitrobenzenesulfonic Acid," *Journal of Agricultural and Food Chemistry*, vol. 27, no. 6, pp. 1256–1262, 1979, doi: 10.1021/jf60226a042.
- [15] V. L. Singleton, R. Orthofer, and R. M. B. T.-M. in E. Lamuela-Raventós, "[14] Analysis of total phenols and other oxidation substrates and antioxidants by means of folin-ciocalteu reagent," in *Oxidants and Antioxidants Part A*, vol. 299, Academic Press, 1999, pp. 152–178. doi: [https://doi.org/10.1016/S0076-6879\(99\)99017-1](https://doi.org/10.1016/S0076-6879(99)99017-1).
- [16] I. F. F. Benzie and J. J. Strain, "The Ferric Reducing Ability of Plasma (FRAP) as a Measure of 'Antioxidant Power': The FRAP Assay," *Analytical Biochemistry*, vol. 239, no. 1, pp. 70–76, 1996, doi: <https://doi.org/10.1006/abio.1996.0292>.
- [17] P. Alonso-Riaño, M. T. S. Diez, B. Blanco, S. Beltrán, E. Trigueros, and O. Benito-Román, "Water ultrasound-assisted extraction of polyphenol compounds from brewer's spent grain: Kinetic study, extract characterization, and concentration," *Antioxidants*, vol. 9, no. 3, 2020, doi: 10.3390/antiox9030265.
- [18] A. Friedl, E. Padouvas, H. Rotter, and K. Varmuza, "Prediction of heating values of biomass fuel from elemental composition," *Analytica Chimica Acta*, vol. 544, no. 1-2 SPEC. ISS., pp. 191–198, 2005, doi: 10.1016/j.aca.2005.01.041.
- [19] A. Connolly, C. O. Piggott, and R. J. Fitzgerald, "Characterisation of protein-rich isolates and antioxidative phenolic extracts from pale and black brewers' spent grain," *International Journal of Food Science and Technology*, vol. 48, no. 8, pp. 1670–1681, 2013, doi: 10.1111/ijfs.12137.
- [20] K. M. Lynch, E. J. Steffen, and E. K. Arendt, "Brewers' spent grain: a review with an emphasis on food and health," *Journal of the Institute of Brewing*, vol. 122, no. 4, pp. 553–568, 2016, doi: 10.1002/jib.363.
- [21] N. Sriperm, G. M. Pesti, and P. B. Tillman, "Evaluation of the fixed nitrogen-to-protein (N:P) conversion factor (6.25) versus ingredient specific N:P conversion factors in feedstuffs," *Journal of the Science of Food and Agriculture*, vol. 91, no. 7, pp. 1182–1186, 2011, doi: 10.1002/jsfa.4292.
- [22] A. L. Merrill and B. K. Watt, "Energy Value of Foods: Basis and Derivation. Agriculture Handbook," *Washington, DC: United States Department of Agriculture*, 1973.
- [23] S. Ikram, L. Huang, H. Zhang, J. Wang, and M. Yin, "Composition and Nutrient Value Proposition of Brewers Spent Grain.," *Journal of food science*, vol. 82, no. 10, pp. 2232–2242, Oct. 2017, doi: 10.1111/1750-3841.13794.
- [24] D. M. Waters, F. Jacob, J. Titze, E. K. Arendt, and E. Zannini, "Fibre, protein and mineral fortification of wheat bread through milled and fermented brewer's spent



- grain enrichment," *European Food Research and Technology*, vol. 235, no. 5, pp. 767–778, 2012, doi: 10.1007/s00217-012-1805-9.
- [25] P. J. Arauzo, M. P. Olszewski, and A. Kruse, "Hydrothermal carbonization brewer's spent grains with the focus on improving the degradation of the feedstock," *Energies*, vol. 11, no. 11, 2018, doi: 10.3390/en11113226.
- [26] S. M. Heilmann, L. R. Jader, M. J. Sadowsky, F. J. Schendel, M. G. von Keitz, and K. J. Valentas, "Hydrothermal carbonization of distiller's grains," *Biomass and Bioenergy*, vol. 35, no. 7, pp. 2526–2533, 2011, doi: 10.1016/j.biombioe.2011.02.022.
- [27] M. Jackowski *et al.*, "Hydrothermal Carbonization of Brewery's Spent Grains for the Production of Solid Biofuels," *Beverages*, vol. 5, no. 1, p. 12, 2019, doi: 10.3390/beverages5010012.
- [28] J. Poerschmann, B. Weiner, H. Wedwitschka, I. Baskyr, R. Koehler, and F. D. Kopinke, "Characterization of biocoals and dissolved organic matter phases obtained upon hydrothermal carbonization of brewer's spent grain," *Bioresource Technology*, vol. 164, pp. 162–169, 2014, doi: 10.1016/j.biortech.2014.04.052.
- [29] L. Du, P. J. Arauzo, M. F. Meza Zavala, Z. Cao, M. P. Olszewski, and A. Kruse, "Towards the properties of different biomass-derived proteins via various extraction methods," *Molecules*, vol. 25, no. 3, 2020, doi: 10.3390/molecules25030488.
- [30] I. Sereewatthanawut, S. Prapintip, K. Watchirarujj, M. Goto, M. Sasaki, and A. Shotipruk, "Extraction of protein and amino acids from deoiled rice bran by subcritical water hydrolysis," *Bioresource Technology*, vol. 99, no. 3, pp. 555–561, 2008, doi: 10.1016/j.biortech.2006.12.030.
- [31] S. O. Lourenço, E. Barbarino, P. L. Lavín, U. M. Lanfer Marquez, and E. Aidar, "Distribution of intracellular nitrogen in marine microalgae: Calculation of new nitrogen-to-protein conversion factors," *European Journal of Phycology*, vol. 39, no. 1, pp. 17–32, 2004, doi: 10.1080/0967026032000157156.
- [32] S. Niamke, L. P. Kouame, J. P. Kouadio, D. Koffi, B. M. Faulet, and S. Dabonne, "Effect of some chemicals on the accuracy of protein estimation by the Lowry method," *Biokemistri*, vol. 17, no. 2, pp. 73–81, 2006, doi: 10.4314/biokem.v17i2.32591.
- [33] T. Rogalinski, S. Herrmann, and G. Brunner, "Production of amino acids from bovine serum albumin by continuous sub-critical water hydrolysis," *Journal of Supercritical Fluids*, vol. 36, no. 1, pp. 49–58, 2005, doi: 10.1016/j.supflu.2005.03.001.
- [34] H. J. Lee, P. S. Saravana, Y. N. Cho, M. Haq, and B. S. Chun, "Extraction of bioactive compounds from oyster (*Crassostrea gigas*) by pressurized hot water extraction," *Journal of Supercritical Fluids*, vol. 141, no. January, pp. 120–127, 2018, doi: 10.1016/j.supflu.2018.01.008.
- [35] K. Watchararujj, M. Goto, M. Sasaki, and A. Shotipruk, "Value-added subcritical water hydrolysate from rice bran and soybean meal," *Bioresource Technology*, vol. 99, no. 14, pp. 6207–6213, 2008, doi: 10.1016/j.biortech.2007.12.021.

- [36] W. Abdelmoez and H. Yoshida, "Production of amino and organic acids from protein using sub-critical water technology," *International Journal of Chemical Reactor Engineering*, vol. 11, no. 1, pp. 369–384, 2013, doi: 10.1515/ijcre-2013-0017.
- [37] A. Lamp, M. Kaltschmitt, and O. Lüdtke, "Protein recovery from bioethanol stillage by liquid hot water treatment," *Journal of Supercritical Fluids*, vol. 155, 2020, doi: 10.1016/j.supflu.2019.104624.
- [38] Widyarani, Y. W. Sari, E. Ratnaningsih, J. P. M. Sanders, and M. E. Bruins, "Production of hydrophobic amino acids from biobased resources: wheat gluten and rubber seed proteins," *Applied Microbiology and Biotechnology*, vol. 100, no. 18, pp. 7909–7920, 2016, doi: 10.1007/s00253-016-7441-8.
- [39] M. B. Esteban, A. J. García, P. Ramos, and M. C. Márquez, "Kinetics of amino acid production from hog hair by hydrolysis in sub-critical water," *Journal of Supercritical Fluids*, vol. 46, no. 2, pp. 137–141, 2008, doi: 10.1016/j.supflu.2008.04.008.
- [40] N. Doctor, G. Parker, K. Vang, M. Smith, B. Kayan, and Y. Yang, "Stability and extraction of vanillin and coumarin under subcritical water conditions," *Molecules*, vol. 25, no. 5, pp. 1–9, 2020, doi: 10.3390/molecules25051061.
- [41] C. Fabian, N. Y. Tran-Thi, N. S. Kasim, and Y. H. Ju, "Release of phenolic acids from defatted rice bran by subcritical water treatment," *Journal of the Science of Food and Agriculture*, vol. 90, no. 15, pp. 2576–2581, 2010, doi: 10.1002/jsfa.4123.
- [42] K. Kang *et al.*, "Optimization of amino acids production from waste fish entrails by hydrolysis in sub- and supercritical water," *Canadian Journal of Chemical Engineering*, vol. 79, no. 1, pp. 65–70, 2001, doi: 10.1002/cjce.5450790110.

# CHAPTER 4

---

**Preliminary study of subcritical water treatment scale-up from laboratory to pilot system for brewer's spent grain valorization**

**Based on the article:**

P. Alonso-Riaño, M. T. Sanz, S. Beltrán, E. Trigueros, C. Ramos.

“Preliminary study of subcritical water treatment scale-up from laboratory to pilot system for brewer's spent grain valorization”.



## Capítulo 4

### Estudio preliminar del escalado del sistema de tratamiento con agua subcrítica desde el modelo de laboratorio hasta planta piloto para la valorización del bagazo de cerveza

---

#### Resumen

En este capítulo se ha investigado la viabilidad del tratamiento con agua subcrítica a escala industrial, mediante la ampliación del sistema desde una escala de laboratorio hasta una planta piloto, en un modo de operación discontinuo, para la valorización del bagazo de cerveza.

En primer lugar, se analizaron los extractos obtenidos en el sistema a escala de laboratorio, recolectados periódicamente durante 45 min, a una temperatura fija de 170 °C. En base a los resultados obtenidos se definió un tiempo de reacción de 22 minutos, con el objetivo de obtener un buen rendimiento de azúcares, liberados principalmente de la fracción de hemicelulosa del bagazo, manteniendo al mismo tiempo una concentración relativamente baja de productos de degradación, para evitar la inhibición enzimática y/o de la fermentación, en un paso posterior de valorización de los oligosacáridos, dentro de un concepto de biorrefinería. Bajo estas condiciones, se alcanzó un rendimiento total de pentosas del 87%, liberadas principalmente en forma de oligómero.

El tratamiento del bagazo con agua subcrítica en la planta piloto a 170 °C y 22 min, dio lugar a la liberación del 56% de los carbohidratos presentes en el bagazo de cerveza. Se alcanzó un rendimiento total de pentosas del 78% (18% como monómero y 82% como oligómero), mientras que la concentración de inhibidores en el hidrolizado subcrítico fue relativamente baja, 0.22 g/L, 0.31 g/L y 0.13 g/L de furfural y ácidos acético y fórmico, respectivamente. Además, se obtuvieron los siguientes compuestos de alto valor: 6,5 g/L de péptidos (64% de rendimiento proteico), 21 mg de aminoácidos libres por gramo de proteína en el bagazo inicial (2,17% de rendimiento de aminoácidos), y un contenido fenólico total de 17,84 mg<sub>GAE</sub>/g<sub>bagazo-seco</sub>.

En general, los resultados mostraron una buena reproducibilidad al escalar el proceso de tratamiento con agua subcrítica desde el sistema de laboratorio a la planta piloto ya que no se encontraron diferencias estadísticamente significativas ( $p$ -valor  $< 0.05$ ), entre los dos sistemas para el rendimiento de oligómeros totales ni para el rendimiento de proteínas y aminoácidos libres. Sin embargo, el rendimiento de xilooligosacáridos fue un 13% mayor a escala de laboratorio que a escala piloto y se encontraron mayores concentraciones de monómeros y compuestos fenólicos en los hidrolizados subcríticos obtenidos a escala de laboratorio.

Por otra parte, el tratamiento con agua subcrítica modificó la composición química del sólido residual, ya que se observó una notable disminución de la concentración de hemicelulosa y un aumento en el contenido de glucano, lo que podría mejorar el rendimiento de glucosa en una hidrólisis enzimática posterior.

---

**Palabras clave:** tratamiento con agua subcrítica, biorrefinería, bagazo de cerveza, escalado, carbohidratos, oligosacáridos, proteínas, aminoácidos, compuestos fenólicos.

## Abstract

---

The feasibility of industrial-scale subcritical water (subW) system by scaling-up from laboratory to pilot scale in a discontinuous operation mode has been investigated regarding the valorization of brewer's spent grain (BSG). The optimum reaction time was 22 min at lab-scale at a fixed temperature of 170 °C.

The subW treatment of BSG at pilot-scale in a discontinuous mode at 170 °C and 22 min, resulted in the release of 56% of the total carbohydrates present in the BSG. A total pentose yield of 78% was achieved (18% as monomer and 82% as oligomer). The concentration of inhibitors in the hydrolysate was relatively low, 0.22 g/L, 0.31 g/L, and 0.13 g/L of furfural and acetic and formic acids respectively. Other high value compounds were obtained, such as 6.5 g/L peptides (64% protein yield), 21 mg/g<sub>protein</sub> of free amino acids (2.17% aa yield), and a total phenolic content of 17.84 mg<sub>GAE</sub>/g<sub>dry-BSG</sub>. In general, the results showed good reproducibility when scaling up from laboratory to pilot subW process. Good reproducibility of the scale-up was found for the release yield of total oligomers, arabinoxylo-oligomers, and gluco-oligomers from BSG, also for the protein yield and the release of free amino acids. However, the xylo-oligomers yield was 13% higher at lab-scale than at pilot-scale and higher concentrations of monomers and phenolic compounds were found in the subW hydrolysates obtained at lab-scale. subW treatment modified the composition of the residual solid, as a decrease in the concentration of hemicellulose and an increased in the glucan content was observed, that may enhance the digestibility of the solid improving a further enzymatic release of glucose from the remaining solid.

---

**Keywords:** Subcritical water treatment, scale-up, carbohydrates, oligosaccharides, protein, amino acids, phenolic compounds, valorization, brewer's spent grain, biorefinery.





## 1. Introduction

Nowadays, efforts are being made to move towards a more sustainable economy with a better use of natural resources and a reduction of greenhouse gases emissions. The development of sustainable biorefineries will contribute to the transition from an economy based on fossil feedstocks to a biobased economy. The use of biomass as raw material opens the possibility to obtain different products and energy through new biorefineries based on a sustainable economy, converting biomass into bio-based products. For that, good quality and low-cost biomass availability and the development of innovative and environmentally friendly technologies for its valorization, are key aspects to implement the bioeconomy.

Regarding the biomass, brewery spent grain (BSG) is a second-generation biomass based on non-food lignocellulosic biomass generated in the brewing industry in large quantities at low cost. Around  $38.6 \cdot 10^6$  tons of BSG are annually globally generated from the brewing industry of which  $3.4 \cdot 10^6$  tons are produced in Europe [1]. After brewing, BSG contains around 80% of moisture [2]. Due to the high humidity and fermentable sugar content, BSG is susceptible to microbial growth and deteriorates quickly (around 7-10 days) [3]. Therefore, BSG is commonly discarded in landfills, used for cattle feed, or incinerated. Nevertheless, BSG is a sustainable resource of valuable bio compounds based on its chemical composition: cellulose (12-26%), hemicellulose (19-42%), lignin (12-28%), proteins (14-31%), and lipids (3-13%), expressed on a dry weight basis [4]. BSG is also an excellent source of bioactive ingredients such as phenolic compounds, mainly hydroxycinnamic acids (p-coumaric, ferulic, sinapic, and caffeic acids) as well as vitamins and minerals [5]. Therefore, BSG valorization in a biorefinery is a powerful strategy not only from an economic point of view, but also from an environmental perspective [6].

An integral valorization of biomass requires extraction and fractionation of its building blocks including extractives, lipids, proteins, and structural components of the biomass (cellulose, hemicellulose, and lignin). However, due to the recalcitrant structure of lignocellulosic materials, one of the most limiting steps for their conversion is fractionation. As reviewed by Sganzerla et al. [6], different pretreatments have been applied to BSG, such

as chemical treatment by acid, alkali, or acid-alkali, supercritical fluids, pulsed electric, hydrothermal, and enzymatic hydrolysis.

Among these techniques, hydrothermal treatment, which includes liquid hot water treatment (also known as autohydrolysis, water extraction, pressurized hot water, and subcritical water treatment) and steam explosion pretreatment, is a low-cost and environmentally friendly process as no chemicals are required. This technic applies water above its normal boiling point at a pressure high enough to maintain its liquid state and under subcritical conditions (critical point 373 °C and 22.1 MPa). Under these conditions, the physical and chemical properties of water as a solvent, comprising its dielectric constant and solubility, are modified, resulting in certain extraction improvements due to the high diffusivity, low viscosity, low surface tension, and higher polarizability. When temperature increases under subW conditions, ionization constants gradually increase, as the hydrogen bonds of subW gradually weaken, producing more acidic hydronium ions ( $\text{H}_3\text{O}^+$ ) and alkaline hydroxide ions ( $\text{OH}^-$ ). In addition, the contribution of  $\text{H}_3\text{O}^+$  generated by the ionization of the acetyl groups present in hemicelluloses may promote the depolymerization process of polysaccharides [7]. In a subW system, temperature and reaction time are the most important parameters to be considered. The higher the temperature and time are, the greater hemicellulose solubilization is achieved; although, if these two variables are too high, hemicellulose sugars and oligomers start to degrade producing inhibitors such as furfural derived from pentoses and hydroxymethylfurfural (HMF), derived from hexoses [7]. Middle temperatures (175–190 °C) and short treatment time (15–60 min) enhance the production of oligosaccharides, while longer treatment times (60–120 min) and lower temperature (160–175 °C) may allow a high yield of monosaccharides [8].

According to Sganzerla et al. [6], the utilization of hydrothermal technology with subW may be a promising alternative to produce different concentrated sugars in an industrial plant from BSG, but it is still rarely explored. Specially, considering that most of the studies regarding the use of BSG as source of several valuable bioproducts have been performed at laboratory-scale with no account for their feasibility and processing costs in pilot and/or industrial plants.

Recently, a techno-economic evaluation of subcritical water hydrolysis process for sugars production from BSG simulating two different capacity vessels of 10 L and 500 L,

coupled or not to a separation system, has been published [9]. In that work, the authors concluded that (1) BSG is best hydrolyzed in the extractor vessel of 500 L, as the arabinose cost of manufacturing (the highest concentrated sugar obtained from BSG) decreased from 64.10 USD/kg to 7.22 USD/kg when scaling-up the reactor volume from 10 L to 500 L. (2) To achieve positive profitability indicators in the process, the purification system (a five-zone simulated moving bed process) should be integrated enhancing the feasibility of the process. In this regard, the cost of manufacturing for the subW process at industrial scale (3x500 L) was 2.92 USD/kg increasing to 6.63 USD/kg with the adoption of the separation system. However, the selling price of purified arabinose (59 USD/kg) is by far higher than the market price of the hydrolysate by considering the non-concentrated sugars (3 USD/kg).

Nevertheless, to make full use of the feedstock, enhancing the feasibility of the process, an integral valorization of biomass should be integrated. Among the different compounds produced by subW treatment, oligosaccharides attract extensive attention in food, cosmetics, agriculture, pharmacy, and biomedicine [8]. As reported in the literature, subW treatment at 170 °C for 20 min in a batch reactor enabled the production of oligosaccharides from BSG, maintaining the generation of acetic acid and the sugar degradation products quite low [10]. In addition, when hemicellulose is solubilized from the biomass, most of the cellulose and lignin remain in the solid fraction after subW treatment, which can be submitted to saccharification and fermentation to produce second generation ethanol [11]. Moreover, subW treatment has been found to be able to extract/hydrolyze up to 78% of the protein fraction from BSG in a semi-continuous fixed bed reactor at 180 °C, producing hydrolysates with high antioxidant capacity as well as phenolic compounds, such as vanillin and p-coumaric and ferulic acids and a minor amount of free amino acids, mainly aspartic acid [12]. However, in that work, the concentration of HMF and furfural in the hydrolysates were significantly higher at 185 °C than at 160 °C, while the concentration of free amino acids and hydroxycinnamic acids were higher at 160 °C, suggesting that some of the valuable compounds of BSG are labile at 185 °C.

Therefore, a subW temperature of 170 °C was chosen mainly focused on the release of oligosaccharides from the hemicellulose fraction of BSG, but also considering other valuable biocompounds, while maintaining a relatively low concentration of degradation products.

This work aimed to verify if subW treatment of BSG is a suitable technology to be performed at an industrial scale through scaling-up from lab to pilot system. Accordingly, the purposes of this work were: (1) to perform a detailed characterization of the liquid and solid streams generated after the subW process, at different reaction times, at laboratory and pilot-scales, considering the main valuable BSG components, such as carbohydrates, released as monomer and oligomers, protein and free amino acids, phenolic compounds, the presence of inhibitors, such as acetic acid, furfural, and HMF, as well as the potential uses of the subW solid residue and (2) to evaluate the reproducibility of the results obtained when scaling up from laboratory to pilot subcritical water process.

## 2. Materials and methods

### 2.1. Raw material

The BSG was kindly supplied by San Miguel S.A with an initial average humidity of 85% (w/w). This raw material was first preconditioned by washing it and drying in an air convection oven at 45 °C until reaching a final moisture content of 8 % (w/w). Dry BSG was milled in a Retsch SM100 mill and the fraction with particle size lower than 0.5 mm was selected. The particle size distribution was determined by a vibratory sieve shaker (CISA, RP.09). **Table 4.1** collects the particle size distribution of the BSG as received (whole BSG), together with the fraction of milled BSG selected for this work.

**Table 4.1.** Particle size distribution of BSG as received (whole BSG) and the fraction of BSG selected after milling.

Particle size (mm)	Whole BSG (%)	Selected BSG (%)
> 1	5.19	—
1 – 0.5	52.49	—
0.5 – 0.25	28.45	68.93
0.25 – 0.125	8.69	22.98
< 0.125	1.73	8.09

The selected fraction of BSG (from now on it will be called BSG to simplify) was characterized following the NREL protocols [13] to determine structural carbohydrates (cellulose and hemicellulose), lignin, moisture, total solids, ash, total extractives, and protein as has been detailed in Chapter 1.

Starch and  $\beta$ -Glucan contents were determined by using the total starch (amyloglucosidase/ $\alpha$ -amylase method) and the mixed linkage  $\beta$ -glucan assay kit, according to the manufacturer's (Megazyme International Ltd.) instructions. The lipid content of the BSG was determined by Soxhlet extraction (Buchi B-8111) using hexane as solvent. Cellulose was estimated as the difference between glucose determined after hydrolysis and glucose due to starch and  $\beta$ -glucans. Hemicellulose was estimated from the xylan, arabinan, and acetyl groups content in the biomass.

## 2.2. Subcritical water equipment

### 2.2.1. Laboratory-scale assay

Subcritical water experiments at laboratory-scale level were carried out in a lab-built discontinuous reactor (see **Figure 4.1**).

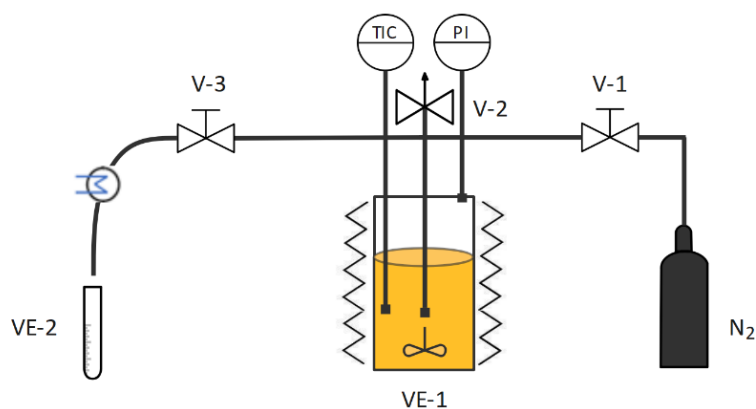


**Figure 4.1.** Diagram of laboratory-scale subcritical water equipment. VE-1: extractor; VE-2: sample collector; V-1: vent valve; V-2: pressure relief valve; V-3: needle valve.

The total capacity of the high-pressure stainless-steel vessel was 0.5 L. Pressurization of the vessel was performed with nitrogen gas. To reach the working temperature, the reactor was covered by a ceramic heating jacket (230 V, 4000 W,  $\phi$  95 cm, 160 mm height). A Pt100 sensor, connected to a PID system and placed inside the reactor, allowed to control and register the temperature during the extraction. A needle valve (Autoclave Engineers) followed by a cooling system was connected to collect samples along the assay.

In a typical run, dry BSG was loaded into the reactor and filled with water at biomass to distilled water ratio of 1:20, corresponding to a biomass loading of 5% (w/v) in a dry weight basis. The temperature was set at 170 °C, agitation rate at 500 rpm, and extraction pressure at 50 bar and maintained during all the process. Extraction/hydrolysis kinetics were followed by withdrawing samples through a sampling pipe provided with a metallic filter to avoid the clogging of the pipe. After 60 minutes from the beginning, the extraction vessel was cooled and depressurized when the temperature was lower than 90 °C. The temperature inside the reactor was registered from the beginning (ambient temperature) until it was cooled down below 100 °C after the treatment (cooling stage). Samples were stored at -18 °C until analysis

### **2.2.2. Pilot-scale assay**

SubW experiments at pilot-scale level were performed at Hiperbaric's facilities (<https://www.hiperbaric.com/es/>) by using a discontinuous system.

The prototype was mainly composed of a vessel of 25 L capacity, a steam boiler as the heating system, a pump to recirculate and homogenize the biomass inside the reactor, a heat exchanger to avoid cooling during the recirculation process, and a solid/liquid separation system (see **Figure 4.2**). The maximum specifications of the system were 185 °C and 20 bar. A software built by Hiperbaric was used to execute the operation and control of the process.

The experiments were performed as follows. Firstly, all the system was pre-heated at 80 °C by heating water up to 80 °C in the steam boiler and circulating it through the heat exchanger. Then, the system was totally drained, and the BSG was loaded into the reactor. After that, the reactor was filled with the pressurized water and the desired temperature

was reached by the steam boiler system. Nitrogen gas was used to pressurize the system. At this moment, the recirculation pump was turned on to improve external mass transfer in the extraction/hydrolysis process. The maximum specifications of the pump were a solid concentration of 40% (w/v) with a maximum particle size of 0.5 mm, which determined the particle size of the biomass to be used, as mentioned above. The heat exchanger was placed in the recirculation pipe to permit contact with the steam boiler outlet pipe, avoiding heat loss in the recirculation process. A sampling system inserted at the base of the reactor, allowed periodical sampling to follow the extraction/hydrolysis kinetics. At the end of the treatment, the liquid stream was separated from the solid residue by employing a filtration tank.

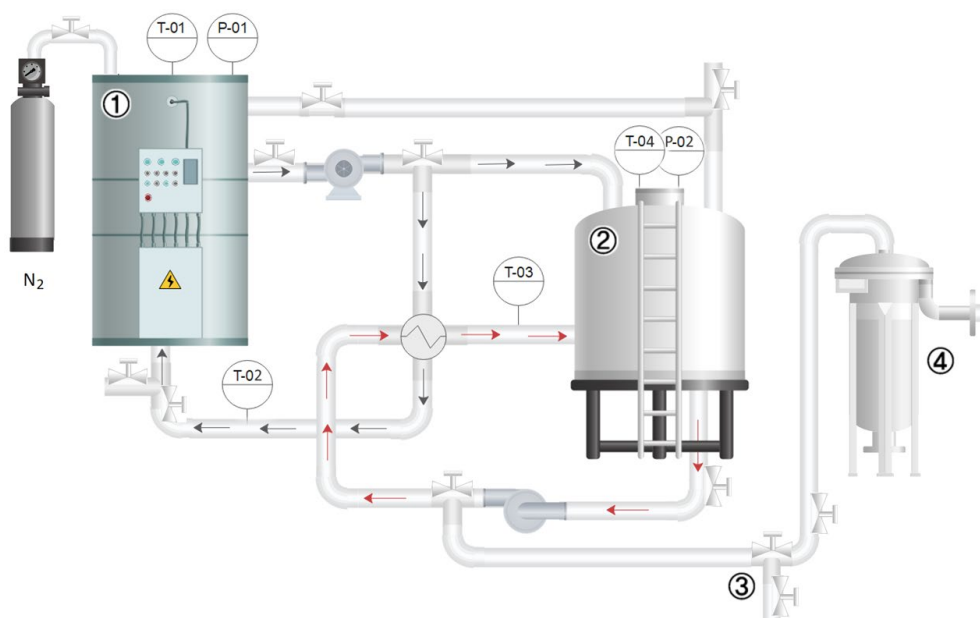


**Figure 4.2.** Diagram of pilot-scale subcritical water plant designed and built in Hiperbaric.

1: boiler preheater and water tank; 2: 25 L extractor; 3: liquid sample collector;

4: filtration tank.

Experiments were carried out at 5% (w/v) biomass loading, temperature of 170 °C and a working pressure of 20 bar. The treatment time was established from the results obtained in the laboratory-scale assay.

## 2.3. Analytical methods

### 2.3.1. Carbohydrate fraction and their degradation products in liquid streams

Monosaccharides and their degradation products were determined by HPLC as described by Alonso-Riaño et al. [12]. The HPLC equipment mainly consists of a Biorad Aminex-HPX-87H column and its corresponding pre-column and two detectors, a variable wavelength detector (VWD), and a refractive index detector (RID). Sulfuric acid (0.005 M) was the mobile phase. The temperature of the column and the refractive index detector was maintained at 40 °C. After filtering through a 0.2 µm syringe filter, 10 µL of sample were injected. Sugars, acetic, and formic acid were quantified by RID while 5-hydroxymethyl-2-furaldehyde (HMF), and furfural were determined by VWD at 284 and 275 nm, respectively. Calibration was performed with pure standards of xylose, arabinose, glucose, and furfural (99%), purchased from Sigma-Aldrich, HMF (97%) from Alfa Aesar, formic acid (98%) from Fluka and acetic acid (99.8%) from VWR.

Monomeric yield was evaluated as the ratio of the amount of sugar monomer released to the medium over the maximum potential yield of sugar obtained from the BSG composition:

$$\text{Monomeric yield (\%)} = \frac{\text{Monomeric sugar in the hydrolysate}}{\text{Sugar in the raw material}} \cdot 100 \quad [4.1]$$

Total sugars were determined after a first acid hydrolysis step to release monomeric sugars from oligomers for quantification following the NRLE protocols [14]. Total yield of each sugar was determined according to Equation 4.2.

$$\text{Total yield (\%)} = \frac{(\text{Monomeric and Oligomeric Sugar})_{\text{hydrolysate}}}{\text{Sugar in the raw material}} \cdot 100 \quad [4.2]$$

Oligomer yield was calculated by difference between total and monomer yield.



### 2.3.2. Protein and free amino acids

Total protein content was determined from the nitrogen content measured by using a TOC/TN analyzer (Shimadzu TOC-V CSN analyzer) using  $\text{KNO}_3$  as standard after applying a nitrogen factor of 6.25.

Free amino acids were determined by using the EZ:faast Phenomenex procedure as described by Alonso Riaño et al. [12].

### 2.3.3. Total organic carbon

Total carbon and inorganic carbon were measured with a TOC Analyzer Shimadzu by using  $\text{C}_6\text{H}_{14}(\text{COOK})(\text{COOH})$ ,  $\text{NaHCO}_3$  and  $\text{Na}_2\text{CO}_3$  as standards. Total organic carbon (TOC) was calculated by subtracting the inorganic carbon from total carbon content.

### 2.3.4. Polyphenolic compounds

Total Polyphenols Content (TPC) was determined by using the Folin–Ciocalteu reagent following the method described by Singleton et al. [15]. A calibration curve was prepared with standard solutions of gallic acid by following the same colorimetric method, and results were expressed as mg of gallic acid equivalent (GAE) per gram of dry BSG.

Individual phenolic compounds were identified and quantified according to the method previously described by Alonso-Riaño et al. [2]. The sample was filtered through a 0.2  $\mu\text{m}$  syringe filter. After that, 80  $\mu\text{L}$  of sample were injected in the HPLC system. The separation was performed at 25 °C on a Kinetex®  $\mu\text{m}$  Biphenyl 100 Å, 250 × 4.6 mm column (Phenomenex). The mobile phase consisted of ammonium acetate 5 mM with acetic acid (1%; v/v) in water (solvent A) and ammonium acetate 5 mM with acetic acid (1%; v/v) in acetonitrile (solvent B). The composition of the mobile phase varied during the run according to a nonlinear gradient as follows: from 0 to 7 min, 2% of solvent B (isocratic), from 7 to 20 min, from 2% to 8% solvent B, from 20 to 35 min, from 8% to 10% solvent B and from 35 to 55 min, from 10% to 18% solvent B and post time of 10 min, at a flow rate of 0.8 mL/min. Detection and quantification were performed at 240, 280, 330, 340, 350, and 370 nm. The HP ChemStation software was employed to collect and analyze the chromatographic data delivered by the diode array detector and our own library was used

to identify the different phenolic compounds by comparing retention times and spectral data with those of authentic standards: syringic aldehyde, protocatechuic aldehyde, vanillin, p-coumaric acid, ferulic acid, catechin, vanillic acid, 4-vinylphenol and 4-vinylguaicol standards (Sigma-Aldrich). Peak purity was checked to exclude any contribution from interfering peaks. Individual stock solutions of the above phenolic compounds, and their mixtures, were prepared in methanol to plot the calibration curves.

### 2.3.5. Elemental composition

Elemental composition (C, H, N, S) of raw material and solid residue after subW treatment was determined by an organic elemental micro-analyzer equipment (Thermo Scientific Model Flash 2000). Oxygen content was determined by difference. The high heating value (HHV) of BSG and the solid remaining after subW treatment was evaluated according to Equation 4.3 [16]:

$$HHV (kJ/kg) = 3.55C^2 - 232C - 2230H + 51.2C \cdot H + 131N + 20600 \quad [4.3]$$

### 2.4. Statistical analysis

All values were expressed as mean  $\pm$  standard deviation from triplicate measurements. The significance of the differences was determined based on an analysis of the variance with the Fisher's Least Significant Difference (LSD) method at p-value  $\leq 0.05$  using the Statgraphics X64 software. Error bars in all graphs are 95% confidence intervals.

## 3. Results and discussion

### 3.1. BSG composition

Chemical composition of the BSG employed in this work is presented in **Table 4.2**, in a weight percentage dry basis. Polysaccharides represent up to 50% of the BSG dry weight, comprising xylan (21.6%), glucan (19.1%), and arabinan (9.5%). The cellulose and hemicellulose content of the BSG used in this work was 14% and 32%, respectively. Besides carbohydrates, the BSG also contained a significant amount of protein (22.1% w/w) and lignin (20.8% w/w), and minor amounts of lipids, ash, starch, and  $\beta$ -glucans.

**Table 4.2.** Chemical composition of the selected fraction of BSG (particle size < 0.5 mm) expressed in weight percentage on a dry basis

Component	Composition of selected BSG (%)
Extractives in water (24 h, 50 °C)	9.2 ± 0.1
TOC	6.08 ± 0.06
Protein	5.53 ± 0.01
TPC	0.365 ± 0.009
Extractives in ethanol (24 h, 50 °C)	5.3 ± 0.1
Protein	0.513 ± 0.004
TPC	0.109 ± 0.004
Total Protein	22.1 ± 0.5
Glucan content	19.1 ± 0.2
Cellulose	14.0 ± 0.2
Starch	4.11 ± 0.06
β-Glucan	0.99 ± 0.01
Hemicellulose content	32.0 ± 0.6
Xylan	21.6 ± 0.4
Arabinan	9.5 ± 0.4
Acetyl groups	0.93 ± 0.05
Lignin	20.8 ± 0.2
Acid Soluble lignin	5.3 ± 0.2
Acid Insoluble lignin	15.5 ± 0.1
Lipids	6.2 ± 0.3
Ash	3.32 ± 0.06

Values are expressed as mean ± standard deviation from triplicate determination.

Extractives in water and extractives in ethanol (water insoluble) comprised non-structural compounds accounted for 9.2% and 5.3% dw, with a TPC of 3.65 and 1.09 mg<sub>GAE</sub>/g<sub>BSG, dry</sub>, respectively. The protein content in water and ethanol extractives were 5.53% and 0.51%, respectively, determined by the TN content and applying the factor 6.25. However, according to Qin et al. [17], the value of total nitrogen in the sample might include non-protein nitrogen compounds, such as free amino acids degraded from protein during the mashing process. These authors reported a protein yield of 64-66% from BSG in water at 60 °C for 24 h. In the present work, the amount of crude protein in water extractives (5.53%) accounted for 25% of BSG protein which was water-soluble. This value agrees with

values reported in the literature for this type of biomass [12], [18]. Total organic carbon in water extractives was also determined, corresponding to 6.08% on a dry weight basis.

### 3.2. Heating rate

Temperature profiles for the subW experiments performed at lab-scale and pilot-scale are shown in **Figure 4.3**.

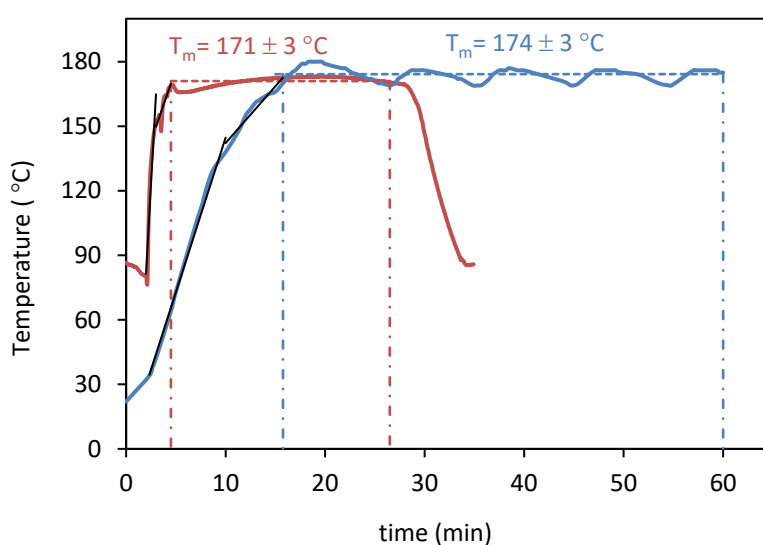


**Figure 4.3.** Hydrothermal temperature profile during subW treatment performed at lab-scale, continuous blue lines (—), and at pilot-scale, continuous red lines (—).

Discontinuous lines delimit the isothermal period in each system.  $T_m$ : medium temperature during the isothermal period.

Different heating rates were observed for both systems. Specifically, the time needed to reach the desired working temperature, 170 °C, was 15.7 min at lab-scale, while it was achieved after only 4.5 min when subW treatment was performed at the pilot plant, since water was placed into the pilot plant reactor at 80 °C. It is worth describing the differences between the temperature profiles in as much detail as possible since heating rate influences the results regarding the biocompounds release from BSG. The pre-heating time was defined as the time needed to reach the working temperature. From now on, the time when

the working temperature was reached will be referred to as time 0, which will be the beginning of the isothermal period. In each system, two different heating rates were observed, being faster at the beginning. The initial heating rate at pilot-scale was 83.4 °C/min, decreasing until 13.4 °C/min after 3 min, whereas the heating rate at lab-scale was 14.4 °C/min for the first 10 min, with a reduction after that down to 5.3 °C/min. Typically, the heating time to achieve the desired reaction temperature in subW ranges from 15 to 80 min, and heating rates vary from 2 to 7.1 °C/min [19]. Furthermore, medium operating temperature during the isothermal period was  $174 \pm 3$  °C and  $171 \pm 3$  °C at lab-scale and pilot-scale, respectively.

Additionally, it must be highlighted that cooling was almost instantaneous at pilot-scale, while it took around 75 min to decrease the temperature below 80 °C inside the reactor at lab-scale. Therefore, considering the three stages, pre-heating time, isothermal time, and cooling time, the total time that the solid was in contact with water at a temperature higher than 80 °C was around 135 min at lab-scale for a defined isothermal time of 45 min. In contrast, experiments performed at pilot-scale could be considered under isothermal operation as both, the pre-heating and the cooling periods were truly short. In consequence, the combined effect of temperature and reaction time during hydrothermal processes was evaluated by the severity factor parameter according to Equation 4.4:

$$R_0 = t \cdot \exp\left(\frac{T-100}{14.75}\right) \quad [4.4]$$

where  $R_0$  is the severity factor,  $t$  is the treatment time (min),  $T$  is the operating temperature (°C),  $T_{ref}$  is 100 °C because under this temperature practically no solubilization neither depolymerization of the hemicellulose take place and the value 14.75 is a typical activation energy for glycosidic bond cleavage of carbohydrates under hydrothermal treatment assuming conversion is first order. The severity factor is commonly determined considering only the isothermal stage and expressed as  $S_0 = \log R_0$ , being in this case, 3.83 (45 min, 174 °C) and 3.43 (22 min, 171 °C) for lab-scale and pilot-scale, respectively. However, the severity factor can be modified to incorporate the effect of non-isothermal stages by integrating the temperature vs time profile at heating, isothermal, and cooling periods [20], [21]:

$$\begin{aligned}
 R_o &= R_{o, \text{Heating}} + R_{o, \text{Isothermal}} + R_{o, \text{Cooling}} \\
 &= \int_{t_0}^{t_H} \exp\left(\frac{T(t)-100}{14.75}\right) \cdot dt + t \cdot \exp\left(\frac{T-100}{14.75}\right) + \int_{t_F}^{t_C} \left(\frac{T(t)-100}{14.75}\right) \cdot dt
 \end{aligned} \quad [4.5]$$

where  $T(t)$  is the function of the temperature vs time determined from the temperature profile (**Figure 4.3**) at each stage.  $t_0-t_H$  is the time range to reach the work temperature ( $T$ ),  $t$  is the isothermal time and  $t_F-t_C$  is the time range to decrease temperature from  $T$  to  $100^\circ\text{C}$  after the isothermal period.

Therefore, the severity factor of the treatment at lab-scale calculated according to Equation 4.5 increased up to 7.47 by considering the three stages during the hydrothermal process. Nevertheless, this value may be used with caution to compare the results with those reported in the literature for two reasons: (1) the severity factor is often calculated in the literature only for the isothermal period even if higher heating times were employed and (2) this value should be used only to compare the composition of the residual solid since samples from the liquid stream were collected periodically through the sampling pipe, so, the stage of cooling time was not considered.

### 3.3. Polysaccharide fraction extraction/hydrolysis

**Figure 4.4a** shows the kinetic release of glucose, xylose, and arabinose monomers in the laboratory-scale extracts (LSE) and the pilot-scale extracts (PSE) from BSG. **Figure 4.4b** shows total sugars (released as monomer and oligomer) expressed as monomer equivalent. Moreover, the individual sugar yield in each system, obtained at different reaction times as monomer and as oligomer (expressed as monomer equivalent) has been represented in **Figure 4.5**. During the preheating time (15.8 min for laboratory-scale and 4.5 min for pilot-scale) a fraction of the sugars, mainly in oligomeric form, was released. At that time, glucose, xylose, and arabinose equivalent concentrations were 1.41 g/L, 1.55 g/L, and 1.27 g/L, respectively, in LSE and 1.46 g/L, 1.29 g/L, and 0.36 g/L, respectively, in PSE, released as total sugars (monomers and oligomers). Moreover, arabinose was found as monomer in concentrations of 0.43 g/L and 0.11 g/L in LSE and PSE, respectively, while the amounts of xylose and glucose monomers were negligible in both systems at zero time (time when the selected temperature was reached). Similarly, Vallejos et al. [22] found that a fraction of

hemicellulose was hydrolyzed from sugarcane bagasse during the time needed to reach 170 °C and de Camargos et al. [23] reported a concentration of arabinose and xylose in oligomeric form of 3.42 g/L in hydrolysate of BSG treated at 80 °C for 10 min which probably were not covalently bonded to the BSG structure.

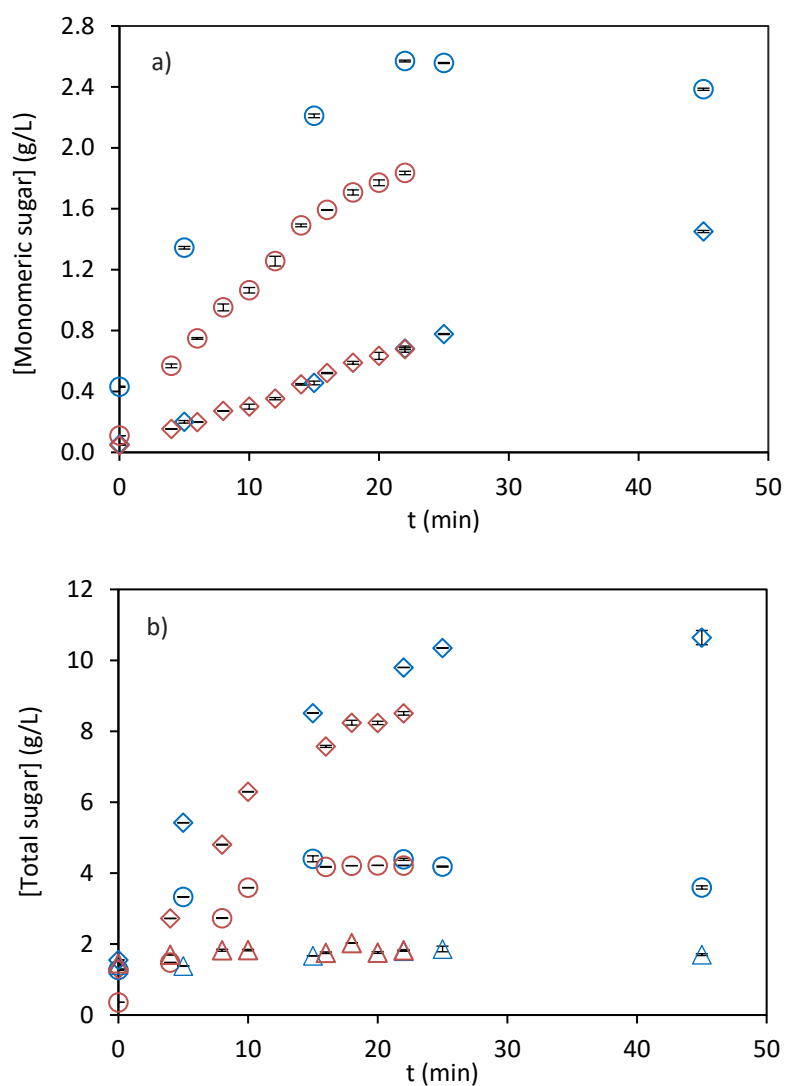


**Figure 4.4.** Sugar concentration in subW extracts released as **(a)** monomers: xylose ( $\diamond \diamond$ ) and arabinose ( $\circ \circ$ ) and **(b)** as total sugars (monomer + oligomer): xylose ( $\diamond \diamond$ ) and arabinose ( $\circ \circ$ ), and as gluco-oligomers ( $\triangle \triangle$ ) along assays performed at laboratory-scale (blue symbols) and at pilot-scale (red symbols).

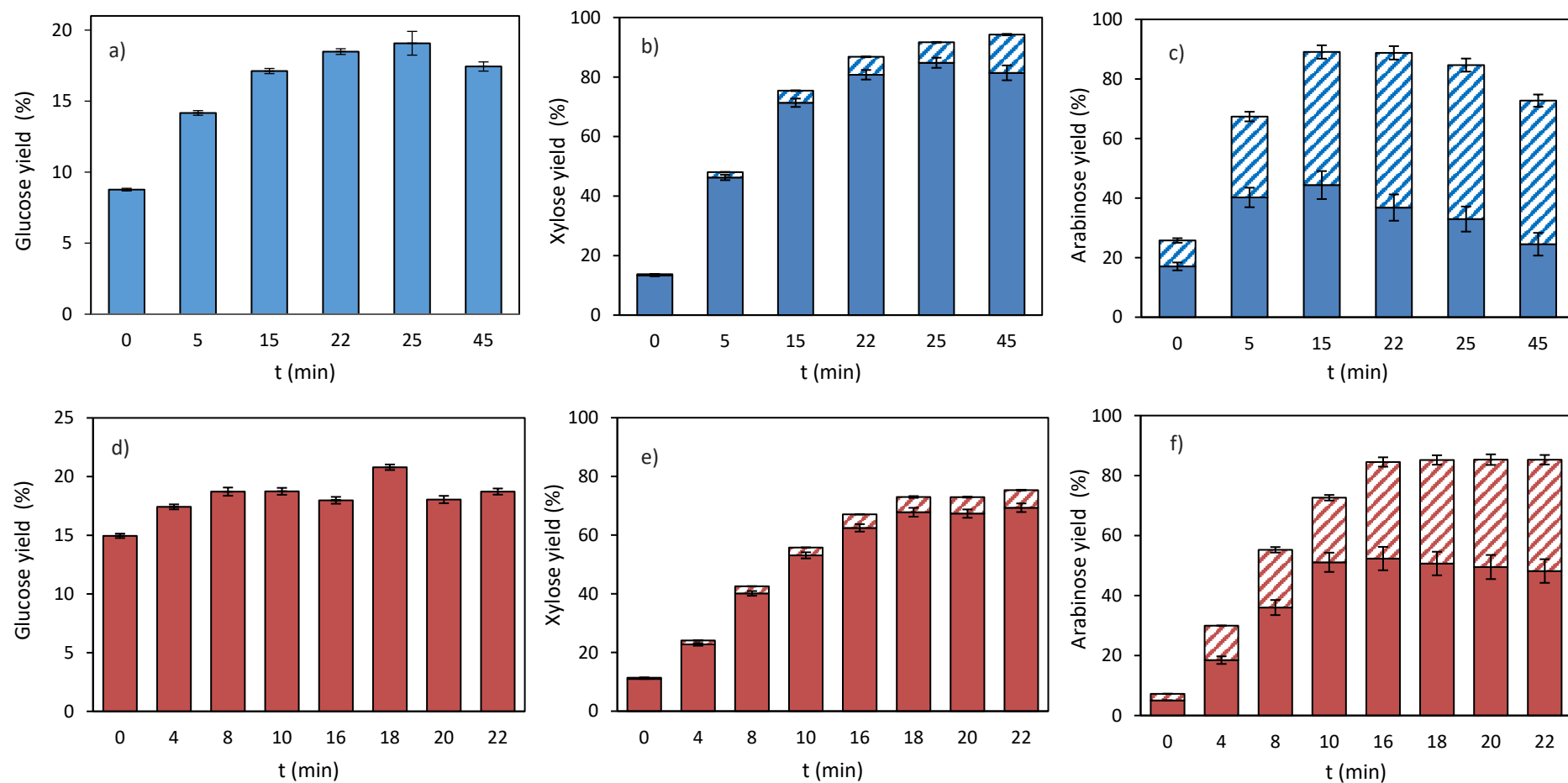


**Figure 4.5.** Sugar yield in subcritical water extracts from BSG collected at the different time intervals as oligomers (■, ■) and monomers (▨, ▨) at laboratory-scale (blue): (a) glucose, (b) xylose and (c) arabinose, and at pilot-scale (red): (d) glucose (e) xylose and (f), arabinose at 170 °C.



As expected, the release of monomeric sugars was lower than oligomeric sugars for both systems, since subW, with no acid addition, produces mostly oligomers with minor amounts of monomers, being necessary a lower pH to hydrolyse most of the hemicellulose into monomers [24]. Monomer arabinose content in PSE increased with time up to 1.83 g/L at the end of the assay (22 min), while a higher concentration of arabinose, 2.57 g/L, was found in LSE at the same time, probably due to the higher pre-heating time needed in this system. After that, arabinose concentration decreased due to the formation of degradation products, mainly furfural. As can be seen in **Figure 4.6a**, furfural concentration increased from 0.29 g/L to 0.73 g/L in the range-time from 22 to 45 min in LSE while slightly lower concentration of furfural, 0.20 g/L, corresponding to 0.43 g/100 g<sub>dry-BSG</sub>, was found in PSE at 22 min. This notwithstanding, the arabinose content in PSE after 22 min of treatment was slightly higher (3.98 g/100 g<sub>dry-BSG</sub>) than the highest value of 3.1 g<sub>arabinose</sub>/100g<sub>BSG</sub> reported by Torres-Mayanga et al. [24] in a semi-continuous reactor, employing a flow rate of 10 mL/min, with 112 g<sub>water</sub>/g<sub>BSG</sub> and 180 °C (log R<sub>0</sub> = 3.32), while higher furfural content was reported by these authors in the hydrolysates, 1.2 g/100 g<sub>BSG</sub>.

Regarding total arabinose, similar amounts were released in both systems, reaching a plateau after 15 and 16 min of treatment in LSE and PSE, respectively (**Figure 4.4b**). Although the total arabinose yield was not significantly different in both systems (p-value < 0.05), the monomer/oligomer ratio was higher in LSE than in PSE. The arabinose yield obtained in monomeric and in oligomeric form in each system can be seen in **Figure 4.5c** and **4.5f**.

The concentration of xylose, both in monomeric and oligomeric form, increased with time in the experiments carried out in both systems, reaching a maximum concentration of total xylose of 10.64 g/L, corresponding to 94% yield, and a monomeric xylose concentration of 1.45 g/L (12.8% yield) in LSE after 45 minutes of treatment. After 22 min of treatment a total xylose yield of 87% was achieved in LSE, being slightly lower in PSE, 75%. Although the highest xylose yield was obtained at the highest time assayed, the concentration of degradation compounds was noticeably higher (**Figure 4.6**). In this period (22-45 min), furfural concentration increased from 0.27 g/L to 0.73 g/L, acetic acid concentration increased from 0.32 to 0.64 g/L and formic acid concentration increased from 0.07 to 0.15 g/L. Therefore, increasing time of treatment resulted in furfural formation as dehydration product of pentoses (C5) sugars and small amounts of HMF from glucose (C6) sugar. Degradation of these compounds produces formic acid, acetic acid and levulinic acid.

These compounds are strong inhibitors of fermentation [26], so, their formation should be avoided if subsequent fermentation of the subW hydrolysates is planned. However, acetic acid was mainly released due to deacetylation of the hemicellulose fraction.

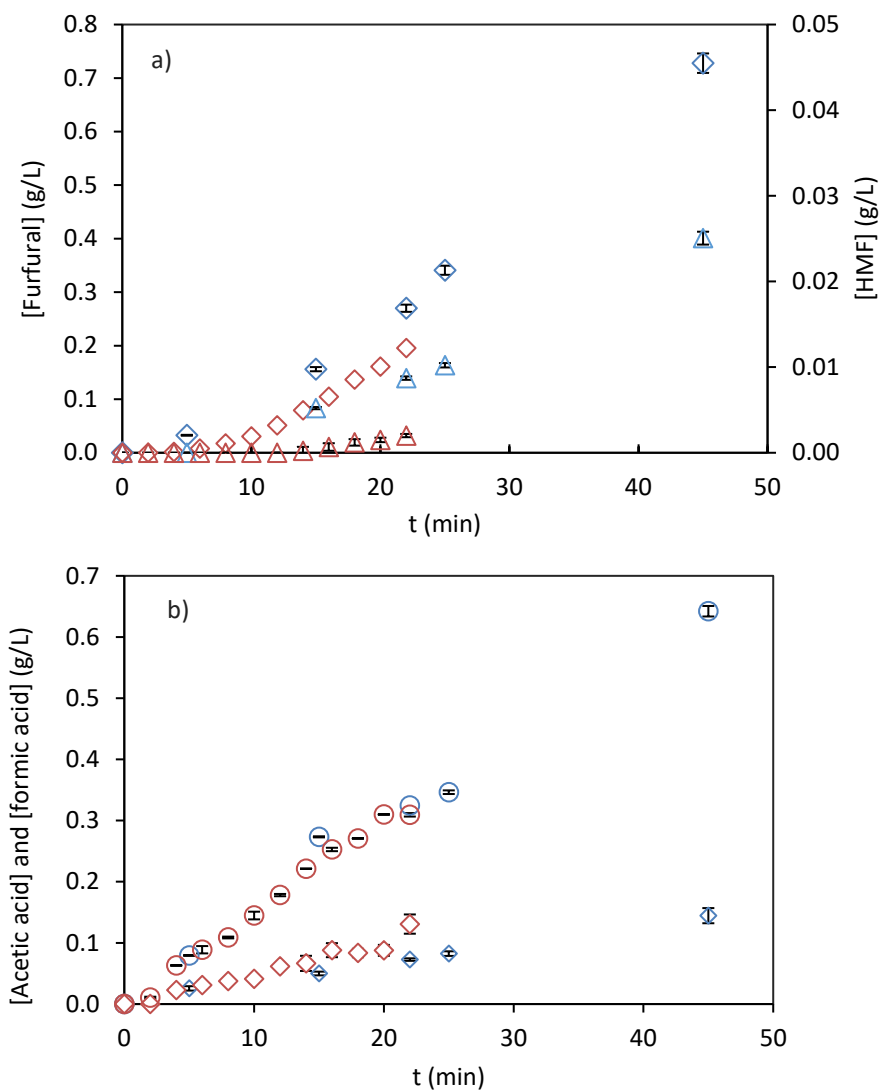


**Figure 4.6.** Concentration of sugar-derived compounds **(a)** furfural ( $\diamond \diamond$ ) and hydroxymethylfurfural, HMF ( $\triangle \triangle$ ) and **(b)** acetic acid ( $\circ \circ$ ) and formic acid ( $\diamond \diamond$ ) in subW extracts collected along assays performed at laboratory-scale (blue symbols) and at pilot-scale (red symbols).

As can be seen in **Figure 4.6b** the formation of acetic acid was similar in laboratory-scale and in pilot-scale during the first 22 min of extraction, suggesting that hemicellulose

deacetylation occurred parallelly in both systems. Notwithstanding, pentosan yield (as total xylose + total arabinose) was higher in laboratory scale (87%) than in pilot-scale (78%). According to Cocero et al. [27], hemicellulose hydrothermal fractionation comprises numerous physical phenomena such as hemicellulose cleaving into decreasing molecular weight oligomers, hemicellulose deacetylation, hemicelluloses dissolution and mass transfer between the solid and the liquid, production of sugars and sugars degradation into furfural or other compounds. The results obtained in this work suggested that production of sugars and sugars degradation into furfural occurred earlier in laboratory-scale than in pilot-scale, probably due to the higher preheating time needed to reach the work temperature. According to Rodríguez et al. [19] the main factor of discrepancies within different hydrothermal studies performed under the same conditions lies in the preheating time, being necessary to study the treatment under rigorous isothermal operation to successful scale up from laboratory to pilot plant. In addition, the pressure was higher in the laboratory assay (5 MPa) than in pilot-scale (2 MPa). Although the pressure has very little influence on the properties of water, as long as the water remains in the liquid state, a recent study about the influence of pressure (2.5 and 10 MPa), on the release of the main components of sugarcane bagasse, during hydrothermal treatment in a continuous flow mode, showed that the monomer xylose content was similar at both pressures considered, while xylooligosaccharides yield was 27% higher operating at 10 MPa [28].

Regarding glucose, it was not detected as monomer in any of the systems. Consequently, small concentrations of HMF were found in the subW extracts, indicating that probably, small amounts of glucose monomer were released and quickly dehydrated to produce HMF. Levulinic acid was not detected in the subW extracts, as it comes from HMF degradation. The concentration of gluco-oligomers was similar in all extracts collected at different times in both systems, reaching a maximum level of 1.86 g/L and 2.03 g/L in LSE (25 min) and in PES (18 min), respectively. Gluco-oligomers were not released from the cellulosic fraction. As can be seen in **Table 6.2**, 26.7% of glucans were non-cellulosic glucans. They mainly came from starch, which is easily hydrolyzed during the subcritical water treatment, while the cellulosic fraction was not hydrolyzed under the subcritical water conditions performed on this work [29]. Consequently, the maximum yields of gluco-oligomers obtained in laboratory and in pilot scale were 19.07% and 20.8%, respectively, (see **Figure 4.5a** and **4.5d**).

The results obtained in this work are consistent with those found in the literature. The value of xylan susceptible to be hydrolysed has been reported for the hydrothermal treatment for different biomass, such as sugarcane bagasse with a high fraction of hydrolysed xylan, 92 % [22] and 85-89 % [30] and sugar maple with percentage of hydrolysed xylan in the range from 78 to 87 % [31]. All these results indicate that a high fraction of the total amount of xylans present in the solid are susceptible to hydrolysis by subW from different biomass.

Likewise, Carvalheiro et al. [10] reported that the release of monomeric xylose from BSG by subW at 170 °C, 60 min and a liquid/solid ratio of 8 g/g, increased with reaction time, whereas the maximal concentration of free arabinose was obtained after 20 min. The amount of solubilized xylan reported by these authors were 84–90% (from 150 to 190 °C) while arabinan was almost completely solubilized. On the other hand, the maximum percentages of soluble saccharides (xylo-oligosaccharides and xylose) recovered from xylan, at the range of temperature studied by these authors were lower (53-72%) and was reached after 20 min of treatment when working at 170 °C, compared to 94% of xylan recovery obtained in the present work at the longest time assayed (45 min). The lower time needed for achieving the maximal xylo-oligosaccharides yield at 170 °C, reported by these authors, may be explained by the high initial concentration of xylo-oligomers (11.08 g/L) in the hydrolysates, suggesting that the hydrolysis of the hemicellulose started during the higher preheating time employed in that work (32-44 min). Moreover, the higher yield of total xylose obtained in the present work, could be explained by the better heat and mass transfer achieved by operating at higher liquid/solid ratio and by reducing the biomass particle size by milling.

#### **3.4. Protein fraction extraction/hydrolysis**

Protein content was determined as the total nitrogen content in subW extracts per 100 g of dry BSG, after applying the nitrogen factor 6.25. The kinetics of protein extraction/hydrolysis obtained at laboratory and pilot scale have been represented in **Figure 4.7**, together with protein yield. At the beginning of the isothermal treatment,  $2.10 \pm 0.03$  and  $5.33 \pm 0.05$  g/100 g<sub>dry-BSG</sub> of protein were found in PSE and LSE, respectively. As mentioned above, BSG water-soluble protein accounted for 5.53 % (w/w). Thus, the results indicated that almost all the soluble protein fraction was extracted during the

preheating time at laboratory-scale assay, while a fraction of water-soluble protein remained unextracted at time 0 min when the assay was performed at pilot-scale.

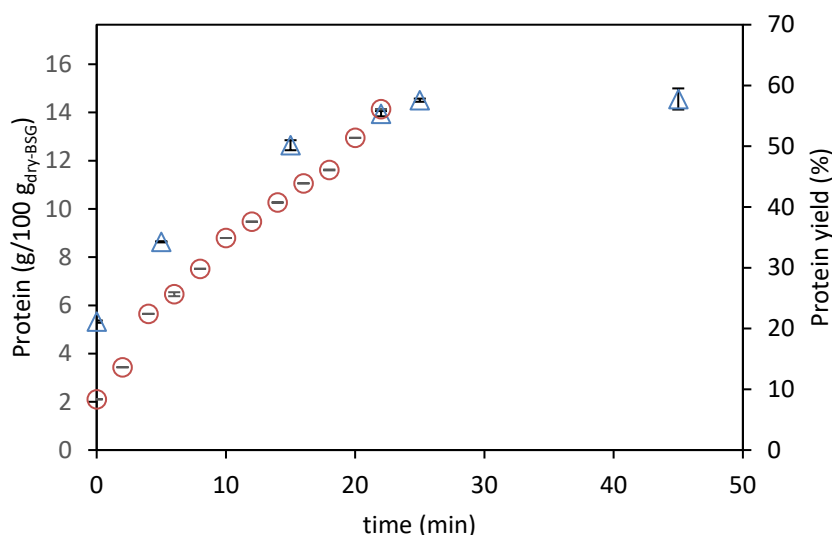


**Figure 4.7.** Protein content, expressed as g per 100 g of dry BSG and protein yield in subW extracts obtained along time at lab-scale (△) and at pilot-scale (○).

As can be seen in the pilot-scale protein curve, the rate of released protein increased after 4 min of isothermal treatment, suggesting that at this moment, protein hydrolysis from BSG matrix was happening. After 22 min of treatment, protein content in LSE and PSE were 13.95 and 14.14 g/100 g<sub>dry-BSG</sub>, respectively, corresponding to protein yields of 63 ± 2% and 64 ± 2%, respectively. Despite these minor differences in the curves of the release of protein fraction between both systems, there was no significant difference between protein yield after 22 min of treatment between the two systems (p-value < 0.05). Therefore, the release of protein in subW showed great reproducibility at different scales.

Furthermore, when increased time from 22 min to 45 min at lab-scale, the value of protein yield (66 ± 3%) was not statistically different than that obtained at 22 min (p-value < 0.05), suggesting a temperature limitation of the protein release. According to Lamp et al. [32], this fact may be due to two reasons: (1) a limitation of the protein solubility due to the subW polarity, which remains constant at each temperature, while a temperature increase, associated to a decrease in the subW polarity, could lead to an increase in protein solubility, and (2) higher activity energies of hydrolysis for some peptide bonds, which require elevated temperatures to be broken.

Higher protein yield (78%) was achieved from BSG by subW extraction at 185 °C in a semi-continuous fixed-bed reactor in a previous work [12]. However, protein concentration in subW extracts was greater in this work (6.5 g/L) than that obtained when operated in semi-continuous mode at 185 °C and a flowrate of 4 ml/min, accumulated after 4 h of treatment (2.8 g/L). Furthermore, the protein yield reached in this work was higher than those obtained by other hydrolytic methods such as enzymatic hydrolysis (47.1%, 6% protease, 4 h), alkaline hydrolysis (50.5%, 0.1 M NaOH, 4 h) [12] or ultrasound assisted extraction (UAE) (46.6%, water, 50 °C, 30 min) [2]. The results obtained in this work were in good agreement with those reported in the literature. For instance, Lamp at al. [32] found that protein solubilization started at 89 °C, achieving the highest protein yield in the hydrolysate (75%) at 170 °C and 20 min, when studying the protein recovery from the insoluble fraction of stillage by subW at different temperatures and times (110–210 °C for 10–90 min).

Likewise, a minor fraction of the protein content was hydrolysed as free amino acids in the subW extracts. Free amino acids in subW extracts were determined by the sum of individual free amino acids measured by gas chromatography, as has been plotted in **Figure 4.8**.

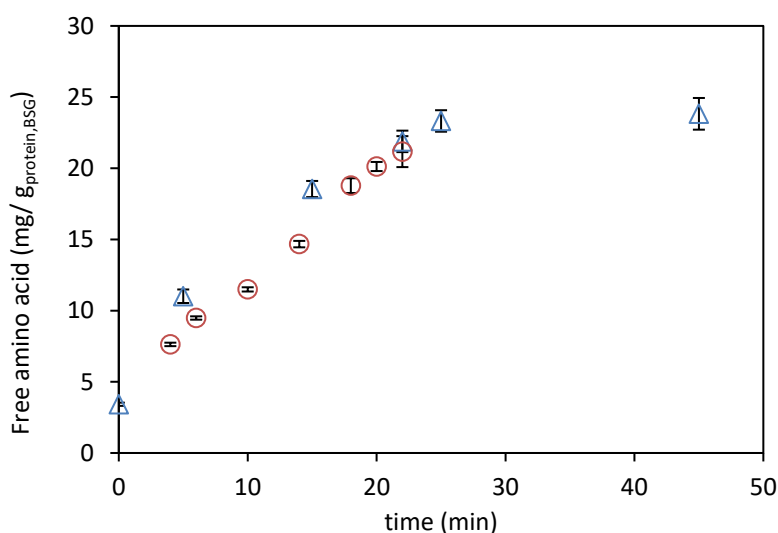


**Figure 4.8.** Free amino acids, expressed as mg per g of protein in dry BSG, in subcritical water extracts obtained along time at lab-scale (△) and pilot-scale (○).

The amount of free amino acids presented in the subW extracts obtained by both systems, around 21 mg/g<sub>protein, BSG</sub>, after 22 min of treatment, was not significantly different. After that, the concentration of free amino acids in LSE slightly increased up to 23.8 ± 0.5 mg/g<sub>protein, BSG</sub> at 45 min, although the difference of this value with that obtained at 22 min was not statistically significant ( $p < .05$ ).

The release curves for individual amino acids by subW at lab and pilot-scale systems have been represented in **Figure 4.9**, grouped into non-polar (**4.9a** and **4.9b**) and polar amino acids (**4.9c** and **4.9d**). The concentration of non-polar amino acids in PSE and LSE increased or remained constant when increasing time. Conversely, the degradation of some polar amino acids was observed in the time range studied in this work. Specifically, glutamic acid showed a concentration decrease after 5 min of treatment in both systems. Glutamic acid has been reported as one of the most labile amino acids since it lactamizes with temperature to form pyroglutamic acid [33]. In general, according to Lamp et al. [32], the constant rate of degradation for the polar amino acids is about one order of magnitude higher than for the non-polar amino acids, taking place at 170 °C for almost all polar amino acids. Furthermore, polar amino acids present a high tendency to undergo Maillard reactions with carbonyl groups or reducing carbohydrates that have been released during subW treatment.

**Table 4.3** shows free amino acid yields as the ratio of individual amino acids in the extracts and in the raw material. Free amino acids yield obtained in this work, around 2.1% after 22 min of extraction in both systems, were lower than those obtained from BSG in a semi-continuous reactor, accumulated after 4 h of subW treatment, at different temperatures (125-185 °C), which varied from 2.9% at 125 °C to the maximum level, 5.5%, obtained at 160 °C [12]. Aspartic acid showed by far the highest yield in both systems, 19% in laboratory-scale and 21% in pilot-scale after 22 min of treatment, exhibiting a decrease until 19% when reaction time increased up to 45 min.

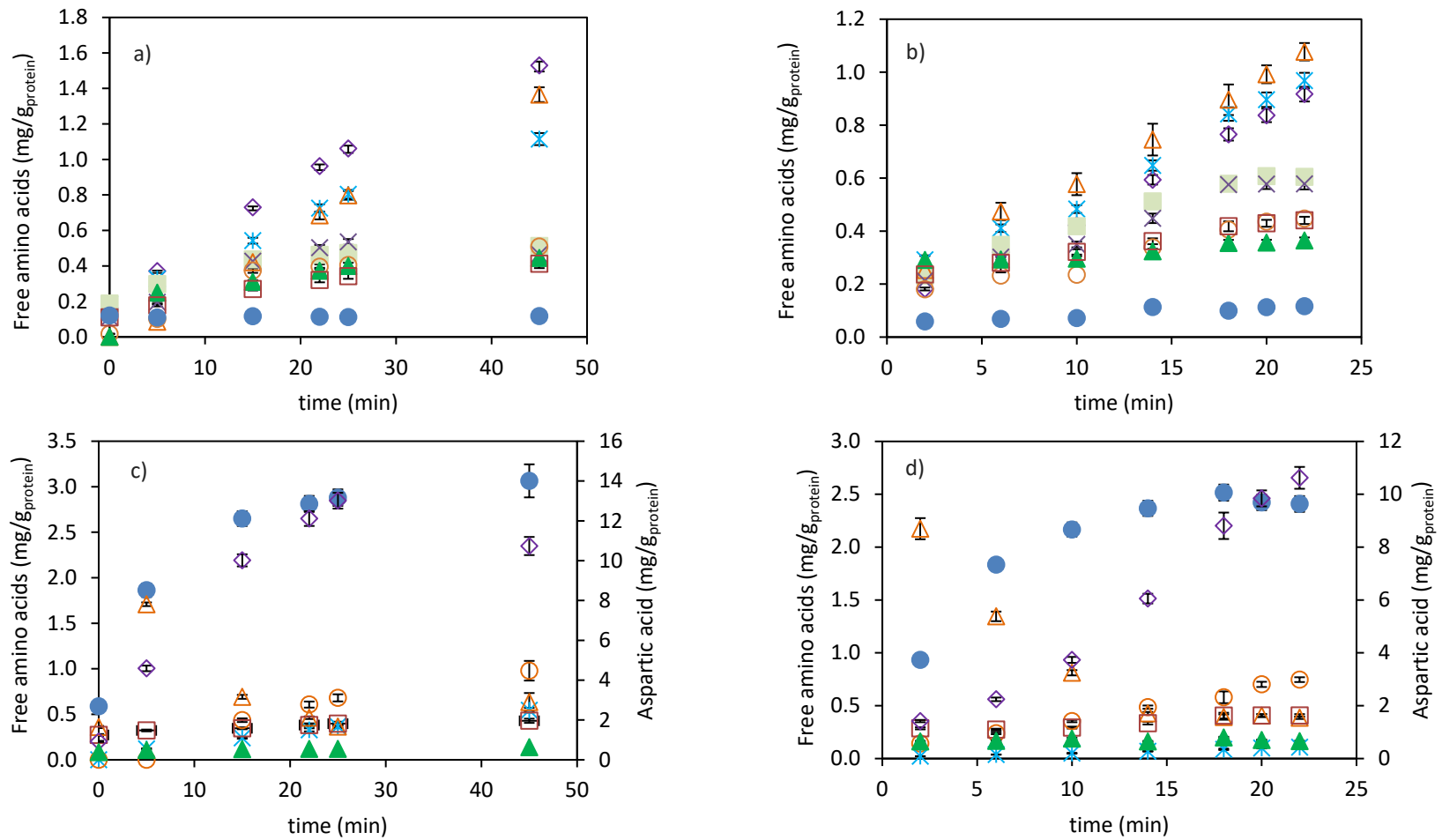


**Figure 4.9.** Accumulative formation of individual amino acids. Non-polar amino acids **(a)** at lab-scale **(b)** at pilot-scale (\* alanine,  $\diamond$  glycine,  $\triangle$  valine,  $\times$  leucine,  $\circ$  isoleucine,  $\blacksquare$  proline,  $\square$  phenylalanine,  $\blacktriangle$  methionine and  $\bullet$  tryptophan). Polar amino acids **(c)** at lab-scale **(d)** at pilot-scale ( $\bullet$  lysine,  $\circ$  serine,  $\triangle$  glutamic acid,  $\square$  histidine,  $\diamond$  aspartic acid,  $*$  threonine and  $\blacktriangle$  tyrosine). (Experimental data includes standard deviations,  $n = 3$  technical replicates).



**Table 4.3.** Amino acid profile of BSG and free amino acid yields in the subW extracts obtained in pilot-scale at 22 min and in lab-scale at 22 and 45 min, expressed as mg aa/gprotein and percent yield as the ratio of individual amino acids in the extracts and in the raw material.

Amino acid	BSG		Pilot-Scale SWE, 22 min		Lab-Scale SWE 22 min		Lab-Scale SWE 45 min	
	mg/g <sub>protein</sub>		mg/g <sub>protein</sub>	Yield (%)	mg/g <sub>protein</sub>	Yield (%)	mg/g <sub>protein</sub>	Yield (%)
Alanine	61 ± 2		0.97 ± 0.03 <sup>b</sup>	1.59 ± 0.07	0.72 ± 0.02 <sup>a</sup>	1.19 ± 0.05	1.11 ± 0.03 <sup>c</sup>	1.83 ± 0.08
Aspartic acid	57 ± 2		10.6 ± 0.4 <sup>a</sup>	19 ± 1	12.1 ± 0.4 <sup>b</sup>	21 ± 1	10.7 ± 0.5 <sup>a</sup>	19 ± 1
Glutamic acid	97 ± 3		0.41 ± 0.01 <sup>a</sup>	0.42 ± 0.02	0.46 ± 0.01 <sup>a,b</sup>	0.48 ± 0.02	0.63 ± 0.10 <sup>b</sup>	0.65 ± 0.11
Glycine	48 ± 1		0.92 ± 0.03 <sup>a</sup>	1.92 ± 0.08	0.96 ± 0.03 <sup>a</sup>	2.01 ± 0.09	1.53 ± 0.05 <sup>b</sup>	3.19 ± 0.14
Histidine <sup>e</sup>	30 ± 1		0.41 ± 0.01 <sup>a</sup>	1.37 ± 0.07	0.38 ± 0.02 <sup>a</sup>	1.28 ± 0.08	0.43 ± 0.02 <sup>a</sup>	1.44 ± 0.10
Hydroxylysine	6.4 ± 2.1		n.d.	-	n.d.	-	n.d.	-
Hydroxyproline	7.8 ± 0.2		n.d.	-	n.d.	-	0.34 ± 0.01 <sup>a</sup>	4.3 ± 0.2
Isoleucine <sup>e</sup>	76 ± 2		0.45 ± 0.02 <sup>a</sup>	0.59 ± 0.03	0.40 ± 0.01 <sup>a</sup>	0.52 ± 0.02	0.51 ± 0.02 <sup>b</sup>	0.67 ± 0.03
Leucine <sup>e</sup>	87 ± 3		0.58 ± 0.02 <sup>b</sup>	0.67 ± 0.03	0.50 ± 0.01 <sup>a</sup>	0.58 ± 0.03	0.47 ± 0.02 <sup>a</sup>	0.54 ± 0.03
Lysine <sup>e</sup>	67 ± 2		2.41 ± 0.07 <sup>a</sup>	3.6 ± 0.2	2.81 ± 0.03 <sup>b</sup>	4.2 ± 0.2	3.1 ± 0.2 <sup>b</sup>	4.6 ± 0.31
Methionine <sup>e</sup>	25.3 ± 0.8		0.36 ± 0.01 <sup>a</sup>	1.4 ± 0.06	0.37 ± 0.02 <sup>a</sup>	1.47 ± 0.08	0.44 ± 0.01 <sup>b</sup>	1.76 ± 0.08
Phenylalanine <sup>e</sup>	76 ± 3		0.44 ± 0.01 <sup>b</sup>	0.58 ± 0.02	0.32 ± 0.01 <sup>a</sup>	0.42 ± 0.02	0.41 ± 0.02 <sup>b</sup>	0.54 ± 0.04
Proline	137 ± 4		0.60 ± 0.02 <sup>c</sup>	0.44 ± 0.02	0.46 ± 0.02 <sup>a</sup>	0.34 ± 0.02	0.51 ± 0.02 <sup>b</sup>	0.38 ± 0.02
Serine	22.1 ± 0.7		0.75 ± 0.02 <sup>b</sup>	3.4 ± 0.2	0.61 ± 0.04 <sup>a</sup>	2.7 ± 0.18	1.0 ± 0.1 <sup>c</sup>	4.4 ± 0.51
Threonine <sup>e</sup>	30 ± 1		0.43 ± 0.01 <sup>b</sup>	1.4 ± 0.06	0.33 ± 0.02 <sup>a</sup>	1.08 ± 0.07	0.54 ± 0.03 <sup>c</sup>	1.79 ± 0.10
Tryptophan <sup>e</sup>	11.2 ± 0.3		0.12 ± 0.02 <sup>a</sup>	1.0 ± 0.05	0.113 ± 0.004 <sup>a</sup>	1.01 ± 0.04	0.12 ± 0.01 <sup>a</sup>	1.04 ± 0.11
Tyrosine	24 ± 1		0.66 ± 0.02 <sup>b</sup>	2.8 ± 0.1	0.54 ± 0.02 <sup>a</sup>	2.3 ± 0.32	0.63 ± 0.04 <sup>b</sup>	2.7 ± 0.20
Valine <sup>e</sup>	141 ± 4		1.08 ± 0.03 <sup>b</sup>	0.76 ± 0.03	0.68 ± 0.02 <sup>a</sup>	0.48 ± 0.02	1.36 ± 0.04 <sup>c</sup>	0.97 ± 0.04
TAA	1002 ± 9		21.2 ± 0.4 <sup>a</sup>	2.11 ± 0.05	21.8 ± 0.4 <sup>a</sup>	2.17 ± 0.04	23.8 ± 0.5 <sup>a</sup>	2.38 ± 0.06
TEAA	543 ± 7		6.3 ± 0.1 <sup>a</sup>	1.15 ± 0.02	5.9 ± 0.1 <sup>a</sup>	1.09 ± 0.02	7.4 ± 0.2 <sup>a</sup>	1.35 ± 0.04
TEAA/TAA (%)	54.2 ± 0.8 <sup>b</sup>		30 ± 1 <sup>a</sup>		27.1 ± 0.5 <sup>a</sup>		31 ± 1 <sup>a</sup>	

n.d., not detected. TAA, total amino acids. TEAA, total essential amino acids. TEAA/TAA: ratio of essential amino acids to total amino acids. Values are expressed as mean ± standard deviation from triplicate determination. Values with different letters in each column are significantly different when applying the Fisher's least significant differences (LSD) method ( $p \leq .05$ ) for mg aa/g<sub>protein</sub> and yield values. Aspartic acid includes asparagine. Glutamic acid includes glutamine.

### 3.5. Polyphenolic compounds

#### 3.5.1. Total polyphenol content in subW extracts

Total phenolic content (TPC) in LSE and PSE was determined by the Folin-Ciocalteu method and has been represented at different treatment times in **Figure 4.10**.

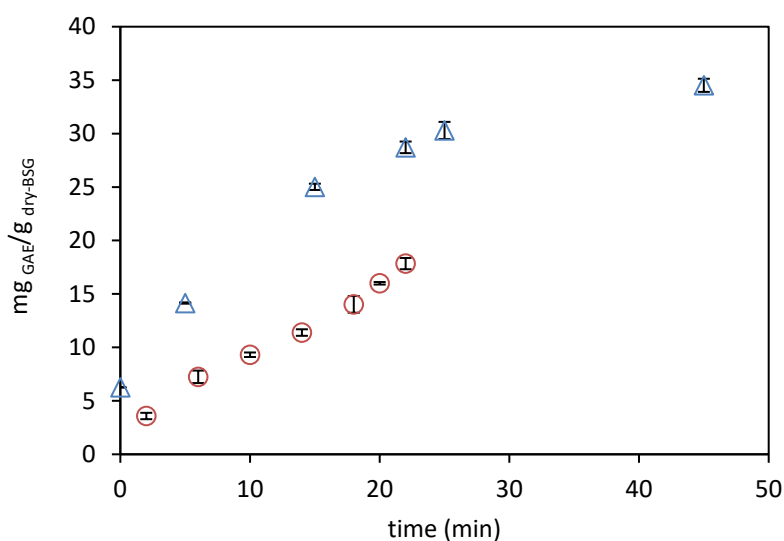


**Figure 4.10.** Total phenolic content, expressed as mg of GAE per g of dry BSG in lab-scale extracts (△) and pilot-scale extracts (○), released from BSG, along time

The difference between both systems was noticeable. In the lab-scale system, the initial phenolic content was  $6.27 \text{ mg}_{\text{GAE}}/\text{g}_{\text{dry-BSG}}$  and increased with time up to a TPC of  $34 \text{ mg}_{\text{GAE}}/\text{g}_{\text{dry-BSG}}$  after 45 min of isothermal treatment. This TPC in LSE was 38% higher than in PSE, although an increase in the extraction rate after 18 min of treatment was observed in the TPC kinetic curve obtained at pilot-scale, suggesting that the higher preheating time at lab-scale determined higher TPC at the same isothermal time of treatment in both systems. In a previous work about the release of phenolic compounds from BSG in a semi-continuous subW extractor, in the temperature range from  $125 \text{ }^{\circ}\text{C}$  to  $185 \text{ }^{\circ}\text{C}$  [12], it was found that  $23.01 \text{ mg}_{\text{GAE}}/\text{g}_{\text{dry-BSG}}$  and  $33.03 \text{ mg}_{\text{GAE}}/\text{g}_{\text{dry-BSG}}$  were obtained by the Folin–Ciocalteu method, at  $160 \text{ }^{\circ}\text{C}$  and  $185 \text{ }^{\circ}\text{C}$ , accumulated after 240 min of subW treatment, at a flow rate of 4 ml/min. Thus, the TPC in LSE after 45 min of treatment was comparable with

the highest TPC obtained in that study. In this previous study, higher release of hydroxycinnamic acids was found at 160 °C than at 185 °C. According to Fabian et al. [34], the optimal temperature for the extraction of coumaric and ferulic acids from defatted rice bran was 175 °C, decreasing at higher temperatures because thermal decomposition of these compounds started at around 172 °C. In this work, p-coumaric acid, ferulic acid and vanillin were found in both PSE and LSE and the kinetic curves of the release of these compounds has been represented in **Figure 4.11**.

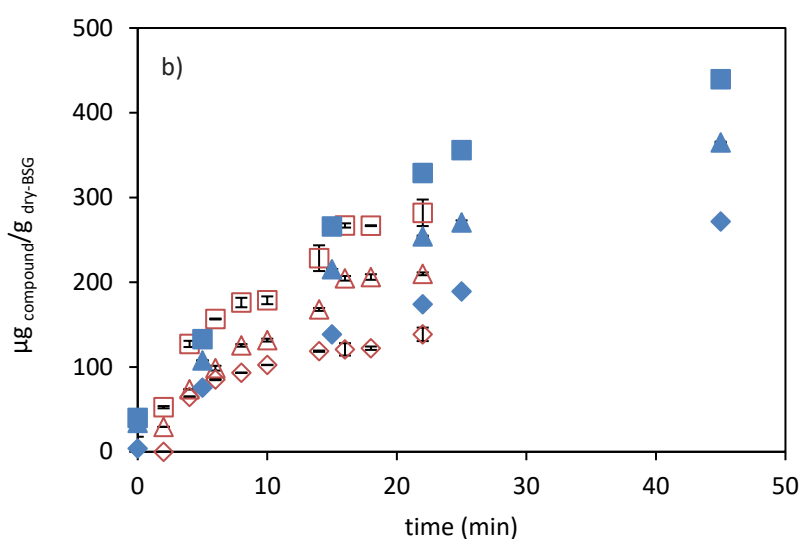


**Figure 4.11.** Accumulative individual phenolic compounds released from BSG at pilot-scale (red open symbols) and lab-scale (blue filled symbols): p-coumaric acid ( $\diamond$   $\blacklozenge$ ), ferulic acid ( $\triangle$   $\blacktriangle$ ) and vanillin ( $\square$   $\blacksquare$ ).

The same trend than for TPC was observed for the release of the identified phenolic compounds, the concentration of these compounds increased along time in both systems, being higher in LSE than in PSE, even after 22 min of treatment. At this moment, the amounts of p-coumaric acid, ferulic acid and vanillin were 20%, 17% and 14% higher in LSE than in PSE, respectively. The maximum concentration of p-coumaric acid, ferulic acid and vanillin were  $272 \pm 1 \mu\text{g/g}_{\text{dry-BSG}}$ ,  $365.1 \pm 0.9 \mu\text{g/g}_{\text{dry-BSG}}$  and  $439.7 \pm 0.4 \mu\text{g/g}_{\text{dry-BSG}}$ , respectively achieved in LSE at the highest time studied, 45 min. Moreover, other phenolic compounds were also identified in LSE after 45 min of treatment, such as protocatechuic

aldehyde ( $65 \pm 3 \mu\text{g/g}_{\text{dry-BSG}}$ ), catechin ( $72 \pm 3 \mu\text{g/g}_{\text{dry-BSG}}$ ), vanillic acid ( $25.0 \pm 0.4 \mu\text{g/g}_{\text{dry-BSG}}$ ) and 4-vinylguaicol ( $90 \pm 2 \mu\text{g/g}_{\text{dry-BSG}}$ ), coming the last one from the thermal decarboxylation of ferulic acid [35]. Therefore, the total amount of phenolic compounds identified in LSE after 45 min of treatment was  $1.38 \text{ mg/g}_{\text{dry-BSG}}$ , a value remarkable lower than  $34 \text{ mg}_{\text{GAE}}/\text{g}_{\text{dry-BSG}}$ , as determined by the Folin-Ciocalteu assay. The great difference between these values could be explained by different facts. On the one hand, some individual phenolic compounds could not be properly identified by our system due to lack of standards. For instance, together with phenolic acids, several isomeric ferulate dehydromers and one dehydrotrimer have been reported as components of the BSG matrix [36]. On the other hand, compounds related to Maillard reactions, such as protein-carbohydrate conjugates, melanoidins, and heterocyclic compounds may interfere in the TPC determination by the Folin-Ciocalteu assay, being possible to consider HMF and furfural as indicators of these reactions [12]. At this regard, it is worth recalling that lower amount of furfural was found in PSE than in LSE at 22 min, growing up to  $0.73 \text{ g/L}$  after 45 min.

### 3.6. Organic carbon in the subcritical water extracts

The total organic carbon (TOC) present in the subW extracts obtained at laboratory and pilot scales has been plotted in **Figure 4.12**. TOC extraction yield increased with time; although, after 25 min of isothermal extraction at lab-scale, a plateau was reached. The same trend in the release of TOC was observed for the release of other biocompounds, a higher initial value in the LSE than in PSE at the beginning of isothermal treatment due to the release of some compounds from milled BSG that were water-soluble or easily hydrolysable during the pre-heating time. This behaviour suggests that these compounds were not linked to the cell-wall polysaccharide matrix. Specifically, the amount of TOC at time 0 in LSE, 6.21%, was in good agreement with TOC in water extractives 6.08% in a dry weight basis. The extraction rates of both systems were evaluated in each lineal range, from 0 to 25 min at lab-scale and for all time range studied at pilot-scale (0-22 min). There were not statistically significant differences among the slopes at the 90% or higher confidence level, while there were statistically significant differences among the intercepts at the 99% confidence level. Therefore, the difference between TOC in LSE and PSE at the same isothermal time (22 min), accounted of  $6.3 \text{ g}/100 \text{ g}_{\text{dry-BSG}}$ , could be explained as a delay in

the pilot-scale assay as the total time that solids were in contact with water was lower considering the higher pre-heating time employed at lab-scale.

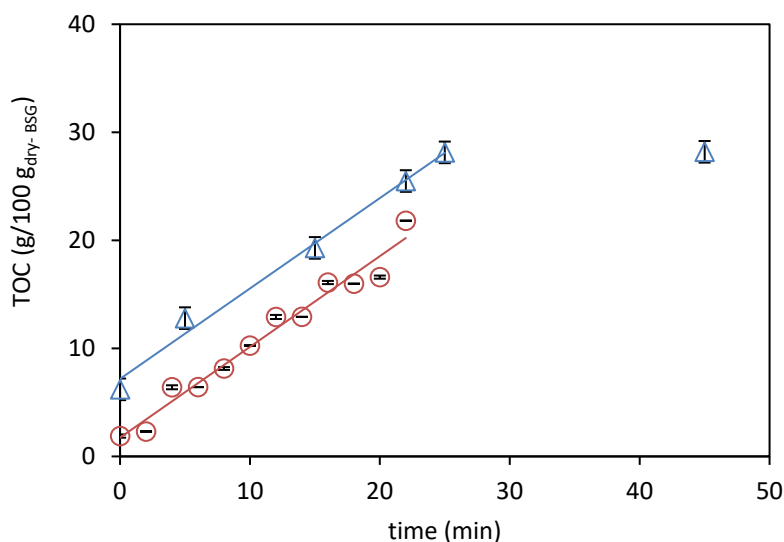


**Figure 4.12.** TOC content in subcritical water extracts collected in subcritical water extracts obtained along time at lab-scale (△) and pilot-scale (○). Lines represent the extraction/hydrolysis rate of TOC in the lineal range at lab-scale:

$$\text{TOC} = 0.8365 \text{ time} + 7.178, R^2 = 0.9902 \text{ and at pilot-scale:}$$

$$\text{TOC} = 0.8397 \text{ time} + 7.1740, R^2 = 0.9696$$

### 3.7. Solid residue after subW treatment

The solid residue obtained after the subcritical water treatment was characterized in the same way as the initial feedstock, according to NREL protocols. The characterization of this solid is important for two reasons. On the one hand, it allows the evaluation of the material balances of the different components present in the biomass that have been partially hydrolysed. In addition, the characterization of these solids is fundamental, as they may constitute the feed for a second stage of biomass valorization, for instance bioconversion of cellulose into ethanol by saccharification and fermentation. The results of these characterizations are shown in **Table 4.4**.

**Table 4.4.** Chemical composition of solid residues remained after subW treatment of BSG performed at lab-scale (LSWR) and at pilot-scale (PSWR)

Compound	LSWR (% dwb)	PSWR (% dwb)
Glucans	34.7 ± 0.6 <sup>b</sup>	30.2 ± 0.4 <sup>a</sup>
Starch	Not determined	0.22 ± 0.02
Cellulose	34.7 ± 0.6 <sup>b</sup>	30.0 ± 0.4 <sup>a</sup>
Hemicellulose	2.31 ± 0.48 <sup>a</sup>	14.9 ± 0.3 <sup>b</sup>
Xylan	2.31 ± 0.06 <sup>a</sup>	11.7 ± 0.2 <sup>b</sup>
Arabinan	Not detected	2.7 ± 0.2
Acetate	Not detected	0.56 ± 0.02
Lignin	47.1 ± 0.4 <sup>b</sup>	40 ± 1 <sup>a</sup>
Acid insoluble lignin	42.7 ± 0.4 <sup>b</sup>	35 ± 1 <sup>a</sup>
Acid soluble lignin	4.4 ± 0.1 <sup>a</sup>	5.6 ± 0.1 <sup>b</sup>
Protein	12.3 ± 0.1 <sup>a</sup>	16.2 ± 0.7 <sup>b</sup>
Ash	2.71 ± 0.01 <sup>a</sup>	2.77 ± 0.09 <sup>a</sup>
Yield (% dwb)	56.5	Not determined

Values are expressed as mean ± standard deviation from triplicate determination. Values with different letters in each row are significantly different when applying the Fisher's least significant differences (LSD) method at p-value ≤ 0.05.

After subW treatment at lab-scale, 43.5% of solids were recovered, whereas the amount of solid that remained after the subW treatment at pilot plant scale could not be properly determined, due to the difficulty of a complete recovery. The total extraction yield at lab-scale was 56.5%, evaluated according to Equation 4.6:

$$Yield (\%) = \frac{W - W_i}{W} \cdot 100 \quad [4.6]$$

where  $w$  is the weight of the dry BSG placed into the reactor and  $w_i$  is the weight of the washed and dry solid residue remaining after the subW treatment.

In the two systems studied, the concentration of glucans increased in the residue with respect to the composition of the initial feedstock, due to the solubilization of other components and the fact that cellulose is not hydrolysed in subcritical water, as discussed above. The presence of glucose in the hydrolysates is derived mainly from the solubilization

of starch, as can be seen in the reduction of the starch content from 4.11% in BSG to 0.22% determined in PSWR. In addition, an increase of insoluble lignin was observed in both residues, which confirmed that this fraction of the biomass was not released under subW treatment. The insoluble lignin-soluble lignin ratio is a parameter indicative of the effects of heat treatment in BSG [23]. This ratio was 3.3 and 2.1-fold higher in the residue obtained in the laboratory and in the pilot plant respectively, compared to the ratio in the original BSG, suggesting that the heat treatment caused changes in the chemical structure of lignin. The increase in the proportion of glucans and insoluble lignin in the residues was more pronounced in the residue from the laboratory assay, due to the higher severity conditions employed in this experiment (see Section 3.2). When subW treatment was performed at lab-scale, almost total solubilization of the hemicellulose was observed, remaining a small proportion of xylans in the residue,  $2.31 \pm 0.06\%$ , while arabinans and acetyl groups were not detected. The cellulose/hemicellulose ratio in the original BSG was 0.44, while after subW hydrolysis this ratio increased up to 15 and 2 in LSWR and PSWR, respectively. Furthermore, the protein content was reduced from  $22.1 \pm 0.1\%$ , initially present in the BSG, to  $12.3 \pm 0.1\%$  and  $15.7 \pm 0.1\%$  in LSWR and PSWR, respectively, due to the protein solubilization by the subW treatment.

The elemental composition of the solid residues after extraction was collected in **Table 4.5**. The carbon content (C) in LSWR and PSWR was higher than in BSG, while no significant differences were found between the values obtained in both residues. The oxygen content (O) was not affected by the subW treatment; however, the molar ratio O:C was significantly lower after subW at lab-scale than in feedstock, which is associated with a decrease in the amount of OH, carboxyl (COOH) and carbonyl (C=O) groups. Additionally, the decrease of both, nitrogen content (N) and molar ratio N:C in the solid was observed when increased the severity of the treatment.

Furthermore, the estimated higher heating value (HHV) calculated for LSWR and PSWR, although slightly higher than the calculated for BSG, differences between such values were found not to be significant, neither between LSWR and PSWR HHV values nor between PSWR and BSG HHV values.

**Table 4.5.** Elemental analysis, ash content, H:C, O:C and N:C molar ratios and estimated heating value (HHV) of BSG and the solid residues remained after subW treatment performed at lab-scale (LSWR) and at pilot-scale (PSWR)

Compound	BSG	LSWR	PSWR
C (% dwb)	49.2 ± 0.5 <sup>a</sup>	52 ± 1 <sup>b</sup>	51.3 ± 0.1 <sup>b</sup>
H (% dwb)	6.64 ± 0.01 <sup>a</sup>	6.9 ± 0.1 <sup>b</sup>	6.66 ± 0.06 <sup>a,b</sup>
N (% dwb)	3.77 ± 0.01 <sup>c</sup>	1.97 ± 0.02 <sup>a</sup>	2.8 ± 0.1 <sup>b</sup>
O (% dwb)	37.0 ± 0.6 <sup>a</sup>	36 ± 1 <sup>a</sup>	36.4 ± 0.2 <sup>a</sup>
Ash (% dwb)	3.32 ± 0.06 <sup>b</sup>	2.71 ± 0.02 <sup>a</sup>	2.77 ± 0.09 <sup>a</sup>
H:C	1.62 ± 0.02 <sup>a</sup>	1.57 ± 0.04 <sup>a</sup>	1.56 ± 0.01 <sup>a</sup>
O:C	0.57 ± 0.01 <sup>b</sup>	0.52 ± 0.02 <sup>a</sup>	0.532 ± 0.003 <sup>a,b</sup>
N:C	0.066 ± 0.002 <sup>c</sup>	0.0323 ± 0.0007 <sup>a</sup>	0.047 ± 0.002 <sup>b</sup>
HHV (MJ/kg)	20.2 ± 0.3 <sup>a</sup>	21.5 ± 0.7 <sup>b</sup>	21.1 ± 0.2 <sup>a,b</sup>

Values are expressed as mean ± standard deviation from triplicate determination. Values with different letters in each column are significantly different when applying the Fisher's least significant differences (LSD) method ( $p$ -value ≤ .05).

**Table 4.6.** shows the mass balance obtained for the different components of BSG evaluated in this work after the subW treatment performed at lab scale. The feed mass,  $m_{\text{feed}}$ , of each compound has been calculated from the chemical composition of the BSG and the initial amount of BSG charged into the reactor (**Table 4.2**). The outlet mass of each component was evaluated considering the remaining amount in the solid residue after cooling the extractor and washing the solid (**Tables 4.4** and **4.5**) and the amount of each compound present in the LSE after 45 min of isothermal treatment. The mass balance for each compound was calculated according to Equation 4.7:

$$\text{Mass balance, MB (\%)} = \frac{\text{Compound}_{\text{outlet}}(g)}{\text{Compound}_{\text{feed}}(g)} \cdot 100 \quad [4.7]$$



**Table 4.6.** Mass balance of subW treatment performed at lab-scale from 100 g of dry BSG.

Compound	$m_{\text{feed}}$ (g)	$m_{\text{outlet}}$ (g)	MB (%)
Solid	100	43.5	-
Glucan	19.1 ± 0.2	18.4 ± 0.3	96 ± 1
Xylan	21.6 ± 0.4	21.4 ± 0.4	99 ± 2
Arabinan	9.5 ± 0.4	6.88 ± 0.09	73 ± 3
Acetic acid <sup>1</sup>	0.95 ± 0.04	1.4 ± 0.03	148 ± 6
Lignin	20.8 ± 0.2	20.5 ± 0.2	99 ± 1
AIL	15.5 ± 0.1	18.6 ± 0.2	120
ASL	5.3 ± 0.2	1.93 ± 0.06	36
C	49.2 ± 0.5	51.0 ± 0.9	104 ± 1
N	3.53 ± 0.08	3.19 ± 0.07	90 ± 2

“AIL” and “ASL” stand for acid insoluble lignin and acid soluble lignin, respectively. Values are expressed as mean ± standard deviation from triplicate determination. <sup>(1)</sup> Acetic acid mass in feed was calculated from acetyl groups present in the BSG.

In general, mass balances present deviations lower than 10% that can be considered acceptable mass balance errors for hydrothermal treatments of a complex matrix such as BSG, specially, considering the long time of the cooling stage. As expected, the highest MB deviation was observed for arabinan balance, which is in concordance with the degradation of arabinose that was observed from 22 min of treatment (**Figure 4.7 a**). At this regard, the arabinan mass loss observed, 2.62 g, would contribute to a furfural production of 1.90 g while 1.6 g were formed after 45 min of isothermal treatment. However, the concentration of furfural increased to 1.5 g/L (3.3 g/100 g<sub>dry-BSG</sub>) during the cooling time (data not shown), indicating that not only arabinan but also xylan underwent degradation along this period. In addition, the value of MB corresponding to acetic acid, noticeably higher than 100, suggests that acetic acid was formed not only from the deacetylation of acetyl groups present in BSG hemicellulose but also from the degradation of other compounds such as amino acids, among others. Regarding amino acids, their degradation under hydrothermal conditions could be followed in different pathways such as decarboxylation to produce carbonic acid and amines, and deamination to produce ammonia and organic acids. The results suggested that the second pathway was major as a mass loss was observed for N but not for C. Moreover, the higher amount of aspartic acid found in the subW extracts together

with its high rate of degradation by a predominant deamination mechanism was consistent with the loss of N [37]. As described by Lamp et al. [32] volatile degradation products associated to the Maillard reaction (e.g., pyrroles, pyridines, imidazoles, pyrazines, oxasoles, thiazoles or aldol condensation products) could be also smelled as “a typical coffee-like aroma” during reactor depressurization after subW treatment. These authors reported a total mass loss inside the reactor of 25% due to the formation of volatile degradation products, at a severity factor of 5.4, while decreasing protein yield.

On the other hand, MB fitted well for total lignin; but was over and under 100 for acid insoluble lignin and acid soluble lignin, respectively, suggesting that changes in the lignin structure took place during the subW treatment. According to the literature, hydrothermal treatment may cause condensation reactions and structural alteration in the lignin, while lignin droplets have been observed on the surface of the treated solid [38].

## 4. Conclusions

The results of this preliminary study may contribute to a proper scale-up process from laboratory to pilot system for brewer's spent grain valorization by subcritical water treatment. Operating conditions of 170 °C and 22 min ( $S_0 = 3.43$ ) were chosen mainly focused on the release of oligosaccharides from the hemicellulose fraction of BSG, while maintaining a relative low concentration of sugar degradation compounds to avoid enzymatic and/or fermentation inhibition in a further step of oligosaccharides valorization within a biorefinery concept. Under these conditions, 56% of the total CH's present in the BSG was found in the pilot-scale hydrolysates, while the yield of total pentose release (as monomer and oligomer) was 78 %. Among the total pentoses recovered, 82% were released in the oligomeric form. The concentration of inhibitors in the PSE were 0.22 g/L of furfural and 0.31 g/L and 0.13 g/L of acetic and formic acids, respectively. Moreover, the concentration of HMF in the PSE was negligible and levulinic acid was not detected. In addition to oligosaccharides, other high value compounds were obtained, such as 6.5 g/L of peptides (64% protein yield), 21 mg/g<sub>protein</sub> of free amino acids (2.17% aa yield) and total phenolic content of 17.84 mg<sub>GAE</sub>/g<sub>dry-BSG</sub>.

In general, scaling up from laboratory to pilot subcritical water system resulted in reproducible results with some differences that have been studied along this work. In this

regard, there were neither statistically significant differences ( $p < .05$ ) between both systems after 22 min of isothermal treatment for the release yield of total polysaccharide oligomers (arabinoxylan-oligomers, arabino-oligomers, and gluco-oligomers from BSG), nor for the protein yield and the free amino acids release. However, differences were observed for individual xylo-oligomers release differences for both systems being the release yield 13% higher at lab-scale than at pilot-scale. Statistically significant differences were also found regarding the release yield of carbohydrate monomers and the total phenolic content between both hydrolysates.

In addition, based on the results obtained at the laboratory scale at longer operation times, fractionation of the different bio-compounds could be achieved. For instance, longer operation times led to lower concentration of hemicellulose in the residual solid and a greater accumulation of glucans that could be convenient for a further enzymatic release of glucose from the remained solid. In addition, if the target compound was furfural, a high-value platform compound, it has been shown that increasing the treatment time increased the concentration of this compound in the hydrolysate.

The feasibility of an industrial-scale subcritical water system through scaling-up from lab to pilot systems has been showed. Future research about operation at higher solid concentrations to increase the economic viability of the system and proposal of different strategies to valorize the different streams under a biorefinery concept is still needed.

## References

- [1] M. Kavalopoulos *et al.*, "Sustainable valorisation pathways mitigating environmental pollution from brewers' spent grains," *Environmental Pollution*, vol. 270, Feb. 2021, doi: 10.1016/j.envpol.2020.116069.
- [2] P. Alonso-Riaño, M. T. S. Diez, B. Blanco, S. Beltrán, E. Trigueros, and O. Benito-Román, "Water ultrasound-assisted extraction of polyphenol compounds from brewer's spent grain: Kinetic study, extract characterization, and concentration," *Antioxidants*, vol. 9, no. 3, 2020, doi: 10.3390/antiox9030265.
- [3] S. A. L. Bachmann, T. Calvete, and L. A. Féris, "Potential applications of brewery spent grain: Critical an overview," *Journal of Environmental Chemical Engineering*, vol. 10, no. 1. Elsevier Ltd, Feb. 01, 2022. doi: 10.1016/j.jece.2021.106951.
- [4] K. M. Lynch, E. J. Steffen, and E. K. Arendt, "Brewers' spent grain: a review with an emphasis on food and health," *Journal of the Institute of Brewing*, vol. 122, no. 4, pp. 553–568, 2016, doi: 10.1002/jib.363.
- [5] S. Ikram, L. Huang, H. Zhang, J. Wang, and M. Yin, "Composition and Nutrient Value Proposition of Brewers Spent Grain.," *Journal of food science*, vol. 82, no. 10, pp. 2232–2242, Oct. 2017, doi: 10.1111/1750-3841.13794.
- [6] W. G. Sganzerla, L. C. Ampese, S. I. Mussatto, and T. Forster-Carneiro, "A bibliometric analysis on potential uses of brewer's spent grains in a biorefinery for the circular economy transition of the beer industry," *Biofuels, Bioproducts and Biorefining*, p. bbb.2290, Sep. 2021, doi: 10.1002/bbb.2290.
- [7] M. J. Cocero *et al.*, "Understanding biomass fractionation in subcritical & supercritical water," *The Journal of Supercritical Fluids*, vol. 133, no. August 2017, pp. 550–565, Mar. 2018, doi: 10.1016/j.supflu.2017.08.012.
- [8] P. Yue, Y. Hu, R. Tian, J. Bian, and F. Peng, "Hydrothermal pretreatment for the production of oligosaccharides: A review," *Bioresource Technology*, vol. 343. Elsevier Ltd, Jan. 01, 2022. doi: 10.1016/j.biortech.2021.126075.
- [9] W. G. Sganzerla, G. L. Zobot, P. C. Torres-Mayanga, L. S. Buller, S. I. Mussatto, and T. Forster-Carneiro, "Techno-economic assessment of subcritical water hydrolysis process for sugars production from brewer's spent grains," *Industrial Crops and Products*, vol. 171, Nov. 2021, doi: 10.1016/j.indcrop.2021.113836.
- [10] F. Carvalheiro, M. P. Esteves, J. C. Parajó, H. Pereira, and F. M. Gírio, "Production of oligosaccharides by autohydrolysis of brewery's spent grain," *Bioresource Technology*, vol. 91, no. 1, pp. 93–100, 2004, doi: 10.1016/S0960-8524(03)00148-2.
- [11] J. Chen *et al.*, "Integrating enzymatic hydrolysis into subcritical water pretreatment optimization for bioethanol production from wheat straw," *Science of the Total Environment*, vol. 770, May 2021, doi: 10.1016/j.scitotenv.2021.145321.
- [12] P. Alonso-Riaño, M. T. Sanz, O. Benito-Román, S. Beltrán, and E. Trigueros, "Subcritical water as hydrolytic medium to recover and fractionate the protein fraction and phenolic compounds from craft brewer's spent grain," *Food Chemistry*, vol. 351, Jul. 2021, doi: 10.1016/j.foodchem.2021.129264.

- [13] J. B. Sluiter, R. O. Ruiz, C. J. Scarlata, A. D. Sluiter, and D. W. Templeton, "Compositional analysis of lignocellulosic feedstocks. 1. Review and description of methods," *Journal of Agricultural and Food Chemistry*, vol. 58, no. 16, pp. 9043–9053, 2010, doi: 10.1021/jf1008023.
- [14] A. Sluiter, B. Hames, R. Ruiz, C. Scarlata, J. Sluiter, and D. Templeton, "Determination of Sugars, Byproducts, and Degradation Products in Liquid Fraction Process Samples: Laboratory Analytical Procedure (LAP); Issue Date: 12/08/2006," 2006. Accessed: May 05, 2019. [Online]. Available: [www.nrel.gov](http://www.nrel.gov)
- [15] V. L. Singleton, R. Orthofer, and R. M. B. T.-M. in E. Lamuela-Raventós, "[14] Analysis of total phenols and other oxidation substrates and antioxidants by means of folin-ciocalteu reagent," in *Oxidants and Antioxidants Part A*, vol. 299, Academic Press, 1999, pp. 152–178. doi: [https://doi.org/10.1016/S0076-6879\(99\)99017-1](https://doi.org/10.1016/S0076-6879(99)99017-1).
- [16] A. Friedl, E. Padouvas, H. Rotter, and K. Varmuza, "Prediction of heating values of biomass fuel from elemental composition," *Analytica Chimica Acta*, vol. 544, no. 1-2 SPEC. ISS., pp. 191–198, 2005, doi: 10.1016/j.aca.2005.01.041.
- [17] F. Qin, A. Z. Johansen, and S. I. Mussatto, "Evaluation of different pretreatment strategies for protein extraction from brewer's spent grains," *Industrial Crops and Products*, vol. 125, no. June, pp. 443–453, 2018, doi: 10.1016/j.indcrop.2018.09.017.
- [18] P. J. Arauzo, L. Du, M. P. Olszewski, M. F. Meza Zavala, M. J. Alhnidi, and A. Kruse, "Effect of protein during hydrothermal carbonization of brewer's spent grain," *Bioresource Technology*, vol. 293, no. July, p. 122117, Dec. 2019, doi: 10.1016/j.biortech.2019.122117.
- [19] F. Rodríguez, E. Aguilar-Garnica, A. Santiago-Toribio, and A. Sánchez, "Polysaccharides Release in a Laboratory-Scale Batch Hydrothermal Pretreatment of Wheat Straw under Rigorous Isothermal Operation," *Molecules*, vol. 27, no. 1, p. 26, Dec. 2021, doi: 10.3390/molecules27010026.
- [20] H. A. Ruiz *et al.*, "Severity factor kinetic model as a strategic parameter of hydrothermal processing (steam explosion and liquid hot water) for biomass fractionation under biorefinery concept," *Bioresource Technology*, vol. 342. Elsevier Ltd, Dec. 01, 2021. doi: 10.1016/j.biortech.2021.125961.
- [21] Z.-W. Wang, M.-Q. Zhu, M.-F. Li, J.-Q. Wang, Q. Wei, and R.-C. Sun, "Comprehensive evaluation of the liquid fraction during the hydrothermal treatment of rapeseed straw," *Biotechnol Biofuels*, vol. 9, p. 142, 2016, doi: 10.1186/s13068-016-0552-8.
- [22] M. E. Vallejos, F. E. Felissia, J. Kruyeniski, and M. C. Area, "Kinetic study of the extraction of hemicellulosic carbohydrates from sugarcane bagasse by hot water treatment," *Industrial Crops and Products*, vol. 67, pp. 1–6, May 2015, doi: 10.1016/j.indcrop.2014.12.058.
- [23] A. B. de Camargos *et al.*, "Production of biogas and fermentable sugars from spent brewery grains: Evaluation of one- and two-stage thermal pretreatment in an integrated biorefinery," *Journal of Environmental Chemical Engineering*, vol. 9, no. 5, Oct. 2021, doi: 10.1016/j.jece.2021.105960.

- [24] N. Mosier *et al.*, "Features of promising technologies for pretreatment of lignocellulosic biomass," *Bioresource Technology*, vol. 96, no. 6, pp. 673–686, 2005, doi: 10.1016/j.biortech.2004.06.025.
- [25] P. C. Torres-Mayanga *et al.*, "Subcritical water hydrolysis of brewer's spent grains: Selective production of hemicellulosic sugars (C-5 sugars)," *Journal of Supercritical Fluids*, vol. 145, no. September 2018, pp. 19–30, 2019, doi: 10.1016/j.supflu.2018.11.019.
- [26] G. Vanmarcke, M. M. Demeke, M. R. Foulquié-Moreno, and J. M. Thevelein, "Identification of the major fermentation inhibitors of recombinant 2G yeasts in diverse lignocellulose hydrolysates," *Biotechnology for Biofuels*, vol. 14, no. 1, p. 92, Dec. 2021, doi: 10.1186/s13068-021-01935-9.
- [27] M. J. Cocero *et al.*, "Understanding biomass fractionation in subcritical & supercritical water," *Journal of Supercritical Fluids*, vol. 133, no. August 2017, pp. 550–565, 2018, doi: 10.1016/j.supflu.2017.08.012.
- [28] C. R. M. Monteiro, L. G. G. Rodrigues, K. Cesca, and P. Poletto, "Evaluation of hydrothermal sugarcane bagasse treatment for the production of xylooligosaccharides in different pressures," *Journal of Food Process Engineering*, no. October 2021, 2022, doi: 10.1111/jfpe.13965.
- [29] S. Deguchi, K. Tsujii, and K. Horikoshi, "Crystalline-to-amorphous transformation of cellulose in hot and compressed water and its implications for hydrothermal conversion," *Green Chemistry*, vol. 10, no. 2, pp. 191–19, Feb. 2008, doi: 10.1039/b713655b.
- [30] G. Garrote, H. Domínguez, and J. C. Parajó, "Kinetic modelling of corncob autohydrolysis," *Process Biochemistry*, vol. 36, no. 6, pp. 571–578, 2001, doi: 10.1016/S0032-9592(00)00253-3.
- [31] A. Mittal, S. G. Chatterjee, G. M. Scott, and T. E. Amidon, "Modeling xylan solubilization during autohydrolysis of sugar maple and aspen wood chips: Reaction kinetics and mass transfer," *Chemical Engineering Science*, vol. 64, no. 13, pp. 3031–3041, 2009, doi: 10.1016/j.ces.2009.03.011.
- [32] A. Lamp, M. Kaltschmitt, and O. Lüdtke, "Protein recovery from bioethanol stillage by liquid hot water treatment," *Journal of Supercritical Fluids*, vol. 155, p. 104624, 2020, doi: 10.1016/j.supflu.2019.104624.
- [33] W. Abdelmoez, T. Nakahasi, and H. Yoshida, "Amino acid transformation and decomposition in saturated subcritical water conditions," *Industrial and Engineering Chemistry Research*, vol. 46, no. 16, pp. 5286–5294, 2007, doi: 10.1021/ie070151b.
- [34] C. Fabian, N. Y. Tran-Thi, N. S. Kasim, and Y. H. Ju, "Release of phenolic acids from defatted rice bran by subcritical water treatment," *Journal of the Science of Food and Agriculture*, vol. 90, no. 15, pp. 2576–2581, 2010, doi: 10.1002/jsfa.4123.
- [35] E. Zago *et al.*, "Sustainable production of low molecular weight phenolic compounds from Belgian Brewers' spent grain," *Bioresource Technology Reports*, vol. 17, no. January, p. 100964, 2022, doi: 10.1016/j.biteb.2022.100964.

- [36] M. M. Moreira, S. Morais, A. A. Barros, C. Delerue-Matos, and L. F. Guido, "A novel application of microwave-assisted extraction of polyphenols from brewer's spent grain with HPLC-DAD-MS analysis," *Analytical and Bioanalytical Chemistry*, vol. 403, no. 4, pp. 1019–1029, May 2012, doi: 10.1007/s00216-011-5703-y.
- [37] N. Sato, A. T. Quitain, K. Kang, H. Daimon, and K. Fujie, "Reaction kinetics of amino acid decomposition in high-temperature and high-pressure water," *Industrial and Engineering Chemistry Research*, vol. 43, no. 13, pp. 3217–3222, 2004, doi: 10.1021/ie020733n.
- [38] X. Zhuang *et al.*, "Liquid hot water pretreatment of lignocellulosic biomass for bioethanol production accompanying with high valuable products," *Bioresource Technology*, vol. 199. Elsevier Ltd, pp. 68–75, Jan. 01, 2016. doi: 10.1016/j.biortech.2015.08.051.





# CHAPTER 5

---

**Pervaporation behaviour of subcritical water hydrolysates of lignocellulosic biomass: brewer's spent grain**

**Based on the article:**

P. Alonso-Riaño, M. T. Sanz, S. Beltrán.

"Pervaporation behaviour of subcritical water hydrolysates of lignocellulosic biomass: brewer spent grain".



## CAPÍTULO 5

### Pervaporación de hidrolizados de agua subcrítica de biomazas lignocelulósicas: bagazo de cerveza

---

#### Resumen

El tratamiento de biomazas lignocelulósicas con agua subcrítica genera unos hidrolizados que contienen carbohidratos procedentes del hemicelulosas, pero también una serie de compuestos orgánicos que pueden actuar como inhibidores en un proceso de fermentación posterior. Estos compuestos orgánicos son también compuestos intermedios, o moléculas plataforma de base biológica, que constituyen la materia prima para procesos de producción de compuestos químicos con interesantes aplicaciones industriales.

En este capítulo, se estudió el uso de dos membranas poliméricas de pervaporación para la recuperación de algunos de los compuestos orgánicos producidos durante la hidrólisis del bagazo de cerveza mediante agua subcrítica, en un reactor discontinuo a 175 °C. El principal azúcar encontrado en los hidrolizados subcríticos fue la xilosa, en forma de monómero y oligómero, seguido de la glucosa y la arabinosa. Además, se encontraron cantidades importantes de furfural (~1.5 g/L), procedente de la deshidratación de las pentosas, y de ácido acético (~0.8 g/L), generado tras la hidrólisis de los grupos acetilo presentes en las hemicelulosas. También se detectaron otros compuestos orgánicos en los hidrolizados, como el ácido fórmico, el ácido levulínico y el 5-hidroximetilfurfural, aunque en menor concentración.

Se estudiaron los efectos de la composición de la alimentación y la temperatura en el flujo del permeado, el factor de enriquecimiento y el índice de separación por pervaporación (PSI), para el agua pura y para diferentes disoluciones modelo que contenían los compuestos orgánicos mencionado anteriormente. Se observó que la membrana de polidimetilsiloxano (PDMS) y la membrana de polioctilsiloxano (POMS) mostraron una alta selectividad por el furfural, en los experimentos de pervaporación realizados con los compuestos puros, mientras que los factores de enriquecimiento para los ácidos orgánicos evaluados fueron inferiores a la unidad.

Se realizaron experimentos de pervaporación para la recuperación del furfural de los hidrolizados subcríticos con membranas de PDMS y POMS y se encontró que ambas membranas fueron capaces de separar selectivamente el furfural. Si bien se obtuvo un flujo de permeado más bajo utilizando la membrana de POMS, esta membrana fue la que mejor funcionó para eliminar y recuperar el furfural, recuperando el 93.9% del mismo, con una concentración de furfural en el permeado de 20.9 g/L, 16 veces superior que en la alimentación inicial.

En este capítulo se evaluó la posibilidad de incorporar la tecnología de pervaporación en un proceso integrado de biorrefinería, tras el pretratamiento del bagazo de cerveza con agua subcrítica, para permitir el uso de los hidrolizados generados como caldos de fermentación, mediante la eliminación y la recuperación del furfural generado, que puede ser empleado como molécula plataforma para producir compuestos químicos renovables.

---

**Palabras clave:** hidrolizados con agua subcrítica, bagazo de cerveza, pervaporación, furfural.

## Abstract

---

Subcritical water hydrolysates from lignocellulosic biomass present important amounts of organic compounds that can act as inhibitors in further fermentation processes. These organic compounds are also biobased platform chemicals used in a wide variety of industrial applications. In this work, two commercially pervaporation membranes were evaluated for the recovery of some of the organic compounds produced during hydrolysis of brewer's spent grain (BSG) by subcritical water (subW) in a discontinuous reactor at 175 °C. The main sugar found in the subW hydrolysate was xylose, as monomer and oligomer, followed by glucose and arabinose. The main sugar-derived compounds generated were furfural and acetic acid. Other organic compounds, such as formic acid, levulinic acid, and 5-hydroxymethylfurfural, were found in lesser level in the subW hydrolysates. The effects of feed composition and temperature on permeate flux, enrichment factor and pervaporation separation index (PSI) were studied for pure water and for different dilute synthetic organic mixtures of the pure compounds found in the subW hydrolysates. It was observed that the polydimethylsiloxane membrane (PDMS) and the polyoctylmethylsiloxane membrane (POMS) show a high affinity towards furfural in the pervaporation experiments carried out with the pure components, while the enrichment factors for the organic acids evaluated were less than the unity. Pervaporation experiments were performed for the recovery of furfural from the BSG subW hydrolysates with PDMS and POMS membranes. Both membranes were able to selectively separate furfural. The lowest permeation flux was obtained by using the POMS membrane, but also the best performed to remove and recover the furfural, with a 93.9% of furfural recovery and 16-folds higher furfural concentration in the permeate, 20.9 g/L, than in the initial feed, 1.3 g/L.

In this study, we assess the possibility of incorporating the pervaporation technology, after the subW pretreatment of BSG, to allow the use of subW hydrolysates as fermentation broths, by selectively removing and recovery the furfural generated, to a further use as a biomass-derived platform chemical, under an integrated biorefinery concept.

---

**Keywords:** Subcritical water hydrolysates, pervaporation, furfural, brewer's spent grain

---



## 1. Introduction

The generation of lignocellulosic biomass by different industries is encouraging the implementation of a biorefinery approach to obtain different valuable products from one residue stream. In this sense, lignocellulosic biomass is one of the most attractive options to achieve sustainable production of energy and chemicals as substitutes for petroleum-based products. The brewer industry generates different by-products during beer production being the most important the solid residue generated after mashing and wort filtration process, the brewer's spent grains (BSG), accounting for about 85% of the total by-products [1].

BSG presents a valuable chemical composition with a high content of protein and carbohydrates, being also an important source of phenolic compounds [2], [3]. Among the different technologies proposed to valorize lignocellulosic biomass, the use of subcritical water (subW) has been growing attention to fractionate the biomass into its individual building blocks by its hydrolysis [4]. SubW is water in its liquid state in the temperature range from 100 °C up to 374 °C, its critical temperature. An increase in temperature in the subcritical state leads to higher ionic product and lower density and dielectric constant than at ambient conditions [5]. The incorporation of lignocellulosic biomass into a biorefinery concept also involves the separation and recovery of the valuable compounds generated during the treatment. In this regard, different membrane separation processes have gained special interest for bioenergy and biomaterial production [6]. Membrane technologies are environmentally friendly, low energy consuming and easy to scale up. Pervaporation (PV) is a membrane separation process that has been proposed to remove and recover some of the compounds generated during the hydrolysis process of biomass by subW [7], [8]. Pervaporation is a membrane process that uses non-porous membranes to separate mixture of liquids by vaporization of the permeate phase. The mass transport through the membrane involves three steps: sorption, diffusion of the components through the membrane and desorption by evaporation at the permeate side. The driving force of the process is usually obtained by lowering the pressure on the permeate side of the membrane. The main advantage of pervaporation process is that the selectivity of the process can be optimized by choosing the appropriate membrane material. By using

organophilic membranes, hydrophobic solute may be sorbed in the non-porous membrane and diffuse across the membrane [6].

The selectivity of PV membranes can be useful considering a double objective. On one hand, lignocellulosic subW hydrolysates can contain inhibitors that should be removed for further use of these hydrolysates as fermentation broths such as furan derivatives or some organic acids. On the other hand, separation and purification of these bio-based chemicals are important for production of chemical compounds with enough purity. Biomass rich in hemicellulose, such as BSG, is a source of furan derivatives such as furfural, being one of the main degradation products of the hemicellulose fraction. Furfural has recently been emphasized as one of the top value-added chemicals derived from biomass, which can be used to produce more than 1600 kinds of chemical products [9]–[11]. According to Shan et al. [11], despite the great potential of PV in furfural recovery, related studies are barely reported. Terblanche [8] proposed the recovery of acetic acid and furfural from an acidic hydrolysate from steam treated wood by using a polydimethylsiloxane membrane (PDMS) and a polyether block amine (PEBA) membrane. PDMS provided better separation of acetic acid and furfural from the acidic hydrolysate due interaction between PEBA membrane and the organic compounds generated in the acidic hydrolysates. Cai et al. [12] proposed the use of PDMS pervaporation membrane for the detoxification of sweet sorghum bagasse hydrolysate by using dilute acetic acid as well as the subsequent removal of butanol generated during fermentation of the hydrolysate. Good removal of furfural from the hydrolysates was obtained achieving a 94.5% of furfural removal. All of these studies proposed the use of dilute acetic acid to obtain the acid hydrolysates. From our knowledge no previous studies have been found in literature to remove some of the organic components generated during the hydrolysis of biomass by subW by using organophilic membranes.

This work discusses the use of organophilic pervaporation membranes for the removal and recovery of furfural produced as degradation product from subcritical water hydrolyses of brewer's spent grain. Therefore, in this work, identification, and quantification of the main components of subW hydrolysates was first carried out. Two pervaporation membrane were tested to study the separation of aliphatic acids and furfural



from the hydrolysate in terms of permeate flux, enrichment factor and performance separation index.

## 2. Materials and methods

### 2.1. Raw material

The raw material used in this work was the brewer's spent grain supplied by San Miguel S.A. This raw material was first preconditioned, as soon as obtained, by washing it and drying in an air convection oven (45 °C, 3 h) until reaching a final moisture content of 8% (w/w). Dehydration is necessary to reduce the storage, and transportation costs as well to reduce the microbial spoilage. The dry BSG was milled in a Retsch SM100 mill and the particle size distribution was determined by a vibratory sieve shaker (CISA, RP.09), with the following final mass percentage distribution: > 1mm, 5.2%; 1 – 0.5 mm, 52.2%; 0.5-0.25 mm, 28.5%; 0.25-0.125 mm, 8.7% and < 0.125 mm, 1.7%.

Biomass characterization was performed according to the NREL protocols [13]. Carbohydrates were quantified by high-performance liquid chromatography (HPLC) with a Bio-Rad Aminex-HPX-87 H column, a variable wavelength detector (VWD) and a refractive index detector (RID) using a mobile phase constituted by 0.005 M sulphuric acid. The column and RID were maintained at 40 °C. Megazyme Total Starch Assay (amyloglucosidase/ $\alpha$ -amylase method) was followed to determine starch in the BSG. Likewise,  $\beta$ -glucans content was performed using Megazyme  $\beta$ -Glucan Assay Kit (Mixed Linkage). Protein in the raw material was estimated from the nitrogen content present in the samples as measured by the elemental analysis and considering a nitrogen factor of 6.25, according to Alonso-Riaño et al. [2]. The oil content of the BSG was determined by Soxhelt extraction (Buchi B-8111) using hexane as solvent.

### 2.2. Pervaporation membranes

Two different organophilic dense membranes supplied by GKKS Research Centre (Germany) were used in this study: (1) PERVAP TM 4060 a membrane whose active layer was based on polydimethylsiloxane (PDMS) (2) another membrane whose selective layer was based on polyoctylmethyl siloxane (POMS).

### 2.3. Subcritical water hydrolysis

Subcritical water hydrolysis treatment was carried out at laboratory-scale in a discontinuous stainless-steel reactor of 500 mL maximum capacity, as described in Chapter 4. The heating system consisted of a heating jacket of 230 V and 400 W covering the reactor, used to reach the working temperature. A Pt100 sensor connected to PID system and placed inside the reactor helps to control and register the temperature during the hydrolysis. Biomass was loaded into the reactor and filled with water. The mixture was heated up to the desired temperature and pressured was fixed at 50 bars by using nitrogen gas and maintained during all the process. SubW hydrolysis was carried out at 175 °C for a treatment time of 60 min and a biomass loading of 5 % (w:v). The final hydrolysate was allowed to cool, filtered, and subjected to further analysis.

### 2.4. Pervaporation experiments

Pervaporation equipment and performance has been previously described elsewhere [14], [15]. The pervaporation equipment consisted of a feed tank, a peristaltic pump and a plate and frame laboratory stainless steel permeation cell (Sulzer Chemtech®) with a specific membrane, which provides a radial flow over the membrane surface. The effective area of the membrane in contact with the feed was 170 cm<sup>2</sup>. The temperature of the feed liquid mixture was kept constant ( $\pm 1$  °C) by means of a thermostat to heat the jacketed stirred tank feed reactor. The feed flow rate was set to 70 kg·h<sup>-1</sup>. In the permeate side, the permeate was condensed on two parallel glass cold traps cooled by liquid nitrogen to assure all the permeate was collected. Permeate pressure was kept constant by using a vacuum pump (Edwards RV12),  $3 \pm 2$  mbar, and a vacuum controller (CVC-3000).

Two types of pervaporation experiments were carried out for each type of membrane. First, steady state pervaporation experiments were carried out for the pure compounds by using a feed tank of 5 L capacity. This way, due to the small amount of permeate product, the concentration of the compound in the feed tank was kept approximately constant along operation. Pervaporation experiments for pure components were performed at different temperatures in the range from 30 to 59 °C and different feed composition with pure acetic, formic and levulinic acids, furfural and hydroxymethyl furfural. Finally, pervaporation of subW hydrolysates was carried out under unsteady state operation at constant

temperature of 59 °C. For that, a smaller feed tank reactor with initially 500 mL of the hydrolysate in the feed side was used to increase the ratio membrane area to initial feed volume and observe a decrease in compounds present in the hydrolysates that preferentially permeate through the membrane.

Organic compounds flux was obtained from the total permeation flux and the mass fraction of the component in the permeate:

$$J_i = J_{tot} \cdot w_i \quad [5.1]$$

where  $J_{tot}$  and  $J_i$  are the total and individual permeation flux, expressed as  $\text{g}\cdot\text{m}^{-2}\cdot\text{h}^{-1}$ , and  $w_i$  is the concentration of component  $i$  in the permeate

The chemical stability of the membrane was checked periodically by measuring pure water permeation flux at reference operating conditions. The separation performance of the pervaporation membranes was checked by the enrichment factor ( $\beta$ ), defined for a specific component as the relationship between its concentration in the permeate and the feed:

$$\beta = w_{i,p}/w_{i,f} \quad [5.2]$$

The performance of PV membranes was also evaluated through the pervaporation separation index, PSI, which is the tradeoff relationship between permeation flux and separation factor [16]:

$$\text{PSI} = J_{tot} \cdot \beta \quad [5.3]$$

## 2.5. Analytical methods

Identification and quantification of the hydrolyzed polysaccharide fraction and its degradation products was performed by HPLC following the same method as for biomass characterization and described in section 2.1.1. Monosaccharides and degradation products were directly analyzed in the subW hydrolysates previously filtered through a 0.22  $\mu\text{m}$  pore size syringe filter (Scharlab). Total sugars were determined after hydrolysis of the sample according to the Laboratory Analytical Procedure [13] to hydrolyze all the oligomers in

monomers sugars. Oligomeric sugar was calculated as the difference between the total sugar content after hydrolysis and the monomers present in the subcritical water hydrolysates.

For the pervaporation experiments of pure compounds and subW hydrolysates the same analysis protocol as previously described for the hydrolysates was followed.

The standards employed for the HPLC analysis were cellobiose (99%), glucose (99.5%), xylose (99%), rhamnose (99%), galactose (99%), arabinose (99%), mannose (99%), glyceraldehyde (98%), glycoaldehyde (99%), acrylic acid (99%), pyruvaldehyde (40%) and furfural (99%) purchased from Sigma Aldrich (Spain), fructose (99%), lactic acid (50%) and formic acid (98%) purchased from Fluka, 5-hydroxymethylfurfural (97%) from Alfa Aesar, acetic acid (99.8%) from VWR Chemicals and levulinic acid (98%) from Merck.

## 2.6. Statistical analysis

Statistical analyses were conducted using the software Statgraphics X64. The results were presented as a mean  $\pm$  standard deviation of at least three replicates. To confirm significant differences, the Fisher's least significant differences method at p-value  $\leq 0.05$  was applied.

## 3. Results and discussion

### 3.1. Biomass characterization

The chemical composition of the BSG employed in this work has been collected in **Table 5.1** in a weight percentage dry basis. The easily extractive compounds of BSG accounted for  $14.5 \pm 0.2\%$  (w/w), ( $9.2 \pm 0.1\%$  and  $5.3 \pm 0.1\%$  for water and ethanol soluble fraction, respectively). Total protein content was  $22.1 \pm 0.5\%$  (w/w) and the lipid fraction was  $6.2 \pm 0.3\%$  (w/w). The main polysaccharide fraction was hemicellulose, with  $32.0 \pm 0.6\%$  (w/w) and the cellulose fraction was  $14.0 \pm 0.2\%$  (w/w).

**Table 5.1.** Chemical composition of BSG expressed in weight percentage on a dry basis

Component	g/100 <sub>dry-BSG</sub>
Extractives in water	9.2 ± 0.1
Extractives in ethanol	5.3 ± 0.1
Protein*	22.1 ± 0.5
Cellulose	14.0 ± 0.2
Starch	4.10 ± 0.06
β-Glucan	0.99 ± 0.01
Hemicellulose	32.0 ± 0.6
Xylan	21.6 ± 0.4
Arabinan	9.5 ± 0.4
Acetyl groups	0.93 ± 0.05
Soluble lignin	5.3 ± 0.2
Insoluble lignin	15.5 ± 0.1
Lipids	6.2 ± 0.3
Ash	3.32 ± 0.06

\*Protein includes the protein content in the extractives fraction Values are expressed as mean ± standard deviation from triplicate determination.

### 3.2. Subcritical water treatment of BSG in a discontinuous reactor

Subcritical water treatment was performed at 175 °C with a biomass loading of 5% (w/v) and a treatment time of 60 min. After cooling, the hydrolysates were filtered and analyzed. Hydrolysis was performed in duplicated and the corresponding composition of the hydrolysates was collected in **Table 5.2**. Hydrolysates were a complex mixture of different organic compounds. Similar composition was obtained for each experiment; however, detailed composition was presented for each hydrolysate since they were used as feed for pervaporation experiments immediately after subW hydrolysis to avoid further degradation of the compounds along time, even under refrigeration conditions. According to the chemical composition of BSG, the main sugar released to the medium was xylose, as monomer and oligomer, followed by glucose and arabinose. Sugars degradation products were also determined in the hydrolysates, being the main compound furfural from pentose dehydration reactions (from 1.3 to 1.7 g/L). In subW hydrolysates organic acids were also determined, being acetic and formic acid, the major organic acids found.

**Table 5.2.** Composition of subcritical water hydrolysates of BSG and feed composition after pervaporation experiments (g/L)

Compound		$C_{o,PDMS}$	$C_{PV-PDMS-hd}$	$C_{o,POMS}$	$C_{PV-POMS,hd}$
Glucose	Monomer	0.35	0.44	0.35	0.37
	Oligomer	1.0	1.22	0.78	0.82
Xylose	Monomer	1.51	1.79	1.47	1.53
	Oligomer	0.59	0.64	0.43	0.33
Arabinose	Monomer	0.28	0.34	0.28	0.30
	Oligomer	0.06	0.09	0.10	0.08
	Furfural	1.7	0.35	1.3	0.17
	HMF	0.18	0.20	0.15	0.16
Other compounds	Formic acid	0.46	0.55	0.36	0.41
	Acetic acid	0.83	1.0	0.79	1.0
	Lactic acid	0.27	0.32	0.30	0.31
	Levulinic acid	--	0.03	0.032	0.033
	Succinic acid	0.35	0.50	0.43	0.45

### 3.3. Evaluation of PDMS and POMS membranes performance with pure compounds.

Pervaporation performance of some of the degradation compounds determined in the subW hydrolysates was first considered. Diluted model organic solutions were prepared according to the subcritical water hydrolysates composition (see **Table 5.2**).

#### 3.3.1. Effect of temperature on pervaporation performance

The effect of temperature on PV flux and selectivity was studied by varying the working temperature in the range from 30 to 59 °C at a fixed permeate pressure of 300 Pa. The pervaporation experiments were carried out for pure water and different dilute synthetic organic mixtures of pure compounds determined as degradation products of sugar monomers in the subW hydrolysates (see **Table 5.2**): acetic acid, formic acid, levulinic acid, hydroxymethyl furfural and furfural. **Figure 5.1** shows the water and organic compounds permeation flux determined for both type of membranes.

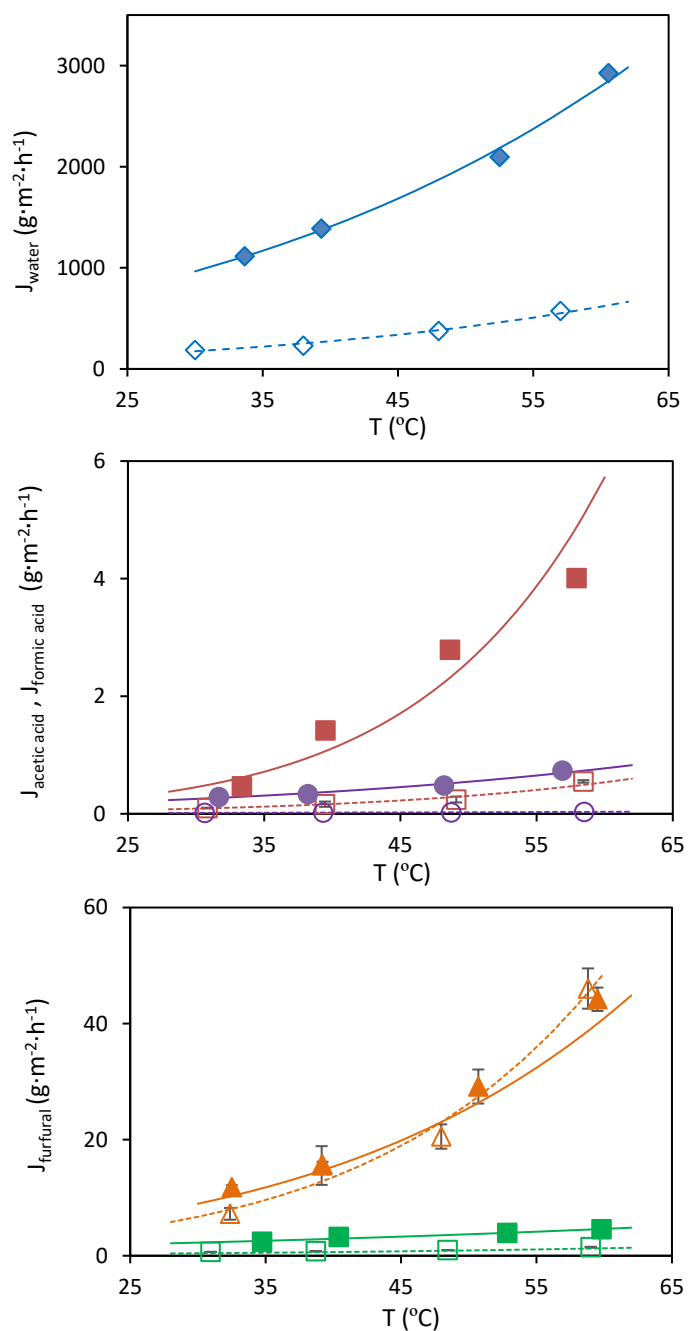


**Figure 5.1.** Permeation flux as a function of temperature (a)  $\blacklozenge$   $\diamond$  water (b)  $\blacksquare$   $\square$  acetic acid (1 g/L) and  $\bullet$   $\circ$  formic acid (0.3 g/L), and (c) furfural  $\blacksquare$  0.17 g/L,  $\square$  0.14 g/L,  $\blacktriangle$  1.3 g/L and  $\triangle$  1.5 g/L. Filled symbol PDMS membrane, open symbols POMS membrane. Lines represent the Arrhenius relationship.

In general, the total permeation flux of the organic model solutions was of the same order as water permeation flux, due to the low concentration of the organic compounds in the feed. In the case of hydroxymethyl furfural and levulinic acid, organic permeation flux was negligible due to the low vapor pressure of these compounds and at the low-level concentrations determined in the subW hydrolysates, so the removal was not feasible.

Permeation flux increased exponentially with temperature, for both types of membranes, in the temperature range covered in this work, due to increase in the driving force of the process, although higher permeation flux was obtained for PDMS than for POMS membrane. The effect of temperature on permeation flux was described by an Arrhenius type equation:

$$J_i = J_{i,o} \exp\left(-\frac{E_{a,i}}{RT}\right) \quad [5.4]$$

where  $J$  is the permeation flux ( $\text{g}\cdot\text{m}^{-2}\cdot\text{h}^{-1}$ ),  $E_{a,i}$  is the apparent activation energy of permeation,  $J_{i,o}$  is the preexponential factor and  $T$  is the absolute temperature.

Apparent activation energies were calculated from the slope and the intercept of a  $\ln J$  versus  $(RT)^{-1}$  plot and are listed in **Table 5.3**. The positive values of the activation energy indicated that an increase in temperature will increase water and organic permeation flux. By increasing temperature, the driving force increased due to the increasing vapour pressure. Additionally, an increase in temperature, causes an increase in the motion of the polymer chains improving diffusion of the permeant molecules [14], [15]. Similar values of activation energy of water permeation were obtained for PDMS and POMS membranes, showing a similar temperature sensitivity, although higher water permeation flux was obtained for PDMS membrane. Terblanche [8] reported a similar value for water activation energy through a PDMS membrane,  $34 \pm 2 \text{ kJ}\cdot\text{mol}^{-1}$ . However, higher values for the apparent activation energy of water through PDMS and POMS membranes were also found in the literature, with values of  $46.7$  and  $43.1 \text{ kJ}\cdot\text{mol}^{-1}$  for POMS and PDMS membranes, respectively [14], [15].

Among the different organic compounds explored in this work, acetic acid and furfural, at the highest concentration studied, showed the highest sensitivity to a temperature increase. A higher value of the apparent activation energy indicates a more sensitive



behaviour toward temperature changes, inferring that, for both compounds, permeation flux is more dependent on temperature than water permeation. Other values reported in the literature for the apparent activation energy of these compounds through PDMS membrane were  $22.5 \pm 9.5$  and  $45.6 \pm 4.5$   $\text{kJ}\cdot\text{mol}^{-1}$  for acetic acid (4.8 g/L) and furfural (1g/L), respectively, while no data were found for POMS membrane.

**Table 5.3.** Apparent activation energies ( $E_{a,i}$ ,  $\text{kJ}\cdot\text{mol}^{-1}$ ) for water, acetic acid, formic acid and furfural at each feed concentration (C, g/L) through PDMS and POMS membranes.

Component	PDMS		POMS	
	C (g/L)	$E_{a,i}$ ( $\text{kJ}\cdot\text{mol}^{-1}$ )	C (g/L)	$E_{a,i}$ ( $\text{kJ}\cdot\text{mol}^{-1}$ )
Water	-	$30 \pm 1$	-	$35 \pm 3$
Acetic acid	1.0	$77 \pm 15$	1.0	$51 \pm 6$
Formic acid	0.3	$31 \pm 3$	0.3	$20.3 \pm 0.7$
Furfural	0.17	$20 \pm 3$	0.14	$23 \pm 3$
Furfural	1.3	$42 \pm 2$	1.5	$55 \pm 7$

To evaluate the selectivity of each membrane towards the different organic compounds, the enrichment factor ( $\beta$ ) and the PSI were evaluated at different temperatures (**Figure 5.2**). As a general trend, increasing temperature induced an increase on the enrichment factors for the different organic compounds for POMS membrane, but this effect was not observed for PDMS membrane. Due to the more hydrophobic nature of POMS than PDMS polymers, hydrophobic compounds could be preferentially adsorbed on POMS membrane surface. Therefore, an increase in temperature induced an increase of the diffusivity of the organic compounds through the polymer membrane, increasing the enrichment factors in case of POMS membrane. For both membranes, the enrichment factors obtained for organic acids were lower than the unity, since lower concentrations of organic acids in the permeate than in the feed were determined. Terblanche [8]. obtained similar results regarding the selectivity of PDMS membranes towards acetic acid when worked with a feed concentration of 4.6 g/L, with an enrichment factor about 0.2 at 80 °C. However, according to the literature, PDMS membranes are slightly more selective towards acetic acid than water when the acetic acid concentration was higher, 100 g/L [17]. Therefore, the organic acid concentration in the feed may play an important role regarding the selectivity of the membranes.

On the other hand, the enrichment factors obtained for furfural, for both membranes, were higher than one, since higher furfural concentration in the permeate than in the feed were found. As it can be observed in **Figure 5.2c** and **5.2d**, the furfural enrichment factors were higher for POMS than for PDMS membranes. The incorporation of longer chain alkyl group in POMS could increase the furfural sorption, enhancing the subsequent diffusion through the membrane. For PDMS membrane, Terblanche [8] showed lower enrichment factors for furfural than the values reported in this work, with values between 1.4 and 2.1 in the temperature range from 40 to 80 °C and for a furfural feed concentration of 1 g/L. The furfural enrichment factors for the POMS membrane greatly increased with temperature, specially at the highest furfural concentration level assayed in this work, 1.3-1.5 g/L. The increase of furfural selectivity with temperature for POMS membranes was probably due to a higher increase of diffusion with temperature of furfural than that of water. Similarly, Ghosh et al. [18], also observed an increase of furfural concentration in the permeate with temperature when using a furfural feed concentration of 2 wt (%) and a polyurethaneurea membrane. These authors expected this behaviour considering that the hydrophobic segments of the membrane interacts more with furfural than with water and diffusion of furfural increased more rapidly than that of water with temperature.

Conversely, PDMS membranes showed higher total permeation flux but lower enrichment factors for furfural than POMS membranes. Therefore, to consider the overall performance of the membrane, the PSI must be also considered. As a general trend, the PSI for all the organic compound studied in this work increased with temperature. For organic acids, PSI for POMS membranes were lower than for PDMS membranes due to the higher permeation flux through PDMS, while enrichment factors were of the same order for both membranes. For furfural, PSI was higher for PDMS than for POMS membrane at the lowest furfural feed concentration assayed in this work, 0.15 g/L. However, by increasing feed concentration PSI for furfural was of the same order for both membranes, even higher for POMS at the highest temperature assayed in this work, due to higher enrichment factor that compensated the lower permeation flux.

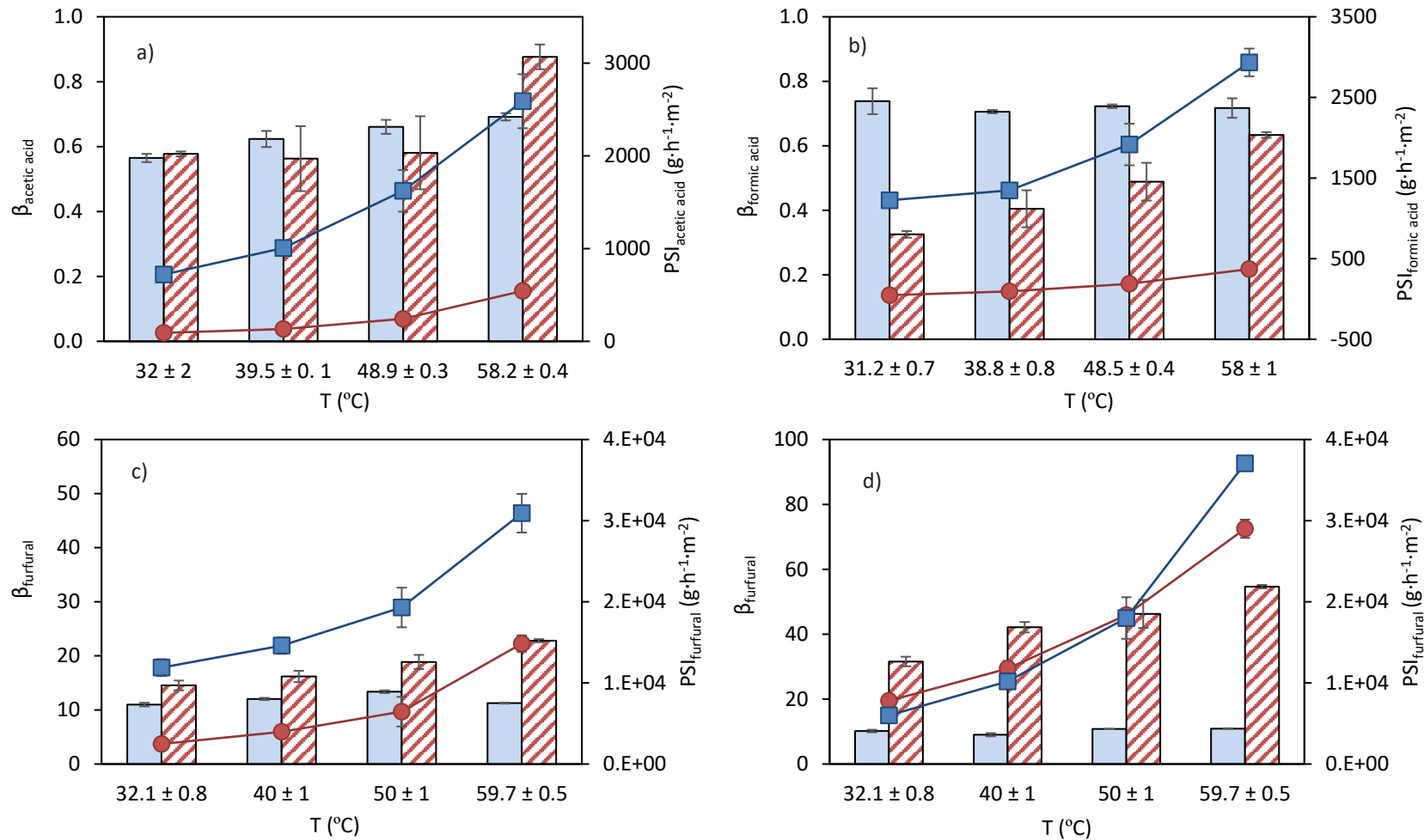


**Figure 5.2.** Enrichment factor,  $\beta$  (□ PDMS, ▨ POMS) and PSI (■ PDMS, ● POMS), determined for each compound (a) acetic acid, 1g/L; (b) formic acid, 0.35g/L, and furfural at two different feed concentration levels (c) 0.15-0.17 g/L and (d) 1.5-1.7 g/L.

### 3.3.2. Effect of furfural concentration in the feed

According to the results presented in section 3.3.1, furfural is the main degradation compound in subW hydrolysates that can be removed by PV. Due to the selective removal of furfural by PV its concentration will not be constant during subW hydrolysate PV in a non-steady state process. Therefore, the effect of the furfural feed composition was studied in the concentration range from 0.15 to 2.2 g/L, at 59 °C, on permeate flux, enrichment factor and PSI for both types of membranes. By increasing the furfural concentration in the feed, the furfural permeation flux increased, observing a relationship between furfural permeation flux and furfural feed concentration (**Figure 5.3**); although the total permeation flux did not change significantly, due to the low furfural concentration in the feed. By increasing the furfural concentration in the feed, sorption of furfural was higher and diffusion through the membrane was enhanced, resulting in a higher furfural permeation flux. Quin et al. [10] also found an increase of furfural permeation flux by increasing feed concentration in the feed concentration range from 0.5 to 6.5 wt (%) at different temperatures (from 308.15 to 353.15 K) for PDMS membranes. These authors explained that the increase in furfural feed concentration tended to facilitate the dissolution of furfural in the membrane which would increase the swelling degree of membrane, as a result, the free volume of the membrane was enhanced, leading to a decrease in the mass transfer resistance of furfural. These authors also found that water flux was relative constant by increasing the furfural feed concentration, although higher total permeation flux was obtained due to the increase of furfural permeation flux. Ghosh et al. [18] also observed an increase of furfural permeation flux and total permeation flux with increasing furfural concentration in the feed from 2 to 8 wt (%), by using a polyurethaneurea membrane. The increase of total permeation flux observed by these authors was related to the so-called bulk flow [18]. This phenomenon was not observed in this work, as the total permeation fluxes were constant for both membranes, due to the lower concentration of furfural in the feed used in this study.

**Figure 5.3b** shows the enrichment factor and PSI for furfural as a function of furfural concentration in the feed. Enrichment factor for PDMS membrane remained more or less constant by increasing the furfural concentration, in the range studied in this work, while it increased until reaching a plateau around 0.85 g/L for POMS membrane. According to these

results, the PSI remained constant for PDMS, while for POMS increased up to furfural concentrations around 1.3 g/L.

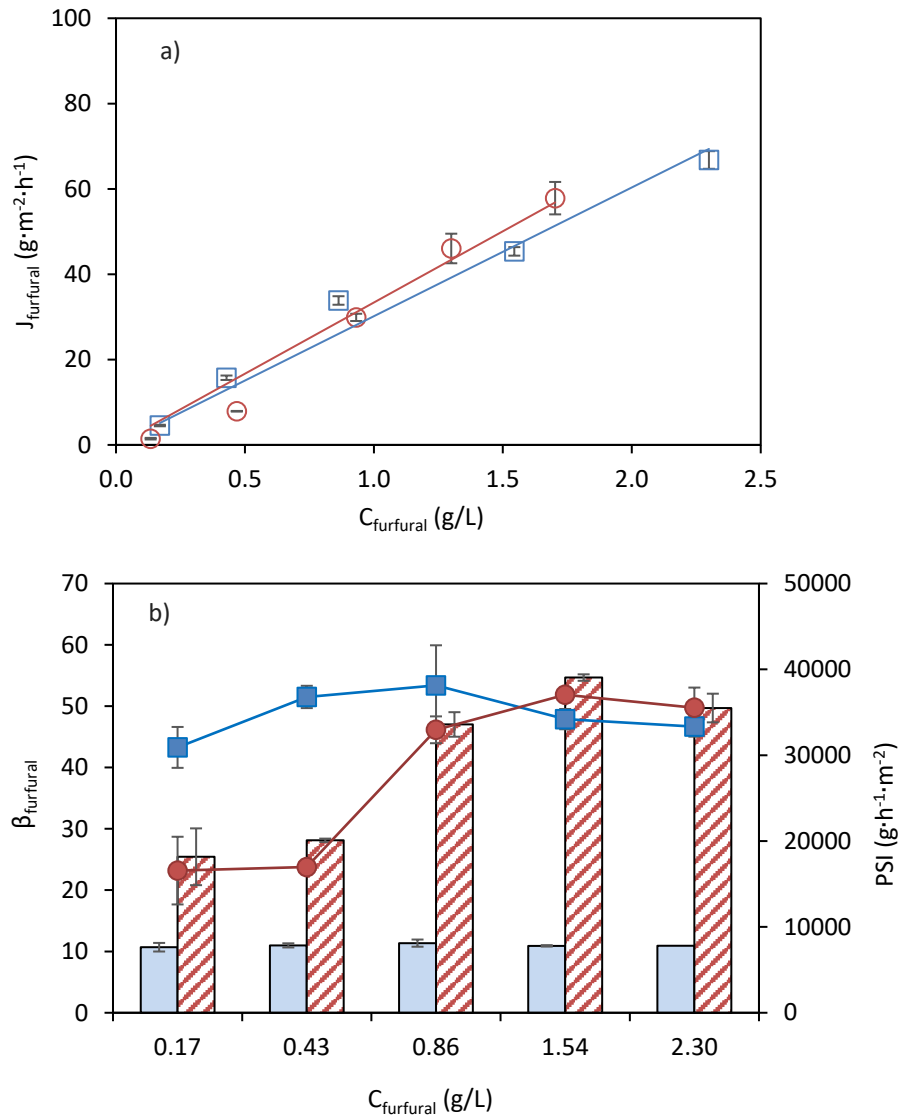


**Figure 5.3. a)** Furfural permeation flux as a function of furfural feed concentration:

(□ PDMS membrane,  $J_{\text{furfural}} = 30.17 \cdot C_{\text{furfural,feed}}$ ,  $R^2 = 0.9676$ ; ○ POMS,

$J_{\text{furfural}} = 33.38 \cdot C_{\text{furfural,feed}}$ ,  $R^2 = 0.9662$ ) and **b)** enrichment factor,  $\beta$  (□ PDMS, ▨ POMS)

and PSI (■ PDMS, ● POMS) for furfural as a function of furfural concentration in the feed.

### **3.4. Pervaporation of subcritical water hydrolysates. Permeate and retentate composition.**

Furfural removal and recovery by PV from subW hydrolysates was studied under unsteady state by using a smaller reactor at a pervaporation temperature of  $55.5 \pm 0.5$  °C, and a permeate pressure of 300 Pa, for both type of membranes. The initial feed concentration for both types of membranes were collected in **Table 5.2**. The permeate concentration of the components present in the subW hydrolysates was determined along the PV process. The composition of the retentate after PV was also collected in **Table 5.2**.

The total permeation fluxes of synthetic organic mixtures were registered along the PV time and compared with water permeation flux, for both types of membranes, in section 3.3.1 (see **Figure 5.1**). The total permeation flux for subW hydrolysates registered along PV time for both membranes has been represented and compared with the total permeation flux obtained for diluted synthetic mixtures with each membrane in **Figure 5.4**. It can be noted that for POMS membranes the presence of other compounds in the subW hydrolysates did not affect the permeation flux. However, for PDMS membranes the total permeation flux for subW hydrolysates was lower than for diluted synthetic mixtures, due to the presence of additional components in the subW hydrolysate that might influence the total permeation through the membrane. Similarly, Terblanche [8] observed that, for PDMS membranes, the total permeation flux for acidic hydrolysates were lower than the total permeation flux during the PV of binary mixtures at the same concentration as the acidic hydrolysates (4.8 g/L of acetic acid and 1 g/L of furfural). This decrease was more notable at high temperatures. For instance, at 70 °C a total permeation flux around  $1700 \text{ g}\cdot\text{m}^{-2}\cdot\text{h}^{-1}$  was obtained for synthetic binary mixtures, while this value was reduced to  $1300 \text{ g}\cdot\text{m}^{-2}\cdot\text{h}^{-1}$  in the acidic hydrolysates, indicating a permeation flux decrease of 24%. However, when PV was performed at 60 °C the decrease of permeate flux was lower than at 70 °C, around 14% of decrease. These authors also performed PV of acidic hydrolysate by using a poly(ether-block-amide), PEBA, membrane, observing a higher reduction in the total permeation flux than for synthetic dilute mixture compared to PDMS membranes. At 60 °C, the total permeation flux decreased from  $1250 \text{ g}\cdot\text{m}^{-2}\cdot\text{h}^{-1}$  for binary dilute mixtures to  $650 \text{ g}\cdot\text{m}^{-2}\cdot\text{h}^{-1}$  for the acidic hydrolysate; while, at 70 °C the decrease was even higher, about 68% from  $2400 \text{ g}\cdot\text{m}^{-2}\cdot\text{h}^{-1}$  to  $750 \text{ g}\cdot\text{m}^{-2}\cdot\text{h}^{-1}$ .

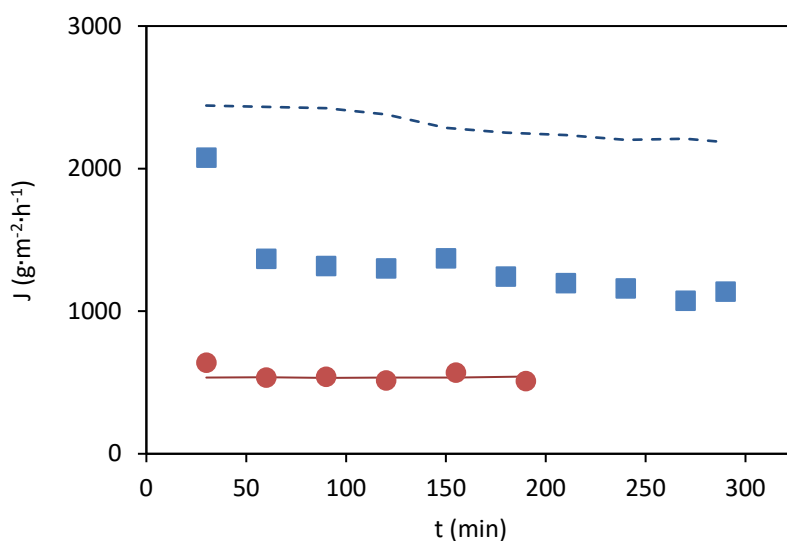


**Figure 5.4.** Total permeation flux for subW hydrolysates registered along PV time for ■ PDMS and ● POMS membranes. Lines represent the total permeation flux obtained for diluted synthetic mixtures with each membrane (--- PDMS, — POMS).

The permeate composition consisted of water, furfural, and small amounts of organic acids for both type of membranes. **Figure 5.5** shows the concentration of furfural in the permeates along the pervaporation experiments for both membranes. The furfural concentration in the permeates continuously decreased since furfural concentration in the retentate side decreased along the PV time. The furfural concentration in the permeate was higher for POMS membrane than for PDMS membrane, according to the higher furfural selectivity of POMS membrane than PDMS. The furfural percentage removal is also presented in **Figure 5.5**. It was evaluated considering the permeate volume and furfural concentration in the permeate at the different time intervals analyzed according to Equation 5.5:

$$\% \text{ Furfural removal} = \frac{V_{\text{permeate}} \cdot C_{p,\text{furfural}}}{V_{o,\text{feed}} \cdot C_{f,\text{furfural}}} \cdot 100 \quad [5.5]$$

where  $V_{\text{permeate}}$  is the volume of permeate in L,  $V_{o,\text{feed}}$  the initial feed volume in L,  $C_{p,\text{furfural}}$  and  $C_{f,\text{furfural,feed}}$  the concentration of furfural in the permeate and in the initial feed, respectively in g/L.

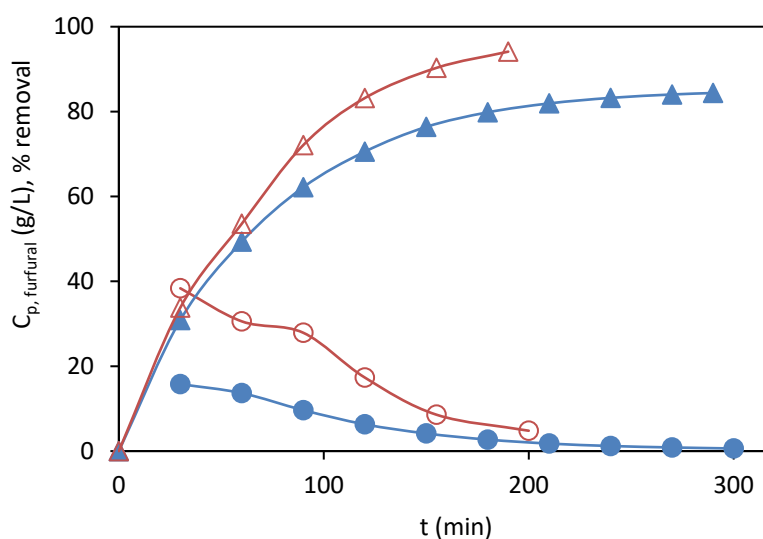


**Figure 5.5.** Furfural concentration in the permeate ( $C_{p, \text{furfural}}$ ) for each membrane (● PDMS, ○ POMS) and percentage removal (▲ PDMS, △ POMS) as a function of PV time.

After 190 min of PV, POMS membrane reached a removal of furfural of 93.9 %, while 84.4 % was obtained for PDMS membrane at 290 min. The final retentate was analyzed and the furfural concentration was 0.35 g/L and 0.17 g/L in the PDMS and POMS membrane, respectively from initial feed concentrations of 1.7 and 1.3 g/L (see **Table 5.2**). The decrease in the furfural concentration in the retentate was due to the furfural removal by PV. A small control sample of subW hydrolysate was subjected at the same temperature/time conditions as during PV, and furfural concentration did not vary due to chemical reactions. The percentage removal, evaluated from the final furfural concentration of the retentate, yielded values of 80 and 87% for PDMS and POMS membrane respectively, which indicates a good mass balance performance with deviations of 5 % and 8 % for PDMS and POMS membrane, respectively.

The concentration of the other components of the subcritical water hydrolysates was also followed in the different permeate collected. However, only acetic and formic acids could be determined, with negligible amounts for the other compounds present in the subW hydrolysates (see **Table 5.2**). **Figure 5.6** shows the concentration of acetic and formic acids in the permeate. According to the results previously presented, the enrichment factor



of both organic acids was less than the unity, as the concentration of these compounds was lower in the permeate than in the initial feed and remained more or less constant. The final concentration of the components in the subW hydrolysates after PV is listed in **Table 5.2**. Since furfural was the only component that permeated preferentially through the PDMS and POMS membranes, the concentration for the other components of the subW hydrolysates, slightly increased after the PV process, due to the removal of water in the permeate side. Geer et al. [7] also indicated that PV leaves the sugars intact and therefore, if water is removed, they will be slightly concentrated in the retentate.

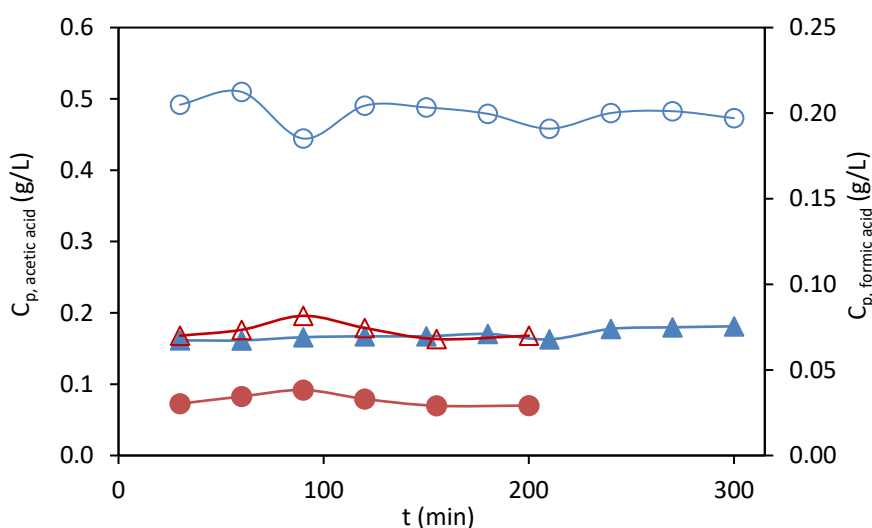


**Figure 5.6.** Acetic and formic acids concentration in the permeate ( $C_{p,i}$ ) for each membrane ( $C_{p, \text{acetic acid}}$ : ● PDMS, ○ POMS,  $C_{p, \text{formic acid}}$ : ▲ PDMS, △ POMS) as a function of pervaporation time.

**Table 5.4** summarizes the comparison between the PDMS and POMS performance in terms of permeate yield and composition. The comparison was established at a similar PV time of 210 and 200 min for PDMS and POMS, respectively. The permeate yield,  $Y_{\text{permeate}}$ , was calculated according to Equation 5.6 [19]:

$$Y_{\text{permeate}} = \frac{\text{mass of permeate}}{\text{initial feed mass}} \cdot 100 \% \quad [5.6]$$

**Table 5.4.** Comparison of permeates after PV of subW hydrolysates through PDMS and POMS membranes. Permeate yield ( $Y_{\text{permeate}}$ ) and furfural recovery ( $R_{\text{furfural}}$ ) are expressed as percentage. Organic compounds concentration in the permeate ( $C_{p,i}$ ) is expressed in g/L.

Membrane	t (min)	$Y_{\text{permeate}}$	$R_{\text{furfural}}$	$C_{p, \text{furfural}}$	$C_{p, \text{acetic acid}}$	$C_{p, \text{formic acid}}$
PDMS	210	16.8	81.9	8.5	0.61	0.07
POMS	200	6.0	94.1	20.9	0.57	0.08

The PDMS membrane presented higher permeation flux, which means a higher permeate yield, but also a lower furfural concentration in the permeate (8.5 g/L), due to the higher water permeation flux through PDMS membranes. On the other hand, the POMS membrane generated lower permeate yield but higher furfural concentration in the permeate (20.9 g/L), due to the higher selectivity of the membrane towards furfural and the lower water permeation flux. The concentrations of the organic acids in the permeate were of the same order for both types of membranes. Based on these results, we can conclude that for a furfural removal efficient process PDMS membrane is a good option since similar furfural recovery was achieved by both types of membranes while higher permeation flux was obtained by PDMS membrane. However, by using POMS membrane, higher furfural concentration in the permeate was obtained that could be useful for further uses of furfural as chemical platforms.

Some studies about the PV treatment applied to acid hydrolysates from different biomass have been found in the literature. Greer et al. [7] hydrolysed *Miscanthus × giganteus* with 1.5% (w/w) of sulfuric acid, at a 25% (w/w) of biomass loading, at 190 °C for 1 min. The PV processing of the acidic hydrolysates containing 0.69 g/L of furfural resulted in an aqueous permeate with 6.3 g/L of furfural, with a PV separation factor of 8.6, by using a PDMS membrane. Terblanche [8] carried out PV experiments for acidic hydrolysate of wood at various temperatures (40-80 °C) with a feed concentration of furfural, formic and acetic acids of 1.5, 0.71 and 4.58 g/L, respectively. When using a PDMS membrane, the permeate concentration of each compound varied with the PV temperature in the following ranges: furfural (1.32 - 3.28 g/L), formic acid (0.06 - 0.09 g/L) and acetic acid (0.77 - 1.43 g/L). The highest selectivity of furfural and acetic acid was obtained at 50 and

80 °C, respectively. The highest furfural and organic acids enrichment factors obtained in that study were,  $2.12 \pm 0.07$  and  $0.25 \pm 0.02$ , respectively.

However, to the best of the author's knowledge, no pervaporation study has been conducted to investigate the fractionation of subcritical water hydrolysates with organophilic membranes.

## 4. Conclusions

Both membranes, PDMS and POMS were selective towards furfural in the pervaporation experiments carried out with pure components. However, both membranes were more selective to water than to acetic or formic acid with enrichment factors lower than the unit.

The pervaporation separation of furfural from subcritical water hydrolysate helped to reduce the furfural concentration in the subcritical water hydrolysates from the initial feed concentrations of 1.7 and 1.3 g/L to retentate concentrations of 0.35 g/L and 0.17 g/L by using PDMS and POMS membranes, respectively. Furthermore, the sugars concentration in the retentate slightly increased after the PV process, due to the removal of water in the permeate side.

The commercial PV membranes, POMS and PDMS, have demonstrated the ability to remove and recover furfural from the subcritical water BSG hydrolysates. (93.9% and 84.4%, respectively). The use of POMS membranes allows the recovery of high concentrated furfural in the permeate (20.9 g/L).

Pervaporation has been demonstrated as an efficient technology to be incorporated in a biorefinery process, after the subcritical water pretreatment of BSG, considering a double objective. On one hand, to remove furfural from the subcritical water hydrolysates, being furfural, the main fermentation inhibitor found in the subW hydrolysates, which may allow their use as fermentation broths. On the other hand, to recover and concentrate furfural with high purity to be used as a biomass-derived platform chemical to produce renewable chemicals.

## References

- [1] V. Kitryte, A. Šaduikis, and P. R. Venskutonis, "Assessment of antioxidant capacity of brewer's spent grain and its supercritical carbon dioxide extract as sources of valuable dietary ingredients," *Journal of Food Engineering*, vol. 167, pp. 18–24, 2015, doi: 10.1016/j.jfoodeng.2014.12.005.
- [2] P. Alonso-Riaño, M. T. Sanz, O. Benito-Román, S. Beltrán, and E. Trigueros, "Subcritical water as hydrolytic medium to recover and fractionate the protein fraction and phenolic compounds from craft brewer's spent grain," *Food Chemistry*, vol. 351, no. February, p. 129264, 2021, doi: 10.1016/j.foodchem.2021.129264.
- [3] P. Alonso-Riaño, M. T. Sanz Diez, B. Blanco, S. Beltrán, E. Trigueros, and O. Benito-Román, "Water Ultrasound-Assisted Extraction of Polyphenol Compounds from Brewer's Spent Grain: Kinetic Study, Extract Characterization, and Concentration," *Antioxidants*, vol. 9, no. 3, p. 265, 2020, doi: 10.3390/antiox9030265.
- [4] M. J. Cocero *et al.*, "Understanding biomass fractionation in subcritical & supercritical water," *Journal of Supercritical Fluids*, vol. 133, no. August 2017, pp. 550–565, 2018, doi: 10.1016/j.supflu.2017.08.012.
- [5] N. Akiya and P. E. Savage, "Roles of water for chemical reactions in high-temperature water," *Chemical Reviews*, vol. 102, no. 8, pp. 2725–2750, 2002, doi: 10.1021/cr000668w.
- [6] A. Bokhary, L. Cui, H. J. Lin, and B. Q. Liao, "A review of membrane technologies for integrated forest biorefinery," *Journal of Membrane Science and Research*, vol. 3, no. 3, pp. 120–141, 2017, doi: 10.22079/jmsr.2016.22839.
- [7] D. R. Greer *et al.*, "Fermentation of hydrolysate detoxified by pervaporation through block copolymer membranes," *Green Chemistry*, vol. 16, no. 9, pp. 4206–4213, 2014, doi: 10.1039/c4gc00756e.
- [8] H. A. Terblanche, "Fractionation of an acidic hydrolysate from steam-treated wood using pervaporation," *North-West University (South Africa), Potchefstroom Campus*, May 2017, <https://repository.nwu.ac.za/handle/10394/25888>.
- [9] R. Mariscal, P. Maireles-Torres, M. Ojeda, I. Sádaba, and M. López Granados, "Furfural: A renewable and versatile platform molecule for the synthesis of chemicals and fuels," *Energy and Environmental Science*, vol. 9, no. 4, pp. 1144–1189, 2016, doi: 10.1039/c5ee02666k.
- [10] F. Qin, S. Li, P. Qin, M. N. Karim, and T. Tan, "A PDMS membrane with high pervaporation performance for the separation of furfural and its potential in industrial application," *Green Chemistry*, vol. 16, no. 3, pp. 1262–1273, 2014, doi: 10.1039/c3gc41867g.
- [11] H. Shan *et al.*, "Molecular dynamics simulation and preparation of vinyl modified polydimethylsiloxane membrane for pervaporation recovery of furfural," *Separation and Purification Technology*, vol. 258, no. P2, p. 118006, 2021, doi: 10.1016/j.seppur.2020.118006.

- [12] D. Cai *et al.*, "Biobutanol from sweet sorghum bagasse hydrolysate by a hybrid pervaporation process," *Bioresource Technology*, vol. 145, pp. 97–102, 2013, doi: 10.1016/j.biortech.2013.02.094.
- [13] J. B. Sluiter, R. O. Ruiz, C. J. Scarlata, A. D. Sluiter, and D. W. Templeton, "Compositional analysis of lignocellulosic feedstocks. 1. Review and description of methods," *Journal of Agricultural and Food Chemistry*, vol. 58, no. 16, pp. 9043–9053, 2010, doi: 10.1021/jf1008023.
- [14] R. Martínez, M. T. Sanz, and S. Beltrán, "Concentration by pervaporation of representative brown crab volatile compounds from dilute model solutions," *Journal of Food Engineering*, vol. 105, no. 1, 2011, doi: 10.1016/j.jfoodeng.2011.02.009.
- [15] R. Martínez, M. Teresa Sanz, and S. Beltrán, "Concentration by pervaporation of brown crab volatile compounds from dilute model solutions: Evaluation of PDMS membrane," *Journal of Membrane Science*, vol. 428, pp. 371–379, 2013, doi: 10.1016/j.memsci.2012.10.035.
- [16] R. Castro-Muñoz, F. Galiano, and A. Figoli, "Chemical and bio-chemical reactions assisted by pervaporation technology," *Critical Reviews in Biotechnology*, vol. 39, no. 7, pp. 884–903, 2019, doi: 10.1080/07388551.2019.1631248.
- [17] S. Y. Lu, C. P. Chiu, and H. Y. Huang, "Pervaporation of acetic acid/water mixtures through silicalite filled polydimethylsiloxane membranes," *Journal of Membrane Science*, vol. 176, no. 2, pp. 159–167, 2000, doi: 10.1016/S0376-7388(00)00434-8.
- [18] U. K. Ghosh, N. C. Pradhan, and B. Adhikari, "Separation of furfural from aqueous solution by pervaporation using HTPB-based hydrophobic polyurethaneurea membranes," *Desalination*, vol. 208, no. 1–3, pp. 146–158, 2007, doi: 10.1016/j.desal.2006.04.078.
- [19] T. M. Brueckner, P. G. Pickup, and K. A. Hawboldt, "Improvement of bark pyrolysis oil and value added chemical recovery by pervaporation," *Fuel Processing Technology*, vol. 199, no. September 2019, p. 106292, 2020, doi: 10.1016/j.fuproc.2019.106292.



# CHAPTER 6

---

**Second generation bioethanol production from subcritical water pretreated brewer's spent grain within a biorefinery concept**

**Based on the article:**

P. Alonso-Riaño, A. Xavier, M. Amândio, S. Beltrán, M. T. Sanz

“Second generation bioethanol production from subcritical water pretreated brewer's spent grain within a biorefinery concept”.





## CAPÍTULO 6

### Producción de bioetanol de segunda generación a partir de bagazo de cerveza pretratado con agua subcrítica en un concepto de biorrefinería

---

#### Resumen

En este capítulo se estudió la producción de bioetanol a partir de bagazo de cerveza pretratado con agua subcrítica. El pretratamiento con agua subcrítica se realizó en un reactor discontinuo a  $174 \pm 3$  °C, durante 60 minutos y se introdujo en el reactor un 5% de BSG seco (p/v). Después de este pretratamiento, la hidrólisis enzimática con celulasa (Celluclast, 40 FPU/g) arrojó un rendimiento de glucosa cercano al 100%. Se utilizó tampón citrato de sodio (0,05 M), a pH = 4,8, como medio de reacción. La posterior fermentación del hidrolizado enzimático mediante la levadura *Ethanol Red*<sup>®</sup>, resultó en una producción de etanol del 83% del rendimiento teórico máximo (0,511 g de etanol/g de glucosa), lo que corresponde a una productividad volumétrica de  $0,754 \text{ g}\cdot\text{L}^{-1}\cdot\text{h}^{-1}$ . La mayor productividad de etanol ( $1,073 \text{ g}\cdot\text{L}^{-1}\cdot\text{h}^{-1}$ ) se alcanzó mediante la sacarificación y fermentación simultánea del bagazo pretratado con agua subcrítica, con una alta carga de sólidos (25%), siguiendo una estrategia de alimentación por lotes. En estas condiciones, la mayor concentración de bioetanol (32,18 g/L) se obtuvo tras 30 h de fermentación. Estos resultados sugieren que el pretratamiento con agua subcrítica es una tecnología prometedora para la utilización de bagazo de cerveza como materia prima para la producción de bioetanol de segunda generación, dentro de un concepto de biorrefinería.

---

**Palabras clave:** tratamiento con agua subcrítica, biorrefinería, bagazo de cerveza, bioetanol, sacarificación y fermentación simultáneas



## Abstract

---

In this study, the production of bioethanol from subcritical water pretreated brewer's spent grain (BSG) was investigated. The subcritical water pretreatment was performed in a discontinuous reactor at  $174 \pm 3$  °C, during 60 min and 5 % of dry BSG (w/v) was charged into the reactor. After this pretreatment, the enzymatic hydrolysis yield of glucose was almost 100% by using the enzyme cocktail Celluclast at 40 FPU/g in 0.05 M sodium citrate buffer at pH = 4.8 as reaction medium. Subsequent fermentation of the enzymatic hydrolysate by *Ethanol Red*<sup>®</sup> yielded 83% of the theoretical ethanol yield (0.511 g ethanol/g glucose), corresponding to a volumetric ethanol productivity of  $0.754 \text{ g}\cdot\text{L}^{-1}\cdot\text{h}^{-1}$ . The highest ethanol productivity ( $1.073 \text{ g}\cdot\text{L}^{-1}\cdot\text{h}^{-1}$ ) was achieved by simultaneous saccharification and fermentation of the hydrothermal pretreated BSG at high solid loading following a fed-batch strategy. At these conditions, the highest concentration of ethanol (32.18 g/L) was obtained after 30 h of fermentation. These results suggest that subcritical water pretreatment is a promising technology for increasing the valorization of BSG as a feedstock for the second-generation bioethanol production within a biorefinery concept.

---

**Keywords:** Subcritical water pretreatment, biorefinery, brewer's spent grain, bioethanol, high solid loading, simultaneous saccharification and fermentation.



## 1. Introduction

Biorefinery has been considered a promising concept for processing biomass into different products and energy, being very important in the context of circular economy, closing loops of streams, and valorizing multiple outputs [1]. In this regard, Sganzerla et al. [2] demonstrated the possibility of developing a biorefinery using brewer's spent grain (BSG) as raw material to obtain several valuable compounds such as arabinoxylans, proteins, ferulic acid, xylitol, xylose, lactic acid, butanol, biogas, fertilizer, and bioethanol.

BSG is the main solid by-product generated in breweries, which remains after the mashing and wort filtration process, representing 85% of the total by-products generated. It was estimated that about 20 kg of BSG are produced per 100 L of beer [3]. BSG is a lignocellulosic material mainly composed of hemicelluloses, cellulose, protein, and lignin, being the polysaccharide fraction more than 50% of the BSG composition on a dry weight basis [4]. The monomeric sugars required to feed the fermentation processes to produce biofuels can be released by enzymatic saccharification of cellulose and hemicelluloses. However, a pretreatment step is needed before performing enzymatic saccharification due to the complex morphological macrostructure of lignocellulosic materials and their characteristic recalcitrance. Different pretreatment methods have been applied, being acid and alkaline treatments the most commonly used. However, the use of subcritical water (subW) as an eco-friendly method for lignocellulose pretreatment has been proposed in recent studies [5]–[7]. SubW is pressurized water in its liquid state in the temperature range from 100 °C to 374 °C. Under these conditions, water presents unique properties such as higher ionic product and lower dielectric constant than at ambient conditions [8]. During subW pretreatment different bioactive compounds can be released from the biomass, such as phenolic compounds, protein, and amino acids [4]. The recovery of these valuable compounds during the pretreatment, as well as fermentable carbohydrates, constitutes a significant advance that could enhance the feasibility of the industrial implementation of lignocellulosic biomass-based biorefineries [1].

The subW pretreatment was performed in a discontinuous reactor at 174 °C during a total treatment time of 60 min, which includes the preheating time of around 15 min. These conditions were selected according to the results obtained in a previous work (Chapter 4).

In that work, when subW pretreatment of the BSG was performed under the mentioned conditions, almost a complete solubilization of the hemicellulose fraction was observed and the remaining solid was enriched in cellulose and lignin. After the pretreatment, enzymatic hydrolysis was carried out at different solid loadings. It has been found that the lower the hemicellulose and lignin content in the sample, the higher the efficiency of cellulose hydrolysis [9]. However, according to Chen et al. [7], the glucose concentration after enzymatic hydrolysis is a more appropriate response value for optimising subcritical water process than the sugar content in the liquid fraction, the cellulose retention rate or lignin removal rate in solid residues. Therefore, the main objective of this work was to evaluate the enzymatic yield by using cellulases for raw BSG and subW-pretreated BSG to assess the effect of subW pre-treatment.

In the context of bioethanol production, different fermentation strategies can be employed, such as separate hydrolysis and fermentation (SHF) or simultaneous saccharification and fermentation (SSF). The main advantage of SHF is that the hydrolysis and the fermentation processes can be performed under their different optimal conditions. However, using SSF instead of SHF may reduce the total time required for ethanol production from BSG [10] increasing productivity. Furthermore, the use of high solids loading in the saccharification, and fermentation processes may increase bioethanol concentration and, consequently, reduce distillation costs of the lignocellulose-to-ethanol process [5].

This work aimed to evaluate the integral valorization of brewer's spent grain within a biorefinery concept using environmentally friendly subcritical water, focusing on cellulosic ethanol production. The effectiveness of subW as pretreatment to improve the BSG enzymatic yield of glucose by using cellulases at different solids loadings was evaluated. A comparison of different fermentation configurations, such as SHF and SSF was performed, namely in terms of ethanol concentration and productivity. Furthermore, one of the main goals of this work was to improve ethanol productivity from BSG by increasing solids loading up to 25% by following a fed-batch strategy and reducing overall time when performing SSF. In addition, the overall process mass balance for ethanol production from BSG under the different conditions was investigated to valorize all fractions obtained along the process in the context of a biorefinery concept.

## 2. Materials and methods

### 2.1. Raw material

The raw material used in this work was the brewer's spent grain kindly supplied by San Miguel S.A. This raw material was first preconditioned, as soon as obtained, by washing it with water until uncoloured washing water and drying it in an air convection oven (45 °C, 3 h) until reaching a final moisture content of 8% (w/w).

The dry BSG was milled down to a particle size lower than 0.5 mm in a Retsch SM100 mill. Biomass characterization was performed according to the NREL protocols [11]. Carbohydrates were quantified by high-performance liquid chromatography (HPLC) with a Bio-Rad Aminex-HPX-87 H column, a variable wavelength detector (VWD) and a refractive index detector (RID) using a mobile phase constituted by 0.005 M sulfuric acid. The column and the RID detector were maintained at 40 °C. A Megazyme Total Starch Assay (amyloglucosidase/ $\alpha$ -amylase method) was followed to determine starch in the BSG. Moreover,  $\beta$ -glucans content was performed using a Megazyme  $\beta$ -Glucan Assay Kit (Mixed Linkage). Protein in the raw material was estimated from the nitrogen content present in the samples as measured by elemental analysis and considering a nitrogen factor of 6.25 [4]. The oil content of the BSG was determined by Soxhlet extraction (Buchi B-8111) using hexane as solvent.

### 2.2. Subcritical water hydrolysis

Subcritical water hydrolysis treatment was carried out in a discontinuous stainless-steel reactor of 500 mL maximum capacity. The heating system consisted of a heating jacket of 230 V and 400 W covering the reactor, used to reach the working temperature. A Pt100 sensor connected to a PID system and placed inside the reactor helps to control and register the temperature during the hydrolysis. The biomass was loaded into the reactor and filled with water. The mixture was heated up to the desired temperature and pressured was fixed at 50 bars using nitrogen gas and maintained during all the process. SubW hydrolysis was carried out at  $174 \pm 3$  °C for a total treatment time of 60 min and a biomass loading of 5% (w/v).

The liquid stream was analyzed in terms of protein content, monomeric sugars and oligomeric sugars, as it was described in Chapter 4. Monosaccharides and degradation products were determined by HPLC as described in section 2.1. Total sugars (monomeric + oligomeric sugars) were determined following the NRLE protocols [11]. Protein content in the liquid stream was determined from the nitrogen content measured by using a TOC/TN analyzer (Shimadzu TOC-V CSN analyzer) using  $\text{KNO}_3$  as standard after applying a nitrogen factor of 6.25.

The remaining solid after subW treatment (pretreated BSG) was washed to remove the residual sugars and inhibitors before drying it at 45 °C. Chemical characterization of pretreated BSG was performed as described for the raw material. The washing water was analyzed to ensure no residual compounds remained on the solid residue. Several subW batch were performed at the same conditions in the 0.5 L reactor, the remaining solids were collected and the mix of all of them was used as the pretreated BSG for further enzymatic hydrolysis.

### **2.3. Enzymatic hydrolysis**

A cellulolytic cocktail (Celluclast 1.5 L) kindly provided by Novozymes A/S (Denmark) was utilized to hydrolyse both raw BSG and pretreated BSG. Celluclast 1.5 L is a liquid cellulases cocktail with 1.2 g/mL of density and declared activity of 700 endoglucanase units/g. Its filter paper unit (FPU) activity was determined according to NREL standard procedure as 53.7 FPU/mL. The enzymatic loading was always 40 FPU/g of solid in the presence of a 0.05 M sodium citrate buffer at pH 4.8. The effect of solids loading in the enzymatic hydrolysis yield was studied at 5, 10, 15 and 20 % solids loading for BSG and at 5 and 8 % solid loading for subW pre-treated BSG, based on oven-dried material (w/v). The experiments were conducted for 94 h, with a stirring rate of 100 rpm, at 50 °C and samples were taken at 12, 22, 46, 70 and 94 h. The reaction was stopped by heating the samples in boiling water for 5 min for enzymes denaturation. After cooling the samples in ice for 5 min, they were centrifuged at 13000 rpm for 10 min. After proper dilution, the supernatant was analyzed for monomeric sugars, acetic acid, lactic acid, and furfural determination. Furthermore, blanks of the enzymatic solutions were prepared and analyzed by HPLC, to



subtract the sugar content since the commercial cellulolytic complex enzymes could contain some sugar in monomeric or oligomeric forms. These assays were performed in duplicate.

## 2.4. Microorganism

*Saccharomyces cerevisiae* (Ethanol Red<sup>®</sup>) was kindly provided by Leaf by Lesaffre Advanced Fermentations (Marcq-en-Baroeul, France). This strain was grown at 28 °C and maintained at 4 °C on Petri dishes with solid yeast medium (YM) prepared with 10 g/L glucose, 5 g/L xylose, 5 g/L peptone, 3 g/L malt extract and 3 g/L yeast extract (the pH adjusted to 5.5), and 20 g/L agar.

## 2.5. Pre-Inoculum and Inoculum

Pre-inoculum was prepared by transferring a colony from a maintenance YM Petri dish to 10 mL liquid YM (similar to solid YM, except agar) and was incubated for 24 h at 28 °C and 180 rpm. The inoculum was prepared by transferring the pre-inoculum to 40 mL of fresh liquid YM. The inoculum was incubated at 28 °C and 180 rpm for 14 h. These procedures were carried out in duplicate.

## 2.6. Fermentations

### 2.6.1. Separate hydrolysis and fermentation assays (SHF)

The hydrolysate obtained after 46 h of enzymatic hydrolysis of the subW pretreated BSG at 8% (w/v) of solid concentration (section 2.3) was centrifuged for 1 h at 5000 rpm and 4 °C (Megafuge 16R, Thermo Scientific, Osterode am Harz, Germany). The supernatant was sterilized by autoclaving at 121 °C for 20 min (Uniclave 88, AJC, Cacém, Portugal). The resulting hydrolysate was analyzed by HPLC and submitted to fermentations in 250 mL Erlenmeyer flasks with a working volume of 50 mL, incubated at 28 °C and 180 rpm. Supplementation was composed by 2.0 g/L (NH<sub>4</sub>)<sub>2</sub>HPO<sub>4</sub>, 1.0 g/L (NH<sub>4</sub>)<sub>2</sub>SO<sub>4</sub>, 0.5 g/L MgSO<sub>4</sub>·7H<sub>2</sub>O, and 2.5 g/L yeast extract. Fermentation media was composed of 85% (v/v) hydrolysate, the exact volume of inoculum that guarantees an optical density at 620 nm (OD<sub>620 nm</sub>) of about 0.400, 5% (v/v) of supplementation solution and NaCl solution (0.9%) to reach the final volume. Steril samples were collected periodically, and after biomass and

pH monitorisation, they were centrifuged at 13.000 g for 10 min. The supernatant was kept to determine glucose, xylose, glycerol, and ethanol concentrations.

### **2.6.2. Simultaneous saccharification and fermentation (SSF)**

The SSF experiments were performed in 250 mL Erlenmeyer flasks with a total volume of 50 mL of citrate buffer (0.05 M, pH 4.8) containing the nutrients previously described for SHF and the exact volume of inoculum that guarantees an  $OD_{620\text{ nm}}$  of about 0.400. The substrates were subW pretreated BSG at 8%, 15% and 25% (w/v) solids loading based on oven-dried material. SSF was started by adding the enzymatic consortium and inoculum simultaneously. Enzyme dosages used were the same as in the enzymatic hydrolysis experiments. The assays were carried out at 38 °C and 180 rpm. Sampling was performed as described in section 2.6.1.

### **2.6.3. Fed-batch strategy**

A fed-batch approach was followed with an initial solids loading of 8% (w/v) based on the total working volume (50 mL), where 3.5 g of subW-pretreated BSG were fed after 2 h and 2 doses of 2.5 g were added after 4h and 8 h from the beginning, achieving a final concentration of 25% (w/v). The assays were carried out at 38 °C and 180 rpm in a total working volume of 50 mL. Sampling was performed as described in section 2.6.1.

## **2.7. Analytical methods**

The samples pH was measured using an electrode InPro 3030/200 (Mettler Toledo, Columbus, OH, USA) connected to a benchtop meter sensION+ MM340 (Hach, Loveland, CO, USA).

Biomass was monitored by measuring  $OD_{620\text{ nm}}$  (UVmini-1240, Shimadzu, Tokyo, Japan) and converted into concentration using a calibration curve of optical density versus biomass dry weight.

High-performance liquid chromatography (HPLC) was used to quantify glucose, xylose, lactic acid, acetic acid, furfural, glycerol, and ethanol. After centrifuged and filtered for 8 min at 8000 rpm (Eppendorf, Hamburg, Germany), samples were injected by autosampler

L-2200 (MiniSprin centrifuge, Hitachi, Ltd., Chiyoda, Japan) on a Rezex ROA-Organic Acid H+ (8%) 300 × 7.8 mm ion-exchange column (Phenomenex, Torrance, CA, USA) at 65 °C (oven Gecko 2000, CIL Cluzeau, Sainte-Foy-la-Grande, France) and detected by a refraction index detector L-2490 (Hitachi, Chiyoda, Japan). The injection volume was 10 µL and the eluent used was H<sub>2</sub>SO<sub>4</sub> 0.005 N, with a flow rate of 0.5 mL/min (pump L-2130, Hitachi). A standard calibration curve was used for the determination of metabolites concentration.

All analytical determinations were performed in triplicate. Average results, with standard deviations lower than 5%, were reported.

## 2.8. Calculations

The glucose and xylose yields were evaluated as the ratio of the amount of sugar released to the medium over the maximum potential yield of sugar obtained from the solid (raw BSG and subW pretreated BSG) characterization (Equation 6.1):

$$\text{Yield}_{\text{sugar}} (\%) = \frac{\text{Monomeric sugar in the enzymatic hydrolysate}}{\text{Sugar in solid BSG}} \cdot 100 \quad [6.1]$$

The ethanol yield in SHF was calculated according to Equation 6.2 to compare the results with values reported in the literature.

$$\text{Ethanol yield, SHF} (\%) = \frac{\text{Ethanol produced}}{\text{Glucose}_{\text{solution}} \times 0.511} \cdot 100 \quad [6.2]$$

Ethanol yield in SSF was calculated according to Equation 6.3. The ethanol yield in SHF was also calculated according to this equation, to compare the results with the SSF results on the same basis.

$$\text{Ethanol yield, SSF} (\%) = \frac{\text{Ethanol produced}}{\text{Glucan}_{\text{solid}} \times 1.11 \times 0.511} \cdot 100 \quad [6.3]$$

where 1.11 (180/162) is the stoichiometric factor for glucan hydration from glucose and 0.511 (46·2/180) for the glucose conversion into ethanol considering the maximal theoretical yield of ethanol (2 mole of ethanol produced from 1 mole glucose).

The volumetric ethanol productivity,  $\text{Prod}_{\text{vol}}$  (g·L<sup>-1</sup>·h<sup>-1</sup>) was calculated, considering the time when the maximum ethanol concentration was achieved:

$$Prod_{vol}(g \cdot L^{-1}h^{-1}) = \frac{[ethanol]_{max}}{\Delta t} \quad [6.4]$$

The ethanol yield coefficient per glucose,  $Y_{ethanol/glucose}$  ( $g \cdot g^{-1}$ ) and the biomass yield coefficient,  $Y_{biomass/substrate}$  ( $g \cdot g^{-1}$ ), were calculated according to Equations 6.5 and 6.6, respectively, considering glucose and xylose as substrate to biomass growth.

$$Y_{bioethanol/glucose} = -\frac{\Delta[bioethanol]}{\Delta[glucose]} \quad [6.5]$$

$$Y_{biomass/substrate} = -\frac{\Delta[biomass]}{\Delta[substrate]} \quad [6.6]$$

## 2.9. Statistical analysis

All values were expressed as mean  $\pm$  standard deviation from triplicate measurements. The significance of the differences was determined based on an analysis of the variance with the Fisher's Least Significant Difference (LSD) method at  $p$ -value  $\leq 0.05$  using the Statgraphics X64 software. Error bars in all graphs are 95% confidence intervals.

## 3. Results and discussion

### 3.1. Composition of raw BSG and subcritical water pre-treated BSG

The chemical composition of the BSG employed in this work is presented in **Table 6.1**, together with the chemical composition of pretreated BSG under subcritical water conditions, in a weight percentage dry basis. The amount of carbohydrates (glucan, xylan and arabinan) present as oligomers and monomers, and the protein and acid soluble lignin content in the subW hydrolysates per 100 g of dry raw BSG are also collected in **Table 6.1**. After subW treatment, 41.2% of solids remained into the reactor. Total protein content decreased from  $22.1 \pm 0.7\%$  (w/w) in raw BSG to  $12.1 \pm 0.1\%$  (w/w) in subW pretreated BSG, due to the solubilization of 67% of protein content in raw BSG during the treatment. The main polysaccharide fraction of raw BSG was hemicellulose, with  $32.0 \pm 0.6\%$  (w/w) and the cellulose fraction was  $14.0 \pm 0.2\%$  (w/w). In contrast, the subW pretreated BSG showed a 1.8-fold higher glucans content than raw BSG. Furthermore, most of the hemicellulose fraction was removed from the BSG and recovered in the subW hydrolysates. Arabinose

was not detected in the subW pretreated BSG, according to our analytical methodology. The cellulose/hemicellulose ratio in raw BSG was 0.44, while in the subW residue, this ratio significantly increased up to 15. On the other hand, the lignin content was 2.3-fold higher in the pretreated BSG due to the extraction of other compounds more easily hydrolyzed. Additionally, the insoluble lignin-soluble lignin ratio is a parameter indicative of the effects of heat treatment in BSG [6]. This ratio was 3.5-fold higher in the residue obtained after subcritical water treatment than in raw BSG, suggesting that the hydrothermal treatment has caused changes in the chemical structure of lignin. The mass balance of the subW process is included in Section 3.5 (**Figure 3.7**).

**Table 6.1.** Chemical composition of raw BSG and BSG pretreated with subW, and concentration of each compound in the subW hydrolysate expressed as g of compound per 100 g of dry raw BSG.

Compound	Raw BSG (% dwb)	subW pretreated BSG (% dwb)	subW hydrolysate (g/100 gBSG)
Glucans	19.1 ± 0.2	35.1 ± 0.3	3.51 ± 0.02
Starch	4.11 ± 0.06	-	
B-glucan	0.99 ± 0.01	-	
Cellulose	14.0 ± 0.2	-	
Hemicellulose	32.0 ± 0.6	2.22 ± 0.04	
Xylan	21.6 ± 0.4	2.22 ± 0.04	21.95 ± 0.4
Arabinan	9.5 ± 0.4	Not detected	6.85 ± 0.3
Acetate	0.93 ± 0.05	Not detected	
Lignin	20.8 ± 0.2	47.1 ± 0.5	
Acid insoluble	15.5 ± 0.1	42.9 ± 0.4	
Acid soluble	5.3 ± 0.2	4.2 ± 0.1	3.11 ± 0.01
Ash	3.32 ± 0.06	2.7 ± 0.1	
Proteins	22.1 ± 0.7	12.1 ± 0.1	14.82 ± 0.04

Values are expressed as mean ± standard deviation from triplicate determination.

### 3.2. Enzymatic Saccharification of raw BSG and pre-treated BSG

Raw BSG was submitted to enzymatic hydrolysis by using a commercial cellulolytic complex (Celluclast 1.5 L). Different solids loading concentrations (2, 5, 10 and 20% w/v)

were assayed. As can be seen in **Figure 6.1 a**, the maximum glucose concentration was achieved after 22 h for all the solid concentrations evaluated in this work. The concentration of glucose in the hydrolysates drastically decreased after this maximum due to the formation of lactic acid (see **Figure 6.1 d**). According to the literature, lactic acid fermentation may occur spontaneously, when anaerobic conditions, water activity, moisture, salt concentration, and temperature are favourable for the growth of the autochthonous lactic acid bacteria [12]. Lactic acid was not found in the enzymatic hydrolysates from subW pretreated BSG, suggesting that this pretreatment could act also like a sterilizing treatment, avoiding the step of autoclaving and, consequently, reducing costs.

The maximum concentration of glucose reached for each experiment increased from  $1.88 \pm 0.07$  g/L to  $7.24 \pm 0.01$  g/L by increasing the substrate concentration from 5% to 20%, respectively, corresponding to hydrolysis yields of  $18.9 \pm 0.7\%$  and  $18.2 \pm 0.2\%$ . Surprisingly, no substantial differences were found in the hydrolysis yield when solid concentration was increased, although the highest yield ( $20.7 \pm 0.3\%$ ) was reached for 10% of solids. The glucose concentration obtained in these hydrolysates was too low to be submitted to further fermentation to obtain bioethanol in a feasible way. Similar results can be found in the literature for raw BSG. For instance, Michelin and Teixeira [13] achieved a cellulose conversion to glucose of  $36.97 \pm 1.76\%$  when performing enzymatic hydrolysis of 5% (w/v) raw BSG for 72 h with Cellic Ctec2 and NS 22083 (Novozymes).

To improve enzymatic digestibility, BSG was submitted to subW. In the present work, almost a complete conversion of cellulose to glucose has been achieved for both solid concentrations assayed, 98.2% and 99.5% for 5% and 8% (w/v) solids, respectively. That means a glucose concentration of  $19.15 \pm 0.09$  and  $31.05 \pm 0.06$  g/L, respectively, after 94 h of treatment (see **Figure 6.2a**). Nevertheless, after 46 h of treatment, the increase in glucose concentration in the hydrolysates becomes too slow to be convenient in terms of productivity, reaching at this time over 94 % of the maximum glucose concentration achieved during the entire process for both assays.

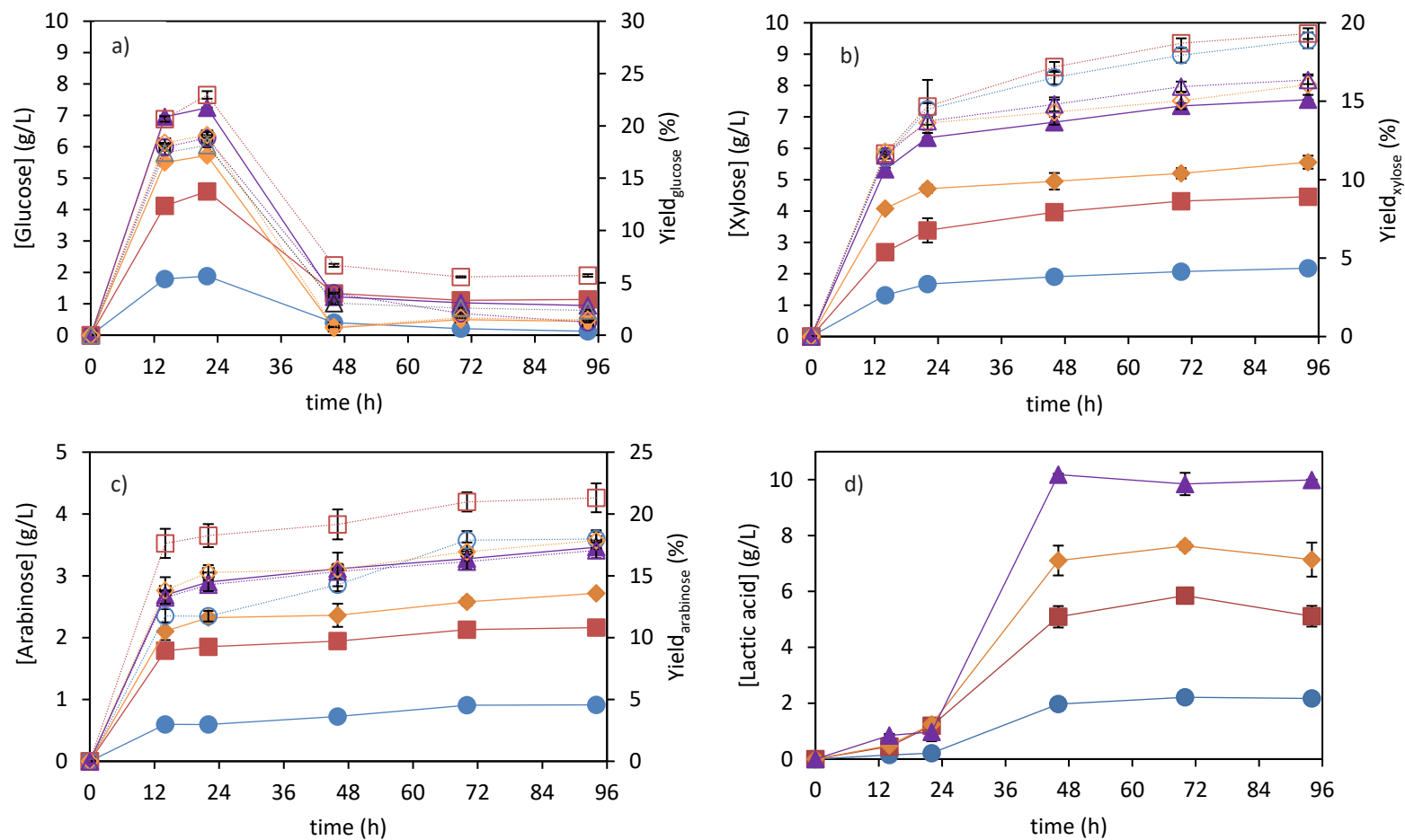


**Figure 6.1.** Kinetics of enzymatic hydrolysis of raw BSG at different solids loading ●○ 5% (w/v), ■□ 10% (v/w), ◆◇ 15% (v/w), ▲△ 20% (v/w); **a)** glucose, **b)** xylose; **c)** arabinose, **d)** lactic acid. Compound concentration (g/L, filled symbol) and yield, expressed as g compound per 100 g of compound in BSG, (open symbol).

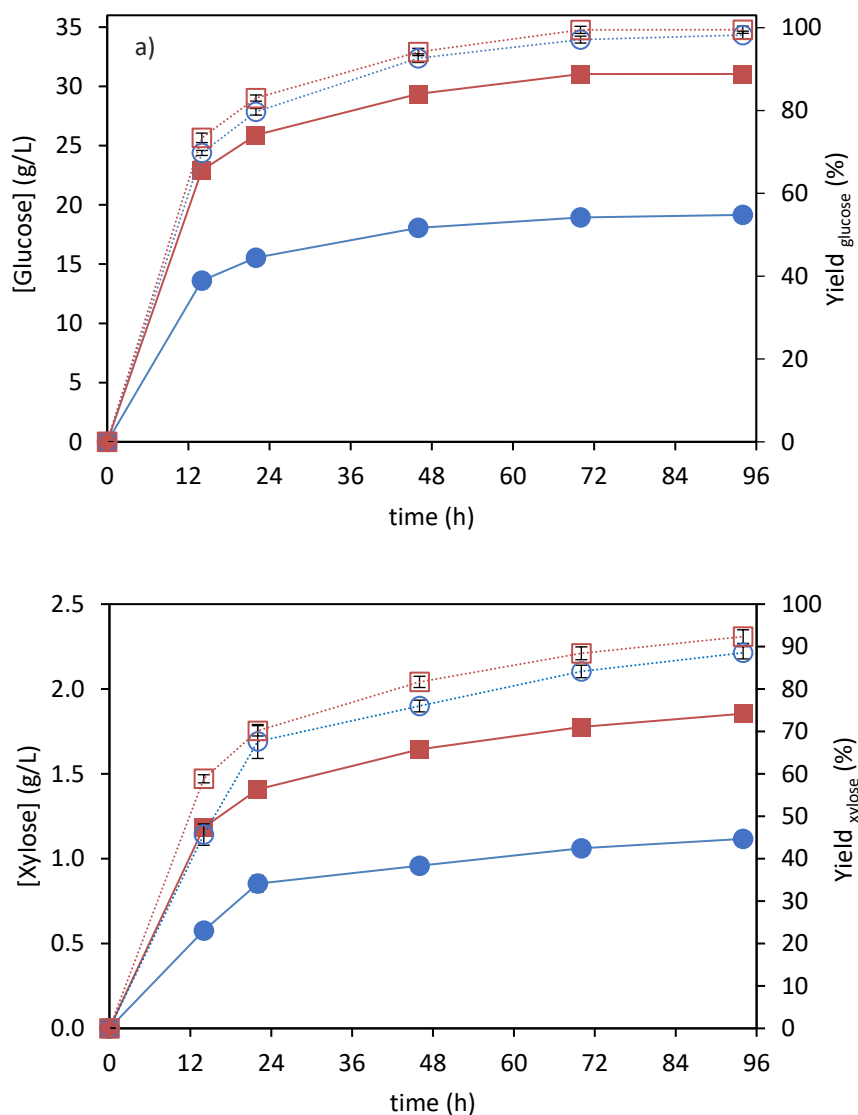


**Figure 6.2.** Kinetics of enzymatic hydrolysis of subW pretreated BSG at different solids loading ● 5% (w/v), ■ 8% (v/w); **a)** glucose, **b)** xylose. Compound concentration (g/L) (filled symbol) and yield, expressed as g compound per 100 g of compound in pre-treated BSG, (open symbol).

Enzymatic hydrolysis assays were not carried out at higher solid concentrations with subW pretreated BSG as the slurry was too viscous and all the buffer solution were retained



by the pretreated solids. Lv et al. [14] reported that the average pore diameter of sugarcane bagasse and the water retention value increased after subW pretreatment at 160 °C, due to the xylan removal during the pretreatment. On the other hand, these structural changes in the pretreated solid can facilitate the enzymatic hydrolysis of subW pretreated lignocellulose [28].

Different pretreatments for BSG have been studied in the literature previous to the enzymatic hydrolysis in order to make the cellulose more accessible to enzymes. **Table 6.2** summarizes the operation conditions and the results reported for pretreatment, enzymatic hydrolysis and fermentation assays from BSG in these studies, together with some results obtained in this work. Mussatto et al. [15] performed a two-step pretreatment with sulfuric acid and sodium hydroxide to obtain a hydrolysate with 59 g/L of glucose (73.8% yield) from 8% of pretreated BSG by using Celuclast 1.5 L for 92 h. Similar to this work, Rojas-Chamorro et al. [16] reached a cellulose-glucose conversion of 70% after pre-treatment of BSG at 160 °C with 6.83% H<sub>3</sub>PO<sub>4</sub> (w/v) and further enzymatic hydrolysis with Cellic CTec3 (Novozymes A/S, Denmark) supplemented by fungal β-glucosidase (Novozyme 50010), during 48 h and a solid concentration of 5% (w/v).

These previous studies reported lower hydrolysis yield than this work. However, Rojas-Chamorro et al. [10] achieved also a high enzymatic digestibility from 97.4 to 99.7% expressed as g glucose by enzymatic hydrolysis per 100 g of glucose in pretreated BSG in an aqueous phosphoric acid solution 2% (w/v) at 155 °C, with solids loading of 5% and 15%, respectively.

Comparing the different results for cellulase treatment of raw BSG and subW pretreated BSG at 5% of solids loading, it can be observed that the maximum concentration of glucose reached in each hydrolysate was more than 10-fold higher for pretreated BSG than for raw BSG. As shown in **Table 6.1**, subW pretreated BSG showed a 1.8-fold higher glucans content than untreated BSG. Furthermore, the glucose yield for subW pretreated BSG was 5.2-fold higher than for raw BSG. The removal of the hemicellulose fraction during the pretreatment favours enzymatic hydrolysis, becoming cellulose chains more accessible to enzymatic attack to be converted into glucose monomers [5]–[7]. In this work, the cellulose/hemicellulose ratio in pretreated BSG was more than 34-fold higher than in raw BSG. Additionally, according to Qing et al. [17]

xylose, xylo-oligomers, and xylan are strong inhibitors of cellulose hydrolysis by enzymes, thus reducing the xylan content during the subW pretreatment is also convenient in this respect.

On the other hand, the lignin accumulation on subW pretreated BSG did not reduce the enzymatic yield. Consequently, a high amount of lignin available for further valorization is expected to be found in the solid remained after saccharification, which can maximize the utilization of this lignocellulosic by-product.

Furthermore, hydrolysis kinetics for xylose and arabinose have been also determined for untreated and subW pretreated BSG and have been plotted in **Figures 6.1b**, **6.1c** and **6.2b**. Lower xylose yields were obtained from untreated BSG than for subW pretreated BSG, whereas arabinose was not detected in enzymatic hydrolysates from pretreated BSG, consistently with its complete release during subW treatment, as discussed above. Therefore, Celluclast 1.5 L was able to release not only glucose but also pentoses from both untreated and pretreated BSG. This agrees with previous reports, which indicated that Celluclast 1.5 L showed hemicellulose-degrading activity [18], [19].

### **3.3. Separate hydrolysis and fermentation (SHF)**

The hydrolysate obtained from subW pretreated BSG, by enzymatic hydrolysis with 8% (w/v) of solid for 48 h at 50 °C, was autoclaved at 120 °C for 20 minutes and then submitted to fermentation by Ethanol Red®. After autoclaving, the hydrolysate composition was 31.23 g/L glucose and 1.43 g/L xylose. The fermentation media contained 85% of this hydrolysate. **Figure 6.3** shows profiles of pH and biomass, glucose, xylose, ethanol, and glycerol concentration. At the beginning of the assay, the fermentation the sugars concentrations were 26.55 g/L glucose and 1.22 g/L xylose. After 13 h of fermentation, 92% of glucose was consumed with a glucose depletion at 15 h of fermentation. At this time, the greatest level of ethanol ( $11.30 \pm 0.01$  g/L) was produced, which corresponds to a conversion efficiency of  $0.426 \pm 0.007$  g of ethanol per gram of initial glucose.

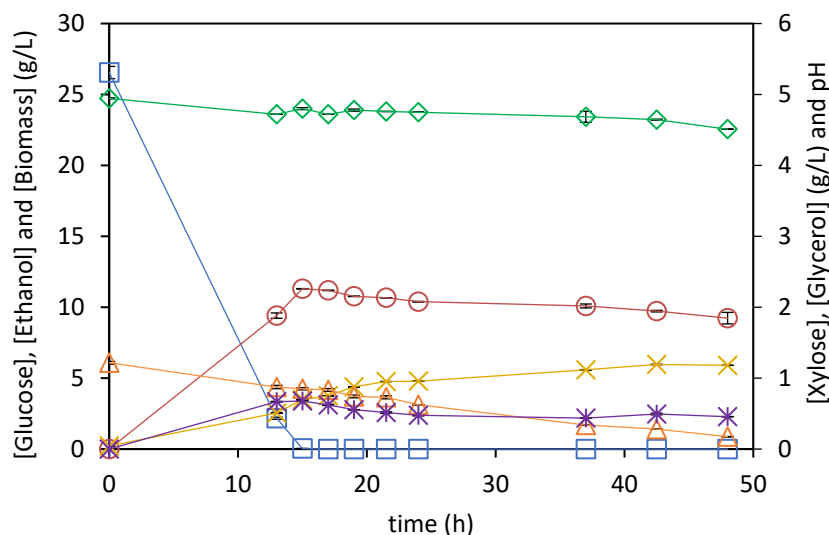


**Figure 6.3.** Evolution of  $\diamond$  pH and  $\square$  glucose,  $\triangle$  xylose,  $\circ$  ethanol,  $*$  glycerol and  $\times$  biomass concentrations (g/L) for fermentation from subW pretreated BSG after enzymatic hydrolysis (48 h and 8% w/v) in a SHF configuration during 48 h.

A slight decrease in ethanol concentration was observed after reaching its maximum, together with an increase in biomass concentration. Branco et al. [20] observed a little increase in biomass concentration when ethanol started to be assimilated due to the ability of *S. cerevisiae* to respire ethanol when the concentration of fermentable sugars has dropped. In this regard, biomass concentration still increased after glucose exhaustion also due to consumption of xylose and probably, other metabolites present in the hydrolysate. After 48 h of fermentation, the biomass concentration was  $5.901 \pm 0.005$  g/L, corresponding to a biomass/substrate yield of  $0.206 \pm 0.003$  g/g.

Although 85.7% of xylose was consumed during the assay, the initial concentration in the medium was only 1.22 g/L, and its contribution to ethanol production was not remarkable. Moreover, a decrease in the xylose concentration did not lead to an increase in ethanol concentration after glucose exhaustion. Amândio et al. [21] also reported slight xylose consumption by Ethanol Red<sup>®</sup>. Regarding glycerol, the maximum concentration,  $0.677 \pm 0.005$  g/L, was achieved after 13 h of fermentation, showing a minor decrease after

that. The reduced glycerol production indicates that most of the glucose was fermented to ethanol. **Figure 6.3** also shows the pH evolution along the assay showing a slight decrease from 4.95 to 4.51 due to the CO<sub>2</sub> released by biomass growth and ethanol production [20].

Some authors have been evaluating different pretreatments for bioethanol production from BSG. In **Table 6.2**, a comparison of *S. cerevisiae* fermentation parameters using pretreated BSG as raw material is also presented. For comparative purposes, the ethanol yield was calculated considering the maximum theoretical ethanol yield of 0.511 g per g of glucose present in the fermentation medium according to Equation 6.2 (see **Table 6.2**). The ethanol yield from this study with 8% of solids loading in SHF configuration was 83 ±1%. This result was consistent with the reported data collected in **Table 6.2**, from 55 to 81%, obtained by using acid or alkali pretreatments. Chen et al. [7] reported a fermentation yield of 90% from subW pretreated wheat straw at 15% solids loading in SHF configuration. This preliminary finding suggests the potential of subcritical water as pretreatment of lignocellulosic material for ethanol production.

**Table 6.2** Comparison between the results obtained for SHF (8% w/v) and SSF (25% w/v) assays from pretreated BSG with *S. cerevisiae* in this work and in the literature.

Pretreatment	Enzyme	Enzyme dosage	Solid loading (% w/v)	[Glucose] (g/L)	Glucose yield (%)	Conf	[Ethanol] g/L	Ethanol yield (%)	Productivity <sup>(2)</sup> (g·L <sup>-1</sup> ·h <sup>-1</sup> )	Reference
SubW, 174 °C, 50 bar, 60 min.	Celluclast 1.5L	40 FPU/g <sub>BSG</sub>	8	31.2	99.5	SHF	11.3	<sup>(1)</sup> 83 ± 1	0.754	This work
			25	-	-	SSF	32.2	65.3 ± 0.6	1.073	
H <sub>3</sub> PO <sub>4</sub> (6.83%), 160 °C	Cellic CTec3 β-glucosidase	15 FPU/g <sub>substrate</sub> 15 IU/g <sub>substrate</sub>	15	59.4		SHF	22.6	72	0.94	[10]
				-	-	SSF	18.5	62	0.595	
H <sub>2</sub> SO <sub>4</sub> (1%), 130 °C, 26 min	Cellic CTec3 β-glucosidase	15 FPU/g <sub>substrate</sub> 15 IU/g <sub>substrate</sub>	25			SSF	27	68		[22]
1. H <sub>2</sub> SO <sub>4</sub> (1.25%), 120 °C, 17 min 2. NaOH (2%), 120 °C, 90 min	Cellulase β-glucosidase (Novozymes)	2.24% (v/v) 1%(v/v)	8	75	97	SHF	12.79	54.8	0.53	[23]
NaOH (5%), 50 °C, 12 h	Cellic®CTec2	51 FPU/g <sub>solid</sub> (calculated)	15	41.7		SHF	17.3	81	N.R.	[24]
1. H <sub>2</sub> SO <sub>4</sub> (1.85%), 90 °C, 19.5 min 2. H <sub>2</sub> SO <sub>4</sub> (1%), 120 °C, 30 min	Cellic® CTec3	0.04 g/g DM	15	46.1	75.5	SHF	16.9	71.6	0.72	[25]

“Conf” stands for configuration. “DM” stands for dry matter. “NR” stands for not reported.

(1) Ethanol yield calculated according to Equation 6.3. (2) Productivity refers to volumetric ethanol productivity of fermentation step.

### 3.4. Simultaneous saccharification and fermentation (SSF)

For comparison purposes, subW pretreated BSG was subjected to an SSF process at 8% solids loading, the same tested in the sequential process. **Figure 6.4** shows profiles of pH, glucose, xylose, ethanol, and glycerol concentration along 48 h of SSF. After 13 h of fermentation, glucose concentration was still 1.21 g/L, while ethanol concentration was 9.24 g/L, increasing slowly until reaching the highest value of 10.23 g/L at 19 h. The glucose concentration needed to produce this ethanol concentration increase (0.99 g/L) is 1.94 g/L, whereas the glucose concentration detected decreased 1.21 g/L. Furthermore, a reduced amount of glycerol was formed during this period, 0.16 g/L, indicating that glucose has been still released from cellulose during the period between 13 and 19 h.

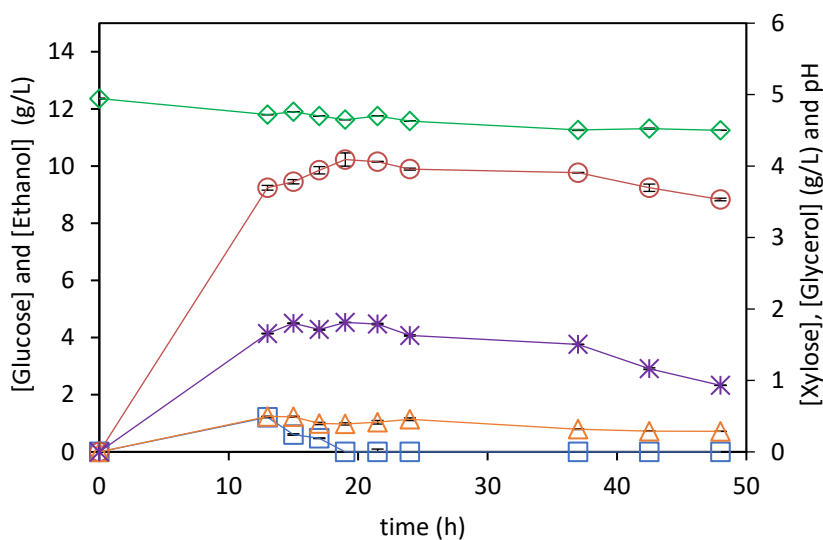


**Figure 6.4.** Evolution of  $\diamond$  pH and  $\square$  glucose,  $\triangle$  xylose,  $\circ$  ethanol and  $*$  glycerol concentrations for fermentation from subW pretreated BSG with an 8% w/v of solids loading in a SSF configuration.

**Table 6.3** summarizes the following parameters: maximum ethanol concentration, yield (as a percentage of the theoretical), yield<sub>ethanol/solid</sub> and volumetric productivity obtained in the SHF and SSF assays carried out in this work. The ethanol yield was calculated according to Equation 6.3 for SHF and SSF to compare the values on the same basis.

The ethanol content of  $10.2 \pm 0.2$  g/L was obtained after SSF fermentation, compared to  $11.30 \pm 0.01$  g/L for SHF mode, corresponding to a yield of  $64.2 \pm 0.8$  and  $83.4 \pm 0.4\%$ , respectively. Similarly, Rojas-Chamorro et al. [10] reported a higher value of ethanol yield for SHF mode (72% after 72 h enzymatic hydrolysis + 24 h fermentation) as compared to SSF (62% after 72 h of fermentation). Glucose accumulation was not observed during the assay, which may indicate a poor conversion of cellulose into glucose by working at 38 °C since cellulases are known to be more efficient at 50 °C. Moreover, the ratio ethanol/glycerol produced by SHF was 17, compared to 6 by fermentation in SSF mode. According to the literature, an increase in glycerol formation lead to a decrease in ethanol production [26]

Although the ethanol yield was lower by using the SSF mode than in SHF configuration, the time reduction should be highlighted when saccharification and fermentation were performed simultaneously, from 63 h in SHF to 19 h in SSF to reach the maximum ethanol concentration. In this regard, the volumetric fermentation productivity in the sequential and SSF processes, at 8% of solids loading, were  $0.754 \pm 0.001$  and  $0.54 \pm 0.01$  g·L<sup>-1</sup>·h<sup>-1</sup>, respectively (see **Table 6.3**). This notwithstanding, the volumetric productivity of the overall SHF process was  $0.179$  g·L<sup>-1</sup>·h<sup>-1</sup>, considering the 48 h of enzymatic hydrolysis performed. Therefore, from an economic point of view, the use of SSF instead of SHF may be advantageous by reducing the total time required.

**Table 6.3.** Parameters obtained in SHF and SSF of subW pretreated BSG at different solids loadings with Ethanol Red®.

Conf.	Solid loading (%)	[Ethanol] <sub>max</sub> (g/L)	Ethanol yield (%)	Y <sub>ethanol/solid</sub> (g/g)	Productivity (g·L <sup>-1</sup> ·h <sup>-1</sup> )
SHF	8	11.30 ± 0.01 <sup>b</sup>	<sup>(1)</sup> 83.4 ± 0.4 <sup>b</sup>	0.1662 ± 0.0002 <sup>b</sup>	<sup>(2)</sup> 0.754 ± 0.001 <sup>d</sup> <sup>(3)</sup> 0.1794 ± 0.0002 <sup>a</sup>
SSF	8	10.2 ± 0.2 <sup>a</sup>	64.2 ± 0.8 <sup>a</sup>	0.128 ± 0.003 <sup>a</sup>	0.54 ± 0.01 <sup>b</sup>
SSF	15	19.1 ± 0.3 <sup>c</sup>	64.0 ± 0.6 <sup>a</sup>	0.128 ± 0.002 <sup>a</sup>	0.74 ± 0.01 <sup>c</sup>
SSF (f-b)	25	32.18 ± 0.08 <sup>d</sup>	64.6 ± 0.3 <sup>a</sup>	0.1287 ± 0.0003 <sup>a</sup>	1.073 ± 0.003 <sup>e</sup>

“Conf” stands for configuration. (1) Ethanol yield calculated according to Equation 6.3.

(2) Productivity considering the time of the fermentation step (15 h). (3) Productivity considering the time of saccharification and fermentation (48+15 h). Values are expressed as mean ± standard deviation from triplicate determination. Values with different letters in each column are significantly different when applying the Fisher's least significant differences (LSD) method at p-value ≤ 0.05

The ethanol content of 10.2 ± 0.2 g/L was obtained after SSF fermentation, compared to 11.30 ± 0.01 g/L for SHF mode, corresponding to a yield of 64.2 ± 0.8 and 83.4 ± 0.4%, respectively. Similarly, Rojas-Chamorro et al. [10] reported a higher value of ethanol yield for SHF mode (72% after 72 h enzymatic hydrolysis + 24 h fermentation) as compared to SSF (62% after 72 h of fermentation). Glucose accumulation was not observed during the assay, which may indicate a poor conversion of cellulose into glucose by working at 38 °C since cellulases are known to be more efficient at 50 °C. Moreover, the ratio ethanol/glycerol produced by SHF was 17, compared to 6 by fermentation in SSF mode. According to the literature, an increase in glycerol formation lead to a decrease in ethanol production [26]

Although the ethanol yield was lower by using the SSF mode than in SHF configuration, the time reduction should be highlighted when saccharification and fermentation were performed simultaneously, from 63 h in SHF to 19 h in SSF to reach the maximum ethanol concentration. In this regard, the volumetric fermentation productivity in the sequential and SSF processes, at 8% of solids loading, were 0.754 ± 0.001 and 0.54 ± 0.01 g·L<sup>-1</sup>·h<sup>-1</sup>,



respectively (see **Table 6.3**). This notwithstanding, the volumetric productivity of the overall SHF process was  $0.179 \text{ g}\cdot\text{L}^{-1}\cdot\text{h}^{-1}$ , considering the 48 h of enzymatic hydrolysis performed. Therefore, from an economic point of view, the use of SSF instead of SHF may be advantageous by reducing the total time required.

All in all, the ethanol concentrations reached by both configurations, SHF and SSF, at 8% solids loading were not high enough to be considered for a second-generation ethanol process, being necessary at least 4% by volume for distillation economic feasibility [27]. For this reason, SSF assays with 15 and 25% solids loading were performed. **Table 6.3** also collects the parameters obtained in SSF at 15% solids loading. Similar ethanol yields were reached at 8% and 15% solids loading, 64.2% and 64.0% of the theoretical ethanol yield, respectively. However, an ethanol concentration of 19.1 g/L was reached at 15% solids loading after 26 h (see **Figure 6.5**). Although the time needed to achieve the maximum level of ethanol was higher at 15% than at 8%, 26 h vs 19 h (see **Figure 6.4** and **6.5**), the volumetric ethanol productivity was higher at 15% than at 8% solids loading with values of  $0.74$  and  $0.54 \text{ g}\cdot\text{L}^{-1}\cdot\text{h}^{-1}$ , respectively.

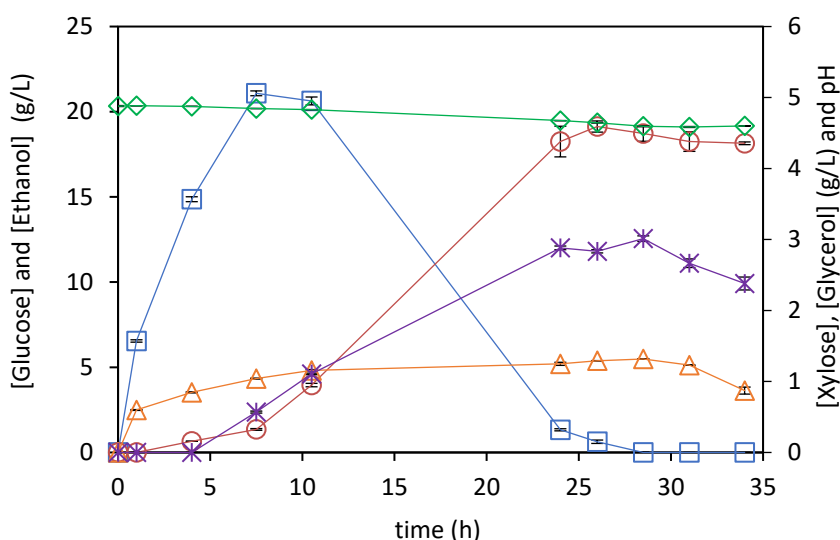


**Figure 6.5.** Evolution of  $\diamond$  pH and  $\square$  glucose,  $\triangle$  xylose,  $\circ$  ethanol and  $*$  glycerol concentrations for fermentation from subW pretreated BSG with a 15% w/v of solids loading in a SSF configuration.

SSF was also performed at 25% of solids loading. However, the viscosity of the mixture was too high, and no liquefaction was achieved, even after 96 h of SSF. To achieve a solid concentration of 25% a feed-batch strategy was defined.

### 3.5. Fed-batch strategy

**Figure 6.6** shows the evolution of pH and glucose, xylose, ethanol, and glycerol concentrations for the SSF assay performed at 25% solids loading following a fed-batch strategy. The assay was initiated with a solid concentration of 8% and subW pretreated BSG was added after 2, 4, and 8 h of fermentation (section 2.6.3), achieving a total solids loading of 25%.

Compared with SSF at 8 and 15% solids loading, a similar yield was reached, 65.3%, whereas a maximum level of ethanol, 32.18 g/L was produced after 30 h. This value corresponds to 4.08 % (v/v), achieving now the threshold of 4%, as discussed above. The same ethanol/glycerol ratio of 6 was found in all the SSF assays performed in this work.

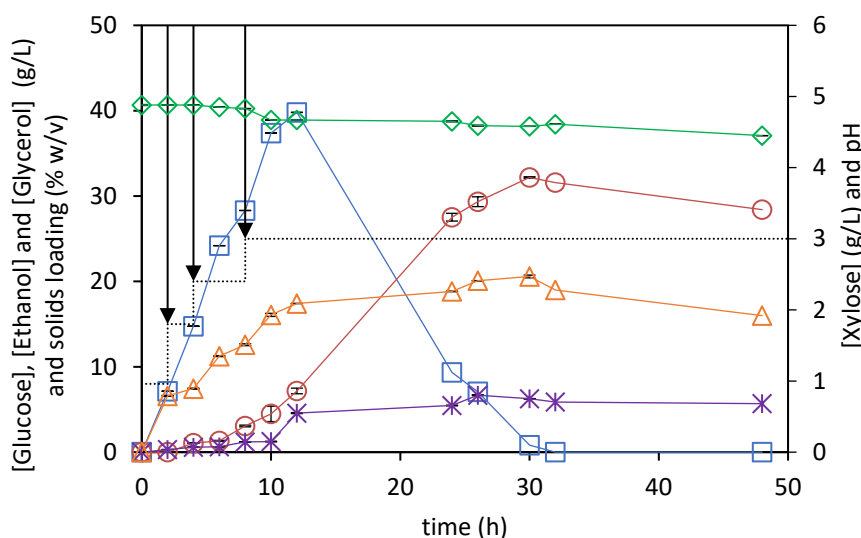


**Figure 6.6.** Evolution of  $\diamond$  pH and  $\square$  glucose,  $\triangle$  xylose,  $\circ$  ethanol and  $*$  glycerol concentrations for fermentation from subW pretreated BSG at a final solids loading of 25% (w/v) following a fed-batch strategy in a SSF configuration. The discontinuous line shows solid concentration along time.

The value of ethanol concentration from BSG obtained in this study was higher than that reported in earlier works using acid and/or alkali pretreated BSG, ranging from 12.79 to 22.7 g/L, as collected in **Table 6.2**, while being lower than that obtained by recent research on BSG (42.29 g/L and 39 g/L) using the whole slurry of pretreated BSG through different co-fermentation strategies [28], [29]. Pinheiro and et al. [29] achieved ethanol concentrations from 28.7 to 42.27 g/L by fermentation of the whole slurry, obtained by hydrolysis of BSG at 160 °C and 25% solids loading, after 120 h of saccharification. According to the authors, the ethanol concentration varied according to the chemical composition of the raw BSG tested. In this regard, the maximum ethanol level was achieved from BSG with a total glucan content of 32.1% (7.6% of soluble glucose polysaccharides) compared with 19.1% glucan content in the BSG used in this work. Otherwise, Rojas-Chamorro et al. [28] reached the concentration of 39 g/L by following a co-fermentation strategy with (*Escherichia coli*) from BSG pretreated with phosphoric acid. However, the time required for the overall process was noticeably higher than that employed in this work, since they employed 24 h for saccharification and 100 h for fermentation. Furthermore, these authors introduced an intermediate step of concentration of the enzymatic hydrolysate by evaporation.

It is also worth pointing out that by using SSF instead of SHF, the total time required for ethanol production from BSG at its maximum level has been reduced to 30 h, with an ethanol productivity of 1.073 g·L<sup>-1</sup>·h<sup>-1</sup>. Likewise, the overall ethanol productivity obtained in this study is the highest reported to produce ethanol from BSG, according to the author's knowledge.

### **3.6. Overall process mass balance**

In the context of a biorefinery concept, all fractions obtained along the overall process should be valorized. **Figure 6.7** shows the mass balance for ethanol production from BSG under the different conditions investigated in this work, pretreatment with subcritical water at 174 °C for 60 min and 5% (w/v), enzymatic hydrolysis of the pretreated biomass at 8% (w/v) solid loading and subsequent fermentation, as well as simultaneous saccharification and fermentation with different solid concentrations. Glucose, xylose and arabinose have been determined in all the streams, as described in the material and

methods section. Overall mass balance is presented considering 100 kg of dry BSG as a calculation basis. The subW pretreatment yielded 41.2 kg of pretreated solid. The subW liquid stream contained 32.28 kg of carbohydrates (3.51 kg glucose, 21.91 kg xylose and 6.85 kg arabinose) mainly in oligomeric form and 14.82 kg peptides, whereas 16.07 kg glucose, 1.04 kg xylose, 4.99 kg protein and 19.41 kg lignin remained in the solid stream. Different options could be followed to valorize the subW liquid stream. For instance, after purification, xylo-oligomers and peptides may be used as a functional food ingredient [30]. On the other hand, the subW liquid stream could be submitted to fermentation after converting the oligomer sugars into monomers, as monomers are present at low concentrations (0.30 g/L glucose, 1.5 g/L xylose and 2.3 g/L arabinose). Furthermore, it could be used to produce other valuable building blocks as xylose, which can be converted to xylitol or furfural [31], [32].

The subW pretreated solid was submitted to enzymatic hydrolysis releasing 16.08 kg glucose and 0.74 kg xylose. The overall recovery of carbohydrates after pretreatment and saccharification was 87% being the glucose recovery 92%. Depending on how the fermentation processes were conducted, the energy and chemical requirements of the process and the amount of ethanol produced varied. For instance, 6.85 kg of ethanol were obtained from 100 kg of dry raw BSG when SHF was performed, while around 5.3 kg were produced by SSF. However, to determine which process configuration is most interesting for the industrial production of ethanol from BSG, it would be necessary to carry out a techno-economic evaluation. Consequently, it should be noted that the working volume for SSF at 25% solid loading is 3.8-fold lower than for SHF at 8% solid loading, and the ethanol concentration is 2.8-fold higher by performing SSF at 25% solids. This fact not only means lower water requirements and lower equipment costs but also reduced distillation costs. Furthermore, the productivity of the overall process was 6-fold higher in SSF at 25% solids loading.

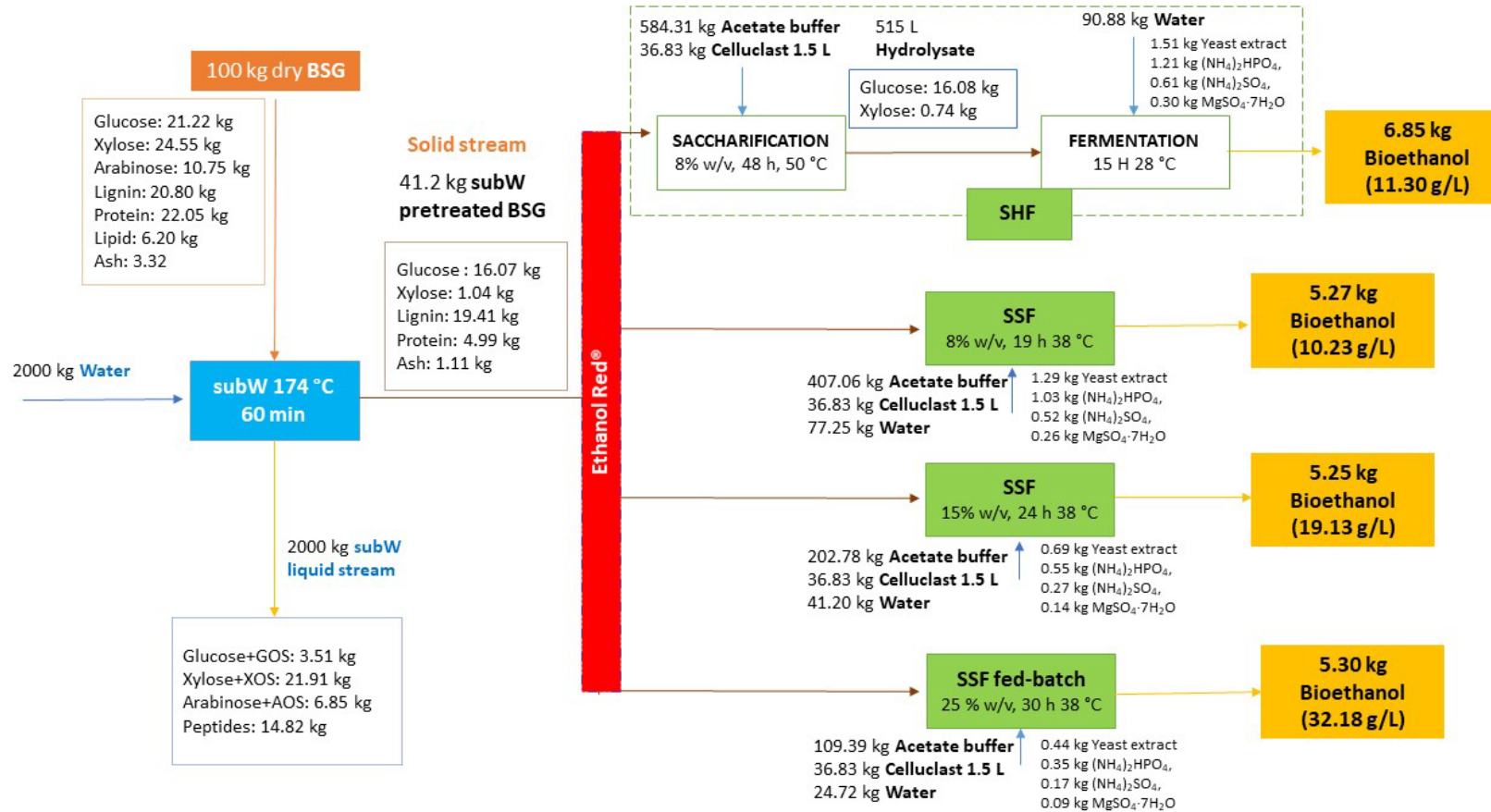


Figure 6.7 Overall mass balance for ethanol production from subW pretreated BSG by saccharification and fermentation at different operational modes.

“GOS”, “XOS” and “AOS” stands for gluco-oligomers, xylo-oligomers and arabino-oligomers, respectively

## 4. Conclusions

The bioconversion of brewer's spent grain using subcritical water as pretreatment, followed by simultaneous saccharification and fermentation by Ethanol Red<sup>®</sup> is a promising option to achieve the integral valorization of this by-product within a biorefinery concept. The subW pretreatment at 174 °C for 60 min resulted in an easily hydrolysable solid with higher glucan content than raw BSG, yielding a glucose release of 99.5%. Separated hydrolysis and fermentation and simultaneous saccharification and fermentation of pretreated BSG, at different solids loading, were evaluated in terms of ethanol production. Fed-batch SSF allowed to increase the total solids loading to 25 %, resulting in relatively high ethanol concentration (> 32 g/L) in only 30 h, achieving to reach the target concentration of 4% by volume. Furthermore, the highest value of ethanol productivity ( $1.07 \text{ g}\cdot\text{L}^{-1}\cdot\text{h}^{-1}$ ) reported for this raw material was attained.

## References

- [1] G. Dragone, A. A. J. Kerssemakers, J. L. S. P. Driessen, C. K. Yamakawa, L. P. Brumano, and S. I. Mussatto, "Innovation and strategic orientations for the development of advanced biorefineries," *Bioresource Technology*, vol. 302, no. January, p. 122847, 2020, doi: 10.1016/j.biortech.2020.122847.
- [2] W. G. Sganzerla, L. C. Ampese, S. I. Mussatto, and T. Forster-Carneiro, "A bibliometric analysis on potential uses of brewer's spent grains in a biorefinery for the circular economy transition of the beer industry," *Biofuels, Bioproducts and Biorefining*, vol. 15, no. 6, pp. 1965–1988, 2021, doi: 10.1002/bbb.2290.
- [3] S. I. Mussatto, G. Dragone, and I. C. Roberto, "Brewers' spent grain: Generation, characteristics and potential applications," *Journal of Cereal Science*, vol. 43, no. 1, pp. 1–14, 2006, doi: 10.1016/j.jcs.2005.06.001.
- [4] P. Alonso-Riaño, M. T. Sanz, O. Benito-Román, S. Beltrán, and E. Trigueros, "Subcritical water as hydrolytic medium to recover and fractionate the protein fraction and phenolic compounds from craft brewer's spent grain," *Food Chemistry*, vol. 351, Jul. 2021, doi: 10.1016/j.foodchem.2021.129264.
- [5] D. G. Gomes, M. Michelin, A. Romani, L. Domingues, and J. A. Teixeira, "Co-production of biofuels and value-added compounds from industrial *Eucalyptus globulus* bark residues using hydrothermal treatment," *Fuel*, vol. 285, Feb. 2021, doi: 10.1016/j.fuel.2020.119265.
- [6] A. B. de Camargos *et al.*, "Production of biogas and fermentable sugars from spent brewery grains: Evaluation of one- and two-stage thermal pretreatment in an integrated biorefinery," *Journal of Environmental Chemical Engineering*, vol. 9, no. 5, Oct. 2021, doi: 10.1016/j.jece.2021.105960.
- [7] J. Chen *et al.*, "Integrating enzymatic hydrolysis into subcritical water pretreatment optimization for bioethanol production from wheat straw," *Science of the Total Environment*, vol. 770, May 2021, doi: 10.1016/j.scitotenv.2021.145321.
- [8] M. J. Cocero *et al.*, "Understanding biomass fractionation in subcritical & supercritical water," *Journal of Supercritical Fluids*, vol. 133, no. August 2017, pp. 550–565, 2018, doi: 10.1016/j.supflu.2017.08.012.
- [9] S. I. Mussatto, M. Fernandes, A. M. F. Milagres, and I. C. Roberto, "Effect of hemicellulose and lignin on enzymatic hydrolysis of cellulose from brewer's spent grain," *Enzyme and Microbial Technology*, vol. 43, pp. 124–129, 2008, doi: 10.1016/j.enzmictec.2007.11.006.
- [10] J. A. Rojas-Chamorro, I. Romero, E. Ruiz, C. Cara, and E. Castro, "Comparison of fermentation strategies for ethanol production from pretreated brewers spent grain," *Chemical Engineering Transactions*, vol. 61, pp. 637–642, 2017, doi: 10.3303/CET1761104.
- [11] J. B. Sluiter, R. O. Ruiz, C. J. Scarlata, A. D. Sluiter, and D. W. Templeton, "Compositional analysis of lignocellulosic feedstocks. 1. Review and description of methods," *Journal of Agricultural and Food Chemistry*, vol. 58, no. 16, pp. 9043–9053, 2010, doi: 10.1021/jf1008023.

- [12] R. di Cagno, P. Filannino, and M. Gobbetti, "Vegetable and Fruit Fermentation by Lactic Acid Bacteria," *Biotechnology of Lactic Acid Bacteria: Novel Applications: Second Edition*, pp. 216–230, 2015, doi: 10.1002/9781118868386.ch14.
- [13] M. Michelin and J. A. Teixeira, "Liquid hot water pretreatment of multi feedstocks and enzymatic hydrolysis of solids obtained thereof," *Bioresource Technology*, vol. 216, pp. 862–869, Sep. 2016, doi: 10.1016/j.biortech.2016.06.018.
- [14] S. Lv *et al.*, "The Influence of Hemicellulose and Lignin Removal on the Enzymatic Digestibility from Sugarcane Bagasse", doi: 10.1007/s12155-013-9297-4.
- [15] S. I. Mussatto, G. Dragone, M. Fernandes, A. M. F. Milagres, and I. C. Roberto, "The effect of agitation speed, enzyme loading and substrate concentration on enzymatic hydrolysis of cellulose from brewer's spent grain," *Cellulose*, vol. 15, no. 5, pp. 711–721, 2008, doi: 10.1007/s10570-008-9215-7.
- [16] J. A. Rojas-Chamorro *et al.*, "Ethanol Production from Brewers' Spent Grain Pretreated by Dilute Phosphoric Acid," *Energy and Fuels*, vol. 32, no. 4, pp. 5226–5233, Apr. 2018, doi: 10.1021/acs.energyfuels.8b00343.
- [17] Q. Qing, B. Yang, and C. E. Wyman, "Xylooligomers are strong inhibitors of cellulose hydrolysis by enzymes," *Bioresource Technology*, vol. 101, no. 24, pp. 9624–9630, Dec. 2010, doi: 10.1016/j.biortech.2010.06.137.
- [18] M. Yoshida *et al.*, "Effects of cellulose crystallinity, hemicellulose, and lignin on the enzymatic hydrolysis of *Miscanthus sinensis* to monosaccharides," *Bioscience, Biotechnology and Biochemistry*, vol. 72, no. 3, pp. 805–810, 2008, doi: 10.1271/bbb.70689.
- [19] A. Berlin, V. Maximenko, N. Gilkes, and J. Saddler, "Optimization of enzyme complexes for lignocellulose hydrolysis," *Biotechnology and Bioengineering*, vol. 97, no. 2, pp. 287–296, 2007, doi: 10.1002/bit.21238.
- [20] R. H. R. Branco, M. S. T. Amândio, L. S. Serafim, and A. M. R. B. Xavier, "Ethanol production from hydrolyzed kraft pulp by mono- and co-cultures of yeasts: The challenge of C6 and C5 sugars consumption," *Energies*, vol. 13, no. 3, 2020, doi: 10.3390/en13030744.
- [21] M. S. T. Amândio, J. M. S. Rocha, L. S. Serafim, and A. M. R. B. Xavier, "Cellulosic bioethanol from industrial *Eucalyptus Globulus* bark residues using kraft pulping as a pretreatment," *Energies*, vol. 14, no. 8, Apr. 2021, doi: 10.3390/en14082185.
- [22] J. A. Rojas-Chamorro, I. Romero, J. C. López-Linares, and E. Castro, "Brewer's spent grain as a source of renewable fuel through optimized dilute acid pretreatment," *Renewable Energy*, vol. 148, pp. 81–90, Apr. 2020, doi: 10.1016/j.renene.2019.12.030.
- [23] R. Liguori, C. R. Soccol, L. P. de Souza Vandenberghe, A. L. Woiciechowski, and V. Faraco, "Second generation ethanol production from brewers' spent grain," *Energies*, vol. 8, no. 4, pp. 2575–2586, 2015, doi: 10.3390/en8042575.
- [24] S. Wilkinson, K. A. Smart, and D. J. Cook, "Optimisation of alkaline reagent based chemical pre-treatment of Brewers spent grains for bioethanol production,"



- Industrial Crops and Products*, vol. 62, pp. 219–227, 2014, doi: 10.1016/j.indcrop.2014.08.036.
- [25] S. Bedő, M. Rozbach, L. Nagy, A. Fehér, and C. Fehér, “Optimised fractionation of brewer’s spent grain for a biorefinery producing sugars, oligosaccharides, and bioethanol,” *Processes*, vol. 9, no. 2, pp. 1–18, Feb. 2021, doi: 10.3390/pr9020366.
- [26] K. T. Scanes, S. Hohrann, and B. A. Prior, “Glycerol production by the yeast *Saccharomyces cerevisiae* and its relevance to wine: a review,” *South African Journal of Enology and Viticulture*, vol. 19, no. 1, pp. 17–24, 1998.
- [27] G. Zacchi and A. Axelsson, “Economic evaluation of preconcentration in production of ethanol from dilute sugar solutions,” *Biotechnology and Bioengineering*, vol. 34, no. 2, 1989, doi: 10.1002/bit.260340211.
- [28] J. A. Rojas-Chamorro, J. M. Romero-García, C. Cara, I. Romero, and E. Castro, “Improved ethanol production from the slurry of pretreated brewers’ spent grain through different co-fermentation strategies.,” *Bioresource technology*, vol. 296, p. 122367, Jan. 2020, doi: 10.1016/j.biortech.2019.122367.
- [29] T. Pinheiro, E. Coelho, A. Romani, and L. Domingues, “Intensifying ethanol production from brewer’s spent grain waste: Use of whole slurry at high solid loadings,” *New Biotechnology*, vol. 53, pp. 1–8, Nov. 2019, doi: 10.1016/j.nbt.2019.06.005.
- [30] K. M. Lynch, E. J. Steffen, and E. K. Arendt, “Brewers’ spent grain: a review with an emphasis on food and health,” *Journal of the Institute of Brewing*, vol. 122, no. 4, pp. 553–568, 2016, doi: 10.1002/jib.363.
- [31] A. George, K. Simet, and A. Carradorini, “Brewer’s Spent Grain to Xylitol & Polylactic Acid,” *Senior Design Reports (CBE)*, pp. 1–368, 2017, [Online]. Available: [http://repository.upenn.edu/cbe\\_sdr/90](http://repository.upenn.edu/cbe_sdr/90)
- [32] D. Steinbach, A. Kruse, and J. Sauer, “Pretreatment technologies of lignocellulosic biomass in water in view of furfural and 5-hydroxymethylfurfural production- A review,” *Biomass Conversion and Biorefinery*, vol. 7, no. 2, pp. 247–274, Jun. 2017, doi: 10.1007/s13399-017-0243-0.





# CONCLUSIONS

---



## CONCLUSIONS

---

Although each chapter contains its own conclusions from the different experimental studies carried out in this PhD Thesis, the following general conclusions can be established:

- The valorization of brewer's spent grain (BSG) generated by large (industrial BSG) and small local companies (craft BSG) within a biorefinery concept is of great interest to obtain different high value biocompounds.

Along the different chapters the main components of the BSG have been recovered by using green technologies.

The chemical analysis of the BSG showed an important amount of water and ethanol extractables compounds, as well as a lipophilic fraction rich in polyunsaturated acids. BSG accounted also for an important fraction of protein, as well as carbohydrate as the main structural components. The carbohydrate fraction included cellulose and hemicellulose. Starch and  $\beta$ -glucans were also determined in the BSG from craft brewery

According to the cascade approach presented in this Thesis the main conclusions raised from the work carried out are the following.

- Ultrasound assisted extraction (UAE) yielded 24 g of **water extractives** from 100 g of dry-craft BSG in 30 min. The aqueous extract contained soluble proteins, water soluble sugars, phenolic compounds, and exhibited antioxidant activity. By a further concentration step via centrifuge ultrafiltration with membranes of NMWL lower than 10 kDa, a permeate rich in hydroxycinnamic acids and sugars was obtained while the retentate was enriched in the protein fraction.

- sc-CO<sub>2</sub> has been confirmed as a green solvent for oil recovery obtaining an **oily extract** rich in linoleic acid, with important amounts of bioactive compounds that provide good antioxidant properties. sc-CO<sub>2</sub> treated BSG yielded higher enzymatic yield, around 18 % of increase, by using cellulase as biocatalyst due to fat removal and to morphological changes of BSG after sc-CO<sub>2</sub>, that facilitates the access of the enzymes to the cellulose fraction

- **Protein fraction** was efficiently extracted and hydrolyzed by subcritical water treatment. About 78% of the protein fraction of the craft BSG was recovered by working in

## CONCLUSIONS

### *Integral valorization of brewer's spent grain by emerging technologies*

---

a semicontinuous fix-bed reactor at 185 °C and 4 mL/min, after 240 min. After 60 min of treatment (the time in which the protein extraction kinetic curve is lineal), the protein content in the extracts was about 5 g/L (67.7% of protein yield). When working in a discontinuous reactor, at 170 °C, 66% of the protein fraction of the industrial BSG was recovered after 45 min, with a protein content of 6.5 g/L. Therefore, higher protein yield was achieved by working at semicontinuous mode, but more concentrated extracts were obtained in the discontinuous reactor. However, it must be noted, that the chemical composition of each BSG type was slightly different and that the industrial BSG was milled before the subW treatment.

A minor fraction of the protein content was hydrolysed as **free amino acids** in the subW extracts. The free amino acids yield obtained in the discontinuous reactor at 170°C (2.38% after 45 min of extraction), was lower than those obtained from BSG in the semi-continuous reactor, at different temperatures (125-185 °C), and residence time around 28-29 min, which varied from 2.9% at 125 °C to the maximum level, 5.5%, obtained at 160°C and decreased to 3.2% at 185°C. Probably, this is due to the higher temperature and reaction time employed in the discontinuous mode which may cause amino acid degradation. Furthermore, above 160 °C, amino acids react by nucleophilic addition with the carbonyl groups of released sugars and be involved in Maillard reactions.

- Subcritical water treatment has also been proven to be an efficient technology to release the **phenolic compounds** from the BSG lignocellulosic matrix. The highest **total phenolic content** (TPC) released by subW treatment in a semicontinuous fix-bed reactor, 33 mg<sub>GAE</sub>/g<sub>dry-BSG</sub> was obtained at 185 °C, from the craft-BSG. Similarly, a TPC of 34 mg<sub>GAE</sub>/g<sub>dry-BSG</sub> was reached from the industrial-BSG in the subW discontinuous reactor at 170°C, after 45 min of treatment.

A positive correlation between reducing capacity, as determined by the FRAP assay, and TPC was established. The high TPC value and **antioxidant capacity** of the extracts obtained at the highest temperatures could be due to newly formed compounds related to Maillard reactions that influence TPC and FRAP responses.

Some individual phenolic compounds were identified in the extracts obtained by the different methods evaluated during this PhD Thesis, being the **hydroxycinnamic acids**,

## CONCLUSIONS

### *Integral valorization of brewer's spent grain by emerging technologies*

---

ferulic acid (FA) and p-coumaric acid (CA), and the phenolic aldehyde, **vanillin**, the ones found in the highest amount. It was found that subW was not as effective as alkaline hydrolysis to release hydroxycinnamic acids from BSG, at the operation conditions evaluated. Around 35 % of the values determined by alkaline hydrolysis were determined in the subW extracts obtained at 170 °C in the discontinuous reactor. Under this conditions vanillin was successfully released from the BSG. By working with subW at different temperatures in the semicontinuous reactor, it was found that hydroxycinnamic acids are more sensitive to temperature than aldehyde phenolic compounds.

- Subcritical water treatment has been successfully employed to hydrolyze the **hemicellulose fraction** of BSG. The subcritical water treatment of industrial BSG at 170 °C and 22 min in a laboratory scale batch reactor released the 87% of the arabinoxylan content in BSG. An increase in the reaction time up to 45 min led to an increase in the total pentosan yield up to 94%, but also to an increase in the degradation products concentration.

- The feasibility of an industrial-scale subcritical water system through **scaling-up from lab to pilot systems** has been proved in a discontinuous configuration. Reproducible results were observed at both scales considering the release of the main valuable BSG components, such as carbohydrates, released as monomer and oligomers, protein and free amino acids, phenolic compounds, the presence of inhibitors, such as acetic acid, furfural, and 5-hydroxymethylfurfural, as well as the chemical composition of the subW solid residues.

- A further step in the valorisation of the BSG was achieved by fractionating the liquid hydrolysate after subW treatment by pervaporation. Organophilic PV membranes allowed the removal and concentration of **furfural** in the permeate side. achieving a double objective: (1) Separation and purification of furfural as sugar-derived building block and (2) Detoxification of the liquid hydrolysate.

- The solid residue generated after subW treatment at 174 °C was suitable to obtain **bioethanol** from lignocellulosic biomass like BSG (second generation bioethanol) via enzymatic hydrolysis. Removal of hemicellulose fraction generated a solid rich in cellulose, being more accessible to enzymatic attack. Simultaneous saccharification with cellulase and fermentation by the yeast Ethanol Red<sup>®</sup> (SSF), in a fed-batch strategy to work with a total solid loading of 25% (w/v), resulted in a relatively high bioethanol concentration (> 32 g/L)

## CONCLUSIONS

### *Integral valorization of brewer's spent grain by emerging technologies*

---

in only 30 h, achieving a great value of bioethanol productivity ( $1.07 \text{ g}\cdot\text{L}^{-1}\cdot\text{h}^{-1}$ ). Separated saccharification and fermentation of subW pretreated BSG with 8% solids loading, allowed higher bioethanol yield, 83%, but also a lower bioethanol concentration (11.3 g/L) and lower productivity ( $0.18 \text{ g}\cdot\text{L}^{-1}\cdot\text{h}^{-1}$ ).

The bioconversion of BSG by using subcritical water as pretreatment, followed by a simultaneous saccharification and fermentation (SSF) in a fed-batch strategy, is a promising approach to achieve the integral valorization of this by-product within a biorefinery concept.

- Further research to valorize the BSG **lignin** fraction is needed in order to achieve a complete valorization of this valuable by-product. By using subcritical water pretreatment followed by enzymatic saccharification, the BSG hemicellulose and cellulose fractions were completely depolymerized and solubilized from the biomass and a high protein fraction (66%) was also released by subW treatment, which addresses the opportunity of valorizing the BSG lignin fraction of the remaining solids enriched in lignin.









# **CURRICULUM VITAE**

---



## PATRICIA ALONSO RIAÑO

Born on October 12<sup>th</sup>, 1989, in Logroño (Spain)

### Contact

e-mail: [patriciaalonsoriano@gmail.com](mailto:patriciaalonsoriano@gmail.com)

Scopus author ID: 57188582857

ORCID: <https://orcid.org/0000-0003-4765-5859>

### Education

---

2018-2022	PhD student in “Advances in Food Science and Biotechnology” University of Burgos, Spain
2007-2012	Bachelor’s Degree in Chemistry University of Burgos, Spain

---

### Employment

---

2018-2022	PhD scholarship in the Department of Biotechnology and Food Science, University of Burgos, Spain (Ref: 422058)
2007-2012	Research support technician in the Department of Biotechnology and Food Science, University of Burgos, Spain (Ref: 376072)

---

### Short research visit

---

2021 (3 months)	Department of Chemistry, University of Aveiro, Portugal
-----------------	---

---

### Publications compiled in the PhD Thesis

1. P. Alonso-Riaño, A. Xavier, M. Amândio, S. Beltrán, M. T. Sanz. "Second generation bioethanol production from subcritical water pretreated brewer's spent grain within a biorefinery concept," *Biomass Conversion and Biorefinery, Food and Bioproducts processing* (summitted).
2. P. Alonso-Riaño, M. T. Sanz, S. Beltrán. "Pervaporation behaviour of subcritical water hydrolysates of lignocellulosic biomass: brewer spent grain," *Separation and Purification Technology* (summitted).
3. P. Alonso-Riaño, M. T. Sanz, S. Beltrán, E. Trigueros, C. Ramos. "Preliminary study of subcritical water treatment scale-up from laboratory to pilot system for brewer's spent grain valorization," *Journal of Environmental Chemical Engineering* (submitted).
4. P. Alonso-Riaño, R. Melgosa, E. Trigueros, S. Beltrán, M. T. Sanz. "Valorization of brewer's spent grain by consecutive supercritical carbon dioxide extraction and enzymatic hydrolysis," *Food Chemistry* (under review)
5. P. Alonso-Riaño, M. T. Sanz, O. Benito-Román, S. Beltrán, E. Trigueros, "Subcritical water as hydrolytic medium to recover and fractionate the protein fraction and phenolic compounds from craft brewer's spent grain," *Food Chemistry*, vol. 351, Jul. 2021, doi: 10.1016/j.foodchem.2021.129264.
6. P. Alonso-Riaño, M. T. S. Diez, B. Blanco, S. Beltrán, E. Trigueros, O. Benito-Román, "Water ultrasound-assisted extraction of polyphenol compounds from brewer's spent grain: Kinetic study, extract characterization, and concentration," *Antioxidants*, vol. 9, no. 3, 2020, doi: 10.3390/antiox9030265.

### Co-authored publications

7. Ó. Benito-Román, P. Alonso-Riaño, E. Díaz de Cerio, M. T. Sanz, S. Beltrán, "Semi-continuous hydrolysis of onion skin wastes with subcritical water: Pectin recovery and oligomers identification," *Journal of Environmental Chemical Engineering*, vol. 10, no. 3, p. 107439, Jun. 2022, doi: 10.1016/J.JECE.2022.107439.
8. E. Trigueros, P. Alonso-Riaño, C. Ramos, C. I. K. Diop, S. Beltrán, M. T. Sanz, "Kinetic study of the semi-continuous extraction/hydrolysis of the protein and polysaccharide fraction of the industrial solid residue from red macroalgae by subcritical water," *Journal of Environmental Chemical Engineering*, vol. 9, no. 6, Dec. 2021, doi: 10.1016/J.JECE.2021.106768.
9. E. Trigueros, M. T. Sanz, P. Alonso-Riaño, S. Beltrán, C. Ramos, and R. Melgosa, "Recovery of the protein fraction with high antioxidant activity from red seaweed

industrial solid residue after agar extraction by subcritical water treatment," *Journal of Applied Phycology*, vol. 33, no. 2, pp. 1181–1194, Apr. 2021, doi: 10.1007/s10811-020-02349-0.

10. E. Trigueros, M. T. Sanz, A. Filipigh, S. Beltrán, P. Riaño, "Enzymatic hydrolysis of the industrial solid residue of red seaweed after agar extraction: Extracts characterization and modelling," *Food and Bioproducts Processing*, vol. 126, pp. 356–366, Mar. 2021, doi: 10.1016/J.FBP.2021.01.014.

### Oral communications

P. Alonso-Riaño, O. Benito-Román, S. Beltrán, E. Trigueros, M. T. Sanz, "Subcritical water extraction and identification of phenolic compounds from Brewer's Spent Grain (BSG)" invited lecture in *18th European Meeting on Supercritical Fluids (EMSF)*. May 2021 Bordeaux (France).

P. Alonso-Riaño, O. Benito-Román, S. Beltrán, E. Trigueros, M. T. Sanz, "Utilización de agua subcrítica para recuperar y fraccionar la fracción proteica y los compuestos fenólicos del bagazo de cerveza" in *VII Jornadas de doctorandos de la Universidad de Burgos*. March 2021, Burgos (Spain).

### Poster communications

P. Alonso-Riaño, R. Melgosa, E. Trigueros, S. Beltrán, M. T. Sanz. "Modification of brewer's spent grain after sc-CO<sub>2</sub> extraction: improvement of sugar and phenolic compounds release" in *Second Iberian Meeting on Supercritical Fluids*. 28 February-2 March 2022, Coimbra (Portugal).

P. Alonso-Riaño, O. Benito-Román, S. Beltrán, E. Trigueros, M. T. Sanz, "Hydrolysis and fractionation of phenolic compounds from brewery's spent grain by subcritical water" in *First Greening International Conference*. February 2021, Costa da Caparica (Portugal).

P. Alonso-Riaño, O. Benito-Román, C. Ramos-Rodriguez, S. Beltrán, E. Trigueros, M. T. Sanz, "Subcritical water fractionation of proteins and free amino acids from Brewer's Spent Grain (BSG)" in *First Iberian Meeting on Supercritical Fluids*. February 2020, Santiago de Compostela (Spain).

P. Alonso-Riaño, R. Melgosa, E. Trigueros, O. Benito-Román, M.T. Sanz, S. Beltrán, "Subcritical Water Fractionation of bioactive compounds from Brewer's Spent Grain (BGS)" in *17th European Meeting on Supercritical fluids*. April 2019, Ciudad Real (Spain).

